

Design of Operable Reactive Distillation Columns

Myrian Andrea Schenk

A thesis submitted for the degree of Doctor of Philosophy
of the University of London.

Department of Chemical Engineering
University College London,
London WC1E 7JE

September, 1999



Abstract

Reactive distillation is an integrated process which considers simultaneous physical and chemical transformations. It is increasingly receiving attention both from industry and academia. Significant advances have been made in the area of modelling and simulation as well as the implementation of such units industrially. However, the area of control and optimisation of such units has not been explored thoroughly.

The thesis presents a general framework for simulation and design, which can handle reactive and non-reactive systems. Various different aspects of the modelling and simulation of distillation have been described in order to understand the behaviour of the reactive distillation columns. In the framework both simulation modes, steady-state and dynamic, are considered and the process is described by equilibrium and non equilibrium-based models. In a rate-based (or non equilibrium) model, mass transfer rates between liquid and vapour phase are considered explicitly, based on the Maxwell-Stefan equations. Equilibrium is attained at the phase interface in the non-equilibrium model. A switching policy makes it possible to go from one model to the other, based on the knowledge gained, by following the Gibbs free energy as a function of time. Tray efficiency has also helped in determining the switch between the non-equilibrium and equilibrium models, and has been studied for various systems.

The existence of multiple steady state has been verified through simulation with the hybrid model. Bifurcation diagrams also confirmed the existence of output multiplicity obtained in the simulations.

Analysis of process controllability at the design stage has been shown to provide guidance for improving process operation. In the thesis controllability measures for the reactive systems studied are presented as a first step towards control structure selection.

A method for obtaining the design of reactive separation columns at minimum total annualised cost (investment and operating costs) and which will be able to maintain stable operation in the presence of variability is also presented.

Acknowledgements

I would like to thank my supervisors David Bogle, Rafiqul Gani and Stratos Pistikopoulos. Their continuous support and guidance has led to the production of this work. It has been a pleasure to work next to them and I also thank them for the opportunity of this joint research.

The many technical discussions at ICI, especially with Tom Malik, are also greatly appreciated.

Financial support from the Centre for Process Systems Engineering, CAPEC-Research Center and ICI is gratefully acknowledged.

Special thanks go to Carlos, Nicolas, Sonia, Alejandro and Marta for introducing me to the challenge of research.

It has been a pleasure to work amongst different groups, in Lyngby and here in London. The time would not have been memorable and enjoyable without the nice people I have had around. I would like to thank particularly to: Eduardo, with whom I have worked and discussed a lot about reactive distillation, and with whom I shared the difficult times far away from home; Cecilia, my office-mate from the old times, it have been a pleasure to work next to her; Celeste, with whom I discussed piles of work and with whom I keep my Spanish 'up-to-date'; my part-time flat-mates in the 'London time', the 'adventure guys', Soraya and Geoff; Vik, my desk neighbour at IRC, who always has a smile ready to start the working day.

My dearest friends Marianne, Ari, Stefan and Angelika will always be remembered for their sincere friendship and for their encouragement in good and bad times.

I would also like to thank my family for their love and everlasting confidence through the years.

Last but not least, I would like to thank Jes, my lovely husband, without whom all this may never have been. His support and infallible trust in my work has motivated me over all these years.

Contents

1	Introduction	12
1.1	Reactive Distillation	12
1.2	Motivation and Aim of the Work	14
1.2.1	Problem Definition	15
1.3	Overview	15
2	Background: Literature Review	18
2.1	Reactive and Non-reactive Distillation in Process Engineering	18
2.2	Modelling-Design-Synthesis Issues	21
2.2.1	Equilibrium Models	21
2.2.2	Non-equilibrium (rate-based) Models	28
3	Modelling Issues	33
3.1	Equilibrium Models	35
3.2	Non-equilibrium Models	35
3.2.1	Maxwell-Stefan Equations	36
3.3	Model Equations	39
3.4	Model Formulation	41
3.5	Equations	42
3.6	Generation of Models	59
3.6.1	Tray Efficiency	66
3.7	Condensers and Reboilers	69

3.8	Computational and Numerical Aspects	71
3.8.1	Specifications for Equilibrium and Non-equilibrium Simulations	71
3.8.2	Solution of Model Equations	71
3.8.3	Initialisation	74
3.8.4	Switching between Models and Monitoring of Phenomena	76
3.9	Conclusions	76
4	Validation of models	78
4.1	Systems Studied	79
4.1.1	MTBE: Methyl-Tert-Butyl-Ether	79
4.1.2	Ethyl Acetate	86
4.1.3	Depropanizer Column	91
4.2	Initialisation	91
4.3	Validation of Models	94
4.3.1	MTBE	94
4.3.2	Ethyl Acetate	102
4.3.3	Depropanizer Column	106
4.4	Bifurcation Analysis	107
4.4.1	Applied Bifurcation Analysis	109
4.5	Conclusions	114
5	Analysis with Hybrid Models	116
5.1	Monitoring of Phenomena through Gibbs Free Energy	117
5.2	Tray Efficiency Analysis	119
5.3	Illustration of Hybrid Modelling Approach	128
5.4	Conclusions	132
6	Controllability Issues and Dynamic Optimization	133
6.1	Controllability Issues	134
6.1.1	Linear Model	135

6.1.2	Scaling	137
6.1.3	Controllability Tools	139
6.1.4	Control Configurations	140
6.1.5	Examples of Application	143
6.2	Dynamic Optimization	150
6.2.1	Optimization problem	153
6.3	Conclusions	159
7	General Conclusions and Future Work	160
	Nomenclature	163
	References	167
A	Properties	179
A.1	Enthalpy	179
A.2	Density	180
A.3	Viscosity	180
A.4	Surface Tension	181
A.5	Thermal Conductivity	181
A.6	Binary Diffusion Coefficients	182
B	Results	184
B.1	Simulation Results for MTBE	184
B.1.1	Controllability Analysis for the MTBE production . . .	189
B.2	Esterification of Acetic Acid with Ethanol	203
C	Optimization	219
C.1	Objective Function and Disturbances	219

List of Figures

1.1	Exemplary reactive distillation column	16
2.1	Residue curve map for MTBE. (P=1atm)(Ung and Doherty, 1995b)	25
2.2	McCabe-Thiele like diagram for MTBE.(Pérez Cisneros <i>et al.</i> , 1997a)	26
3.1	Schematic representation of an stage in the column (Krishnamurthy and Taylor, 1985)	40
4.1	Multiple solutions in the MTBE column	96
4.2	Temperature profiles for low and high conversion in the MTBE column	97
4.3	Equilibrium constant for MTBE synthesis	98
4.4	Simulation results with Rehfinger and Hoffmann, Colombo <i>et al.</i> and DIPPR for the MTBE column	99
4.5	Simulation results compared with those of ASPEN PLUS for the MTBE column	101
4.6	Simulation results with the equilibrium and non-equilibrium model for the MTBE column	102
4.7	Simulation results with different thermodynamic models for the esterification column	103
4.8	Simulation results compared with experimental data for the esterification column	104
4.9	Mass Transfer rate for the esterification column	105
4.10	Comparison of mass transfer rate with literature results	106

4.11	Simulation results with the non-equilibrium model for the depropanizer column	108
4.12	Vapour compositions compared with ChemSep simulations . .	109
4.13	Bifurcation diagram for the esterification column varying reflux flow rate	111
4.14	Bifurcation diagram for the MTBE column varying reflux flow rate	112
4.15	Bifurcation diagram for the MTBE column varying vapour boil-up	113
5.1	Excess Gibbs energy for the esterification column. Trays 1 and 7.	118
5.2	Excess Gibbs energy for the MTBE column. Trays 4 and 10. .	119
5.3	Vapour compositions for the esterification column	120
5.4	Efficiency calculated for the esterification column	121
5.5	Efficiency calculated for the depropanizer column	122
5.6	Vapour composition for the depropanizer column	123
5.7	Efficiency calculated for the depropanizer column far from steady-state	124
5.8	Efficiency calculated for the depropanizer, compared with those of ChemSep: Ethane	125
5.9	Efficiency calculated for the depropanizer, compared with those of ChemSep: Propane	126
5.10	Point Efficiency for the depropanizer column: Propane	127
5.11	Liquid composition profile with equilibrium model with fixed efficiency and non-equilibrium model	129
5.12	Vapour composition profile with equilibrium model with fixed efficiency and non-equilibrium model	130
5.13	Hybrid model applied to the esterification column	131
6.1	Response obtained from the linear and non-linear model (10% step change).	138
6.2	High conversion of MTBE as result of 10% increase in reboiler heat duty.	145

6.3	Low conversion of MTBE as a result of 15% decrease in reboiler heat duty.	146
6.4	Lower purity of MTBE as a result of adding extra reactive stages	147
6.5	Reactive distillation column for the design study	154
6.6	Top and bottom compositions of ethyl acetate. Results from the simulated nominal case with disturbance.	156
6.7	Ethyl acetate composition. Results from the dynamic optimization.	157
6.8	Controlled variable: Reboiler Heat Duty($\times 10^6(MJ/h)$). Results from the dynamic optimization.	158
B.1	Decreasing 10% methanol feed flow-rate.	185
B.2	Increasing 10% methanol feed flow-rate.	185
B.3	Increasing 10% isobutene feed composition.	187
B.4	Decreasing 15% isobutene feed composition.	187
B.5	Decreasing 10% isobutene feed composition.	188
B.6	Poles and Zeroes for Case 1 (MTBE)	190
B.7	RGA element (1,1) as a function of the frequency for Case 1 (MTBE)	191
B.8	Singular values for Case 1(MTBE)	192
B.9	Step response for Case 1 (MTBE). (10% step size)	193
B.10	Poles and Zeroes for Case 2 (MTBE)	195
B.11	RGA element (1,1) as a function of the frequency for Case 2 of MTBE	196
B.12	Step response for Case 2 (MTBE). (10% step size)	198
B.13	Poles and Zeroes for Case 3 (MTBE)	199
B.14	RGA element (1,1) as a function of the frequency for Case 3 (MTBE)	200
B.15	Singular values for Case 3 (MTBE)	201
B.16	Step response for Case 3 (MTBE). (10% step size)	202
B.17	Poles and Zeroes for Case 1 (Esterification)	204

B.18 RGA element (1,1) as a function of the frequency for Case 1 (Esterification)	205
B.19 Step response for Case 1 (Esterification). (10% step size) . . .	207
B.20 Poles and zeroes for Case 2 (Esterification)	209
B.21 RGA element (1,1) as a function of the frequency for Case 2 (Esterification)	210
B.22 Singular values for Case 2 (Esterification)	212
B.23 Step responses for Case 2 (Esterification). (10% step size) . .	213
B.24 Poles and zeros for Case 3 (Esterification)	215
B.25 RGA element (1,1) as a function of the frequency for Case 3 (Esterification)	216
B.26 Singular values for Case 3 (Esterification)	217
B.27 Step responses for Case 3 (Esterification). (10% step size) . .	218

List of Tables

2.1	Thermodynamic equilibrium approaches for the simulation of reactive distillation columns	22
2.2	Design approaches for reactive distillation columns	24
3.1	Thermodynamic models	47
3.2	List of variables per stage in the non-equilibrium model	61
3.3	List of equations per stage in the non-equilibrium model . . .	62
3.4	Various forms of non-equilibrium models	63
3.5	List of variables per stage in the equilibrium model	63
3.6	List of equations per stage in the equilibrium model	64
3.7	Various forms of equilibrium models	65
3.8	Computational times for solution of different sets of model equations	75
4.1	Range of Variables	82
4.2	MTBE Column Design. Data taken from Jacobs and Krishna (1993) except for the tray design which has been calculated in this work	83
4.3	Modelling alternatives for MTBE system	86
4.4	Ethyl Acetate Column Design. Data from Suzuki <i>et al.</i> (1971) except the tray design which has been calculated in this work.	88
4.5	Modelling alternatives for Esterification system	90
4.6	Depropanizer Column Details. Data taken from Taylor and Krishna (1993).	92

4.7	Selected set of numerical statistics for the three distillation systems	94
6.1	Basic control configurations	141
6.2	Ratio control configurations	142
6.3	Measured variables for the controllability study on MTBE production	148
6.4	Controllability indices for the MTBE production	148
6.5	Measured variables for the controllability study on ethyl acetate production	149
6.6	Controllability indices for the ethyl acetate production	149
6.7	Optimization details	155
6.8	Optimization results: nominal and optimal values	159

Chapter 1

Introduction

1.1 Reactive Distillation

Reactive distillation is a hybrid unit which comprises distillation and reaction in a single unit operation.

Recently reactive distillation has become a strong interest in chemical engineering research, although the concept of reactive distillation has been known for a long time. In the 1920's the technique was applied to esterification processes using homogeneous catalysts (Backhaus, 1921). In 1971, Sennewald described a development employing solid heterogeneous catalysts.

The most important benefit of reactive distillation lies in the economics: a reduction in capital cost, energy saving, raw materials and solvent reduction. By carrying out distillation and chemical reaction in the same unit, one process step is eliminated, along with the associated pumps, piping and instrumentation. This gives safer environmental performance (the area or scale of risk and hazards is significantly reduced with just one continuous operating unit) as well as better energy management (the heat of reaction creates more boil-up and better vapour-liquid phase transfer, but no increase in temperature; therefore, no cooling is required).

Particularly good candidates for reactive distillation are processes in which the chemical reactions are characterised by:

unfavourable reaction equilibrium: all chemical reactions have an equilibrium reaction. There are chemical reactions for which, at operating temperature, the mixture at chemical reaction equilibrium conditions still contains considerable concentration of reactants. Even if one of the reactants is present in a high concentration the reaction will not proceed. Such reactions are normally so-called equilibrium-limited. For these chemical reactions the conversion can be increased by continuous removal of products from the reacting mixture.

high heat of reaction: some chemical reactions have large heat of reaction (exothermic or endothermic). If these reactions occur in reactors they will change the temperature and modify the reaction progress. In reactive distillation the heat of reaction will not modify the temperature, the phases will remain at the boiling point, and the heat of reaction will not affect the reaction equilibrium. In the case of exothermic reactions, the heat of reaction is directly used for the distillation process.

large excess of reactants required: reactive distillation is also potentially attractive whenever a liquid phase reaction must be carried out with a large excess of one reactant. In this situation, conventional processes need large recycle cost (for the excess of reactant); however, reactive distillation could be carried out closer to stoichiometric conditions minimising the recycle cost. Reactive distillation prevents side reactions and overcomes limitations due to chemical equilibrium by its natural separation.

azeotropic conditions: reactive distillation can overcome the limitations imposed by azeotropic mixtures: simultaneous chemical and phase equilibrium has the most beneficial effect of reacting away some of the azeotropes and thereby, simplifying the phase behaviour.

systems with solid catalysts: reactive distillation is especially applicable to a certain class of reactions that employ solid catalysts. The important points that characterise the catalyst systems are the activity of the catalyst at distillation conditions and the relative volatility of the reactants and products. The balance between these two characteristics makes some chemical systems perfect candidates for this technique.

The main disadvantage of reactive distillation is that it is highly system specific and its suitability needs to be assessed separately for each process.

Reactive distillation has a strong dependency on the properties of the chemical system that is dealt with. The poor knowledge of the chemical reactions features, (catalyst, kinetics, hold-ups) and distillation (vapour-liquid equilibria, thermodynamics, plate and/or packing behaviour) together with their combination in a reactive distillation unit, makes such a unit difficult to simulate and operate.

Reactive distillation appears to be an interesting process unit. Models capable of dealing with different processes are still not available. Although fully equilibrium considerations may give the limits for reaction and separation, reactive distillation columns will not operate at equilibrium (real operations are not at equilibrium).

1.2 Motivation and Aim of the Work

The motivation of this study has been the interactions between reaction and separation that a reactive column offers. Increased interest in the units for the application to fine chemicals and pharmaceuticals, as well as in the commodity chemical industry has also been an incentive of this work.

The main objective of the present work has been to generate appropriate tools to derive an optimal design of reactive distillation operations.

The objective has been tackled by:

- developing rigorous models for reactive distillation systems;
- formulating a dynamic optimisation problem able to choose the best structure (from all the possible alternatives) for a given task;
- performing controllability analysis on the system studied, using open-loop controllability indicators; and finally,
- applying optimal control (dynamic optimization) for the design of reactive distillation columns.

1.2.1 Problem Definition

Consider the reactive distillation column in Fig. 1.1 where a mixture is to be separated into two product streams. The mixture of A and B will react to C and D. Operational constraints, such as product specifications, must be met in spite of the presence of variability in the feed streams over time (disturbances in composition of A or B). The objective is to design the reactive column at minimum total annual cost with the goal of ensuring feasible operation for all product specifications over time.

In order to undertake such problem, a number of issues need to be addressed:

- Rigorous models (equilibrium and non-equilibrium based) accounting for highly non-ideal mixtures need to be implemented. Simulation and sensitivity analysis should be performed to study whether operability problems, such as multiplicity, can occur.
- Optimisation techniques to choose the best design for a given task should be considered. An objective function including economics of the process and other factors, such as operability indicators, should be included.

1.3 Overview

This thesis is structured as follows,

Chapter 1 gives the introduction, motivation and the aim of this work.

Chapter 2 briefly shows the most relevant literature in the area of reactive distillation. The Chapter is divided into two Sections. The first one addresses the literature in terms of equilibrium models presented. The second one addresses the area of non-equilibrium models.

Chapter 3 gives a full description of the hybrid model presented and used in this work. A brief discussion highlighting the equilibrium and non-equilibrium models is presented. The Maxwell-Stefan equations are also given. A detailed Section with the set of equations describing the hybrid model is presented. Generation of models from the hybrid framework as well as computational and numerical aspects are given at end of the Chapter.

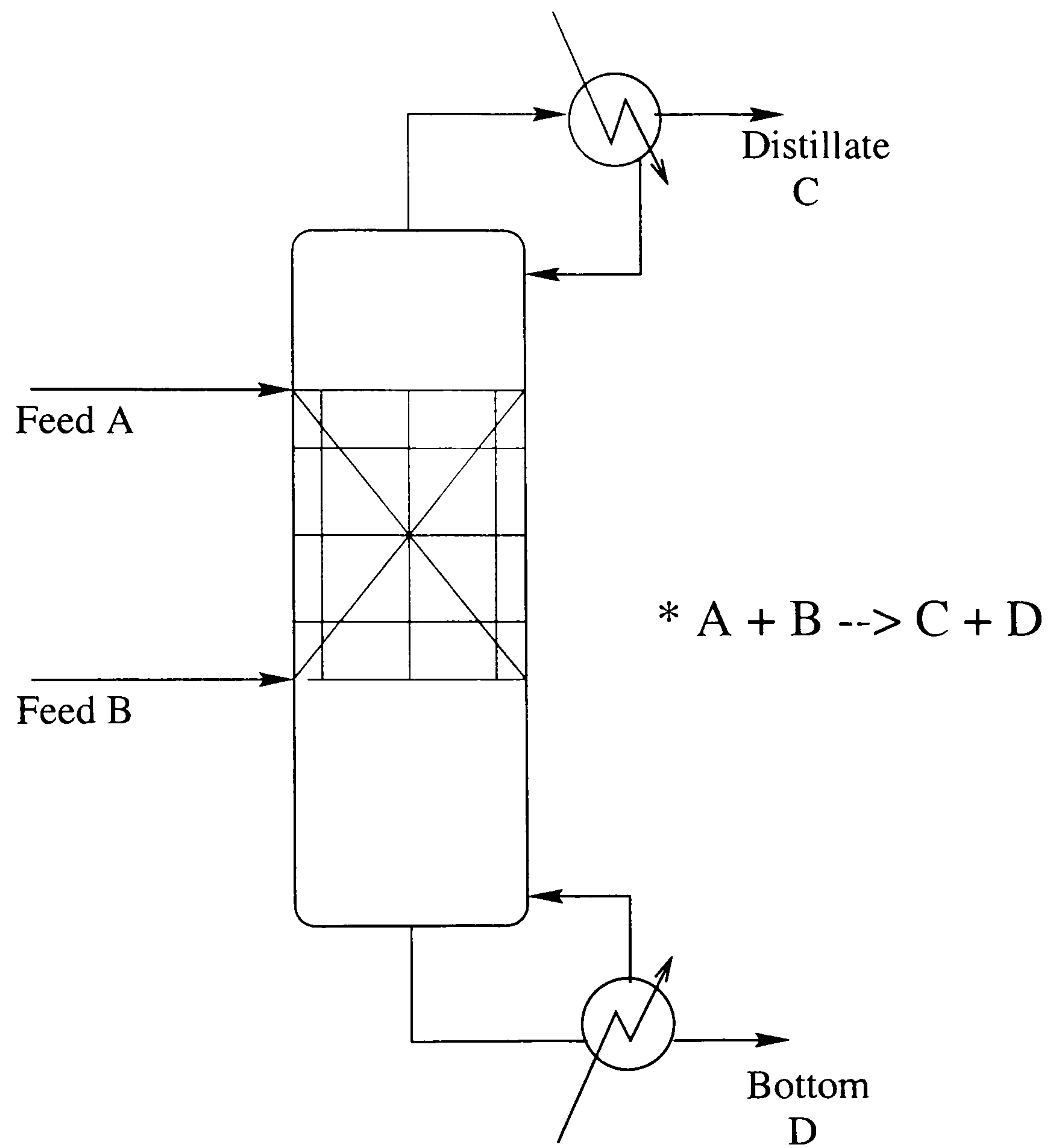


Figure 1.1: Exemplary reactive distillation column

Chapter 4 presents the validation of models. First the systems studied in this thesis are presented, then the model validation for each system is studied. Finally a continuation method integrated into the hybrid approach is also presented showing the bifurcation analysis.

Chapter 5 gives the application of hybrid models. Whenever computational time is to be saved, then combination of non-equilibrium and equilibrium models should be used. To determine when it is possible to switch from one model to another, tray efficiencies and excess tray Gibbs free energy over the simulation time should be analysed. Hybrid modelling results are highlighted.

Chapter 6 gives the controllability issues and dynamic optimization. A brief theory description precedes the results.

Chapter 7, as last Chapter of this thesis, presents the conclusions and future directions from this work, as well as highlighting the main contributions of this thesis.

Chapter 2

Background: Literature Review

“The idea of evolution is closely associated with an increase of organisation giving rise to the creation of more and more complex structures”
(Glansdorf and Prigogine, 1971).

2.1 Reactive and Non-reactive Distillation in Process Engineering

Different pieces of equipment configure a chemical plant. Some of these equipment are likely to be distillation columns. Distillation is one of the oldest unit operations in chemical engineering. The concept of ‘stage’, which describes distillation columns has been known for over a hundred years. The description of a distillation column continues by characterising defined flows entering and leaving any stage. These flows consist of mass or heat and they can be the vapour/liquid flow through the column, feed flows or any draw flows. Distillation displays different types of multiple phenomena such as mass and heat transfer, phase equilibrium, mixing, material and heat flow, etc. The simplest kind of stage in a distillation column is the ‘equilibrium stage’. This implies that the chemical potential of any component has the same value in the vapour and liquid phase.

It is well-known that equilibrium models have one big advantage: a consistent model. However their big weakness is in most cases: that the solution is potentially very far from the real process.

This weakness has been overcome by chemical engineers with the help of the efficiency concept. The Murphree efficiency is commonly used for tray columns mainly because its implementation in equilibrium models is straight forward. When using this efficiency we assume that the vapour composition obtained with the equilibrium model is not the real composition but that the real tray composition is a fraction of the tray composition. For binary separations, where the two efficiencies have the same value, the concept works quite well, but it starts failing when multicomponent mixtures are considered (Wesselingh, 1997). Efficiencies are often assumed ‘constant’ throughout the column. Practical experience helps in deciding which ‘value’ should be used for a particular example.

What is to be done if we do not want to use the efficiency concept? Recently, Wesselingh (1997) suggested the ‘dream of a chemical engineer’, saying: ‘subdivide each piece of equipment into zillions of little elements $dx.dy.dz$, each of which will contain part of one of the phases in the equipment’. Using then the difference form of Navier-Stokes equations for the hydraulics, the Maxwell-Stefan equation to calculate the diffusion flows, and Fourier equations to describe the energy transfer, together with the corresponding balances and boundary conditions we should be able to solve the ‘real problem’. However, unfortunately it won’t be possible to obtain the solution on a short term basis: it is a dream.

Between this ‘dream of engineers’ and the usual equilibrium approach, there is the non-equilibrium model, which in these days takes into account the more important characteristics of the column: it assumes that the vapour and liquid in the column are not at thermodynamic equilibrium. Equilibrium is only assumed at the phase interface. The equations of equilibrium are then used to obtain the driving forces for the mass transfer. Well mixed liquid and vapour phases are mainly considered and the description of the mass and heat transfer between the phases is included.

Significant advances have been made since the early 1970s in the area of modelling and simulation of distillation columns. Simulations of steady state operations and unsteady state operations including start-up and shutdown operations are quite common nowadays.

At the end of the century, the models used for different simulation problems attempt to address the complex modelling and simulation issues, including

those related to separation of azeotropic mixtures and simultaneous separation and reaction: reactive distillation.

The main technical advantage of reactive distillation is the continuous removal of reaction products. However, as reactive distillation still involves longer lead time for research, which kind of models should be applied to the unit? Can a distillation model be extended to consider the simultaneous physical and chemical phenomena? Would one need a 'special' model to describe the proposed problem?.

Reactive distillation units can be modelled as an equilibrium system (simultaneous physical and chemical equilibrium); at physical equilibrium with kinetically controlled reaction; or as a non-equilibrium system (separation through mass/heat transfer plus kinetically controlled reaction); or even maybe as a combination of these models which could also be an interesting way of looking at the process.

The selection of the appropriate model type, form and simulation mode (steady state or dynamic) for a particular simulation problem depends on the problem being solved. The separation task will provide details for the mixture being separated, the required simulation mode, the existence of reactions and/or azeotropes and many more. The choice between non-equilibrium (or rate-based) and equilibrium models, although obvious, is not always followed. That is, since any distillation operation will not attain true equilibrium, the non-equilibrium model is always the most appropriate selection. The equilibrium-based model, however, predominates in terms of application as it is easier to implement and to solve. A question arises here again: is the non-equilibrium model always needed to capture all the phenomena occurring in the reactive column?

Ideally, what is needed is a computer aided system with a general distillation model from which all the necessary model forms can be generated so that our question can be answered. If, for a particular simulation problem, more than one type of model becomes necessary, the computer aided system should be able to generate the problem specific model through the use of a hybrid modelling approach. The hybrid modelling approach consists of generating hybrid models and defining their solution method, for example, modelling of a single distillation column with reactive and non-reactive trays or the use of non-equilibrium-based model on some trays and equilibrium-based model

on the remaining trays. Also, for any design/analysis/control problem, the hybrid modelling approach will allow switching between steady-state and dynamic modes and different forms of models. This will make the transfer of data (information) from one simulation sub-problem to another transparent and ‘noise-free’. Smooth transfer of data also means better initialisation and consequently, a more robust and efficient solution technique. In this thesis an attempt has been made to present such a model.

2.2 Modelling-Design-Synthesis Issues

This section has been divided into two parts, one is related to equilibrium models presented in the open literature. The other one treats non-equilibrium-based models.

2.2.1 Equilibrium Models

The literature review on distillation has been extensively addressed in the past. Several books offer the possibility of understanding, as well as showing how to model, design and control a distillation unit. Examples are, King (1980), Kister (1990, 1992), Luyben (1974), Skogestad and Postlethwaite (1996), to name a few. For this reason we have focused here on the description of the research over the years of only reactive distillation columns.

In recent years a large number of computational algorithms have been reported to solve the mass and energy balance equations together with the phase equilibrium data describing the reactive distillation problem. The unknown variables determined by solving these equations are mole fractions of both phases, stage temperatures, rate of reaction and flow-rates of each phase. The equilibrium model is the standard model for simulating reactive or non-reactive distillation. The key assumption in these models is that the vapour and liquid leaving a reactive or non-reactive stage are in equilibrium and both temperatures (liquid and vapour) on the stage are assumed equal. Table 2.1 summarises some of the simulation approaches using a thermodynamic equilibrium model for reactive distillation (many more are presented in the literature, but all of them offer more or less the same characteristics).

Most of the research has focused upon steady-state solution of the model equations. The earliest algorithms for steady state simulation of staged re-

Authors	Equilibrium-Simulation Features
Suzuki <i>et al.</i> (1971)	Steady-state model. Kinetically controlled reaction. Margules's modified equation for the thermodynamic model Experimental results from a pilot plant.
Saito <i>et al.</i> (1971)	Steady-state model. Instantaneous reaction. Model specific for the esterification example treated.
Komatsu and Holland (1980)	Steady-state model. Kinetically controlled reactions. Homotopy-Continuation method of solution.
Pérez Cisneros <i>et al.</i> (1996)	Dynamic model. Kinetically controlled reactions. General model including non-reactive distillation.

Table 2.1: Thermodynamic equilibrium approaches for the simulation of reactive distillation columns

active distillation columns were reported by Suzuki *et al.*(1971)(general algorithm employing quasi-linearisation Newton methods); Saito *et al.*(1971) (rather specialised, involves instantaneous reaction equilibrium, etc.); and Nelson (1971) (employing modified Newton-Raphson).

During the years several other algorithms with different methods of solution have been studied, for example, Komatsu and Holland (1980), Holland (1981), including quasi-Newton methods combined with the θ -method of convergence. Jelinek and Hlavacek (1976), Komatsu (1977) used relaxation methods (*i.e.* false transient); Chang and Seader (1988) and Bondy (1991) worked on homotopy-continuation methods. The homotopy-continuation method is a way to solve the problem when Newton methods fail. Through parametrisation the problem is transformed into a problem one can solve either by using additional parameters or parameters that occur naturally in the model (parametric continuation).

Inside-out algorithms belong to tearing methods and take a two tier approach

in which the physical properties are approximated by simple models in the outer loop while the model equations are solved at the inner loop (simultaneously by Newton's methods). These kinds of methods are the subject of industrial research, as is shown by Venkataraman *et al.*(1990).

Dynamic equilibrium models for distillation have been presented by Gani *et al.*(1986, 1989), Cameron *et al.*(1986) and Ruiz *et al.*(1988). Their advanced equilibrium stage model including rigorous hydraulics has been applied not only to continuous columns but to shut-down/start-up for columns as well. Recently, the model has been adapted to handle reactive distillation (Pilavachi *et al.*, 1997).

To the best of our knowledge there are few papers in the literature, apart from our own work (Pérez-Cisneros *et al.*, 1996, 1997a; and Pilavachi *et al.* 1997), that addressed dynamic simulation of reactive distillation columns: Ruiz *et al.*(1996) and Schrans *et al.*(1996), Scenna *et al.*(1998).

From the 1980's the interest focused mainly on the design aspects of reactive distillation columns. Several research groups have been dedicated extensively for many years to this area and to the understanding of the interactions between separation and reactions.

The design of reactive columns has followed different kinds of approaches:

- transformed variable approach;
- element balance based approach;
- design techniques through optimization (including synthesis).

Table 2.2 highlights some of the main features obtained for the design of reactive distillation columns.

In the two first approaches, full equilibrium is considered. Doherty and co-workers have been working on the transformed variable approach, while Gani and co-workers have focused on the element balance based approach. Both methods are excellent in terms of visualisation for systems containing less than four components.

Optimization has also been applied for the design as well as synthesis of reactive distillation processes. This kind of approach utilises a superstruc-

Authors	Design Features
Barbosa and Doherty (1987, 1988a, b), Ung and Doherty (1995a,b,c)	Developed tools for analysis of reactive mixtures with a <i>single</i> equilibrium reaction. Later extended to <i>multiple</i> equilibrium reactions with inclusion of inerts.
Pérez Cisneros <i>et al.</i> (1996, 1997a,b)	Development of tools based on the element balance approach for <i>multiple</i> equilibrium reactions.
Ciric and Gu (1994)	MINLP for the optimal reactive column (minimising annualised cost) for multicomponent mixtures and kinetically controlled reaction.
Ismail (1998)	(MINLP) Synthesis framework for multi-component and multi-reactions (kinetically controlled) Hold-ups and catalyst loads are explicitly accounted for.

Table 2.2: Design approaches for reactive distillation columns

ture which is applicable to systems containing multiple feed streams, multicomponent mixtures and multiple reactions which are considered as kinetic rate based expressions, instead of equilibrium reactions. Pistikopoulos and co-workers have been working on developing a superstructure approach for design and synthesis of reactive and non-reactive distillation columns.

Barbosa and Doherty (1987) introduced a new set of composition variables, which reduces the problem considering reaction to a problem which is identical to one without reaction thus reducing the dimensionality of the phase and chemical equilibria problem for multicomponent systems.

Different tools they have developed are: computation of reactive phase diagrams, derivation of conditions and general conditions for reactive azeotropes, computation of residue curve maps (Barbosa and Doherty, 1987, 1988a,b; Ung and Doherty, 1995a,b,c). As an example of the visualisation of the method, the residue curves in transformed variables for the reactive system isobutene-methanol-MTBE with n-butane as inert component is presented in Fig. 2.1.

Image removed due to third party copyright

Figure 2.1: Residue curve map for MTBE. (P=1atm)(Ung and Doherty, 1995b)

The element balance based approach was developed originally by Michelsen (1995) and extended by Pérez-Cisneros *et al.*(1997b). Again, in this approach, the reduction in dimensionality of the problem is used. The approach is based on the fact that the number of ‘elements’ needed to represent a reactive systems is less than the number of components present in the reactive mixture. These elements are not necessarily ‘chemical elements’, but they can be a single chemical element, or a part of molecule or even the component itself. The solution method for this approach reduces to the well-known physical equilibrium problem, which obviously gives a great advantage. Tools developed for this approach for the design of reactive distillation columns include: reactive phase diagrams, general conditions for element reactive azeotropes, McCabe-Thiele-like diagrams (Pérez-Cisneros *et al.*, 1996,

Image removed due to third party copyright

Figure 2.2: McCabe-Thiele like diagram for MTBE.(Pérez Cisneros *et al.*, 1997a)

1997a, b, Pilavachi *et al.*, 1997). As an example of the methodology and visualisation, the McCabe-Thiele like diagram is shown in Fig. 2.2 for the MTBE reactive system.

A design methodology is also described by Pilavachi *et al.*(1997) which includes three steps:

- (i) validation of models (including as well selection of thermodynamic models);
- (ii) identification of variables sensitive to design, and;
- (iii) analysis of these effects on the design and operation of reactive units.

Ciric and Gu (1994) developed a synthesis scheme for reactive distillation processes combining a fairly complex equilibrium model with rate-based kinetic expressions. The resulting optimization model is a MINLP. The total annualised cost is the objective function. The solution of such problems yields the optimal number of trays, reflux ratio, heat exchanger duties and liquid hold-ups throughout the column.

Recently, Ismail (1998) developed a mass/heat transfer framework within a superstructure environment which can handle reactive separation systems. The approach is based on fundamental mass and heat transfer principles. Units of process alternatives are not prepostulated, but instead these are generated according to the synthesis objectives.

Summary

Since the 1950s new algorithms are presented frequently for solving the equilibrium stage model equations for distillation columns. However this is not an implication that everything has been done in the area. Still, many separation problems remain. Some of them are not solved yet or are hard to solve (Taylor and Lucia, 1995). The same problems apply to reactive distillation more strongly due to the fact that research in the area started a few years later (1970s) with equilibrium staged models.

The equilibrium model has been used for reactive distillation without consideration of tray efficiencies, mainly because of the lack of knowledge about the values of these efficiencies. Experimental data are practically not available.

For the design of reactive distillation columns, the variable transformation as well as the element balance based approaches are limited to simultaneous chemical and physical equilibrium. This, of course gives the limits of the possible separation, but units will rarely work at this condition. Variable transformation leads to ‘compositions’ outside the range 0-1. From the element based compositions there is no way to go to component compositions. These element compositions are not always useful. For both approaches, visualisation techniques become difficult for mixtures of more than four components (or elements).

Using the superstructure approach results in a probably more realistic and accurate design of reactive distillation columns. The price of this accuracy is

paid for by computationally demanding models. At present, limited steady state equilibrium models or limited mass/heat transfer models have been used. This highlights the need for a complex model, able to capture all the phenomena present in the reactive distillation process for the superstructure formulation.

2.2.2 Non-equilibrium (rate-based) Models

Rate-based models appear to be the most appropriate for reactive distillation systems, primarily due to the fact that the *a priori* computation of stage efficiency is avoided (Taylor and Krishna, 1993; Sivasubramanian and Boston, 1990).

In general, a non-equilibrium model includes separate mass and energy balances for each phase, equilibrium relations and mass and energy transfer models. The conservation equations for each phase are linked by material balances around the interface, since there is no accumulation at the interface (the mass lost by the vapour phase is gained by the liquid phase). Equilibrium relations are used to relate compositions at either side of the interface. Mass and energy are transferred across the interface at rates that depend on the extent to which the phases are not in equilibrium with each other. These rates are calculated from mass transfer correlations in multicomponent systems (Taylor and Krishna, 1993). Note that equilibrium stage models are a limiting case of the non-equilibrium model. If non-equilibrium simulations are done considering interfacial areas about 100 times larger than they really are, then the results of an equilibrium model can be matched (Powers *et al.*, 1988).

Physical reality is more accurately captured through the non-equilibrium model. Interactions between reaction and separation are considered explicitly through mass and heat balances around the vapour and liquid phases, respectively, in the case of reactive systems.

The non-equilibrium models that have been developed for distillation processes have given interesting insights into the effect of multicomponent mass transfer.

The model developed by Krishnamurthy and Taylor (1985) has been the

‘base’ for any other further development of non-equilibrium models. The model, with or without modifications has been applied for many researchers to the study of non-reactive columns. Recently reactive columns have also been studied with the ‘base-model’.

Well-known applications of reactive distillation include heterogeneous reactive distillation processes in packed columns such as etherifications; processes involving highly non-ideal mixtures such as esterifications or etherifications; and systems with a high reaction equilibrium constant in which at least one of the component concentration is low such as esterification of acetic acid with ethanol. Taylor *et al.*(1994) pointed out that rate-based models are particularly useful for modelling packed columns; strongly non-ideal systems; systems with trace components; columns that exhibit minima or change rapidly; or processes where efficiencies are unknown. A non-equilibrium model seems the way of modelling a reactive distillation column, instead of the well-know equilibrium model.

Another key reason for using a non-equilibrium model instead of an equilibrium model for reactive separation systems is that typically no good predictive methods exist nor is experimental data available for stage efficiencies.

Kooijman and Taylor (1995) have developed a rate-based model for the simulation of dynamic operations of tray columns. The ‘second generation’ of non-equilibrium model, as it is called, considers the dynamic behaviour of the column as well as pressure drop throughout the distillation column.

Górak and co-workers have done extensive research in the area of packed columns, including obtaining experimental results for comparison with their models. Packed columns are continuous contact devices and the more common technique used is a differential mass transfer-based model using multicomponent mass transfer theory (Górak, 1987, Kenig and Górak, 1995). One of the latest developments from this group is the rate-based model for reactive batch packed columns, as well as pilot scale experiments for the case of esterification of acetic acid with methanol (Kreul *et al.*, 1998, 1999). Also, Pelkonen *et al.* (1997) have described experimental validation of the rate-based approach for dynamic simulation of multicomponent distillation; and, Kenig *et al.* (1999) presented a work in which the simultaneous implementation of equilibrium model and non-equilibrium approach for reactive distillation simulation has been addressed.

Although rate-based models for distillation are now quite common (see Seader, 1989; and Taylor and Lucia, 1995, for an interesting review) such models for reactive distillation are still in the development stage. The first work in the field of rate-based model, to the best of our knowledge, was Sawistowski *et al.*(1979) who modelled a packed reactive distillation column for the esterification of acetic acid with methanol to methyl-acetate. An effective diffusivity type was used for the mass transfer model along with irreversible kinetics for the reaction which can lead to a high percentage of error (40%) in the prediction of the mass transfer rates. This may be due to the fact that there is a lack of theoretical and physical understanding with this effective diffusivity method (Taylor and Krishna, 1993).

Zheng *et al.*(1992) and Sundmacher (1995) presented rate-based models for the production of MTBE on a heterogeneous catalyst, which uses the Maxwell-Stefan equations for the description of the mass transfer. The heterogeneous reaction is considered as being pseudo-homogeneous (mass transfer effects to and from the catalyst are lumped together into a catalyst efficiency term).

Just recently more research in the area started to be published (Higler *et al.*, 1997, 1998, 1999a,b; Kreul *et al.*, 1998, 1999) although of a commercial version (ASPEN PLUS User Guide, 1997) of a generalised steady state rate-based model (RATEFRAC) capable of handling reactive systems has been available for almost ten years in the industry. The model which has been described by Sivasubramanian and Boston (1990) is a steady-state model based on that of Krishnamurthy and Taylor (1985) for non-reactive columns. It considers resistance to mass transfer in both phases, but the examples shown in the open literature are simplified to resistance in only one phase (liquid or vapour).

Recently, Higler *et al.*(1997, 1998, 1999 a,b) presented a non-equilibrium model for homogeneous reactive distillation (applied to the esterification of acetic acid with ethanol), where mass transfer accompanied by simultaneous chemical reaction is described using the Maxwell-Stefan continuity equations. In their model no expression for calculating the interfacial area is presented and the Lewis number is fixed for both phases. These assumptions are introduced by the authors in the first paper. Only one phase (liquid phase) mass transfer resistance is considered when applying the model to the case study. Heat transfer is disregarded, so that temperatures in both, liquid and

vapour phases, are the same.

Summary

Reactive distillation involves multicomponent mixtures, but other distillation also involve multicomponent mixtures. Systems containing binary mixtures (which are practically not used) are more simple to model: efficiencies, for example, are equal for both components. In multicomponent systems, however, *diffusive interaction*, *reverse diffusion*, *osmotic diffusion* and *mass transfer barriers* are of importance. It is clear that efficiencies can be different for each component and in each tray (Taylor and Krishna, 1993). Simulation and optimization are then of particular importance together with a good understanding of the process. It has never been presented when and for which range of operation the assumed simplifications to the model (such as equilibrium, constant flows, etc.) are valid. Lack of accurate simulators restricts even more any improvement in this direction, specially for reactive distillation.

Non-equilibrium models will continue to develop. Indeed they will be used massively for the case of multicomponent non-ideal mixtures, reactive separation and low-efficiency processes (Taylor and Lucia, 1995).

The main needs for using a non-equilibrium model at the moment are:

- reaction kinetics;
- better methods of predicting physical and transport properties for pure components as well as for mixtures (specially for dynamic simulation);
- correlations for mass and energy coefficients that cover a large range over the operating conditions;
- hydraulic performance of the units.

Very sophisticated models have been presented, even though it will be possible to extend them further. However, it is still not clear whether such developments can be warranted or give more insights in solving the problem. Most of the non-equilibrium models can, at this stage, accurately represent industrial data. However, it is unfair to say this without remarking here that experimental data is very hard to find and that often the nature of that data is unknown. There comes a point where the value of complex models must be compared with what can be obtained using simplified models. Can it pay to expend time in solving tedious large complex models to get a 0.05%

increase in accuracy? Probably the accuracy of the thermodynamic or transport property data is lower than that.

Model integration, where equilibrium and non-equilibrium models can be accessed for the same distillation unit; where steady-state simulation can be switched to dynamic simulation; where the equilibrium model can be applied for any stage of a column (if thermodynamic equilibrium is attained) while the rest of the unit will continue in the simulation as a non-equilibrium model. Model integration also where different types of models, simplified or rigorous can be accessed directly. In that sense, both types of model, equilibrium and non-equilibrium, have never been integrated. Still today computational time is an important issue, and the non-equilibrium model requires longer time to achieve the solution. A model combining both types of model is called a 'hybrid model'. To be able to account for a specific column configuration and control structure as well as dynamic optimization of the model equations should be implemented in a way such that all these tasks can be performed.

In this thesis an attempt to develop a complete hybrid model is presented together with a way of switching between both models. In addition, steady-state and dynamic modes are considered. Dynamic optimization can also be performed.

Chapter 3

Modelling Issues

Within the chemical industries distillation is the most used unit. Its inherent nature (multicomponent mixtures and complex dynamics) make it difficult to model and to simulate.

In this Chapter a detailed hybrid model (dynamic which can be also switched to steady-state) including both equilibrium and non-equilibrium approaches for continuous distillation and reactive distillation is presented. In the case of the equilibrium model, Murphree efficiency values are added to the equilibrium stage to account for deviation from ideality while for the rate-based (or non-equilibrium) model mass transfer is considered explicitly using the Maxwell-Stefan equations together with binary mass transfer correlations.

The hybrid model approach is presented addressing important characteristics of the processes such as steady-state and dynamic behaviour of multicomponent mixtures. The framework model equations are implemented using the ICAS-integrated simulator (Gani *et al.*, 1997) and *gPROMS* (PSE Ltd., 1997).

Validation of the model is highlighted by matching the results with experimental data available in the open literature (whenever possible) or against other simulation results. The results achieved for several reactive and non-reactive systems show that the model is able to predict accurately the processes over time. Through comparison of equilibrium and non-equilibrium simulation results for reactive distillation it is possible to show that the largest differences occur when the rate of reaction becomes important. The

reaction in the bulk of the liquid affects the mass transfer between the phases, thus moving the equilibrium.

Rate-based models lack appropriate experimental correlations, especially for mass and heat transfer; equilibrium-based model are not accurate (as previously reported, Taylor and Krishna, 1993), hence, a model combining both approaches gives a step forward towards fast and relatively accurate simulation.

In Sections 3.1 and 3.2 some details of equilibrium and non-equilibrium models are given, together with a description of the Maxwell-Stefan equations. From Section 3.3 the model developed in this work is described. Assumptions (with the corresponding justifications) are highlighted.

3.1 Equilibrium Models

Since the 1950's modelling of distillation has been based on the equilibrium stage. The key feature is that vapour and liquid streams leaving the stage are at *equilibrium* with each other.

Three different types of equilibria are presented in the *equilibrium* term: *material equilibrium* (there is no net change of material between the phases), *mechanical equilibrium* (there are no velocity gradients), and *thermal equilibrium* (there is no difference between the phase temperatures) (Bird *et al.*, 1960). Since no distillation unit operates at equilibrium, efficiencies are used to account for departures from equilibrium. For binary systems, efficiencies are equal for both components and they are bounded between 0 and 1. This does not hold for multicomponent mixtures, mainly because of the *diffusional interactions*, as defined by Toor(1964). The *diffusional interactions* include: *reverse diffusion*(when a component is diffusing against its own concentration gradient), *osmotic diffusion*(when a component diffuses even if it has no concentration gradient), and the *mass transfer barrier*(when a component does not diffuse despite its concentration gradient).

3.2 Non-equilibrium Models

When deriving a non-equilibrium model, one of the following theories should be applied at the interface (if fluid-dynamic equations are not considered), for example (there are more than forty theories that can be applied),

- the two-film model theory,
- the boundary-layer theory,
- the penetration theory, or
- film penetration theory.

The two-film model theory (Whitman, 1923) is mostly used because experimental data available is adapted to this theory. This theory is also reported to give accurate results, even when factors such as chemical reactions causes changes in the mass transfer (Taylor and Krishna, 1993). The theory, though, includes various simplifications.

3.2.1 Maxwell-Stefan Equations

The Maxwell-Stefan equation for binary ideal mixtures is written as:

$$\mathbf{df}_1 \equiv \frac{1}{P} \nabla p_1 = -\frac{x_1 x_2 (\mathbf{v}_1 - \mathbf{v}_2)}{D_{12}} \quad (3.1)$$

where \mathbf{df}_1 can be considered to be the driving force for diffusion of species 1 in an ideal gas mixture is at constant temperature and pressure. The symbol D_{12} is the Maxwell-Stefan diffusivity. The Maxwell-Stefan coefficients do not depend on the compositions, and this gives the Maxwell-Stefan equations an advantage over the extended Fick's law for multicomponent systems (Taylor and Krishna, 1993).

The theory for binary ideal systems can be extended to multicomponent ideal systems, so that,

$$\mathbf{df}_i = -\sum_{j=1}^{NC} \frac{x_i x_j (\mathbf{v}_i - \mathbf{v}_j)}{D_{ij}} \quad (3.2)$$

If the approach is to be extended to non-ideal systems, then the driving force for diffusion in non-ideal systems is the gradient of the chemical potential (Taylor and Krishna, 1993). According to this, for liquid mixtures or for dense gases exhibiting deviations from ideal gas behaviour, we can apply the condition,

$$\mathbf{df}_i \equiv \frac{x_i}{RT} \nabla_{T,P} \mu_i \quad (3.3)$$

where the chemical potential gradients give the departure from equilibrium (this driving force reduces to $1/P \nabla p_i$ for ideal gases). Due to the Gibbs-Duhem restriction, only $NC - 1$ driving forces are independent. Hence the sum of the driving forces vanishes:

$$\sum_{i=1}^{NC} \mathbf{df}_i = 0 \quad (3.4)$$

Working with Eq. 3.3 we can obtain,

$$\mathbf{df}_i = \sum_{j=1}^{NC-1} \Gamma_{ij} \nabla x_j \quad (3.5)$$

where for non-ideal liquids,

$$\Gamma_{ij} \equiv \delta_{ij} + x_i \frac{d \ln \gamma_i}{dx_j} \Big|_{T,P,x_k, k \neq j=1, \dots, n-1} \quad (3.6)$$

The above formulation can also be used for non-ideal gases by changing the activity coefficients γ_i for the fugacity coefficients, ϕ_i ,

$$\Gamma_{ij} \equiv \delta_{ij} + x_i \frac{d \ln \phi_i}{dx_j} \Big|_{T,P,x_k, k \neq j=1, \dots, n-1} \quad (3.7)$$

The driving force for the diffusive flux j of the component i within a mixture of NC components, \mathbf{df}_i , is given by (Taylor and Krishna, 1993),

$$\mathbf{df}_i^V = [\Gamma] \sum_{j=1, j \neq i}^{NC} \frac{y_i J_j^V - y_j J_i^V}{\bar{\rho}_V D_{ij}^V} \quad (3.8)$$

D_{ij}^V is the Maxwell-Stefan diffusivity coefficient, which for diluted gases is identical to the binary diffusion coefficient.

The diffusion fluxes J_i^V are given by

$$J_i^V = \bar{\rho}_V \sum_{j=1}^{NC-1} [\Gamma][K]^V \nabla y_j + J_t^V y_i \quad (3.9)$$

where, $J_t^V = \sum_{i=1}^{NC} J_i^V$; and $[K]^V = [C]^{-1}$, with the elements given by,

$$C_{i,i} = \frac{y_{i,NC}}{D_{i,NC}} + \sum_{k=1, k \neq i}^{NC} \frac{y_{i,k}}{D_{i,k}} \quad (3.10)$$

$$C_{i,j} = -y_{i,j} \left(\frac{1}{D_{i,j}} - \frac{1}{D_{i,NC}} \right) \quad (3.11)$$

Because there are $NC - 1$ independent equations, the remaining diffusional flux is calculated by

$$J_{NC}^V = - \sum_{i=1}^{NC-1} J_i^V \quad (3.12)$$

(Note that the equations presented here are for the vapour phase, similar equations are valid for the liquid phase).

Using the two-film theory model requires a value for the film thickness for both phases.

Different types of phenomena, such as entrainment, backmixing, turbulent eddies, and maldistribution, have been usually taken into account by means of mass transfer coefficients, instead of considering only diffusion (given by the Maxwell-Stefan equations).

These mass transfer coefficients are purely empirical parameters and are a function of the diffusion coefficients, among others parameters.

The linearised theory of Toor (1964) and of Stewart and Prober (1964) is a very interesting method for solving the multicomponent diffusion problems, but it is often limited to situations where the diffusion coefficient does not change significantly as the concentration changes during the diffusion process (Taylor and Krishna, 1993). The solution of the linearised model normally compares favourably with fluxes computed with the exact solutions, but composition profiles are often differing (Krishnamurthy and Taylor, 1982). For the exact solution, the approach of Krishna and Standart (1976) may be used in conjunction. The method considers that the matrix of mass transfer coefficients can be calculated from Eq. 3.13 in situations where the film thickness is not known. This method is recommended by Taylor and Krishna (1993) because it is much easier to solve.

$$[K]^V = [C^{ks}]^{-1} \quad (3.13)$$

$$C_{i,i}^{ks} = \frac{y_{i,NC}}{k_{i,NC}} + \sum_{l=1, l \neq i}^{NC} \frac{y_{i,l}}{k_{i,l}} \quad (3.14)$$

$$C_{i,j}^{ks} = -y_{i,j} \left(\frac{1}{k_{i,j}} - \frac{1}{k_{i,NC}} \right) \quad (3.15)$$

The binary k_{ij} can be calculated as a function of the Maxwell-Stefan diffusion coefficients from a correlation or from a physical model. The approach of Krishna and Standart is used and recommended by Taylor and Krishna (1993) only because it is ‘simple and easy to compute’.

3.3 Model Equations

In this section a general distillation model is presented. The model allows the generation of problem specific simulation schemes based on the use of a hybrid modelling approach, where equilibrium and non-equilibrium models can be combined.

The main difference between the equilibrium model and the non-equilibrium model is the way in which the conservation of mass and energy equations are used. For the non-equilibrium model, the balance equations are derived for each phase and linked through mass and energy balance equations at the phase interface. For the equilibrium model, the balance equations are derived around an equilibrium stage (distillation tray) assuming that the liquid and vapour leaving the stage are at thermodynamic equilibrium. Similarly, equilibrium relations are used to relate compositions leaving the stages for the equilibrium model, K-values are calculated at the composition of two well-defined streams and at the stage temperature (usually the same in both phases). For the non-equilibrium model the equilibrium relations are used to relate compositions at each side of the phase interface, so that K-values are evaluated at interface composition and temperature. In this general modelling framework the conservation of mass and energy equations are split for each phase, which makes it easier to consider equilibrium and non-equilibrium models for the same distillation column. For each distillation tray, the necessary equations for each phase and the corresponding defining functions (mass transfer flux for the liquid and vapour phase) is the same throughout the tray, or, it is the same only at the interface. A schematic representation of an stage in this general model is given in Fig. 3.1.

The general distillation model has been incorporated into two computer aided systems providing in both, steady state and dynamic simulation mode, as well as equilibrium and non-equilibrium-based models, of different complexity and

Image removed due to third party copyright

Figure 3.1: Schematic representation of an stage in the column (Krishnamurthy and Taylor, 1985)

form. Both, equilibrium and non-equilibrium models have reactive and non-reactive options and allow the generation of different model forms according to the specified simulation problem. This means that starting from the general distillation model, many of the models reported earlier (for example, Gani *et al.*, 1986, Krishnamurthy and Taylor, 1985, Rovaglio and Doherty, 1990 and Skogestad, 1997) are available for use with respect to a specified simulation problem.

The presence of the various model options in the general distillation model allows the gradual development of problem specific models such that acceptance of every additional assumption makes the models more simple while rejection of an assumption makes the models more complex. Simulation results from a simpler model serve as the initial estimate for a more complex model. The hybrid modelling approach also allows monitoring of important phenomena such as total mass and heat transfer rates, excess Gibbs free energy on each tray, and an efficiency-like parameter during any simulation. Also, during any simulation, a switch from one model form to another as well as from one simulation mode to another can be made.

3.4 Model Formulation

In order to present the proposed model, certain simplifying assumptions have to be made. The simplifications are needed in order to simplify the calculations and are not relevant for the studies made in this work and seem reasonable. Together with the assumptions, the specific column simulated will be assumed to have the conditions and configurations listed in the following:

- Liquid and vapour phases are perfectly mixed for the equilibrium model, while for the non-equilibrium model bulk phases (liquid and vapour) are well mixed.
- For the equilibrium model: liquid and vapour phases leave each stage at thermal equilibrium (same temperature and pressure). For the non-equilibrium model: liquid and vapour leave the stage at conditions determined by the mass and heat transfer rates.
- Murphree-like efficiencies will apply for each plate in the equilibrium model.

- The feed(s) can enter any tray as liquid, vapour or a combination of both. Liquid and vapour products can be withdrawn from any tray.
- No heat is lost from any tray, but heat can be added or taken out at any stage in the column.
- Pressures varies with time as well as from tray to tray.
- The reboiler heat input may be specified or can be used to control temperature or composition at the bottom of the column. The reflux (or distillate) flow may be specified or can be used to control temperature or composition at the top of the column.
- The column can handle sieve or bubble-cap trays. Plate hydraulics, entrainment, weeping and flooding can be determined.
- Physical properties can be determined by using different thermodynamic packages.
- Reaction takes place in the liquid phase for the equilibrium model, and for the non-equilibrium model the reaction occurs in the liquid bulk. Reactions are always considered as kinetically controlled.

The list of assumptions hold for the most complex model, however in order to obtain simplified models from the general model, other simplifications can be made, and they are stated in Section 3.6. The general hybrid model developed in this work is presented as general as possible. Different combination of equations lead to previous models presented in the literature. Different assumptions for solving a specific problem are readily available within the framework. The equations and correlations used here have been used before for equilibrium and non-equilibrium models. The advantage of the general model is that many different models can be generated and it is the choice of the user to select different correlations, mode of simulations, as well as equilibrium or non-equilibrium model equations.

3.5 Equations

The equations for the general distillation model (considering a tray column or a section of a packed column) are derived from:

- Material and energy balance equations (ordinary differential equations for dynamic models and algebraic equations for steady-state models).
- Equilibrium relations and physical properties.
- Kinetic models.
- Mass and energy transfer models.
- Hydraulics.
- Defined functions.

The above set of equations gives a system of differential and algebraic equations (DAEs) for a dynamic model or a system of algebraic equations (AEs) for a steady state model. Typically, the mass and energy balance equations are ordinary differential equations (ODEs) while all other equations are AEs.

The defined functions are the equations that compliment the model, for example the total mass and energy hold-ups equations and efficiencies.

The full set of equations (including differential and algebraic equations) is given below.

1 ODEs

– Mass balances:

* Vapour phase:

$$\begin{aligned} \frac{dm_{i,p}^V}{dt} = & F_{V,p}z_{i,p}^V + V_{p+1}y_{i,p+1} + EV_{p-1}y_{i,p-1} \\ & -(PV_p + V_p + EV_p)y_{i,p} + n_{i,p}^V \end{aligned} \quad (3.16)$$

$$i=1,\dots,NC, p=1,\dots,NP$$

* Liquid phase:

$$\begin{aligned} \frac{dm_{i,p}^L}{dt} = & F_{L,p}z_{i,p}^L + L_{p-1}x_{i,p-1} + EL_{p+1}x_{i,p+1} \\ & -(PL_p + L_p + EL_p)x_{i,p} + S_{i,p} - n_{i,p}^L \end{aligned} \quad (3.17)$$

$$i=1,\dots,NC, p=1,\dots,NP$$

where $m_{i,p}^L$, $m_{i,p}^V$ are the liquid and vapour hold-up of a component i on plate p in Kmol/h, respectively; V_p and L_p , are the vapour and liquid flow-rates leaving stage p respectively in Kmol/h; F is the feed flow (the subscript V or L denotes liquid or vapour feed) in Kmol/h; x, y, z are the mole fractions of component i in stage p for liquid, vapour and feed; EL and EV are liquid and vapour entrainments; PL , PV are liquid or vapour extracted or added to the column; $S_{i,p}$ is the reaction rate in the liquid bulk in Kmol/h; and, $n_{i,p}^V, n_{i,p}^L$ are the net loss or gain of species i due to interface transport, mass transfer rates (note that transport from the liquid to the vapour is assumed to be negative) given by

$$n_{i,p}^V = \int_{a_p} N_{i,p}^V da_p \quad (3.18)$$

$$n_{i,p}^L = \int_{a_p} N_{i,p}^L da_p \quad (3.19)$$

$N_{i,p}$ is the molar flux of species i at a particular point in the two-phase dispersion.

Since there is no mass accumulation at the phase interface, it follows that,

$$M_T = n_{i,p}^V - n_{i,p}^L = 0$$

– Energy balances:

* Vapour phase:

$$\begin{aligned} \frac{dH_{vp}^E}{dt} = & F_{V,p}Hvf_p + V_{p+1}Hv_{p+1} + EV_{p-1}Hv_{p-1} \\ & -(PV_p + V_p + EV_p)Hv_p + Q_p^V + \phi_p^V \end{aligned} \quad (3.20)$$

$$p=1,\dots, NP$$

* Liquid phase:

$$\begin{aligned}
\frac{dH_{lp}^E}{dt} = & F_{L,p}Hl f_p + L_{p-1}Hl_{p-1} + EL_{p+1}Hl_{p+1} \\
& -(PL_p + L_p + EL_p)Hl_p + Q_p^L + DS_p \\
& -\phi_p^L
\end{aligned} \tag{3.21}$$

$p=1,\dots, NP$

where H_v^E , H_l^E , are the enthalpic hold-ups for the vapour and liquid phase respectively; Hvf_p , Hlf , Hv_p , and Hl_p are the vapour-feed, liquid-feed, vapour and liquid enthalpy respectively; Q_p is any heat extracted or added to stage p ; and DS_p is the heat of reaction; ϕ_p^V and ϕ_p^L are the heat transfer rates.

Since there is no accumulation at the interface hence:

$$E_T = \phi_p^V - \phi_p^L = 0.$$

2 Algebraic Equations (AEs)

– Phase equilibrium:

* For the equilibrium model,

$$y_{i,p} = K_{i,p}x_{i,p} \tag{3.22}$$

$K_{i,p}$, the equilibrium constant, is expressed as a function of compositions, temperature and pressure.

$$\sum_{i=1}^{NC} y_{i,p} - 1 = 0 \tag{3.23}$$

* Interface model for the non-equilibrium model,
(the non-equilibrium model assumes that at interface physical equilibrium is attained)

$$y_{i,p}^I = K_{i,p}x_{i,p}^I \tag{3.24}$$

$$\sum_{i=1}^{NC} y_{i,p}^I - 1 = \sum_{i=1}^{NC} x_{i,p}^I - 1 = 0 \tag{3.25}$$

– Physical properties:

- * K-Values: Vapour-liquid equilibrium constant of component i on tray p is given by,

$$K_{i,p} = \frac{\gamma_{i,p} P_{i,p}^{sat}(T)}{\phi_{i,p}^V P} \quad (3.26)$$

$$\text{or } K_{i,p} = \frac{\phi_{i,p}^L}{\phi_{i,p}^V} \quad (3.27)$$

$$i=1,\dots,NC, p=1,\dots,NP$$

Equation 3.26 represents the $\gamma-\phi$ approach, where an activity coefficient model is used to calculate the liquid phase activities while an equation of state is used to calculate the vapour phase fugacities. If an equation of state (EOS) is chosen to calculate the fugacities for both phases ($\phi-\phi$ approach), the vapour-liquid equilibrium constant is given by Eq. 3.27.

Different types of thermodynamic models can be used, according to the mixture of the problem studied. For the systems studied in this thesis, several models have been used and are listed below.

- For systems where the $\gamma-\phi$ approach was needed:
The following models for activity coefficients were used,
 - UNIFAC-vle
 - UNIQUAC-modified (3 parameters)
 - Margules modified equation (Suzuki *et al.*, 1970).

The vapour phase was considered as ideal vapour, so that, $\phi^V = 1$.

- For systems where the $\phi-\phi$ approach was needed:
Two different equation of state were used:
 - Soave-Redlich-Kwong equation of state; and,
 - Peng-Robinson equation of state

The general model of this work is not limited to the thermodynamic models listed above. Table 3.1 give a more complete

list of models available within the framework of ICAS (Gani *et al.*, 1997).

Activity Coefficients Models	Equations of State
UNIFAC-vle; lle	Ideal Gas
UNIQUAC-original	SRK-eos
UNIQUAC-modified	PR-eos
NRTL	ALS-eos
Wilson	SWL-eos
Margules equation	Virial
Van Laar	

Table 3.1: Thermodynamic models

* Enthalpies:

Enthalpies are calculated as a function of temperature, composition and pressure.

$$Hv_p = f(y_{i,p}, P_p, T_p) \quad (3.28)$$

$$Hl_p = f(x_{i,p}, P_p, T_p) \quad (3.29)$$

See Appendix A for details.

* Vapour pressure (Antoine Equation):

$$P_{i,p}^{sat} = \exp[A_i - \frac{B_i}{C_i + T_p}] \quad (3.30)$$

* Density:

Densities for the liquid phase are calculated through a suitable correlation such as DIPPR correlation (Daubert and Danner, 1986) and for the vapour phase are calculated by the Ideal Gas Law or an equation of state (EOS).

$$\bar{\rho}_{L_p} = f(x_{i,p}, T_p, P_p) \quad (3.31)$$

$$\bar{\rho}_{V_p} = f(y_{i,p}, T_p, P_p) \quad (3.32)$$

See Appendix A for details.

* Molecular weight:

$$\overline{M}_{Lp} = \sum_{i=1}^{NC} M_{L,i,p} x_{i,p} \quad (3.33)$$

$$\overline{M}_{Vp} = \sum_{i=1}^{NC} M_{V,i,p} y_{i,p} \quad (3.34)$$

* Viscosity:

Viscosity for liquid and vapour phase are calculated through a suitable correlation such as DIPPR (Daubert and Danner, 1986)

$$\mu_{Lp} = f(x_{i,p}, T_p) \quad (3.35)$$

$$\mu_{Vp} = f(y_{i,p}, T_p) \quad (3.36)$$

See Appendix A for details.

* Surface tension:

Surface tension is calculated through a suitable correlation such as DIPPR (Daubert and Danner, 1986)

$$\overline{\sigma}_p = f(x_{i,p}) \quad (3.37)$$

See Appendix A for details.

* Thermal conductivity:

Thermal conductivity for liquid and vapour phase are calculated through a suitable correlation such as DIPPR (Daubert and Danner, 1986)

$$\overline{\lambda}_{Lp} = f(x_{i,p}, T_p) \quad (3.38)$$

$$\overline{\lambda}_{Vp} = f(y_{i,p}, T_p) \quad (3.39)$$

See Appendix A for details.

* Binary diffusion coefficients:

‘The coefficient of interdiffusion of two liquids must be considered as depending on all the physical properties of the mixture

according to laws which must be ascertained only by experiment' -J.C. Maxwell writing in the Encyclopedia Brittanica, 1952.

$$D_{ij}^V = f(T, \overline{M}, V) \quad (3.40)$$

$$D_{ij}^L = f(x_i, T, \overline{M}, V) \quad (3.41)$$

See Appendix A for details.

– Kinetic models:

Reaction kinetic is assumed to follow, for example, an 'Arrhenius-type' equation in the form,

$$r_{i,p} = k_+(T) \prod^{Nr} A^\alpha - k_-(T) \prod^{Np} A^\beta \quad (3.42)$$

$$\text{with} \quad k_+(k_-) = k_o \exp\left(\frac{-Ea}{RT}\right) \quad (3.43)$$

$$\text{or} \quad k_- = \frac{1}{K_{eq}} \quad (3.44)$$

$$i=1,\dots,NC, p=1,\dots,NP$$

$$\begin{aligned} \text{where } K_{eq} = f(T) = K(T_o) \exp\left(A_1\left(\frac{1}{T} - \frac{1}{T_o}\right) + A_2 \ln\left(\frac{T}{T_o}\right) \right. \\ \left. + A_3(T - T_o) + A_4(T^2 - T_o^2) + A_5(T^3 - T_o^3) \right. \\ \left. + A_6(T^4 - T_o^4)\right) \end{aligned} \quad (3.45)$$

where A can be compositions, concentrations or activity coefficients, Nr represent the reactants, Np represents the products; NR is the number of reactions occurring in the system.

Total reaction rate (sum over all reactions occurring in the stage) for component i in the tray p is given by $S_{i,p}^L$ (term added to the component mass balance in each tray):

$$S_{i,p}^L = \sum_{k=1}^{NR} (r_{k,p} \nu_{i,p}) \quad (3.46)$$

$$i=1,\dots,NC, p=1,\dots,NP$$

In this work, we have assumed the reaction to occur in the bulk liquid only and not in the mass transfer film, although this assumption limits the application range for the general model. The thickness of the liquid film (as well as the vapour film) is very difficult to predict (or estimate) and it is normally considered to be relatively small, also with respect to the vapour film. So that, the interactions between diffusion and chemical reaction in the liquid film have not been taken into account due to the ‘predicted’ small thickness of the liquid film. Moreover, in a recent paper, Higler *et al.*(1997) pointed out that the reaction volume for the mass transfer film is negligible under certain conditions, with respect to the bulk liquid volume. The main limitation of the model under this assumption will be for fast reactions.

– Rate equations

* Mass Transfer

One of the first assumptions here is that the bulk phases are completely mixed. The model for the mass transfer has been based on the model of Krishnamurthy and Taylor (1985) for steady state simulation of distillation columns.

The molar fluxes (mass transfer) in each phase are given by,

$$N_{i,p}^v = J_{i,p}^v + N_T^v y_{i,p} \quad (3.47)$$

$$N_{i,p}^l = J_{i,p}^l + N_T^l x_{i,p} \quad (3.48)$$

$$i=1,\dots,NC-1, \quad p=1,\dots,NP$$

The relationship between the molar fluxes and the mass transfer rates is given by Eq. 3.18 for the vapour phase and Eq. 3.19 for the liquid phase.

Since many multicomponent distillation systems and specially reactive systems are characterised by non-ideal behaviour of the mixtures, the influence of the non-idealities on the mass transfer fluxes should be included when defining the fluxes. The good representation of the mass transfer fluxes can be compared with a good representation of the phase equilibria when equilibrium models are used. Hence, the diffusion fluxes,

J , in our model are given by,

$$J_{i,p}^v = \bar{\rho}_V a [K^v] (y_{i,p} - y_{i,p}^I) \quad (3.49)$$

$$J_{i,p}^l = \bar{\rho}_L a [\Gamma^l] [K^l] (x_{i,p}^I - x_{i,p}) \quad (3.50)$$

$$i=1,\dots,NC-1, p=1,\dots,NP$$

The mass transfer rates ($n_{i,p}^v, n_{i,p}^l$) are obtained by combining Eqs. 3.47-3.48 and 3.49-3.50 and multiplying by the interfacial area available for mass transfer (Krishnamurthy and Taylor, 1985).

$$n_{i,p}^v = \bar{\rho}_V a [K^v] (y_{i,p} - y_{i,p}^I) + n_T^v y_{i,p} \quad (3.51)$$

$$n_{i,p}^l = \bar{\rho}_L a [\Gamma^l] [K^l] (x_{i,p}^I - x_{i,p}) + n_T^l x_{i,p} \quad (3.52)$$

$$i=1,\dots,NC-1, p=1,\dots,NP$$

High flux corrections have not been used because they are unity when $N_t = 0$ (normally the case for distillation units). It can be seen from Eqs. 3.51 and 3.52 that the mass transfer rates are functions of multicomponent mass transfer coefficients ($[K^v], [K^l]$), interfacial area (a), density of the mixture ($\bar{\rho}$), compositions in the bulk and at the interface as well as the total mass transfer rate of the components (n_T^v, n_T^l), present in the mixture.

A further assumption, which is optional depending on the nature of the problem that is going to be solved, is to assume equimolar counter transfer, $n_T^v = 0$ and $n_T^l = 0$. This is valid in general for distillation and for reactive distillation when there is no changes in the total number of moles during diffusion with chemical reaction. Following this, Eqs. 3.51 and 3.52 can be reduced to:

$$n_{i,p}^v = \bar{\rho}_V a [K^v] (y_{i,p} - y_{i,p}^I) \quad (3.53)$$

$$n_{i,p}^l = \bar{\rho}_L a [\Gamma^l] [K^l] (x_{i,p}^I - x_{i,p}) \quad (3.54)$$

$$i=1,\dots,NC-1, p=1,\dots,NP$$

which makes another possible simplified model from the general hybrid model, and is the usual approach when dealing

with distillation. This assumption is equivalent to consider that the heat of vaporisation of the components are equal to each other.

When the assumption is not taken into account, an iterative method is needed to calculate n_T and n_i^l, n_i^v . Repeated substitution of the fluxes starting from an estimate (for example, $n_t = 0$) will take few iterations to converge. If n_T is assumed equal to zero, then the fluxes can be calculated without any iterations.

The interfacial area is calculated through:

- for tray columns the net interfacial area a is (taken from Taylor and Krishna, 1993):

$$a = a' h_f A_b \quad (3.55)$$

where a' is the interfacial area per unit volume of froth; h_f is the froth height; and, A_b is the bubbling area.

The interfacial area per unit volume a' is calculated through the following expression: (Bravo and Fair's correlation)

$$a' = 19.78 A_p (Re^v C a^l)^{0.392} \frac{\bar{\sigma}^{0.5}}{H^{0.4}} \quad (3.56)$$

where, Re^v is the Reynolds number of the vapour phase, and $C a^l$ is the liquid capillary number given by,

$$Re^v = \frac{\bar{\rho}_v u^v}{\mu^v A_p} \quad (3.57)$$

$$C a^l = \frac{u^l \mu^l}{\bar{\sigma}} \quad (3.58)$$

The matrix of multicomponent mass transfer coefficients for mixtures, ($[K^v], [K^l]$), are calculated from binary mass transfer coefficients, following Krishna and Standart (1976) method. This method is applicable when the film thickness is not known, and is the reason why the method is used in this approach. The film thickness is (unfortunately) almost never known.

- for the vapour phase (Krishna and Standart, 1976):

$$[K^v] = [R^v]^{-1} \text{ (dimension } (NC-1) \times (NC-1))$$

with $R_{i,i}^v$ and $R_{i,j}^v$ given by the following expressions:

$$R_{i,i}^v = \frac{y_{i,NC}}{k_{i,NC}} + \sum_{k=1, k \neq i}^{NC} \frac{y_{i,k}}{k_{i,k}} \quad (3.59)$$

$$R_{i,j}^v = -y_{i,j} \left(\frac{1}{k_{i,j}} - \frac{1}{k_{i,NC}} \right) \quad (3.60)$$

$$i=1, \dots, NC-1, \quad p=1, \dots, NP$$

- for the liquid phase (Krishna and Standart, 1976):

$$[K^l] = [R^l]^{-1} \text{ (dimension } (NC-1) \times (NC-1))$$

with $R_{i,i}^l$ and $R_{i,j}^l$ given by the following expressions:

$$R_{i,i}^l = \frac{x_{i,NC}}{k_{i,NC}} + \sum_{k=1, k \neq i}^{NC} \frac{x_{i,k}}{k_{i,k}} \quad (3.61)$$

$$R_{i,j}^l = -x_{i,j} \left(\frac{1}{k_{i,j}} - \frac{1}{k_{i,NC}} \right) \quad (3.62)$$

$$i=1, \dots, NC-1, \quad p=1, \dots, NP$$

The binary mass transfer coefficients $k_{i,k}$ are obtained from a suitable correlation, such as:

- the AIChE Method (AIChE, 1958)
- for the vapour phase,

$$k^v = \frac{(0.776 + 4.57h_w - 0.238F_s + 104.8 \frac{Q_l}{W})}{Sc^{0.5}at_g} \quad (3.63)$$

Eq. 3.63 is derived for the case where mass transfer resistance exists only in the gas phase, and ideal gas law is also assumed to apply. h_w is the exit weir length (m), F_s is the superficial factor (defined by, $F_s = u_s \bar{\rho}_V^{0.5}$), Q_l is the volumetric liquid flow-rate (m^3/sec), W is the

weir length (m), Sc is the Schmidt number for the vapour phase (defined by, $Sc = \frac{\mu^v}{\rho_v D^v}$), a is the interfacial area and t_g is the gas contact time.

- for the liquid phase,

$$k^l = \frac{(19700 D^l)^{0.5} (0.4 F_s + 0.17) t_l}{a t_l} \quad (3.64)$$

where D^l is the Fick liquid diffusivity of the system (m^2/sec), and t_l is the liquid-phase residence time (defined by, $t_l = \frac{Z}{u+l}$).

The AIChE correlations are applicable for bubble cap trays or sieve trays. It is important to note that these binary mass transfer coefficients are functions of tray design and layout (or packing type and size, in a packed column). This means that the column design must be known in advance in order to solve the equations for the rate-based model. However, these parameters can also be determined by carrying out design calculations simultaneously with the solution of the model equations (Taylor *et al.*, 1992).

The correlation for calculating the binary mass transfer fluxes is derived under the assumption of vapour-phase resistance only (as stated earlier), so that this correlations should be used with models which considers only resistance in the vapour phase, as a matter of consistency. Furthermore, the correlation is derived from experiments in steady-state processes. The validity of them for dynamic operations have not been reported in the literature, with exception of the work of Kreul *et al.* (1998) where this correlation has been tested for dynamic packed columns given acceptable results.

In distillation the transfer resistance is almost entirely located on the vapour phase, according to experience and experimental work presented in the literature (Vogelphol, 1979; Kayhand *et al.*, 1977, Dribika and Sandall, 1979). However, there is no evidence that this can hold for reactive distillation. Furthermore, some experimental work

shows that the liquid resistance in a distillation column can be as much as 20% of the entire resistance (Chen and Chuang, 1995).

New correlations are needed when both phases resistances are considered. It is believed that new correlations are also needed for dynamic system and specially for reactive systems. Nevertheless, in this work mass transfer correlations as described above are used for dynamic models and for reactive systems, in an attempt to verify if the correlations lead to acceptable results. Pelkonen *et al.* (1997) proved that steady-state mass transfer correlations can be applied for dynamic simulation of multicomponent distillation.

If the stages of the model are considered very close to each other then we could use the model to simulate packed columns as well. The same equations are used with exception of the binary mass transfer coefficients and interfacial area.

So that, for packed columns the interfacial area is calculated from,

for packed columns the net interfacial area a is (taken from Taylor and Krishna, 1993):

$$a = a' h A_c \quad (3.65)$$

where a' is the interfacial area per unit volume; h is the height of the packing section; and, A_c is the cross-sectional area of the column.

The binary mass transfer coefficients can be calculated through different expressions, for example,

Onda's correlation (Onda *et al.*, 1968) for random packing in packed columns,

- for the vapour phase:

The binary $k_{i,j}$ are calculated from the Sherwood number as:

$$Sh = \frac{k_{i,j}}{D_{i,j}A_p} = A_o Re^v 0.7 Sc^v 0.33 (A_p D_p)^{-2} \quad (3.66)$$

where D_p is the nominal packing size and A_p is the specific surface area of the packing (m^2/m^3). A_o is a constant that takes value of 2 if the nominal size of packing is less than $0.012m$ or 5.23 if D_p is higher or equal to $0.012m$. Re^v is the Reynolds number of the vapour phase (Eq. 3.57). The vapour phase Schmidt number is,

$$Sc^v = \frac{\mu^v}{\bar{\rho}_v D^v} \quad (3.67)$$

- for the liquid phase:

The binary liquid phase mass transfer coefficient is obtained from the following equation,

$$k^l (\bar{\rho}_L / \mu^l g)^{0.333} = 0.0051 (Re'^l)^{0.667} Sc'^l - 0.5 (a_p d_p)^{0.4} \quad (3.68)$$

where Sc'^l is the Schmidt number for the liquid phase

$$Sc'^l = \mu^l / (\bar{\rho}_L D^l) \quad (3.69)$$

and Re'^l is the Reynolds number based on the interfacial area

$$Re'^l = \bar{\rho}_L u^l / (\mu^l a') \quad (3.70)$$

Using this correlation with the expression from Bravo and Fair for the interfacial area will lead to a different value of k^l than if the Onda's correlation for the interfacial area is used. However, there are no explanations about which one of the values is the correct one to the best of our knowledge. Many works presented in the literature are taken this 'combined' equations. Accuracy or consistency is not reported (Taylor and Krishna, 1993).

Each stage model represents a section of packing and the height of this packing section should be specified. Even small

section heights means more stages, therefore, more calculations are as well needed. This is directly reflected in the increasing of computational time. As more stages are then included, the model accuracy increases, but how many stages should be used still remains vague. Experience plays an important role when determining the ‘number of stages’ representing a height of packing.

* Heat transfer equations:

The energy flux for each phase is defined by,

$$\psi_p^v = \alpha_p^v(T_p^v - T_p^I) + \sum_{i=1}^{NC} n_{i,p}^v \bar{H}_{i,p}^v \quad (3.71)$$

$$p=1, \dots, NP$$

$$\psi_p^l = \alpha_p^l(T_p^I - T_p^l) + \sum_{i=1}^{NC} n_{i,p}^l \bar{H}_{i,p}^l \quad (3.72)$$

$$p=1, \dots, NP$$

α are the heat transfer coefficients, and \bar{H}^v , \bar{H}^l are the partial molar enthalpy of component i in stage p , for the vapour and liquid phase respectively.

Heat transfer coefficients are calculated following the well-known Chilton-Colburn analogy. The energy transfer rates for the vapour and liquid phases are obtained after multiplying Eqs. 3.71 and 3.72 by the interfacial area and adding the high flux correction factor $\frac{\epsilon}{\exp \epsilon^v - 1}$, as follows,

$$\phi_p^v = \alpha_p^v a \frac{\epsilon}{\exp \epsilon^v - 1} (T_p^v - T_p^I) + \sum_{i=1}^{NC} n_{i,p}^v \bar{H}_{i,p}^v \quad (3.73)$$

$$p=1, \dots, NP$$

$$\phi_p^l = \alpha_p^l a \frac{\epsilon}{\exp \epsilon^v - 1} (T_p^I - T_p^l) + \sum_{i=1}^{NC} n_{i,p}^l \bar{H}_{i,p}^l \quad (3.74)$$

$$p=1, \dots, NP$$

A simplification of these equations (and the model in general) can be achieved by considering that there is no differences in temperature between the phases. So that, Eq. 3.73 and 3.74 can be reduced to:

$$\phi_p^v = \sum_{i=1}^{NC} n_{i,p}^v \overline{H}_{i,p}^v \quad (3.75)$$

$$\phi_p^l = \sum_{i=1}^{NC} n_{i,p}^l \overline{H}_{i,p}^l \quad (3.76)$$

These are the equations (3.75-3.76) that are used for the simulations in this work.

– Hydraulic equations

The pressure drop between trays is calculated from the pressures of the adjacent trays:

$$\Delta P_p = P_{p-1} - P_p \quad (3.77)$$

Flow-rates of liquid, vapour and entrainments rates (liquid and vapour) are all functions of tray geometry, hold-up and pressure drop between trays (Gani *et al.*, 1986)

$$V_p = f(\Delta P, \text{holdup}, \text{geometry of the tray}) \quad (3.78)$$

$$L_p = f(\text{holdup}, \text{geometry of the tray}) \quad (3.79)$$

$$EL_p = f(\Delta P, \text{holdup}, \text{geometry of the tray}) \quad (3.80)$$

$$EV_p = f(\Delta P, \text{holdup}, \text{geometry of the tray}) \quad (3.81)$$

– Defined functions:

Hold-ups:

$$M_p^v = \sum_{i=1}^{NC} m_{i,p}^v \quad (3.82)$$

$$M_p^l = \sum_{i=1}^{NC} m_{i,p}^l \quad (3.83)$$

$$p=1,\dots, NP$$

$$Hm_p^v = \frac{H_{vp}^E}{\sum_{i=1}^{NC} m_{i,p}^v} \quad (3.84)$$

$$Hm_p^l = \frac{H_{lp}^E}{\sum_{i=1}^{NC} m_{i,p}^l} \quad (3.85)$$

$$p=1,\dots, NP$$

Efficiency parameter:

$$E_{i,p}^M = \frac{y_{i,p+1} - y_{i,p}}{y_{i,p+1} - y_{i,p}^*} \quad (3.86)$$

$$i=1,\dots, NC-1, \quad p=1,\dots, NP$$

3.6 Generation of Models

Hybrid models indicate the use of more than one type of model for the simulation/design of a single distillation column. For example, hybrid models may represent a column having trays that are at equilibrium and trays that are not at equilibrium or a column with reactive and non-reactive trays, or a column with different tray designs.

Also, for a specific simulation of distillation operation, use of different model forms may require the use of mixed simulation modes (steady state and/or dynamic simulation modes). Hybrid models are useful for synthesis/design of separation processes because they indicate how a specified separation can be achieved.

Note that the same hybrid model is applicable even though different distillation operations may be necessary to achieve the specified separation. Use of the hybrid modelling approach may result in improved computational efficiency compared to the single model because it can provide better initialisation and flexibility in terms of modelling options. For example, since the rate-based models usually have more equations than their corresponding equilibrium-based form, if any tray reaches equilibrium, the equilibrium-based form for the remainder of the dynamic simulation run may model it. Also, most reactive distillation columns usually have non-reactive trays. In

such cases, simulations may be started with a totally reactive or non-reactive column and gradually changed to the required hybrid form. In addition, the reactive and non-reactive trays may have rate-based or equilibrium-based models.

The non-equilibrium model is obtained by including mass and energy transfer models and specifying that equilibrium is attained only at the interface of the liquid and vapour phases. The rate-based model consists of Eqs. 3.16-3.17, 3.20-3.21, 3.24-3.25, 3.26 or 3.27, 3.51-3.52, 3.73-3.81, plus defined relations and a selected set of equations for properties. If reaction is to be considered, Eq. 3.46 is added to the system. Models of various degrees of complexity are obtained by using different forms of the algebraic equations. For example, simple expressions for equations 3.26(or 3.27) or 3.51-3.52 or 3.73-3.74 will lead to simpler versions of the rate based model. The number of variables and equations for a single tray (rate-based model) are given in Tables 3.2 and 3.3 respectively. Note that the procedure equations (for example, representation of property models as library routines where the calculated property values are obtained for specified values of temperature, pressure and/or composition) and variables are not listed in these tables. In principle, they can always be calculated with known values of the intensive variables (temperature, pressure and phase compositions). For all the types of non-equilibrium models, dynamic models are derived by using the ODE form of the mass and energy balance equations while steady state models are derived by setting the left hand side (LHSs) of the same set of mass and energy balance equations to zero. Note that all non-equilibrium dynamic models belonging to the general distillation model are represented by a set of differential and algebraic equations (DAEs) of index 1.

From the general non-equilibrium model, various model forms can be generated by making simplifying assumptions. For example, if there are no reactions, $((NC + 1)NR)$ variables and reaction terms drop out. Similarly, if the pressure profile is specified, one variable (tray pressure) and one equation (tray hydraulics) drop out. Three examples of different forms of rate-based models (reactive and non-reactive) are listed in Table 3.4. Similar non-equilibrium models have been reported earlier by Kooijman and Taylor (dynamic model, 1995) and Krishnamurty and Taylor (steady-state model, 1985) for example.

The equilibrium-based model is a special case of the rate-based model, and

Variable	Number
Vapour and Liquid flow-rate	2
Vapour and Liquid compositions	2NC
Vapour and Liquid temperature	2
Vapour and Liquid interface compositions	2NC
Interface temperature	1
Mass transfer rates	2NC
Energy transfer rates	2
Stage pressure	1
Rate of reaction	NC*NR
Heat of Reaction	NR
Total	6NC+8+(NC+1)*NR

Table 3.2: List of variables per stage in the non-equilibrium model

therefore, is a simplification of the rate-based model. Instead of considering equilibrium only at the interface, it is assumed that equilibrium is attained at all points where the vapour and liquid come in contact. Therefore, it is assumed equilibrium at all points in the stage and in the entire column.

This means that Eqs. 3.16-3.17 Eqs. 3.20-3.21 are combined as Eqs. 3.88 and 3.89 respectively.

$$\begin{aligned}
 \frac{dm_{i,p}^T}{dt} = & F_p z_{i,p} + V_{p+1} y_{i,p+1} + L_{p-1} x_{i,p-1} + EV_{p-1} y_{i,p-1} + EL_{p+1} x_{i,p+1} \\
 & - (PV_p + V_p + EV_p) y_{i,p} - (PL_p + L_p + EL_p) x_{i,p} + S_{i,p} \quad (3.87) \\
 & i = 1, \dots, NC, p = 1, \dots, NP
 \end{aligned}$$

where $m_{i,p}^T = m_{i,p}^l + m_{i,p}^v$.

If the vapour hold-up is assumed negligible, the vapour term drops out from the $m_{i,p}^T$, thereby, generating a simpler dynamic model (as for example, the one presented by Gani *et al.*(1986)). The condition for equilibrium at the interface (Eq. 3.24- 3.25) and the mass and heat transfer related equations (Eqs. 3.51-3.52, 3.73-3.74) are not needed, but the equilibrium condition (Eqs. 3.22 and 3.23) are added.

Again, the energy balance equation for an equilibrium-based model is ob-

	Equations	Number
M	Material balances for liquid and vapour	2NC+1
M	Material balances at the interface	NC
E	Heat of reaction	NR
E	Energy balance equations	3
R	Rate of reaction	NC*NR
R	Transfer rate equations	2NC-2
R	Energy transfer rate equations	2
S	Summation equations	2
H	Hydraulic equations	2
Q	Interface equilibrium calculations	NC
	Total	6NC+8+(NC+1)*NR

Table 3.3: List of equations per stage in the non-equilibrium model

tained as a special case of the rate-based model (employing the same assumptions as for mass balance equations).

$$\begin{aligned}
\frac{dH_{Tp}^E}{dt} = & F_p H f_p + V_{p+1} H v_{p+1} + L_{p-1} H l_{p-1} + E V_{p-1} H v_{p-1} + E L_{p+1} H l_{p+1} \\
& - (P V_p + V_p + E V_p) H v_p - (P L_p + L_p + E L_p) H l_p \\
& + Q_p + D S_p \\
& i = 1, \dots, NC, p = 1, \dots, NP
\end{aligned} \tag{3.88}$$

where $H_{Tp}^E = H_{lp}^E + H_{vp}^E$.

If the energy vapour hold-up is assumed negligible, Eq. 3.89 is further simplified as the energy vapour term drops out. Hence, $H_{Tp}^E = H_{lp}^E$.

If reactive distillation is considered, Eq. 3.46 is added to the equation set.

This form of the equilibrium-based model, without the reaction term has been earlier reported by Sørensen (1994) and Skogestad (1997), for example. The dynamic version of the model is again derived by using the ODE form of the mass and energy balance equations while steady state version of the model is derived by setting the LHSs of the same set of mass and energy balance equations to zero. The number of variables and equations for the

Model	Constant pressure	Mass resistance in one phase	Equal temperature in both phases	Number of equations to solve per stage
NEQ-1	yes	no	no	6NC+7 for non-reactive 6NC+7+(NC+1)*NR for reactive
NEQ-2	no	yes	yes	4NC+5 for non-reactive 4NC+5+(NC+1)*NR for reactive
NEQ-3	yes	yes	yes	4NC+4 for non-reactive 4NC+4+(NC+1)*NR for reactive

Table 3.4: Various forms of non-equilibrium models

general equilibrium-based model are listed in Tables 3.5 and 3.6 respectively. Like the non-equilibrium dynamic models, the equilibrium dynamic models are also represented by a set of DAEs of index 1.

Variable	Number
Vapour and Liquid flow-rate	2
Vapour and Liquid compositions	2NC
Temperature	1
Stage pressure	1
Rate of reaction	NC*NR
Heat of Reaction	NR
Total	2NC+4+(NC+1)*NR

Table 3.5: List of variables per stage in the equilibrium model

Various forms of the equilibrium-based models can be generated from the general form of the equilibrium model. For example, Eqs. 3.88 and 3.89 can be simplified by assuming that the molar vapour hold-up is negligible compared to the molar liquid hold-up. Using the general form of the physical equilibrium condition, the case of two liquid phases in equilibrium with one vapour phase is obtained (Bøssen *et al.*(1993), Rovaglio and Doherty (1990)). Further simplification can be made by assuming that the rate of change of

	Equations	Number
M	Material balances	NC+1
E	Heat of reaction	NR
E	Energy balance equation	1
R	Reaction Rate	NC*NR
S	Summation equations	1
H	Hydraulic equations	1
Q	Equilibrium calculations	NC
	Total	2NC+4+(NC+1)*NR

Table 3.6: List of equations per stage in the equilibrium model

the energy accumulation term (LHS of Eq. 3.89) is negligible. This assumption will convert Eq. 3.89 to an algebraic equation. Also, this assumption usually means that the tray pressure is no longer an independent variable. Therefore, the tray pressure is removed from the list of variables and the hydraulic equations are reduced by one (usually, the relationship of pressure drop, liquid hold-up on tray and vapour flow-rate is not used). Each version of these models can be further simplified in terms of models used for tray hydraulics and physical properties. Table 3.7 lists some of the models that can be generated from the general equilibrium-based model. Note that these generated models are not new and have been reported previously (for example, by Gani *et al.*(1986), Gokhale *et al.*(1995), Rovaglio and Doherty, (1990)). Note also that the number of equations in models EQ-2, EQ-3 and EQ-4 do not change but the distribution between ODEs and AEs is different for each model. EQ-4 has the largest number of ODEs while EQ-2 has the lowest number of ODEs (not counting EQ-1).

Hybrid models are useful for different distillation operations where it may be necessary to achieve a specified separation, and it will result in improved computational efficiency compared to the single model because it can provide better initialisation and flexibility. The decision of using a hybrid model can be made *a priori*, for example for the case of reactive distillation with reactive and non-reactive trays, or it can be made *a posteriori*, for example, switching between non-equilibrium and equilibrium models (the simulation should have started to determine which trays have reached equilibrium).

The general distillation model allows the monitoring of a selected set of variables (or phenomena) as a function of time and/or tray. For example, the

Model	Assumption	Number of equations to solve per stage
EQ-1	Rate of change of energy neglected. Constant molar overflow.	NC+1 for non-reactive NC+1+(NC+1)*NR for reactive
EQ-2	Rate of change of energy neglected	2NC+3 for non-reactive 2NC+3+(NC+1)*NR for reactive
EQ-3	Liquid hold-up and energy hold-up considered	2NC+3 for non-reactive 2NC+3+(NC+1)*NR for reactive
EQ-4	Liquid and vapour hold-up considered	2NC+3 for non-reactive 2NC+3+(NC+1)*NR for reactive

Table 3.7: Various forms of equilibrium models

general model computes the values of $\Delta n_l = n_{t+1}^l - n_t^l$, $\Delta n_v = n_{t+1}^v - n_t^v$, excess Gibbs free energy, G^E and an efficiency-like parameter, E^M as a function of time and tray.

For the rate-based model, the excess Gibbs energy for the liquid phase can be estimated without significant additional computation because the liquid phase activities are already known (see Eq. 3.89).

$$\frac{G_p^E}{RT_p} = \sum_i x_{i,p} \ln \gamma_{i,p} \quad (3.89)$$

$$i=1,\dots,NC, p=1,\dots,NP$$

Note that these estimated values of tray excess Gibbs energy change with time for the dynamic model and that the plots of excess Gibbs energy as a function of time are not necessarily the same as plots of excess Gibbs energy as a function of composition. Therefore, it is possible to monitor the transient path of excess Gibbs energy for all trays. Those that approach an

asymptotic minimum value may be considered to be at a pseudo-equilibrium state.

For the non-equilibrium model, the difference of the values of n^l , n^v (represented by Δn_v and Δn_l) can also be monitored as a function of time and tray without significant additional computation time. Generally, the difference of the values of n^l , n^v in a time step before and the present time should be expected to decrease (approaching zero) as the excess Gibbs energy approaches a minimum.

The values of Δn_l , Δn_v and G^E can then be used as a criterion by which the rate-based model may be switched to its corresponding equilibrium-based form. At equilibrium, the Gibbs energy must be at a minimum. Also, at equilibrium, Δn_l and Δn_v must be approximately zero.

Efficiencies are also a way to look for equilibrium. In this work, two different type of efficiency have been investigated.

3.6.1 Tray Efficiency

Two types of efficiencies have been used in this work. ‘Standard’ Murphree efficiency and Murphree vapour phase point efficiency. Both types are described below.

- ‘Standard’ Murphree efficiency

Taken the Murphree tray efficiency (King, 1980) as a basic, an efficiency-like parameter that is a function of only the simulated bulk and interface compositions from the non-equilibrium model, is proposed,

$$E_{i,p}^M = \frac{y_{i,p+1} - y_{i,p}}{y_{i,p+1} - y_{i,p}^*} \quad (3.90)$$

$$i=1,\dots,NC-1, p=1,\dots,NP$$

In the above equation, y_{ki} represents the bulk vapour composition for component i in tray k while y_{ki}^* represents the equilibrium composition

for component i in tray k (at the interface). With the calculated compositions available from the hybrid model, the component efficiencies for all components on each tray can be monitored as a function of time. Note that the use of measured bulk compositions in Eq. 3.90 instead of the simulated bulk compositions may also give different values (see Chapter 5).

- Murphree vapour phase point efficiency

Point efficiencies for multicomponent systems are given by (Toor, 1964),

$$(\Delta y) = [Q](\Delta y^E) \quad (3.91)$$

where $(\Delta y) = (y_p^* - y_p)$, $(\Delta y^E) = (y_p^* - y_{p+1})$, and, $[Q] = \exp[-[N_{OV}]]$, with $[N_{OV}]$ given by

$$\frac{1}{[N_{OV}]} = \frac{1}{[N_V]} + \frac{M(V/L)}{[N_L]} \quad (3.92)$$

$[N_V], [N_L]$ are the numbers of transfer units for the vapour and liquid phases respectively. The elements of the matrix can be calculated by,

$$N_{Vi} = k^v a h_f / u_s \quad (3.93)$$

$$N_{Li} = k^l a h_f Z / (Q_l / W) \quad (3.94)$$

where a is the interfacial area per unit volume, h_f is the froth height, Z is the liquid flow path length, W is the weir length, Q_l is the volumetric liquid flow-rate and u_s is the superficial vapour velocity (based on the bubbling area of the tray). Other models of flow and mass transfer on a distillation tray may lead to a different form of calculating $[Q]$, but the form of Eq. 3.91 can be retained.

The relationship between the elements of $[Q]$ and the component Murphree efficiencies is as follows for a quaternary system:

There are only three independent efficiencies given by

$$E_1^{OV} = 1 - Q_{11} - Q_{12} \frac{\Delta y_{2E}}{\Delta y_{1E}} - Q_{13} \frac{\Delta y_{3E}}{\Delta y_{1E}} \quad (3.95)$$

$$E_2^{OV} = 1 - Q_{22} - Q_{21} \frac{\Delta y_{1E}}{\Delta y_{2E}} - Q_{23} \frac{\Delta y_{3E}}{\Delta y_{2E}} \quad (3.96)$$

$$E_3^{OV} = 1 - Q_{33} - Q_{31} \frac{\Delta y_{1E}}{\Delta y_{3E}} - Q_{32} \frac{\Delta y_{2E}}{\Delta y_{3E}} \quad (3.97)$$

the fourth dependent efficiency can be calculated with the help of the other three equations (3.95-3.97) given,

$$E_4^{OV} = 1 - \frac{\Delta y_1 + \Delta y_2 + \Delta y_3}{\Delta y_{1E} + \Delta y_{2E} + \Delta y_{3E}} \quad (3.98)$$

If the vapour leaving the stage is assumed to be at equilibrium with the liquid leaving the stage, then the matrix $[Q]$ is null, and therefore all the component efficiencies are unity (as can be seen from Eqs. 3.95-3.98)

$[Q]$ will be different from the 0 matrix whenever the stage is not at equilibrium. There could be a case where the approach to equilibrium of all the components is the same. That will be represented by the $[Q]$ matrix being diagonal with all the elements in the diagonal equal one to another, ie. $[Q] = q[I]$, where q is a constant. This is the same as considering that all the components have the same efficiency: $E^{OV} = 1 - q$. According to Agarwal and Taylor (1994) this situation will happen when the mixtures are constituted by similar components in which the binary pair mass transfer coefficients are equal and the mass transfer resistance in the liquid phase is entirely negligible.

$[Q]$ diagonal with unequal diagonal values is the situation most often encountered in practice: to match experimental data some components are given efficiencies of different values. $[Q]$ will also be diagonal when the effective diffusivity model of mass transfer is used. If we assume that $[Q]$ is a function of $[N_{OV}]$ and, since the elements of the matrix $[N_{OV}]$ are a function of the mass transfer coefficients of both vapour and liquid phases, then $[Q]$ will not be any longer diagonal in general. Thus, $[Q]$ will have non-zero off diagonal elements together with unequal diagonal elements. These elements cannot be arbitrarily specified without violating physical constraints (mass balances and non negativity of mole fractions) (Agarwal and Taylor, 1994).

Efficiencies computed with the corresponding mass transfer rates Eq. 3.91 may be quite different than those calculated with Eq. 3.90.

3.7 Condensers and Reboilers

Condensers and reboilers for distillation or reactive distillation are modelled as equilibrium stages. These stages differ from the other equilibrium stages in the column because they are a heat source or a sink of the column. They can be total or partial. Efficiencies of reboiler and condensers are usually taken to be unity (so that the efficiency-like parameter is not applied to these stages): the vapour entering the condenser is at equilibrium with the liquid condensate and, similarly the liquid entering the reboiler is at equilibrium with the vapour leaving the stage. Different specifications are usually made for these stages (two are needed for the simulation of the full distillation column, one for the reboiler and one for the condenser):

- flow-rate of distillate product stream
- flow-rate of bottoms product stream
- reflux ratio or reflux flow-rate
- vapour boil-up or boil-up ratio
- heat duty of condenser or reboiler
- some specific composition of a given component in either the distillate or bottoms product

The independent variables in both cases are the compositions, the stage temperature and the flow-rates. The equations for both condenser and reboiler are listed below.

Condenser

The condenser is a vapour-liquid equilibrium system in which vapour from the top tray condenses as coolant flows through a heat exchange coil. All the vapour or a fraction of it is condensed in the case of a total condenser or a partial condenser, respectively.

* Equations:

- Mass balance:

$$\frac{dm_{i,C}^T}{dt} = V_{NP}y_{i,NP} - rx_{i,D} - Dx_{i,D} \quad (3.99)$$

- Energy balance:

$$\frac{dH_{TC}^E}{dt} = V_{NP}Hv_{NP} - rHl_D - DHl_D - Q_C \quad (3.100)$$

- Physical Equilibrium:

$$y_{i,D} = K_{i,D}x_{i,D} \quad (3.101)$$

In a total condenser, the vapour compositions (used in the equilibrium relations) are those that would be in equilibrium with the liquid stream that actually exist.

Reboiler

The reboiler receives the liquid from the bottom tray of the reactive distillation column and partially (or totally) vaporises the liquid using the heat provided. The vapour is returned to the bottom tray while the remaining liquid is the bottom product of the reactive distillation column.

* Equations:

- Mass balance:

$$\frac{dm_{i,B}^T}{dt} = VB y_{i,B} + L_1 x_{i,1} - Bx_{i,B} \quad (3.102)$$

- Energy balance:

$$\frac{dH_{TB}^E}{dt} = L_1 Hl_1 - BHl_B - VBHv_B + Q_B \quad (3.103)$$

- Physical Equilibrium:

$$y_{i,B} = K_{i,B}x_{i,B} \quad (3.104)$$

3.8 Computational and Numerical Aspects

3.8.1 Specifications for Equilibrium and Non-equilibrium Simulations

Both models require similar specifications in terms of distillation column design variables. Feed flow-rate, feed composition as well as the state of the feed need to be specified for a typical simulation problem. The column details include feed location, number of trays, product flow-rates, and product specifications. Additional specifications such as reflux rate and vapour boil-up are needed for both models if the column has condenser and reboiler, respectively. A rate-based model also needs the specification of model parameters for the transport properties models needed for calculation of mass and heat transfer coefficients. Finally, variables related to column geometry, such as column diameter, tray geometry, etc., need to be specified for dynamic equilibrium models and for the non-equilibrium model (steady state or dynamic simulation modes). In general, the rate-based model needs more properties than the corresponding equilibrium-based model and for some of these properties, if suitable prediction methods are not available, correlations need to be used. Obviously, use of correlations limit the ability to predict the distillation column behaviour. The correlations used in this work, have been chosen not because they are the best but because they are well known and can be easily introduced to the model. Most of the pure component property correlations are taken from DIPPR databank (Daubert and Danner, 1986).

3.8.2 Solution of Model Equations

The model equations listed in Tables 3.4 and 3.7 are solved by a collection of DAE and AE solvers. Details on the various solution approaches have been given earlier (see for example, Cameron *et al.*, 1986).

In general, for the dynamic simulation mode, initial conditions for the ODEs and estimates for the variables related to the AEs need to be supplied. Note that the initial condition and the initial estimates need to be consistent (Gani and Cameron, 1989).

The general model and each of the models which can be generated from it, defines a set of ODEs and a set of procedures to represent the process:

- ODEs: mass balances
- Procedures: thermodynamics, reaction term, mass and energy transfer rates, etc.

The model is set up in a specific manner so that it can easily be switched between solving a steady state or dynamic problem. This allows using the dynamic model as a relaxation method for solving steady state problems (Gani and Cameron, 1989). A problem is started with a steady-state simulation to initialise all the variables. After that, starting from the initial state (all the differential variables are known) the solution of the set of ODEs and algebraic equations representing the model for a particular problem will be as following:

- determining the algebraic variables using mass and energy transfer rates, equilibrium equations, hydraulic equations, reaction equations and defined equations and then, determine the right hand side of all the ODEs.
- determining values of the differential variables at time $t_j = t_{j-1} + \Delta t$, and repeating from a- for $j = 1, \dots, end$.

At each time t_j , a set of ODEs and algebraic equations are solved simultaneously in a similar manner to an equation-oriented package.

(Note that here the procedure is described when solving the model in ODEs form into the ICAS simulator. ICAS simulator also allows to solve the equations as a DAE system. The model is solved as a DAE system with analytical Jacobian when *gPROMS* is used).

The algebraic equation set which includes all the algebraic equations and correlations required to determine all the algebraic variables of the ODEs, for example, prediction of physical properties, defined equations, has been divided into subsets for easy numerical solution (Gani *et al.*, 1986).

The detailed procedure given below is to solve the most general model (most complex non-equilibrium model) inside the ICAS simulator.

Procedure:

Given:

- the differential variables at the initial state;
- the design variables; and,
- the ‘input-output’ variables (for condenser and reboiler): one product rate and one heat duty,

using the definition equations (the total molar liquid and vapour hold-ups) the bulk-liquid and bulk-vapour compositions can be determined. Then,

1. Assume the plate pressure.
2. Given the plate pressure, the compositions of liquid and vapour phase and the enthalpy of the plate, the temperature of the phases in the plate can be determined.
3. Given, pressure, temperature, compositions and an estimate of the liquid composition at the interface, the vapour composition at the interface can be calculated through calculation of the physical equilibrium constant by means of any thermodynamic package (using an iterative method, to solve this ‘flash problem’). If the sum of the vapour compositions at the interface is different from unity, continue, otherwise go to step(5).
4. Assume a new value for the plate pressure (this can be done by using the methods of successive substitution, secant method or newton-Raphson method) go to step(3).
5. Given the compositions in the bulk and at the interface, the mass transfer rate can be calculated and new values for the bulk liquid compositions can be obtained. If the new interface liquid compositions minus the estimated interface liquid compositions are greater than a specified error ($1.0e - 04$) then repeat from step(3) now changing the estimated values to the calculated values for the interface liquid composition.
6. Use the hydraulic model to determine the liquid and vapour flow-rates, entrainments rates (if any).
7. Calculate the reaction rates, given the liquid hold-ups and the composition in the bulk phase.

8. Determine reboiler section variables.
9. Determine condenser section variables.

In the case of the steady state simulation mode, initial estimates for the set of unknown variables need to be supplied. It is important to note the difference between the initial estimates for the set of AEs and the initial condition for the set of ODEs. Naturally, if a reference steady state condition is known, the initial condition (for the ODEs) will be the same as the initial estimate and the RHSs of the balance equations will approach zero. In this thesis, only the use of the hybrid modelling approach with respect to solution efficiency and initialisation has been investigated.

Since the dynamic models are represented by sets of DAEs of index 1, except for initialisation, no attempt has been made to improve the method of solution. The dynamic model employs BDF (backward-differentiation-formulae) solver and the Jacobian of the RHS of all the equations is numerically computed. The method retains a copy of the Jacobian in order to save Jacobian evaluations, which makes the solution of the problem rather fast. The model is not yet optimised for speed or memory requirements.

3.8.3 Initialisation

Initialisation has an important role in the solution of DAE or AE systems. The hybrid modelling approach provides a gradual, step by step procedure for initialisation. That is, for any simulation problem, first a simple model (an equilibrium-based model with only mass balance equations and simple property models) is generated and solved. In the next step, a more complex model is generated and solved using the results from the previous simulation as the initial estimates and providing additional initial values for only the new variables (additional variables are introduced by the more complex model). This step is repeated until the desired model is reached. The advantage of this procedure is that by the time the desired model is to be used for simulation, a large amount of valuable information with respect to the behaviour of the distillation column is generated from the earlier steps. Consequently, a major portion of data needed for design and analysis of the distillation column becomes already available even before the final model equations are solved. Therefore, each new simulation problem becomes easier to solve. This is particularly true for DAE systems, where, the simulation problem is solved in the ODE-mode (the AEs are solved separately as procedure equations)

before switching to the DAE-mode. In this way, the necessary initialisation is obtained for the DAE-mode.

The non-equilibrium model is somewhat more demanding with respect to computer time than the corresponding equilibrium model. Table 3.8 gives an idea of computational times required for each model (the total computational time is divided, for purposes of illustration, into 10 CPU time units). To compare the simulation times, for the same distillation system, one form of non-equilibrium model and the corresponding equilibrium model with the same distillation column design and thermodynamic models have been considered (the depropanizer column is taken as an example). Taylor *et al.*(1994) have also reported similar comparison of computational times between equilibrium and non-equilibrium models.

Model	Non-equilibrium	Equilibrium
K-values	0.1	0.1
Mass transfer	2.0	0.0
Solving equations (RHS calculation)	7.9	5.0
Total (CPU-units)	10.0	5.1

Table 3.8: Computational times for solution of different sets of model equations

The rate-based models need to solve twice as many mass and energy balance equations as the equilibrium-based model. Mass transfer rates are only calculated with the rate-based model. Since the total number of equations for the rate-based models is about three times the number of equations of the equilibrium based, the solution of the non-equilibrium model equations takes longer than the corresponding equilibrium model equations. From the time requirements presented in Table 3.8 it can be noted that the equilibrium model needs approximately 50% of the time needed by the non-equilibrium model for the same simulation problem. Therefore, an incentive to reduce the computational times for the non-equilibrium model (or using the non-equilibrium model only when necessary) is worth considering for dynamic simulation. By introduction of the hybrid approach where equilibrium-based and rate-based models are combined, it may be possible to reduce the simulation time significantly. For example, if in a column with 20 trays we consider that 10 of them are in equilibrium, the simulation with the hybrid modelling approach will take approximately 75 % of the time for the corresponding non-

equilibrium model without any loss of accuracy. This simple analysis serves as an indicator of the opportunities for reduction of computational time. It must be clarified, however, that other means of reduction of computational time, not considered in this thesis, are also possible.

3.8.4 Switching between Models and Monitoring of Phenomena

Excess Gibbs energy for a single phase is a function of the chemical potential:

$$\frac{G^E}{RT} = \sum_i n_i \ln \mu_i^E \quad (3.105)$$

Since during a dynamic simulation (rate-based model), the component compositions and chemical potentials are known in each phase, evaluation of the excess Gibbs energy on the tray at any time (independent variable) does not require additional computational time. Analysis of the transient path of the Gibbs energy for each tray (with the rate-based model) then indicates the approach to equilibrium for each tray. If the Gibbs energy is found to be approximately at a minimum (or asymptotically approaching a minimum value), a switch to the equilibrium-based model can be made. While there is no gain in switching from the rate-based model with respect to simulation results or prediction of dynamic behaviour, there are obvious computational advantages. For example, the number of equations for the tray is reduced by nearly 50 %. Also, from a design and analysis point of view, information on the approach to equilibrium by the trays of the distillation column has importance - the upper limit of conversion will be attained if equilibrium is approached. To ensure that the Gibbs energy is close to a minimum, the values of Δn_l and Δn_v are also monitored. Bifurcation analysis (see Chapter 4) provides a further verification alternative. If the Gibbs energy is not at a minimum (that is, if it can move to a lower value), the bifurcation analysis will point to multiple steady state solutions.

3.9 Conclusions

A general hybrid model has been developed for simulation of distillation columns. The model allows the switch between models of different complexity as well as between simulation modes (steady state and dynamic).

This general framework implemented into ICAS (Gani *et al.*, 1997) permits the simulation of reactive as well as non-reactive systems. The framework within *gPROMS* (PSE Ltd., 1997) allows the use of optimization techniques for the optimal control objective of this thesis as well as simulation. Both models have been implemented almost simultaneously and it was not the idea of this work to compare the results from the two systems. The simulation results obtained from the ICAS simulator have been used as the initial estimate for the *gPROMS* simulation. However, *gPROMS* has showed to be a very reliable tool once the first convergence has been achieved.

In the following Chapters the validity of the general model is presented together with some applications of hybrid modelling. Furthermore, controllability analysis, based on a linearised version of the general model is assessed. Finally the dynamic optimization results, from the *gPROMS* framework, for the design of reactive distillation columns is presented.

Chapter 4

Validation of models

In this Chapter the validity of the hybrid model presented previously (Chapter 3) is shown for the systems studied during this work.

First the systems are presented, given some insights into the phase equilibrium of the mixtures, reaction kinetics and the characteristics of the distillation column where the separation/reaction is taking place. These systems have been chosen in order to cover a wide range of examples.

Different characteristics of the systems make them interesting to analyse, for example, reported multiplicity of the MTBE production, availability of experimental data for the esterification column.

Before going to the simulation results, an initialisation procedure is presented. This procedure allows faster convergence to the more complex models, and even when it may look ‘tedious’ and ‘slow’, it helps finding the solution (convergence) particularly for non-equilibrium models. Without this procedure, many times it was not possible to attain convergence in the more complex models that can be generated from the general hybrid model.

Then, simulation results with different models, generated from the general hybrid model, are validated against experimental data (whenever possible) or against other open literature results.

A detailed study of a vast number of parameters together with simulations with different models shows which model is the more appropriate for a given

system or which set of parameters should be used when simulating the column.

A brief study on bifurcation behaviour of the models is also presented in this Chapter. Bifurcation analysis for the reactive systems is investigated. Bifurcation theory is used to explore all the possible steady states (stable and/or unstable) for reactive systems.

The general hybrid model has shown to be a reliable simulator for distillation columns. It has always been possible to find a model which can match experimental results (or literature results).

4.1 Systems Studied

- Methyl-tert-butyl Ether (MTBE) production
- Esterification of Acetic acid with ethanol
- Depropanizer column

In the following sections the systems are described.

4.1.1 MTBE: Methyl-Tert-Butyl-Ether

What is MTBE?

MTBE, or Methyl Tertiary Butyl Ether, is an ether compound in the same boiling range as gasoline. It is soluble in water, alcohol and other ethers and has a characteristic smell. MTBE is made by combining isobutylene (isobutene) and methanol in presence of a suitable catalyst, typically a cation exchange resin. MTBE is mostly used as an additive for gasolines. Originally its function was to raise the octane of gasolines and it was used instead of lead components. It also raises the oxygen content in the gasolines and reduces hydrocarbon and carbon monoxide emissions from motor vehicles by promoting more complete combustion. MTBE is the preferred additive for producing reformulated gasoline in the USA. However, MTBE has received some negative publicity as a result of health tests although some consider

the tests to be inconclusive. The National Academy of Science (N.A.S.) concluded: *“Based on the available analyses, it does not appear that M T B E exposures resulting from the use of oxygenated fuels are likely to pose a substantial human health risk”*.

However, MTBE has now been banned in the state of California (25th March, 1999). They acted out of concern for water quality. MTBE has been found to enter Californian aquifers and show up in drinking water. As this state goes on environmental regulations so tends the rest of the United States.

Strengths	Weaknesses
High octane	Availability of economical isobutylene feed stocks is limited
Low volatility	
Blending characteristics similar gasoline	Possible methanol supply constraints
Widely accepted in market place by consumers and refinery	Environmental issues not cleared totally
Reduces carbon monoxide and exhaust hydrocarbon emissions	
Economics not dependent on subsidies	

MTBE Production

Methanol and isobutene, under appropriate process conditions, react in the presence of the catalyst to form MTBE. Typically, the isobutene is in a mixed butane stream that contains from about 10% to about 50% isobutene, depending on the source. The other major components are n-butane, isobutane and n-butenes. These other components are inert under the process conditions and the chosen catalyst. In the temperature range of interest (310K-370K), the equilibrium conversion of MTBE is high. With an excess of methanol it is theoretically possible to achieve a conversion of isobutene in the range of 90-97 % with a single-stage conventional process, using two series-flow reactors followed by separation and external recycle of excess of methanol.

Separation of MTBE from the inerts and the excess of methanol is very difficult through distillation. The methanol excess in the distillate is recovered in another separation step and recycled. MTBE (high purity) is obtained as a bottom product. The separation of unreacted isobutene from the normal butenes by distillation is expensive due to the low relative volatility between them. Therefore, the unreacted isobutene leaves with the inerts, thus, a certain amount of isobutene is not converted to MTBE. On the contrary, using reactive distillation technology, instead of the conventional units, is possible to achieve up to 99 % of isobutene conversion.

The MTBE reaction is not severely equilibrium limited. The net reaction rate remains fairly high until a substantial amount of isobutene is converted. Only when the liquid composition (where the reaction takes place) is close to the equilibrium compositions the net reaction rate decrease rapidly.

Conventional processes adopted by industries are, in general, made up of:

- two liquid-phase catalytic reactors placed in series (the isobutene conversion is around 90-95 % and excess of methanol is used)
- the reactors are followed by one or two distillation columns to recover high purity MTBE
- methanol extraction and fractionation columns are required to recover pure methanol for recycling.

The MTBE process using reactive distillation technology consists of a single column.

A particular industrial reactive distillation column (Koch Engineering Co., Inc.) has a diameter of 203cm with a height of 5.2m. It is insulated and equipped with heat compensation for adiabatic operation. The column contains four beds of packing (top and bottom: Flexipac; mid-top and mid-bottom: Katamax), with vapour and liquid distributors above each bed. The Katamax packing contains Amberlyst 15 catalyst. The column was operated for six months for demonstrations runs, and the ranges of variables studied are presented in Table 4.1(Koch Engineering Co., Inc.).

Variable	Value
Total Feed Rate	20-30 bbl./stream day
Feed Isobutene Concentration	11-13 wt %
Feed Methanol-Isobutene Molar Ratio	1.0:1 to 2.6:1
Average Katamax Packing Temp.	333K-353K
Reflux Ratio	1.0:1 to 6.0:1

Table 4.1: Range of Variables

Why Use Reactive Distillation for MTBE Production?

- Reactive distillation achieves higher conversion levels than conventional processes for this selected reaction.
- The preferred temperature range of the catalyst (in which the catalyst can be used more efficiently) match that for the distillation, a characteristic that ensure that this process is excellent for reactive distillation.
- Lower operating cost due to less equipment.
- Lower operating cost due to higher conversion per pass (higher rate of production).

However, one main disadvantage of reactive distillation for MTBE production is the poor knowledge of the reaction kinetics as well as the poor understanding of the plate or packing behaviour.

Case Study

The MTBE column studied in this work differs from the industrial discussed above. The general simulation program is used to simulate the reactive distillation column specified in Table 4.2. The bottom flow rate was specified to 197 mol/sec to obtain the amount of MTBE industrially required.

Reaction Kinetics

The reaction between methanol and isobutene on sulfonic catalytic resins has been studied by several research groups. Ancilotti *et al.*(1978) found that initial rates were zero order in the alcohol and first order in the olefin.

Variable	Value
Feed Rates:	
Methanol	215.5 mol/s
Butenes	535 mol/s
Feed Stages:	
Methanol	4
Butenes	11
Number of Trays	17
Type of tray	Sieve tray
Tray design	<i>Diameter = 2.5m</i> <i>TraySpacing = 0.311m</i> <i>ActiveArea = 5.3m²</i> <i>Weirlength = 3.66m</i> <i>Weirheight = 0.38m</i>
Reactive Section	from tray 4 to tray 11
Catalyst Load	300Kg/stage
Pressure	11 atm.
Reflux Ratio	7.0
Bottom Flow-rate	197 mol/s

Table 4.2: MTBE Column Design. Data taken from Jacobs and Krishna (1993) except for the tray design which has been calculated in this work

The MTBE synthesis reaction catalysed by Amberlyst 15 macroreticular sulfonic resin was also studied by Gicquel and Tork (1983). This catalyst acts through its sulfonic groups bonded to the resin. The porous spherical beads contain 4.9 equivalent protons/kg.

The reaction mechanism and the rate expression are dependent on the relative concentrations of isobutene and methanol which affect the activity of the acidic catalyst particles. When the ratio of isobutene to methanol is less than 0.7, methanol is adsorbed (due to its highly polar nature) and the hydrogen bonds that link the sulfonic groups (protons or catalytic agents) dissociate. Then methanol becomes hydrogen-bonded to the sulfonic group to react with isobutene in solution within the pores and the gel phase. Therefore, it is assumed that MTBE synthesis proceeds by the Eley-Rideal mechanism. The initial surface reaction rate is given by (Al-Jarallah *et al.*, 1988):

$$r_s = k_s K_{MeOH} \left[\frac{C_{IB}^{0.5} C_{MeOH} - C_{MTBE}^{1.5} / K}{(1 + K_{MeOH} C_{MeOH} + K_{MTBE} C_{MTBE})} \right] \quad (4.1)$$

The rate constant k_s is given by:

$$k_s = 1.2 \times 10^{13} \exp(-87900/RT) \quad (4.2)$$

The liquid adsorption constant for methanol and MTBE are:

$$K_{MeOH} = 5.1 \times 10^{-13} \exp(97500/RT) \quad (4.3)$$

$$K_{MTBE} = 1.6 \times 10^{-16} \exp(119000/RT) \quad (4.4)$$

The chemical equilibrium constant is given by an expression like:

$$\begin{aligned} \ln \left[\frac{K(T)}{K(T_o)} \right] = & A_1 \left(\frac{1}{T} - \frac{1}{T_o} \right) + A_2 \ln \left(\frac{T}{T_o} \right) + A_3 (T - T_o) \\ & + A_4 (T^2 - T_o^2) + A_5 (T^3 - T_o^3) + A_6 (T^4 - T_o^4) \end{aligned} \quad (4.5)$$

When the concentration of isobutene begins to be significant, the Langmuir-Hinshelwood mechanism, where both methanol and isobutene absorbed react to give MTBE, starts to be operative. The sorption mechanism for heterogeneous catalysis is (Rehfinger and Hoffmann, 1990):

$$r_s = q k_r \left[\frac{a_{IB}}{a_{MeOH}} - \frac{1}{K} \frac{a_{MTBE}}{a_{MeOH}^2} \right] \quad (4.6)$$

r_s is the rate of reaction per unit catalyst mass, q is the amount of acid groups on the resin per unit mass and a is the activity of the component. The rate constant k_r is presented as:

$$k_r = 3.67 \times 10^{12} e^{\frac{-11110}{T}} \quad (4.7)$$

The chemical equilibrium constant is given as above (Eq. 4.5). When the ratio of isobutene to methanol is around 10 a maximum in the initial rate is observed. Thereafter, when the methanol concentration decreases more, the rate shows a zero order dependence in isobutene and a first order dependence in methanol. Here, diffusion transport begins to control methanol transfer from the bulk liquid phase.

The reaction rate is influenced neither by the diffusion inside the micro-sphere nor by the internal surface area.

In order to preserve selectivity the presence of water should be avoided. Since water is more polar than the alcohol (methanol) it will be preferentially adsorbed on the sulfonic groups. The adsorbed water can react with the isobutene to give tertiary butyl alcohol.

On the basis of the experimental results from the different authors (as discussed above), the following assumptions were made for the reaction system:

- the amount of methanol feed to the column is close to stoichiometric conditions, so the ratio of isobutene to methanol is smaller than unity
- the column operating conditions are chosen so that the amount of methanol in the bottom is very small. This guarantees that the ratio of isobutene to methanol is smaller than unity in the reaction section as well as in the stripping section
- side reactions are negligible (dimerization of isobutene, formation of tert-butyl alcohol from isobutene and water)

With these assumptions the rate of reaction can be accurately described by the expression proposed by Rehfinger and Hoffmann(1990).

Model Formulation

The following assumptions were made when formulating the model:

1. the vapour and liquid on each stage are at equilibrium or not (equilibrium model or non-equilibrium model)
2. Since this section is actually a packed section when formulating the non-equilibrium model this is considered as packed section through a specific number of trays.
3. the chemical reaction occurs only in the liquid phase (not in the liquid film)
4. chemical reaction follows the correspondly kinetic expression: rate-based

5. the pressure drop through the column is negligible
6. there are no external heaters or coolers apart from reboiler and condenser.

Phase Equilibrium

The various physical equilibrium modelling alternatives considered in this work are given in Table 4.3, in terms of liquid and vapour phase models together with the sources for their model parameters.

Liq.Phase Model	Liq.Phase Model Parameters	Vap.Phase Model	Vap.Phase Model Parameters
UNIFAC	Fredenslund <i>et al.</i> (1977)	Ideal	————
UNIFAC	Fredenslund <i>et al.</i> (1977)	SRK	Binary interaction coefficients set to zero
UNIQUAC	Rehfinger and Hoffmann (1990)	SRK	Binary interaction coefficients set to zero

Table 4.3: Modelling alternatives for MTBE system

4.1.2 Ethyl Acetate

Esterification of acetic acid with ethanol to water and ethyl acetate is the most frequently considered reactive system in a reactive distillation column.

In 1921 a patent was published by Backhaus. In the early 70s reactive distillation was described through computer simulations using rigorous equilibrium models (Suzuki *et al.*, 1971). From there on to the present different algorithms and models to solve this system were presented.

Especially compared with the esterification of acetic acid with methanol, this esterification process producing ethyl acetate appears not to be very good for a reactive distillation column (Bock *et al.*, 1997a) and it should be theoretically possible to obtain high purity ethyl acetate with different processes. Bock *et al.* also show that the equilibrium models, which are normally applied to reactive distillation column simulations, are inadequate to model this system, suggesting that a non-equilibrium model will do the task better.

Chang and Seader (1988) reported that the main problems in achieving high purity ethyl acetate in a reactive column are:

- unfavourable reaction conversion
- similar K-values of ethanol, ethyl acetate and water, and
- temperature profile in the column.

In this work ethyl acetate production is considered despite the disadvantages offered for the system when using reactive distillation. There is one big advantage of this system: experimental data is openly available in the literature. This was a major consideration when selecting reactive systems. Experimental data is hard to find.

Moreover, despite the fact that high purity is not obtained with the reactive column, many different as well as interesting phenomena occur in this system: azeotropes, similar volatilities, low and fast reaction in different trays.

The system can definitely test the general model to its limits, pushing the model to its ranges of prediction and accuracy.

The general simulation program was used to simulate the reactive distillation column specified in Table 4.4.

Reaction Kinetics

The equilibrium reaction of the esterification is described as follows:



The rate of reaction is given by:

$$r = k_1 \exp\left(-\frac{E_1}{RT}\right) \prod C_R - k_2 \exp\left(-\frac{E_2}{RT}\right) \prod C_P \quad (4.8)$$

Both the forward and the backward reaction are second order (the forward reaction is first order in acetic acid and first order in ethanol, while the backward reaction is first order in water and first order in ethyl acetate, given

Variable	Value
Feed Rate:	4885.0 mol/h
Composition	
Acetic acid	0.4963
Ethanol	0.4808
Water	0.0229
Feed Stage:	6
Number of Trays	13
Type of tray	Sieve tray
Tray design	
Section 1 to 12	<i>Diameter = 5.60m.</i> <i>TraySpacing = 0.911m</i> <i>ActiveArea = 50.684m²</i> <i>Weirlength = 11.684m</i> <i>Weirheight = 0.18m</i>
Tray 13	<i>Diameter = 6.25m.</i> <i>TraySpacing = 0.911m</i> <i>ActiveArea = 54.684m²</i> <i>Weirlength = 11.684m</i> <i>Weirheight = 1.193m</i>
Reactive Section	from tray 1 to tray 13
Pressure	1 atm.
Reflux Ratio	10

Table 4.4: Ethyl Acetate Column Design. Data from Suzuki *et al.* (1971) except the tray design which has been calculated in this work.

second order reactions). The reaction rate for all the components is the same because the stoichiometric coefficients of all components are equal.

The rate of reaction used in this work is as follows:

$$r = k_1 \exp\left(-\frac{E}{RT}\right) C_{AA} C_{Et} - k_2 \exp\left(-\frac{E}{RT}\right) C_W C_{EtAc} \quad (4.9)$$

where:

$$k_1 = 483.33,$$

$$k_2 = 123.00,$$

$E = 54970.5$,

R is the gas constant, and

C_{AA} , C_{Et} , C_W , C_{EtAc} represent the concentration of acetic acid (AA), ethanol (Et), water (W) and ethyl acetate (EtAC) respectively. The rate of reaction is given in $Kmol/h$.

Model Formulation

The following assumptions were made when formulating the model:

1. the vapour and liquid on each stage are at equilibrium or not (equilibrium model or non-equilibrium model)
2. the reaction zone (all the column, in this case) is modelled as a series of trays
3. the chemical reaction occurs only in the liquid phase (not in the liquid film)
4. the chemical reaction follows the correspond kinetic expression: rate-based
5. the pressure drop through the column is negligible
6. the last tray in the column is bigger than the rest (this facilitates the reaction at the bottom of the reactive distillation column)
7. there are no external heaters or coolers apart from reboiler and condenser.

Phase Equilibrium

The system is strongly non-ideal. The following azeotropes are possible:

- ethanol-water
- water-acetic acid
- ethyl acetate- ethanol

- ethyl acetate-water
- ethanol-ethyl acetate-water.

Suzuki *et al.*(1971) determined the phase equilibrium for the system taking the reaction into account (they fitted coefficients to use in a modified Margules equation). Sawistowski and Pilavachi (1982) mention that the phase equilibrium do not correspond with the experimental data.

Bock *et al.*(1997a) have determined experimentally NRTL parameters without considering the reaction and they have reproduced the experimental mole fraction profile quite well.

In our work (Pérez-Cisneros *et al.*, 1996, 1997; Pilavachi *et al.*, 1997) different thermodynamic models were employed in order to match the experimental data. Table 4.5 summarises the different models used.

Liquid Phase Model	Liquid Phase Model Parameters	Vapour Phase Model	Vapour Phase Model Parameters
UNIFAC	Fredenslund <i>et al.</i> (1977)	Ideal	————
UNIFAC	Fredenslund <i>et al.</i> (1977)	SRK	Binary interaction coefficients set to zero
UNIFAC	Fredenslund <i>et al.</i> (1977)	Virial Eq.	Hayden and O'Connell(1975)
UNIQUAC	Kang <i>et al.</i> (1992)	Ideal	————
UNIQUAC	Kang <i>et al.</i> (1992)	SRK	Binary interaction coefficients set to zero
Margules Modif.	Suzuki <i>et al.</i> (1970)	Ideal	————
Wilson	Suzuki <i>et al.</i> (1970)	SRK	Binary interaction coefficients set to zero

Table 4.5: Modelling alternatives for Esterification system

4.1.3 Depropanizer Column

Taylor and Krishna (1993) have also studied this depropanizer column. The distillation column details are given in Table 4.6. This column has been simulated with the equilibrium model as well as the non-equilibrium model. Models of types RB-3 and EQ-3 have been used in all simulations. For initialisation purposes, simpler model forms have been used.

The depropanizer column is selected as a system to study in this work, mainly due to the availability for data for the column design as well as the property model for the mixture.

Model Formulation

The following assumptions were made when formulating the models:

1. the vapour and liquid on each stage are at equilibrium or not (equilibrium or non-equilibrium model)
2. the pressure drop through the column is negligible
3. there are no external heaters or coolers apart from reboiler and condenser.

Phase Equilibrium

Since the system is a hydrocarbon mixture an equation of state for both phases will represent the mixture quite well. Ideal behaviour is not considered due to the high pressure in the column (15atm.). The Peng-Robinson equation of state is taken as the thermodynamic model for both phases, in order to compare results presented by Taylor and Krishna (1993). SRK-EOS is also used as a thermodynamic model in order to investigate sensitive parameters to simulation.

4.2 Initialisation

For the simulation of the systems, two starting points have been tried. In the first case, a reference condition is not known although the simulation

Variable	Value
Feed Rate	1000.0 mol/s
Feed composition:	
Ethane	0.10
Propane	0.30
Butane	0.50
Pentane	0.10
Feed Stage	16
Number of Trays	35
Type of tray	Sieve tray
Tray design	
Section 1 to 15	<i>Diameter = 4.82m.</i> <i>TraySpacing = 0.5m</i> <i>ActiveArea = 14.96m²</i> <i>Weirlength = 17.6m</i> <i>Weirheight = 0.05m</i>
Section 16 to 35	<i>Diameter = 6.17m.</i> <i>TraySpacing = 0.5m</i> <i>ActiveArea = 24.516m²</i> <i>Weirlength = 0.037m</i> <i>Weirheight = 0.038m</i>
Reactive section	none
Pressure	15 atm.
Reflux Ratio	2.5
Bottom Flow-rate	600 mol/s

Table 4.6: Depropanizer Column Details. Data taken from Taylor and Krishna (1993).

problem needs to predict the transient behaviour due to disturbances around the reference condition -this situation is often encountered in process design where the reference condition or designed condition of operation needs to be determined. This means that first an appropriate reference steady state must be determined before the effect of disturbances can be studied. Since the starting point for dynamic simulation mode is far from the reference condition, simulation is started with the simplest model and after short periods of simulation, a switch to a more complex model is made. This is continued until the desirable model has been reached. In the second case, a reference condition is known and simulations are made from this condition to study effect of changes or disturbances in design variables. For these simulations, the reference condition provides a very good initial estimate and thus the initialisation procedure is not needed unless a switch from one model type or mode is to be made.

For each distillation system, simulations were started with the equilibrium model of type EQ-1 when the corresponding reference conditions were not known. After an arbitrary number of integrations, for example 5 integration steps, a switch to equilibrium model of type EQ-2 was made and after a further 5 integration steps, a switch to model EQ-3 was made. After a further integration ($t=1$ hr), a switch to the steady state mode was made (this step was only taken if a steady state with the equilibrium model was needed for purposes of design or validation). At the computed equilibrium model steady state, a switch to the non-equilibrium model (type RB-3) was made. If a check for stability is included in the simulation problem formulation, dynamic simulation for a further period of time (about 100 hrs) was made. For distillation systems involving reaction, (MTBE production and ethyl acetate production) reactions were introduced in terms of small increments of reaction rate ($\Delta r = 0.001$) after the switch to the final model form (equilibrium or non-equilibrium). The integration statistics (NFE: number of function evaluation; NJE: number of Jacobian evaluation; NSTEP: number of integration steps; Time: time of simulation; and, Residuals: residual values of the differential equations after the simulation time) for the three problems are shown in Table 4.7. Although at first sight, this may seem to be a lot of extra computation, use of the initialisation procedure did result in faster convergence to the desired steady state solution when compared with simulations without use of the initialisation procedure (see also Table 3.8). In most cases, without using the initialisation procedure, it was not possible to obtain the steady state solution with the non-equilibrium model.

Model	ODEs	NFE	NJE	NSTEP	Time	Residuals
MTBE col.: -equilibrium	68	518	7	26	1h.	0.3809e-14
	68	731	7	34	100h.	0.5658e-19
-non-equilibrium	136	2251	18	198	1h.	0.1824e-08
	136	2807	19	101	100h.	0.1257e-12
Esterification col.: -equilibrium	52	393	7	26	1h.	0.3753e-13
	52	873	8	20	100h.	0.8962e-21
-non-equilibrium	104	1069	12	108	1h.	0.5283e-08
	104	1457	13	103	100h.	0.4016e-13
Depropanizer col.: -equilibrium	140	494	7	56	1h.	0.8872e-14
	140	678	8	48	100h.	0.8978e-21
-non-equilibrium	280	2938	22	158	1h.	0.4027e-08
	280	3558	23	147	100h.	0.3075e-14

Table 4.7: Selected set of numerical statistics for the three distillation systems

4.3 Validation of Models

4.3.1 MTBE

In the open literature many authors have presented the MTBE profile in the column (Jacobs and Krishna, 1993; Hauan *et al.*, 1995, Sundmacher and Hoffmann, 1996, Ung and Doherty, 1995a,b). In this thesis different models from the general hybrid model have been used to simulate the process. A set of different thermodynamic models (Table 4.3) has been used in order to determine the set of properties that can be sensitive to the simulation results. The activity coefficient model parameters have been found to be sensitive only in some special cases (see Pérez-Cisneros *et al.*, 1996). There have been hardly any differences between the simulated results when using UNIFAC, UNIQUAC or Wilson equation as thermodynamic models.

With the combination of the UNIFAC model for the liquid phase activity coefficients, ideal gas or SRK equation of state for the vapour phase, the Rehfinger and Hoffmann (1990) expression for the temperature dependent equilibrium constant term, it was possible through steady state and dynamic simulation to match the results (including multiple solutions) reported in the

literature. Fig. 4.1 shows the variation of fractional conversion of isobutene as a function of the methanol feed location, for steady state and dynamic simulation, respectively. Temperature profiles for low and high conversions (for the multiple solutions) are shown in Fig. 4.2.

In order to corroborate the multiplicity presented by this system, different ways of calculating the temperature dependence of the equilibrium constant, K_{eq} , have been studied: Rehfinger and Hoffmann (1990), Colombo *et al.* (1983); and from the expression based on the Gibbs free energy using data from the DIPPR Data Bank (Daubert and Danner, 1986).

K_{eq} for the three expressions is shown in Fig. 4.3.

Simulation results using the three expressions for K_{eq} , are given in terms of fractional conversion of isobutene with the methanol feed location in Fig. 4.4. From this figure it can be noted that while the Rehfinger and Hoffmann expression yields multiple solutions, with the other two expressions multiple solutions cannot be found.

From Fig. 4.3, it can be noted that the differences between the three expressions for K_{eq} increases with increasing temperature while from Fig. 4.4 it can be noted that the differences between the different solutions (considering only one the high conversion solution) lies in stages 10-14. From Fig. 4.3, however, it can be noted that these stages correspond to the 'higher' temperatures where the differences between the expressions for the temperature dependence of the equilibrium constant increases as the temperature increases.

Some pilot plant experiments (Sundmacher, 1995) tend to confirm these multiple solutions for the MTBE column. However, our analysis showed that there are specific cases for which the multiple solutions can occur. The multiplicities, under these specific conditions, remain in the systems, independently of the model used. Three types of models have been used: fully equilibrium, physical equilibrium with kinetically controlled reaction and finally non-equilibrium.

Multiple solutions with the equilibrium model has been validated against other simulated results as shown in Fig. 4.5. The equilibrium model is com-

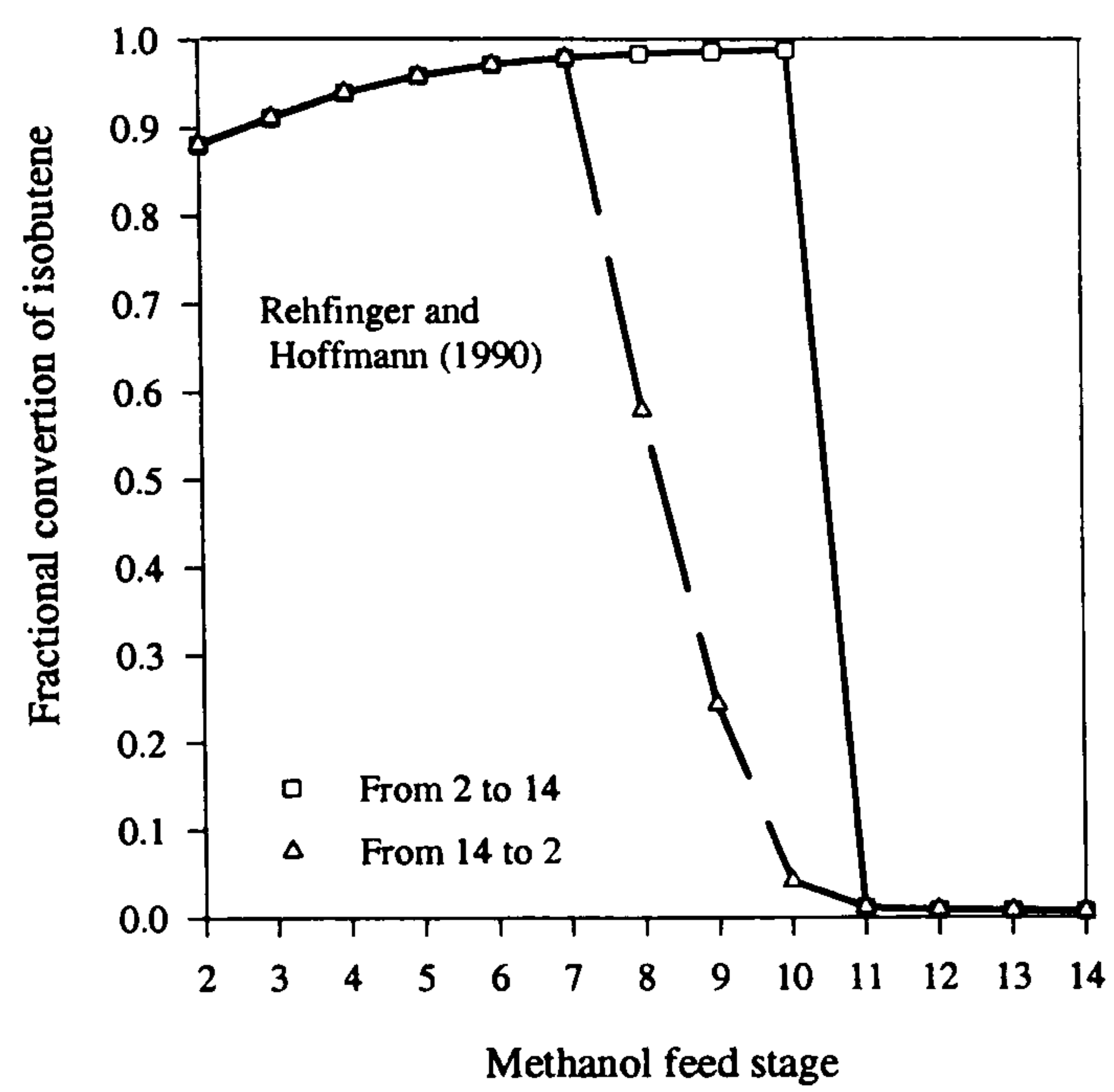


Figure 4.1: Multiple solutions in the MTBE column

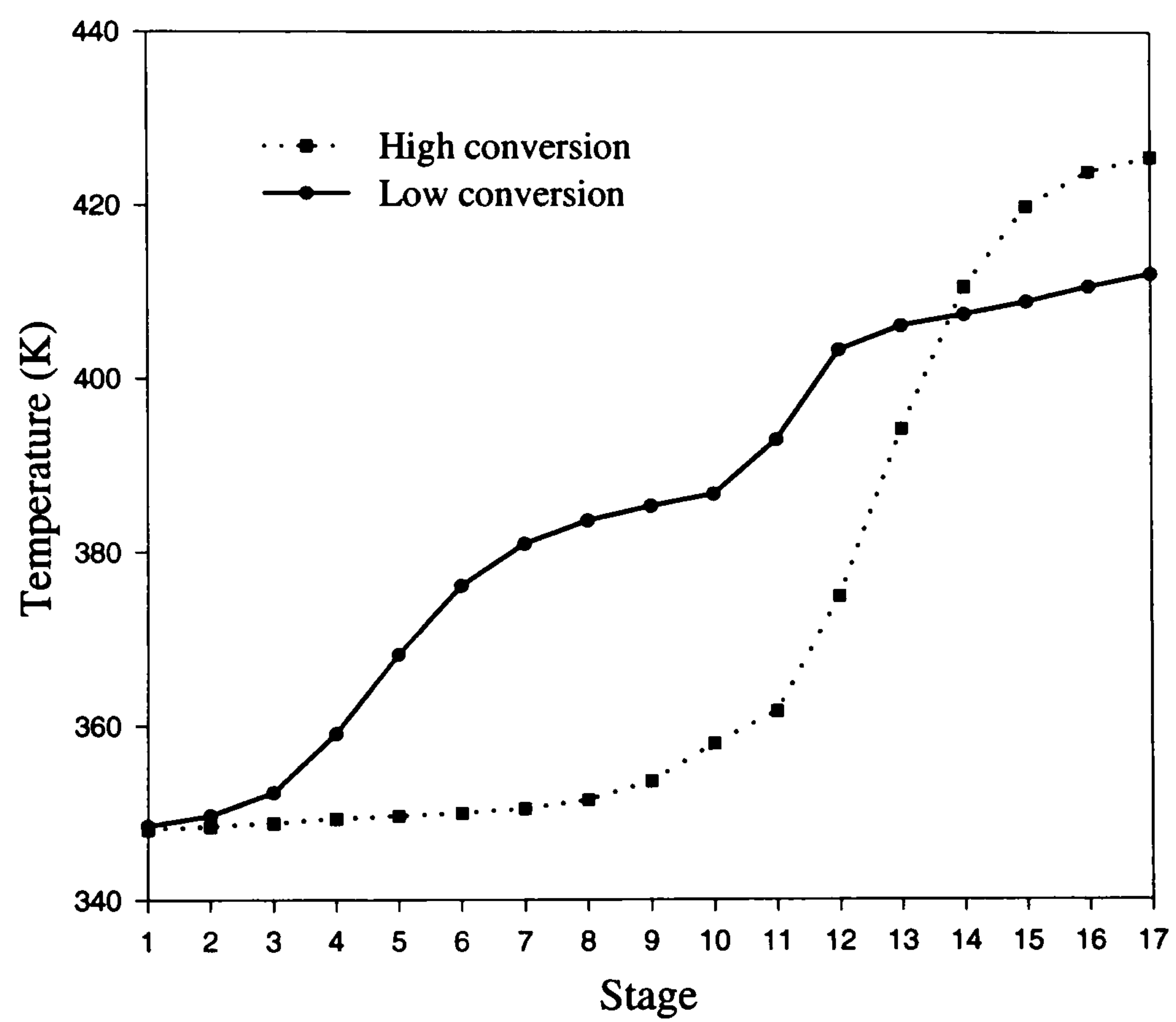


Figure 4.2: Temperature profiles for low and high conversion in the MTBE column

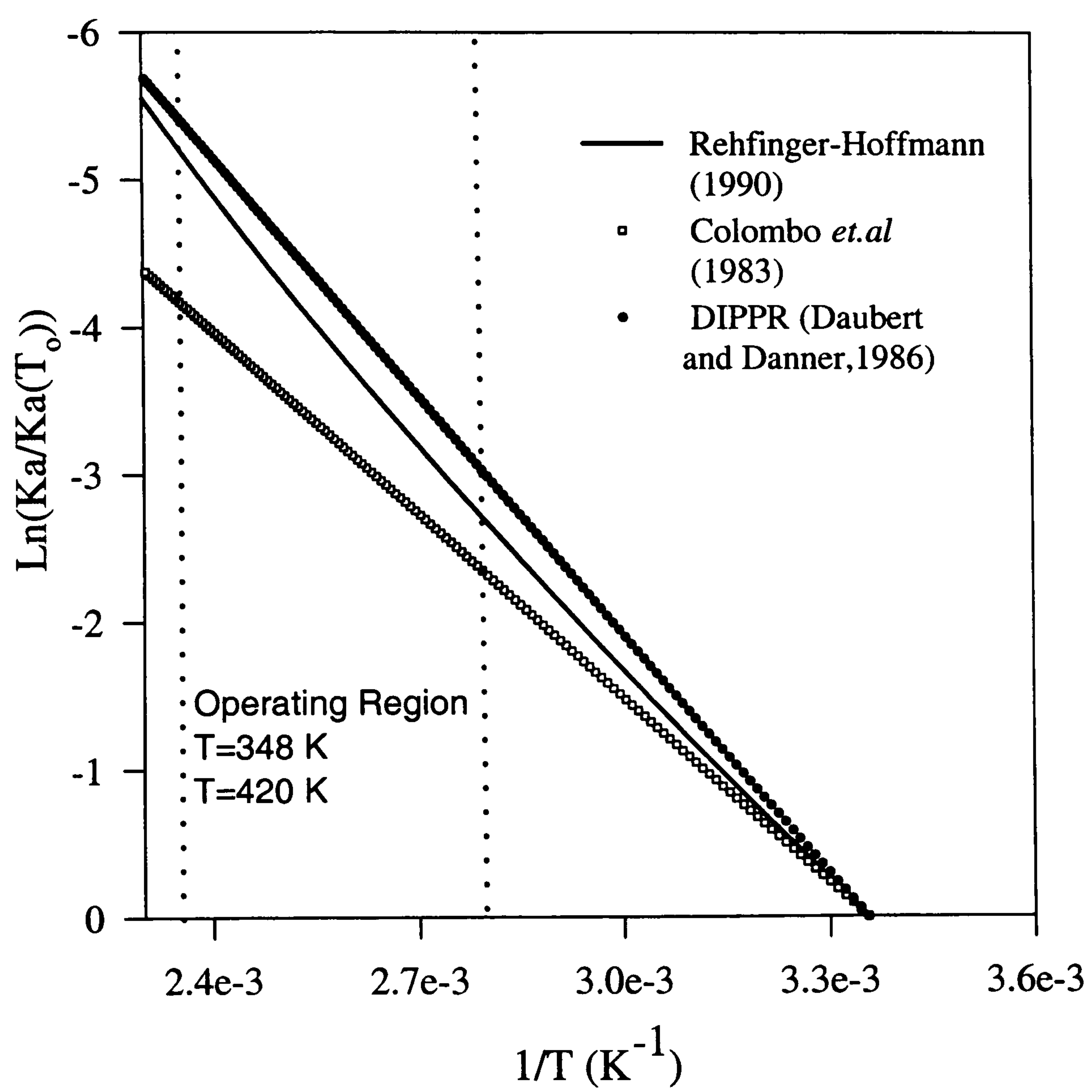


Figure 4.3: Equilibrium constant for MTBE synthesis

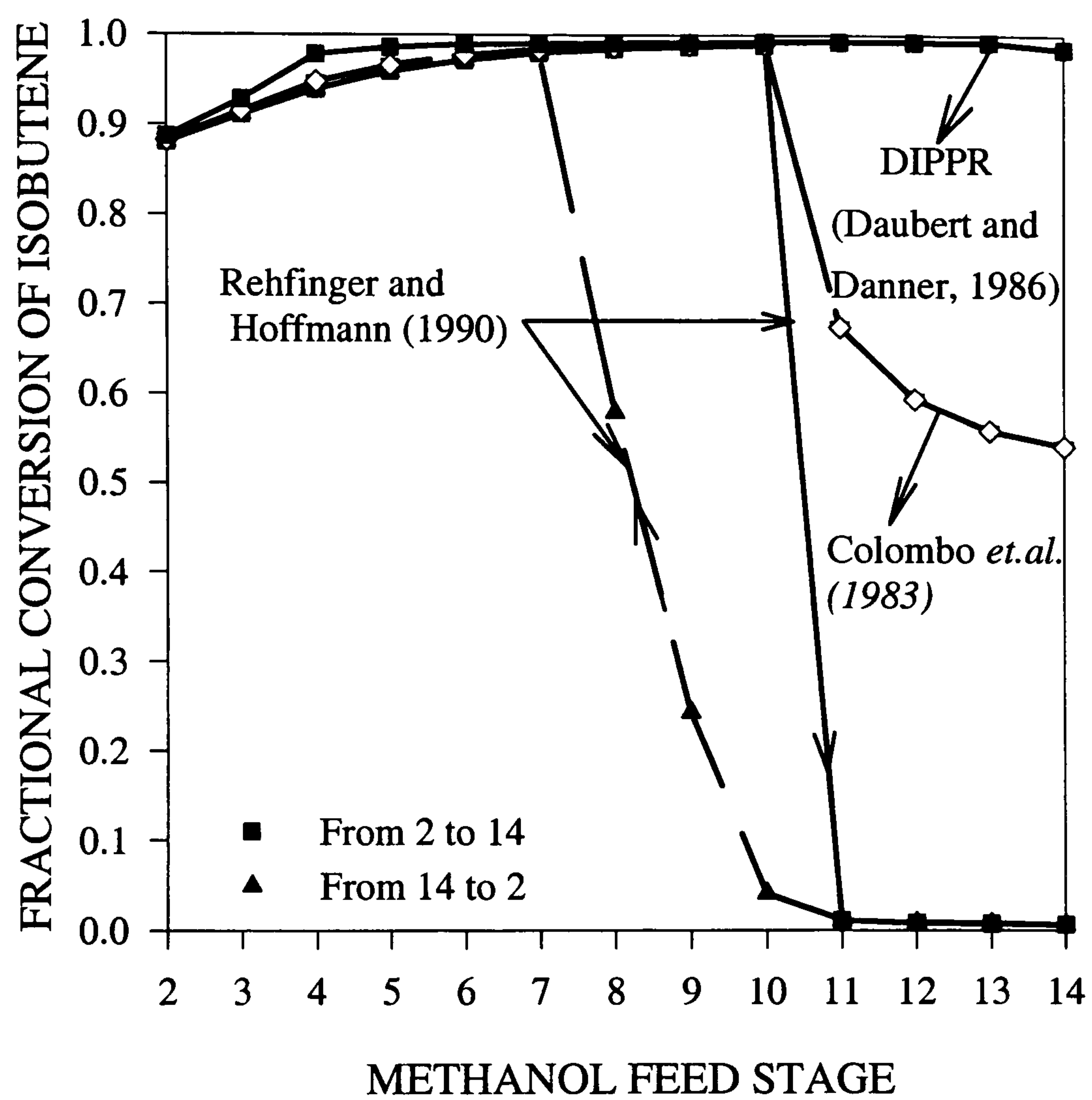


Figure 4.4: Simulation results with Rehfinger and Hoffmann, Colombo *et al.* and DIPPR for the MTBE column

pared against ASPEN PLUS results where full equilibrium (meaning physical and chemical equilibrium) is assumed.

Multiple solutions still remain when using the non-equilibrium model. This results are in agreement with a recent paper of Higler *et al.*(1999) where they also present their non-equilibrium model reproducing the same multiplicities presented earlier with the equilibrium model.

Composition profile in the column with equilibrium and non-equilibrium models are shown in Fig. 4.6. It is interesting to note that deviations between the two models are largest on the reactive stages, but the differences at the top and bottom of the column are almost indistinguishable.

The non-equilibrium model used to simulate the MTBE column assumes constant pressure throughout the column. Furthermore, the packed section of the column has been simulated considering packed column expressions for the binary mass transfer coefficients (Onda *et al.*, 1968) and interfacial area. Mass transfer resistance has been consider to be predominant in the vapour phase, so that the liquid phase resistance has been neglected. The assumptions, however are not limiting the ability to provide a good representation of the system.

The aim of this work has been to determine which model represents accurately the system using as little computational time as possible. The lack of accurate correlations as well as a poor knowledge regarding the number of stages able to represent the height of the packing section compares with the assumptions made. The complex non-equilibrium model, which considers both resistances and variable pressure takes around 40 % extra time during calculations and it is believed that it cannot achieve significantly better performance.

Unfortunately results cannot be compared with experimental data due to the restricted information obtained from the (very small) set of results presented in the open literature. For this reason, high production of MTBE and the existence of a multiplicity region (in order to investigate what actually will happen if for any reason the systems gets into that operating conditions) were the aim of this work. Considering the differences between the models and the lack of experimental data in principle and up to this point any model (equilibrium or non-equilibrium) could be used to simulate the MTBE

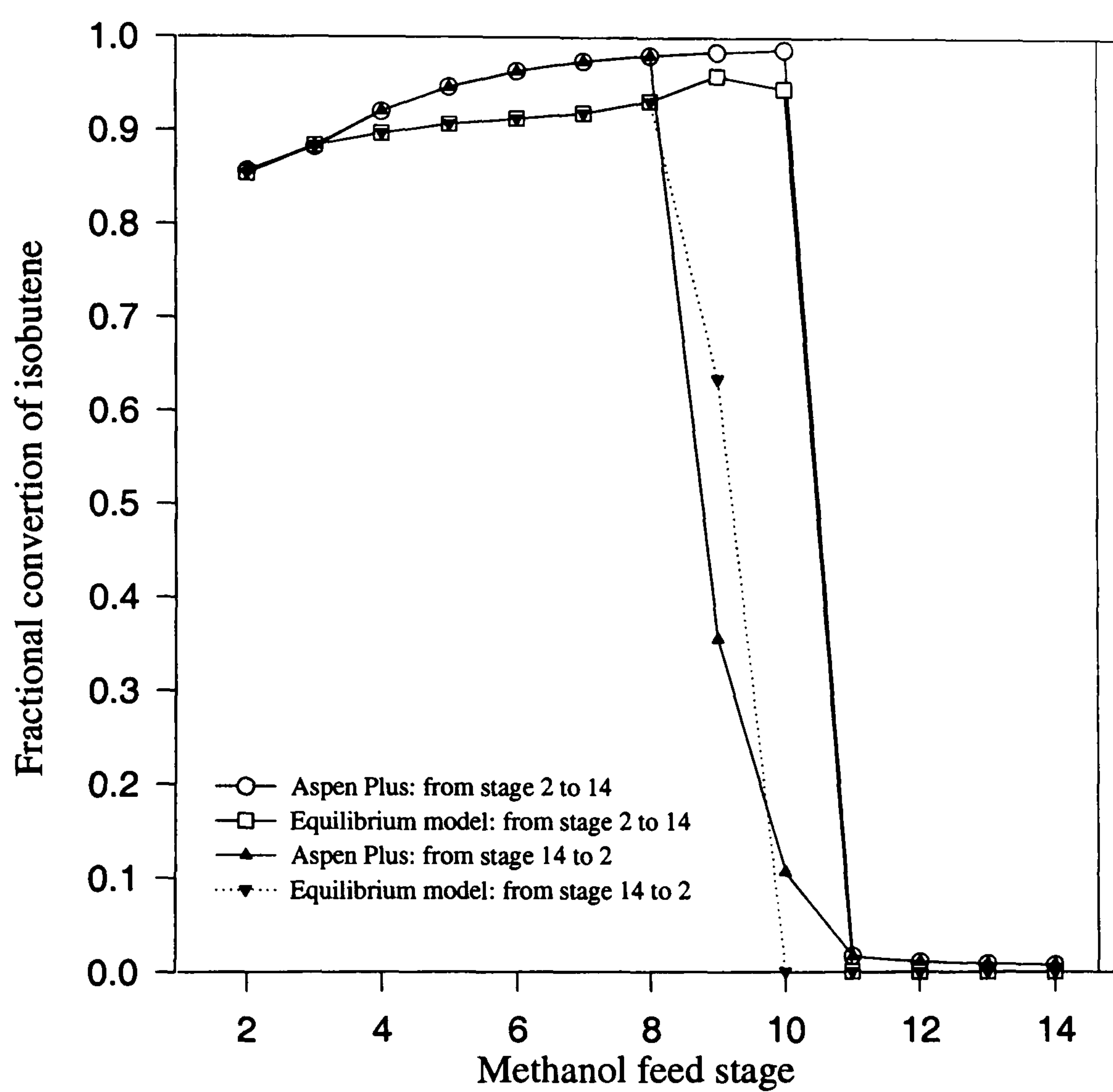


Figure 4.5: Simulation results compared with those of ASPEN PLUS for the MTBE column

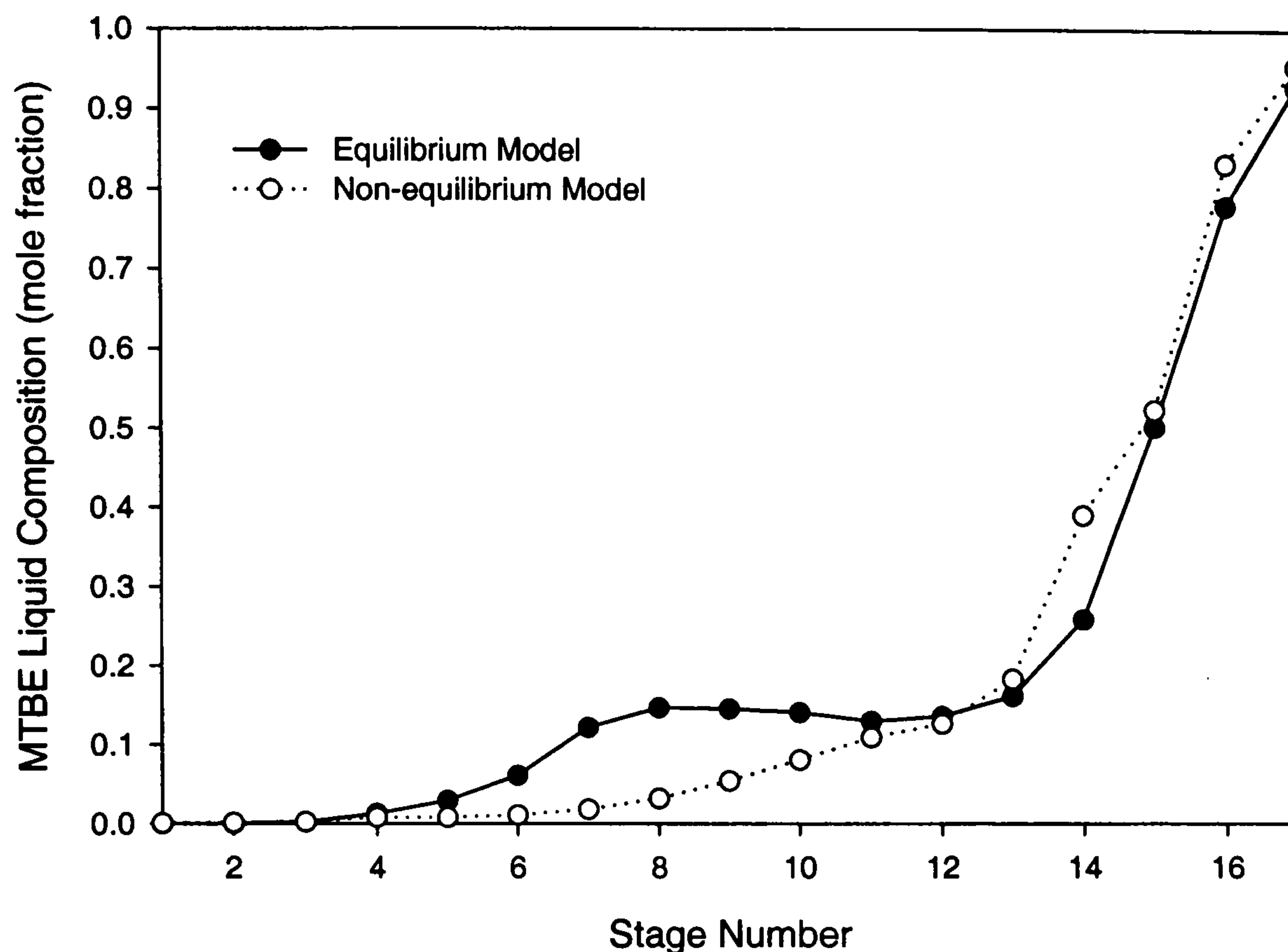


Figure 4.6: Simulation results with the equilibrium and non-equilibrium model for the MTBE column

column. However, later in this work (Chapter 5) it will be show how to determine which one is the best and which one should be used.

4.3.2 Ethyl Acetate

Several thermodynamic models (for activity coefficients) were used in order to reproduce experimental results given by Suzuki *et al.*, 1971. It has been proved that unless the modified Margules equation for activity coefficients given by Suzuki *et al.*(1970) is used or the association and dimerization of the vapour phase (acetic acid) is taken into account, it is not possible to match the experimental results with the equilibrium model. Fig. 4.7 shows different ethyl acetate composition profiles using the thermodynamic models listed in Table 4.5. Activity coefficient model parameters estimated from

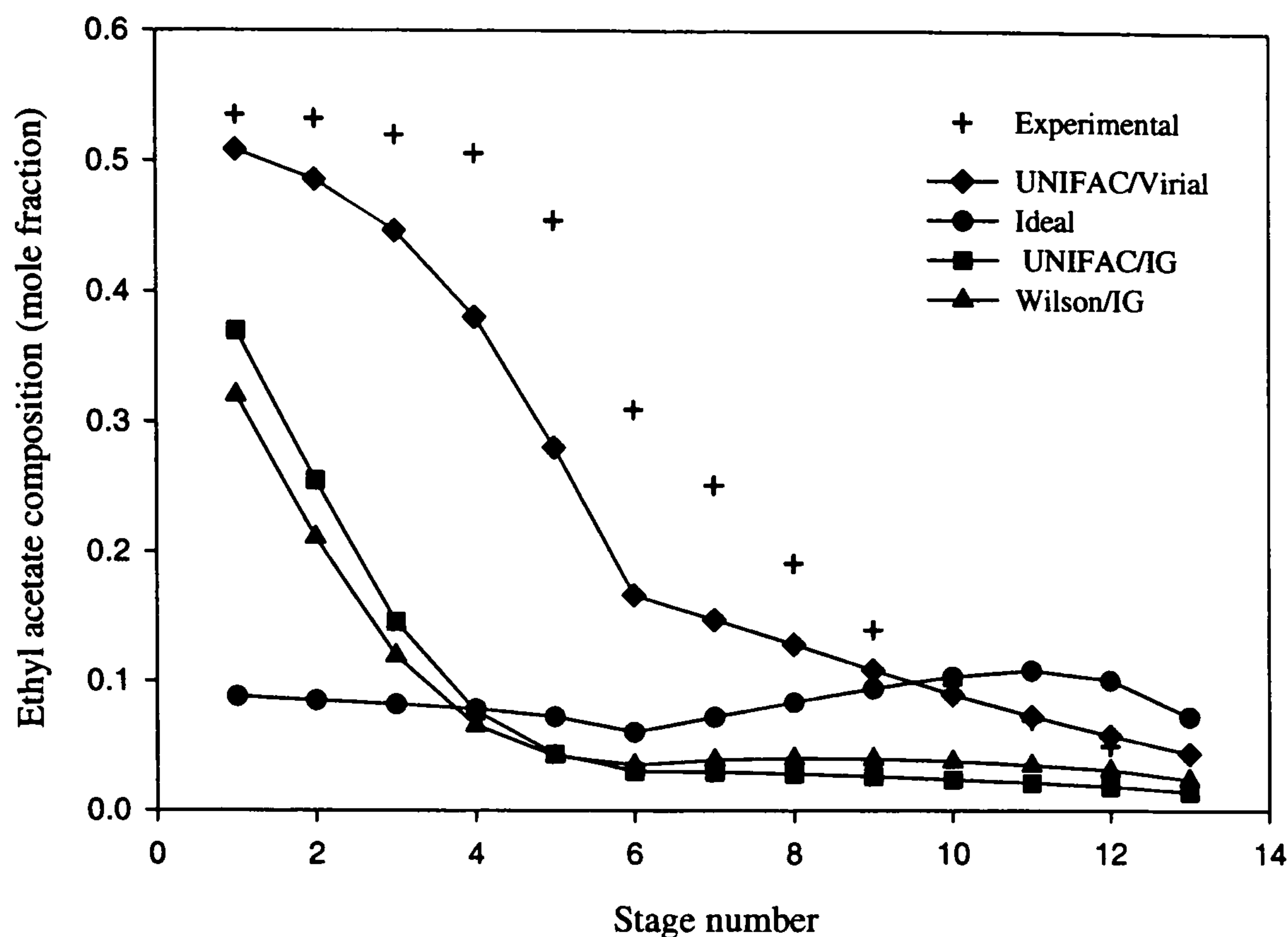


Figure 4.7: Simulation results with different thermodynamic models for the esterification column

vapour-liquid equilibrium data, when used in simulations of reacting systems and physical equilibrium may not give acceptable results.

In Fig. 4.8, the experimental data given by Suzuki *et al.*(1971) are compared with the simulated values from equilibrium (using UNIFAC as thermodynamic model) and non-equilibrium models. Only the final steady state liquid compositions of ethyl acetate on each tray are shown in the plots of Fig. 4.8. Note that no tuning of model parameters has been performed at this stage. The non-equilibrium model performs better than the equilibrium model, a surprisingly good match has been made with the non-equilibrium model for the bottom section of the column, and neither of the models is able to match the reported experimental values for the top section of the column when UNIFAC is used as the activity coefficient model. Using the Margules model

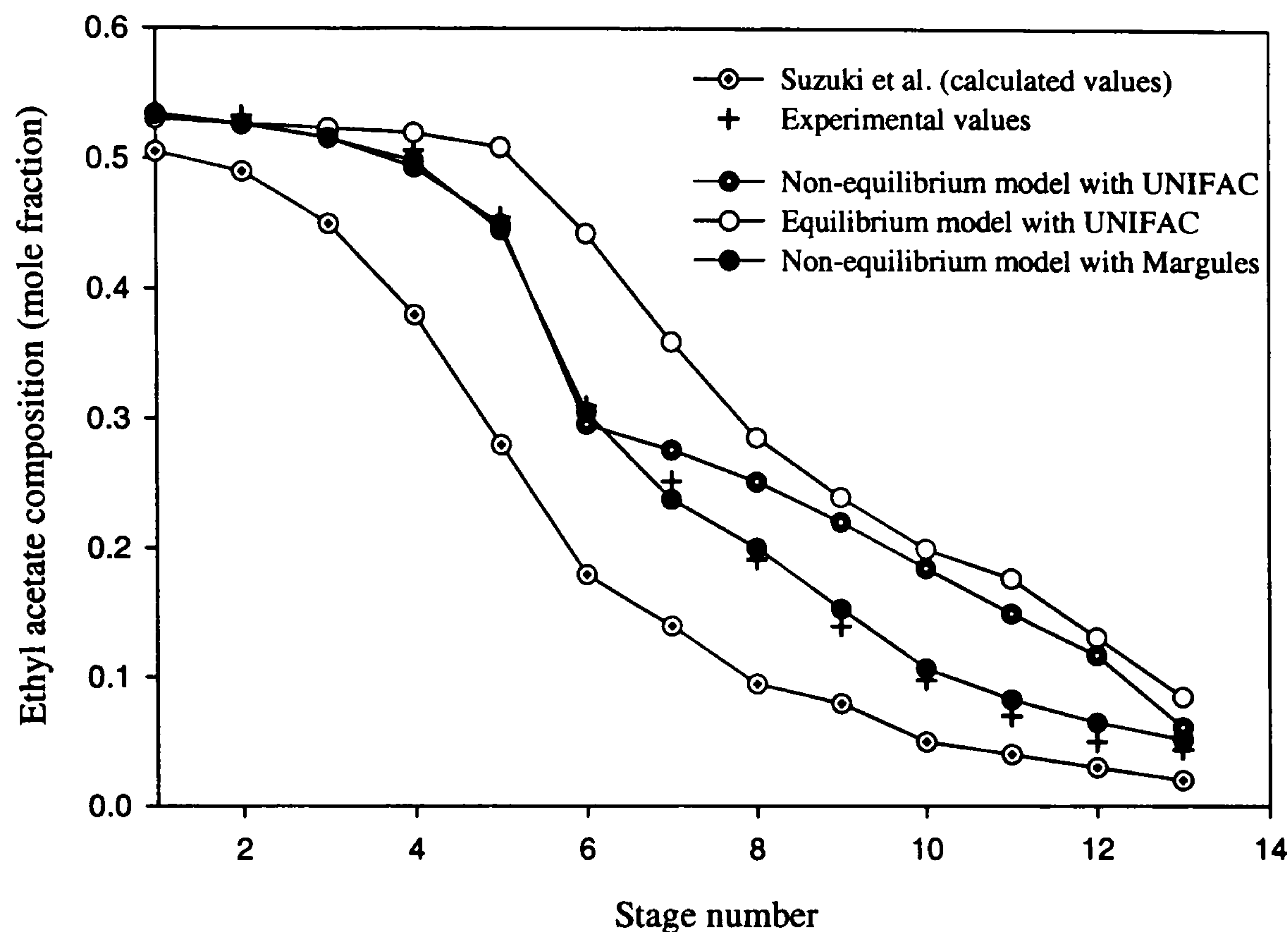


Figure 4.8: Simulation results compared with experimental data for the esterification column

with Suzuki *et al.*(1971) parameters, however, gives a significantly better fit for the entire column with the non-equilibrium model (shown in the plot) as well as for the equilibrium model (not shown in the figure).

Figure 4.9 shows the simulated total mass transfer rates for the four components in this system. Mass transfer from the liquid to the vapour phase is considered to be negative. As can be expected, since ethyl acetate is the more volatile component (but multicomponent mixtures often behave differently from binary systems), it transfers from the liquid to the vapour phase in all the trays. The non-equilibrium model, therefore, qualitatively and quantitatively, gives the correct mass transfer behaviour.

The mass transfer values obtained with the non-equilibrium model, are com-

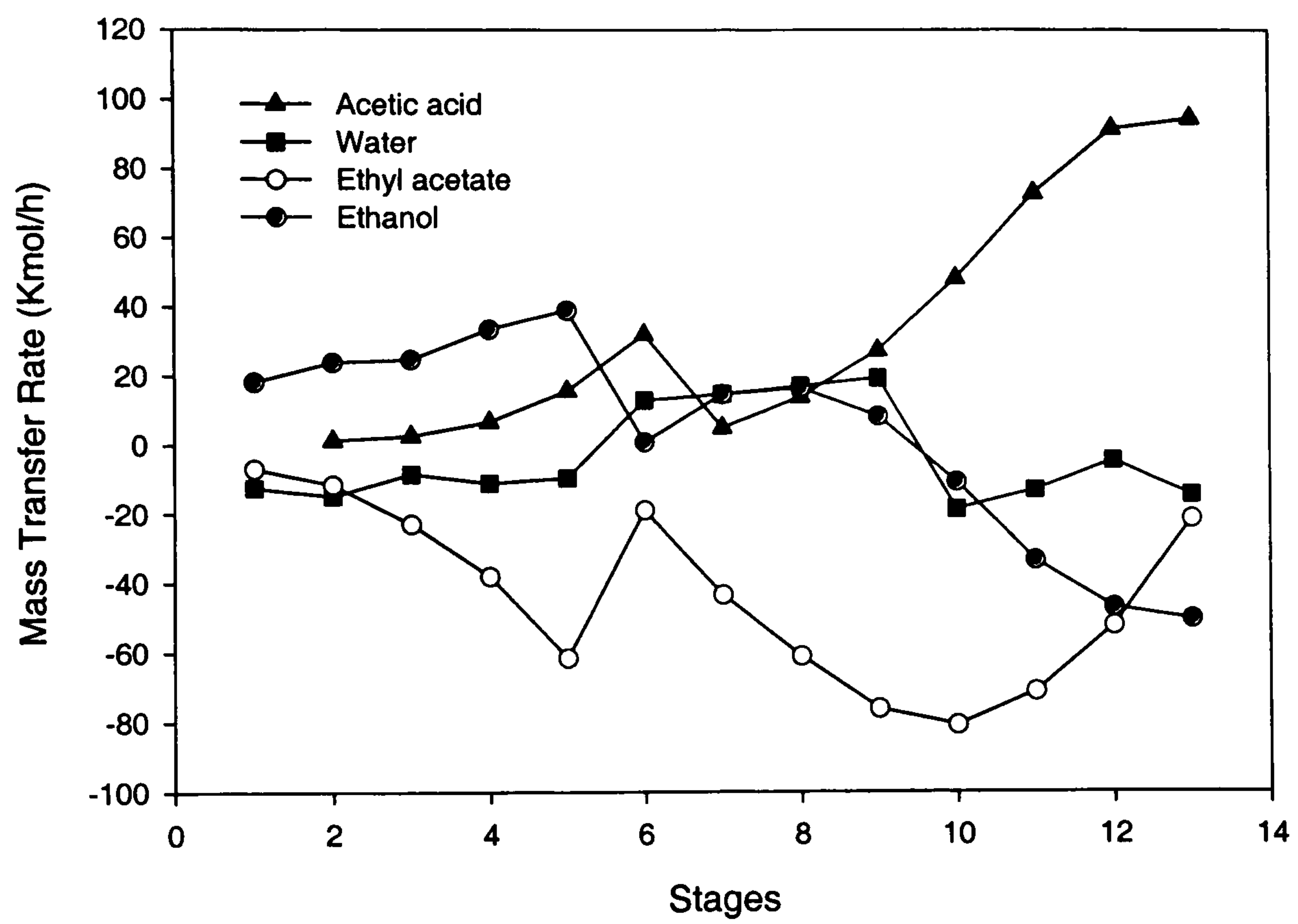


Figure 4.9: Mass Transfer rate for the esterification column

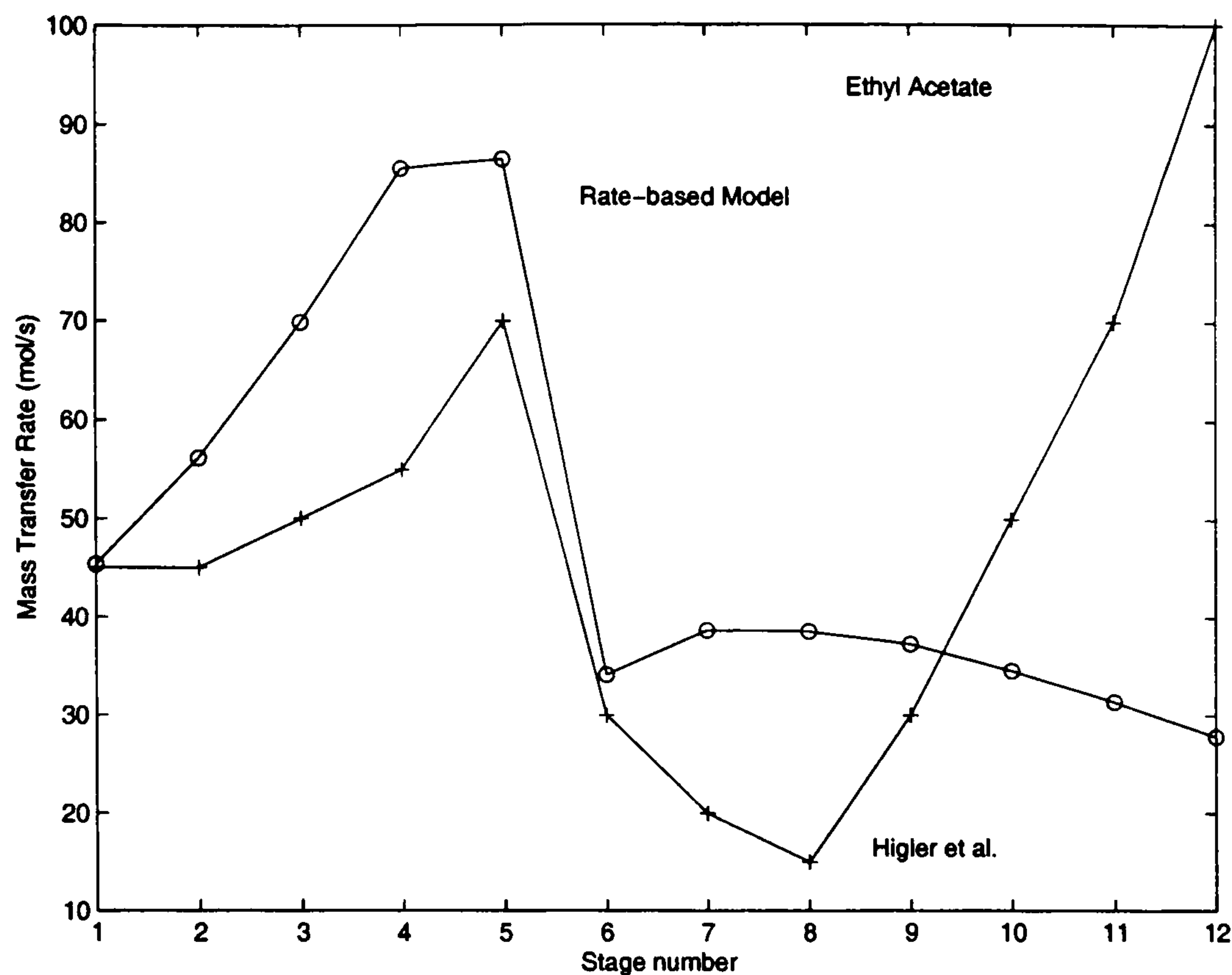


Figure 4.10: Comparison of mass transfer rate with literature results

pared with those of Higler *et al.*(1998). The trend comparison is rather good as can be seen from Fig. 4.10 for one of the components (ethyl acetate).

4.3.3 Depropanizer Column

Different thermodynamic models have been also used for this system, in order to identify possible set of sensitive parameters to the simulation results (as well as good agreement with previous reported results). There are practically no variations between the results obtained with the Peng-Robinson EOS and the SRK-EOS. Since both equations of state lead to similar results, the rest of the work done for this system has used the Peng-Robinson equation of state in order to keep consistency with literature results.

In Fig. 4.11, the simulated steady state liquid composition profiles with the non-equilibrium model for the depropanizer column are shown. The computed composition profiles compare fairly well with those reported by Taylor and Krishna (1993). The results of Taylor and Krishna are not shown in Fig. 4.11. These results validate, at least qualitatively, the non-equilibrium model of this work and the Taylor and Krishna model since approximately

similar simulated behaviour is predicted.

Simulation with the equilibrium model has also been performed. The results differ somehow from those predicted from the non-equilibrium model, but the results from the equilibrium model are not unacceptable.

The ChemSep package (Kooijmann and Taylor, 1996) has been used to compare the results obtained with the general model. Simulations with the ChemSep package are compared with our non-equilibrium model. Fig. 4.12 shows the profiles of the vapour composition for the four components. The differences are acceptable.

4.4 Bifurcation Analysis

In order to explore the dynamic behaviour of the reactive systems, a continuation method has been implemented to use with the equations of the general model.

Due to the non-linearity of the general form of the model equations, it is possible that reactive distillation columns may have unstable behaviour or may have multiple steady states, which has already been shown for the case of the MTBE production.

Bifurcation diagrams are believed to give insight, especially in the cases where multiple solutions are present but also for cases where multiple solutions have not been found. Bifurcation analysis will, furthermore, determine the existence or not of multiple solutions.

The final steady states of the reactive systems obtained by simulation are also verified through bifurcation analysis. To perform continuation, it is possible to use some software already available, for example, PATH (Petersen, 1989); CONT (Kubíček and Marek, 1983; Schreiber and Marek, 1991 (1995); Kubíček, 1976). As an introduction into the theory of bifurcation, several books are available (Mess, 1981; Hilborn, 1994; Solari *et al.*, 1996; Thompson and Stewart, 1986).

In this work, all continuations are performed with the software program

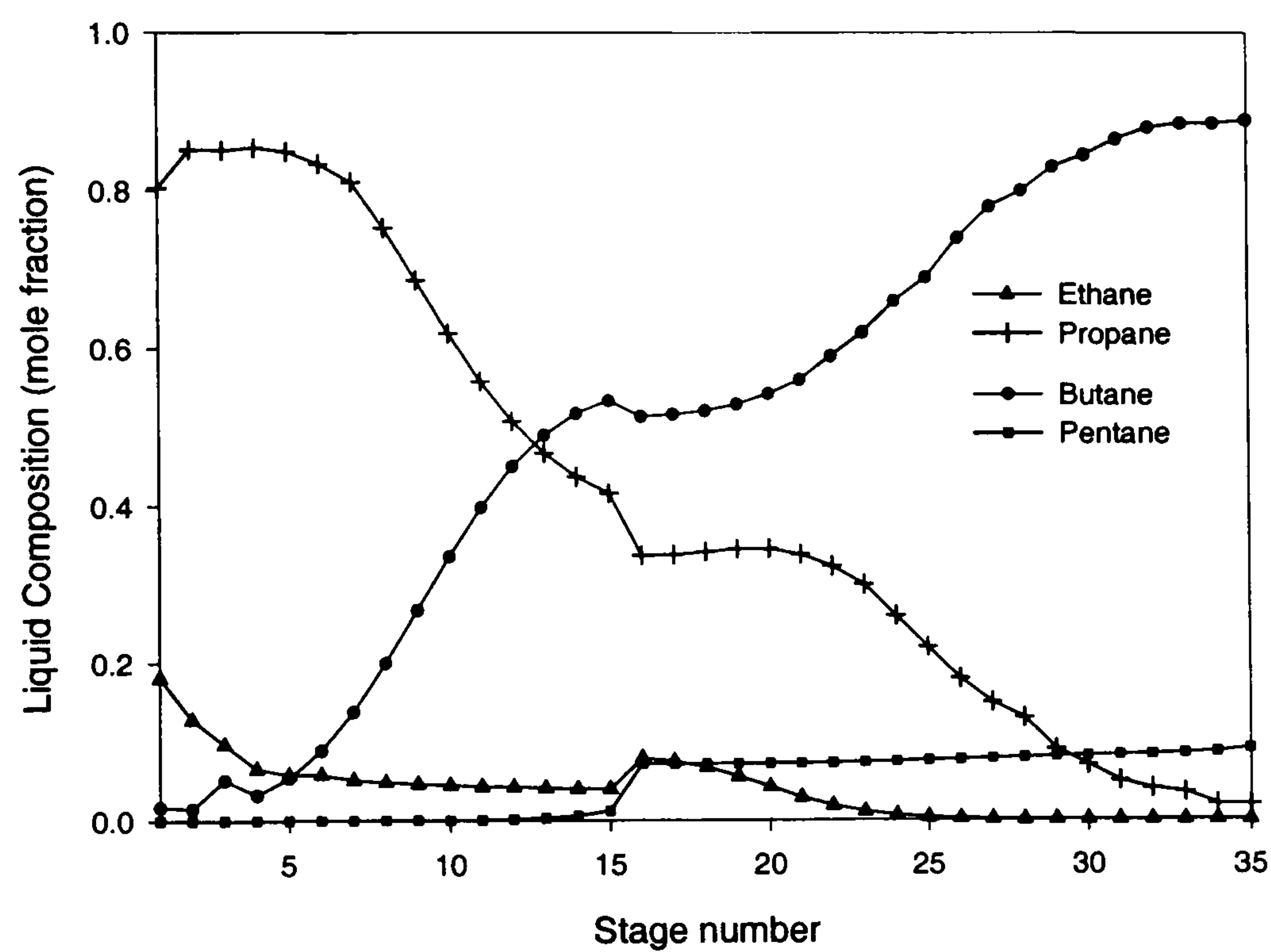


Figure 4.11: Simulation results with the non-equilibrium model for the depropanizer column

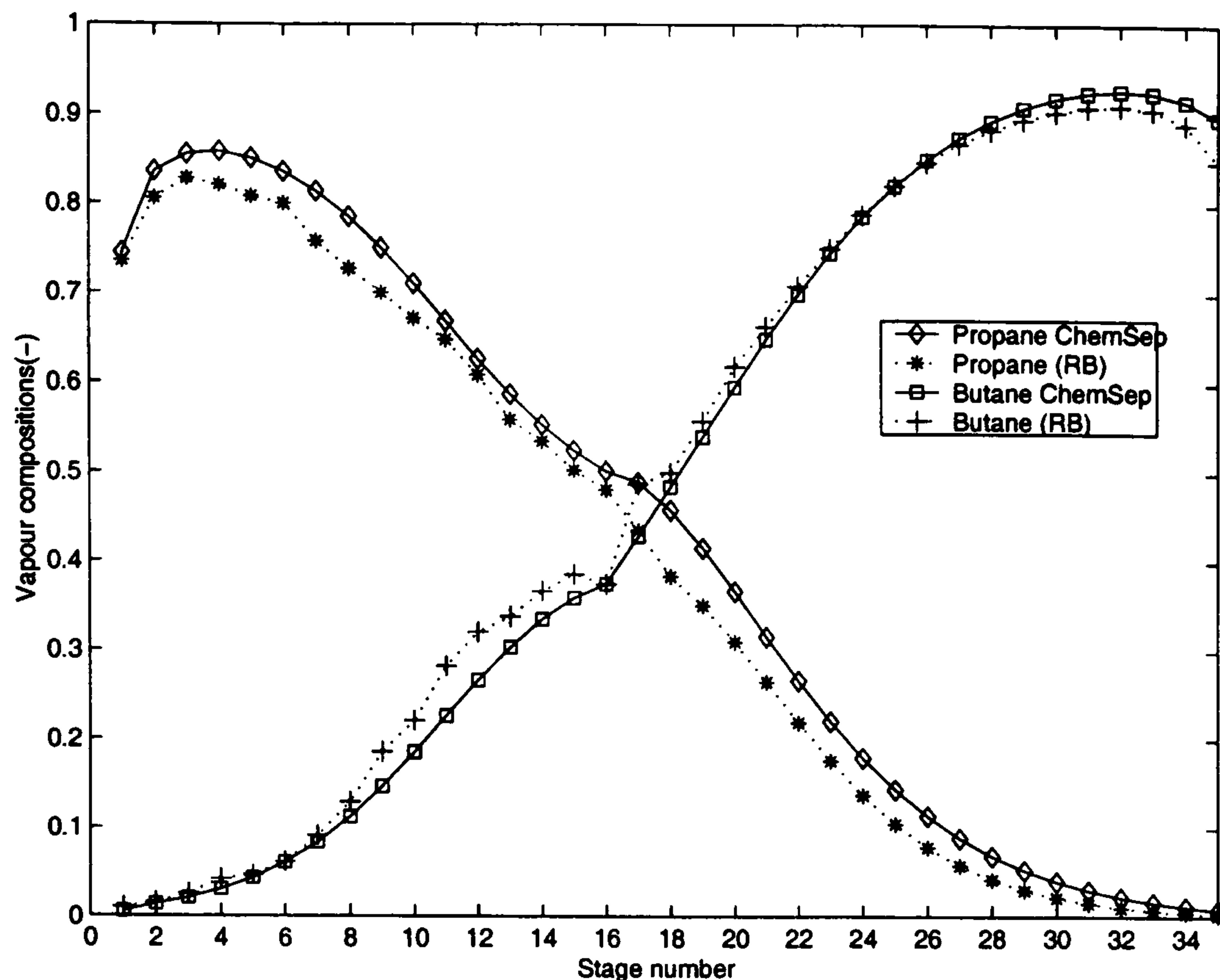


Figure 4.12: Vapour compositions compared with ChemSep simulations

CONT (Kubíček and Marek). The software has been added to the set of solvers for the ODEs, AEs and DAEs.

The continuation method-based solver makes it possible to calculate all the steady-state solutions, stable and/or unstable, with respect to two design variables (bifurcation parameters). Therefore, for any two preselected bifurcation parameters, it is possible to generate bifurcation diagrams and analyse the steady state behaviour of the distillation operation.

After defining the feed stream (compositions, temperature, pressure) in the column there are remaining two degrees of freedom. These are chosen as bifurcation parameters.

4.4.1 Applied Bifurcation Analysis

Bifurcation diagrams have been produced for the two reactive systems, ethyl acetate and MTBE production.

For the bifurcation analysis, two parameters (design variables) were chosen. The results show the analysis for a fixed value of one parameter.

For the esterification column, the bifurcation analysis results are shown in Fig. 4.13. Ethyl acetate composition at the top of the column (product) as a function of reflux rate for a fixed value of the reboiler heat duty is shown in the Figure. As can be seen, only one steady state (stable) is found for all the range of reflux rate studied. The operating point of the nominal design is also marked in the Figure, showing that the design can be optimized to achieve slightly higher product purity.

The analysis has also been made varying reboiler heat duty for a fixed value of the reflux flow rate and again only one solution (stable) has been found in all the range of the variable studied.

For the MTBE column, the bifurcation analysis results are shown in terms of MTBE composition in the bottom product as a function of reflux rate for a fixed value of vapour boil-up in Fig. 4.14 and as a function of vapour boil-up for a fixed value of reflux rate in Fig. 4.15.

It should be noted that for this column, the results of Figs. 4.14 and 4.15 correspond to the fixed configuration of the reactive distillation column where the multiplicities have been already reported (the methanol feed is located in stage 10 and the butenes are fed at stage 11).

It can be noted that while for the esterification case no multiple solutions could be found for the range of reflux ratio or for the range of reboiler heat duty investigated, for the MTBE column, multiple steady states were found for a range of reflux ratios. The region of operation for this system has been calculated as a $\pm 20\%$ of flowrates in the column, starting from the flowrates calculated from the nominal design of the column. According to Fig. 4.14 the operation of this column will have some serious problems, probably changing from a high purity of the product to almost no product recovery.

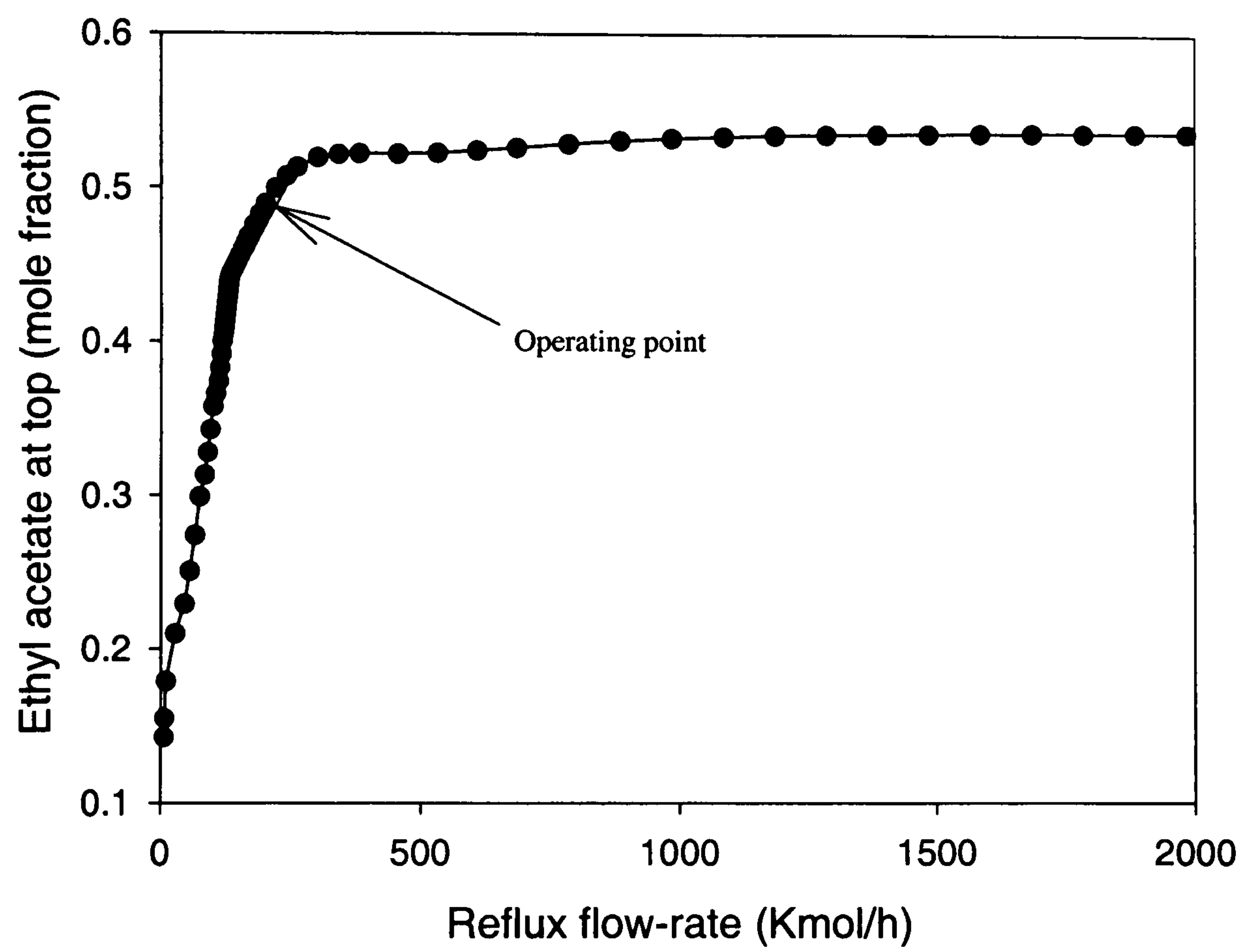


Figure 4.13: Bifurcation diagram for the esterification column varying reflux flow rate

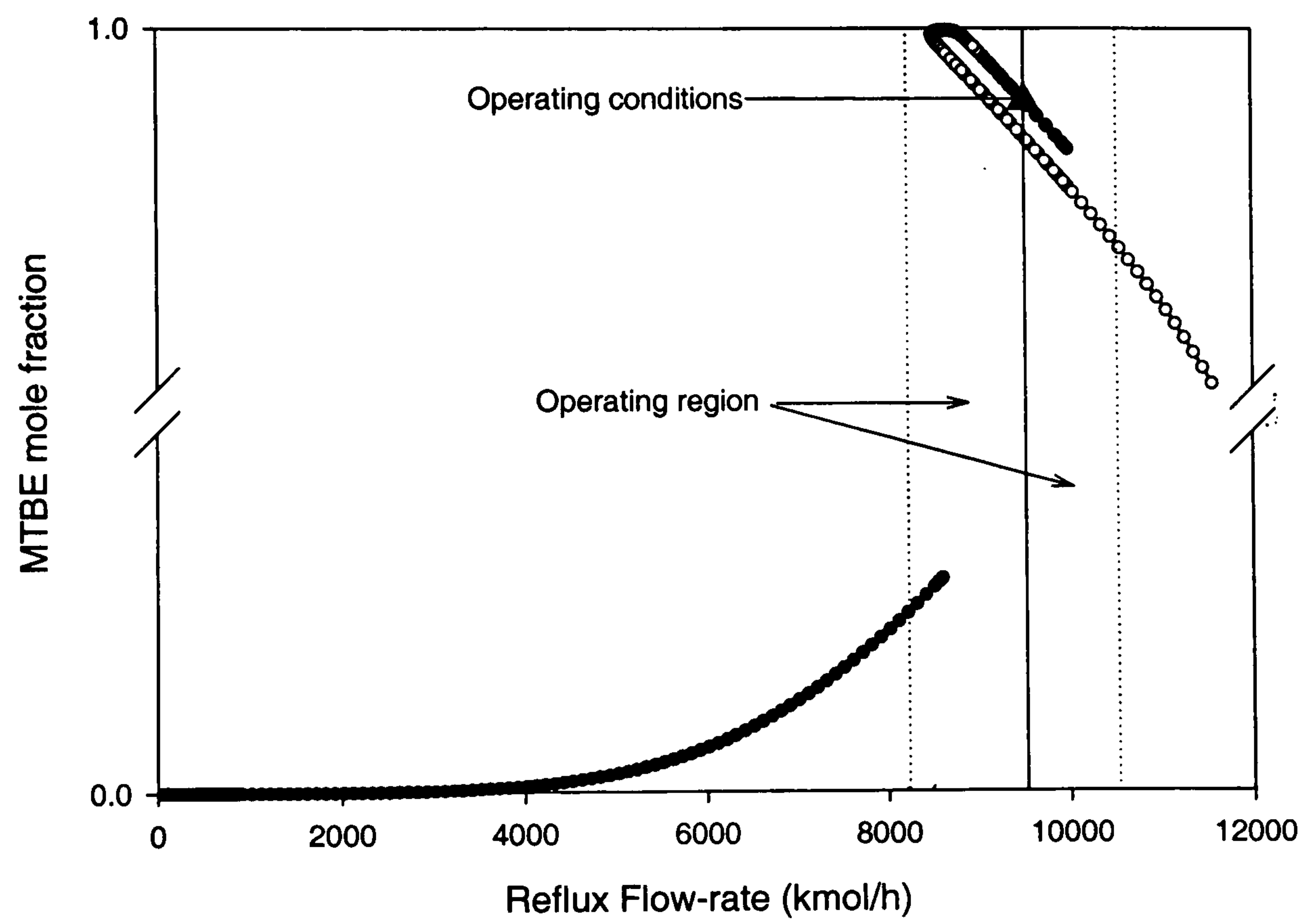


Figure 4.14: Bifurcation diagram for the MTBE column varying reflux flow rate

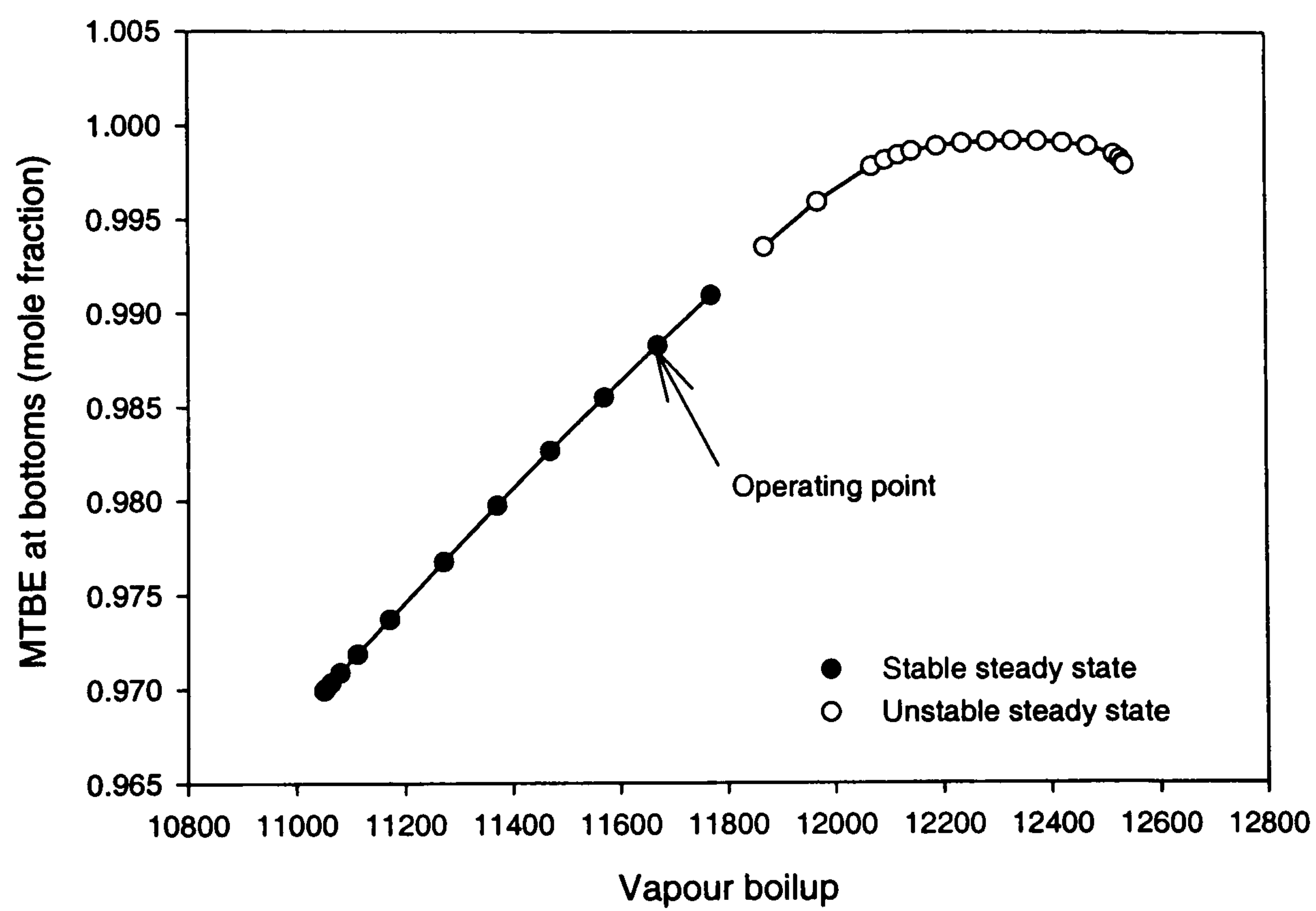


Figure 4.15: Bifurcation diagram for the MTBE column varying vapour boil-up

4.5 Conclusions

The systems selected in this work showed different types of phenomena which helped to demonstrate the strength and the versatility of the general model as well as its applicability.

The non-idealities of the systems have been captured through the general model. The analysis of the mixture to be separated or reacted away together with first simulation results gives an identification of sensitive parameters. The set of sensitive parameters that has been identified for each system helps in the design of a distillation column.

Systems presenting multiple solutions, highly non-ideal mixtures, as well as a ‘simple’ mixture of hydrocarbons for a ‘normal’ distillation column have been selected in order to validate the general (hybrid) model as well as its capability of handling various problems.

Two other systems have been tested with the general model although not presented in this thesis. The systems are, one reactive system: methyl acetate production, (Papaeconomou, 1999) and one non-reactive: methanol-ethanol-acetone (Pilavachi *et al.*, 1999), enhancing the capability of the general model.

The aim of this work was to cover a wide range of systems. Being able to cover different aspects of different systems will definitely help when a new system has to be simulated or analysed.

The bifurcation analysis also contributes to the development of a computer aided environment which facilitates the solution of different simulation problems.

The hybrid modelling approach helps to avoid problems of mismatch between model and simulation results as well as between two forms of models (for any two forms of models, a sub-set of simulation results should be approximately the same).

The results presented in this Chapter have mainly focused on highlighting and validating some of the features of the general model. In the following

Chapter, the application of hybrid models, *i.e.*, the solution of a combined equilibrium and non-equilibrium model, is presented. Through a detailed analysis in terms of tray efficiency, mass transfer and reaction rate, and Gibbs free energy as a function of time a switch between non-equilibrium and equilibrium model can be made.

Chapter 5

Analysis with Hybrid Models

Hybrid models are useful in many distillation operations when a product specification should be met. Hybrid models result in improved computational efficiency compared to the single model because they provide better initialisation and flexibility.

As stated before (Chapter 3) the decision to use a hybrid model can be made *a priori*, or *a posteriori*. In this Chapter we will focus on using hybrid models after the simulation has started, *i.e.*, switching between the non-equilibrium to the equilibrium model.

The general distillation model presented and validated previously, allows the monitoring of a selected set of phenomena as a function of time and/or tray. It computes the values of:

- excess Gibbs free energy, G^E , and,
- efficiency parameter, E^M .

Both can be estimated without significant additional computation time (most of the needed variables and parameters are already known or calculated during the simulation).

The transient path of excess Gibbs energy for all trays is monitored over the simulation time. Those that approach an asymptotic minimum value may be considered to be at a pseudo-equilibrium state. The difference of the values of n^l , n^v (represented by Δn_v and Δn_l) are also monitored at the present

time and are expected to approach zero when the excess Gibbs energy approaches a minimum. Tray (or point) efficiency in the column is calculated during the simulation time, or after the simulation has finished. Efficiency values close to unity represent an equilibrium (or close to equilibrium) stage.

These results can then be used as a criterion by switching between the non-equilibrium model to an equilibrium model.

The main idea of this approach is to obtain useful insights to the reactive distillation operation as well as to save computational time while capturing all the non-idealities of the system. The non-equilibrium model is believed to reproduce accurately the behaviour of the mixture in the column but it is time consuming. Whenever the non-equilibrium model is approaching to simulate an equilibrium model (the limit of any non-equilibrium model is the equilibrium), all the extra equations are no longer needed because an equilibrium model can be used instead.

5.1 Monitoring of Phenomena through Gibbs Free Energy

Since, during a dynamic simulation with the non-equilibrium model, the component compositions and chemical potentials are known in each phase, evaluation of the Gibbs energy on the tray at any time is performed. This analysis of the transient path of the Gibbs energy for each tray will indicate the approach (or not) to equilibrium for each tray.

Studies of tray Gibbs energy as a function of time have been made for the two reactive systems. Plots in Fig. 5.1 show the tray Gibbs energy as a function of time for the esterification system (for trays 1 and 7). It can be noted that while the Gibbs energy value on tray 1 is asymptotically approaching a minimum, the same is not true for tray 7. Note that while plots of Gibbs energy surfaces as a function of composition may not be smooth (possibility of local solutions), Gibbs energy plots as a function of time appeared to be, in all cases studied, first order.

Trays 2 and 3 have also been found to behave the same way as tray 1. The Gibbs free energy is asymptotically approaching to a minimum. The rest of

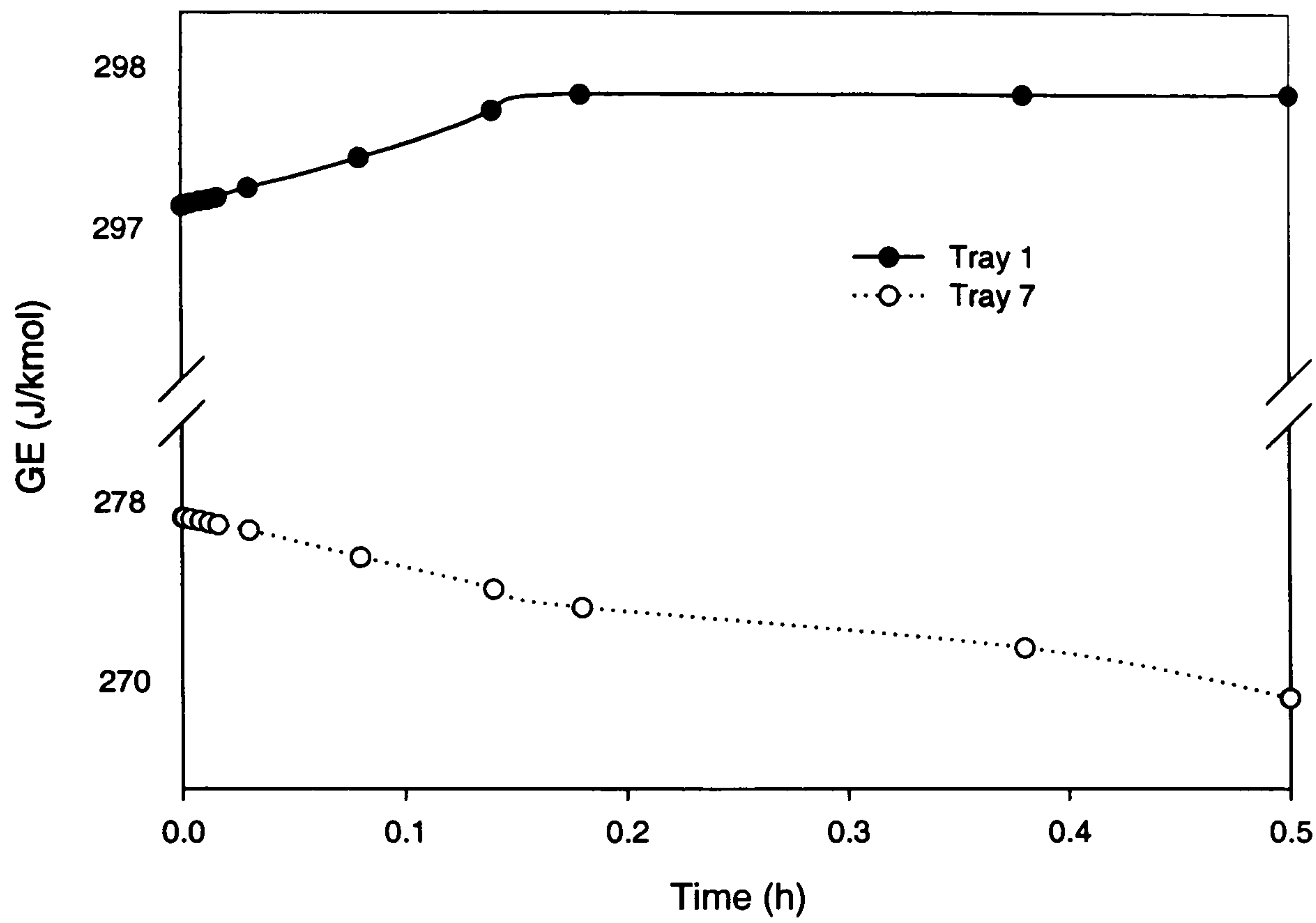


Figure 5.1: Excess Gibbs energy for the esterification column. Trays 1 and 7.

the column follows the behaviour of tray 7. The Gibbs free energy keeps on decreasing as a function of time.

The final steady state is stable and the mass transfer rate differences (Δn_l and Δn_v) are approximately zero. It is highly likely, therefore that these results indicate a state close to equilibrium for trays 1-3.

For the MTBE column, the tray Gibbs energies as a function of time (see Fig. 5.2) show a decreasing trend, thereby indicating a state still further away from equilibrium. In this case, mixed model simulation is not necessary. Note that at steady state, the Gibbs energy for a non-equilibrium process does not have to be at a stationary value. This also means that the non-equilibrium model is the model that should be used when simulating this column. At the

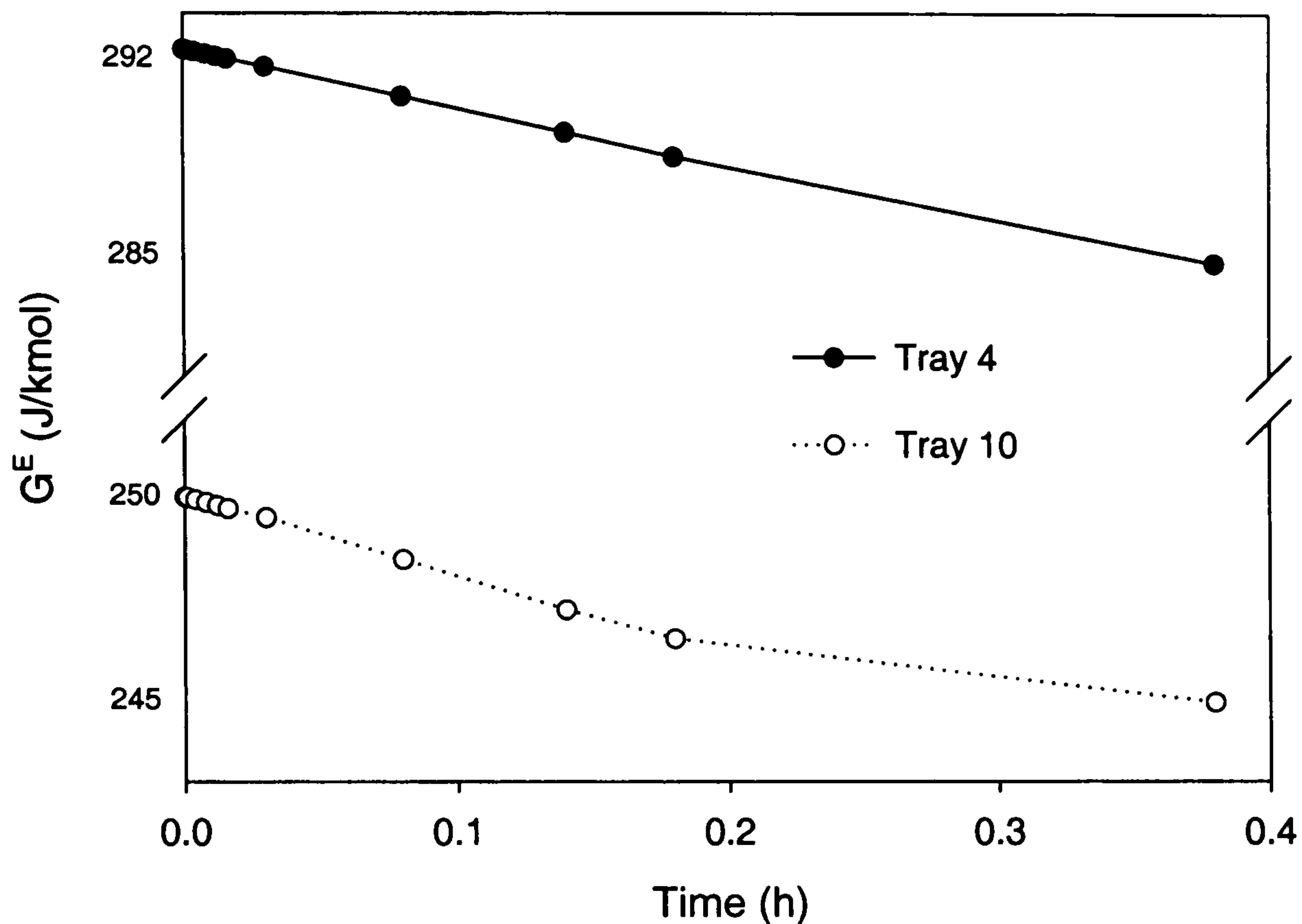


Figure 5.2: Excess Gibbs energy for the MTBE column. Trays 4 and 10.

end of Chapter 4 it was not clear which model should be used. By analysis of the system, this issue becomes clear. All the complex dynamics as well as different non-idealities are better captured through the non-equilibrium model.

5.2 Tray Efficiency Analysis

Efficiency analysis has been studied for the esterification case as well as for the depropanizer column.

For the esterification case, using the composition profiles of Figs. 5.3, the component efficiency-like parameters (shown in Fig. 5.4) have been esti-

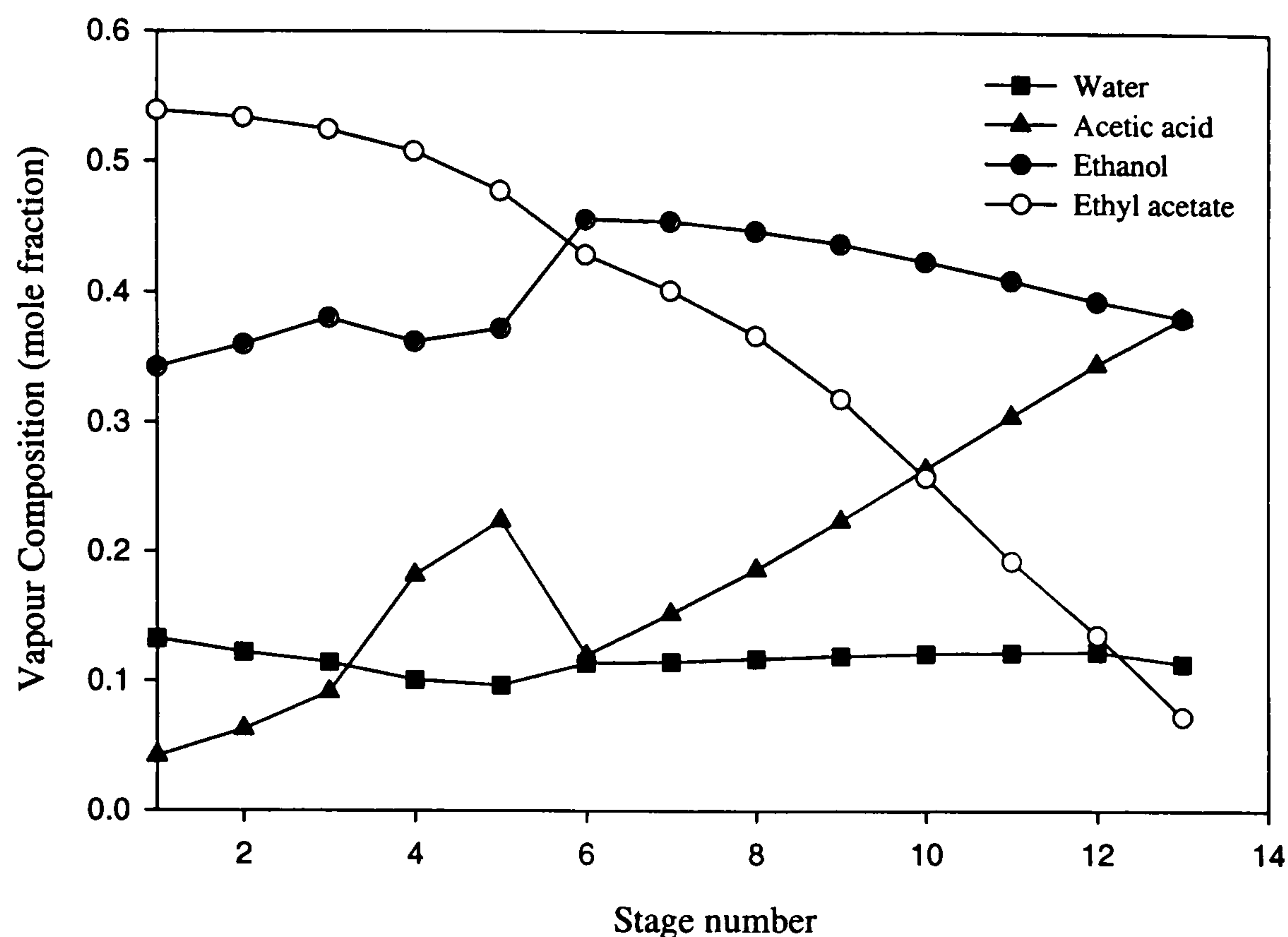


Figure 5.3: Vapour compositions for the esterification column

ated. Figure 5.3 shows the corresponding simulated vapour compositions with the non-equilibrium model. Without any introduction of noise and with assumption of perfect mixing in bulk phases, the component efficiency-like parameters lie between 0 and 1.

As previously predicted through the analysis of the excess Gibbs free energy, component efficiency for trays 1 to 3 are very close to unity, giving an extra reason to believe that these stages are actually at equilibrium.

For the rest of the column (trays 4-13) efficiency values vary between 1 and 0.6. A tray efficiency of 0.7 should predict accurate results for the system.

Tray efficiency analysis is also highlighted for the depropanizer column in Fig.

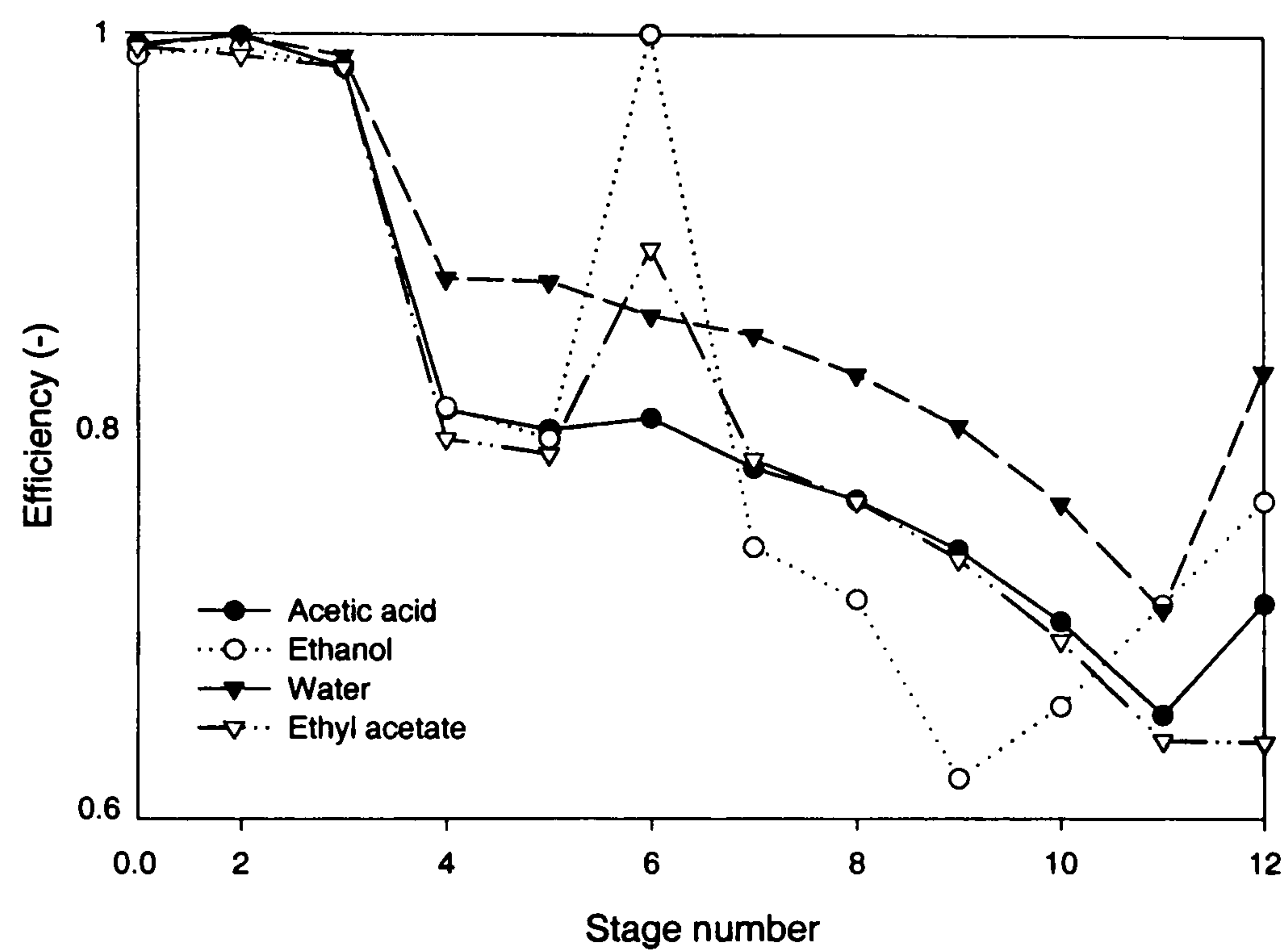


Figure 5.4: Efficiency calculated for the esterification column

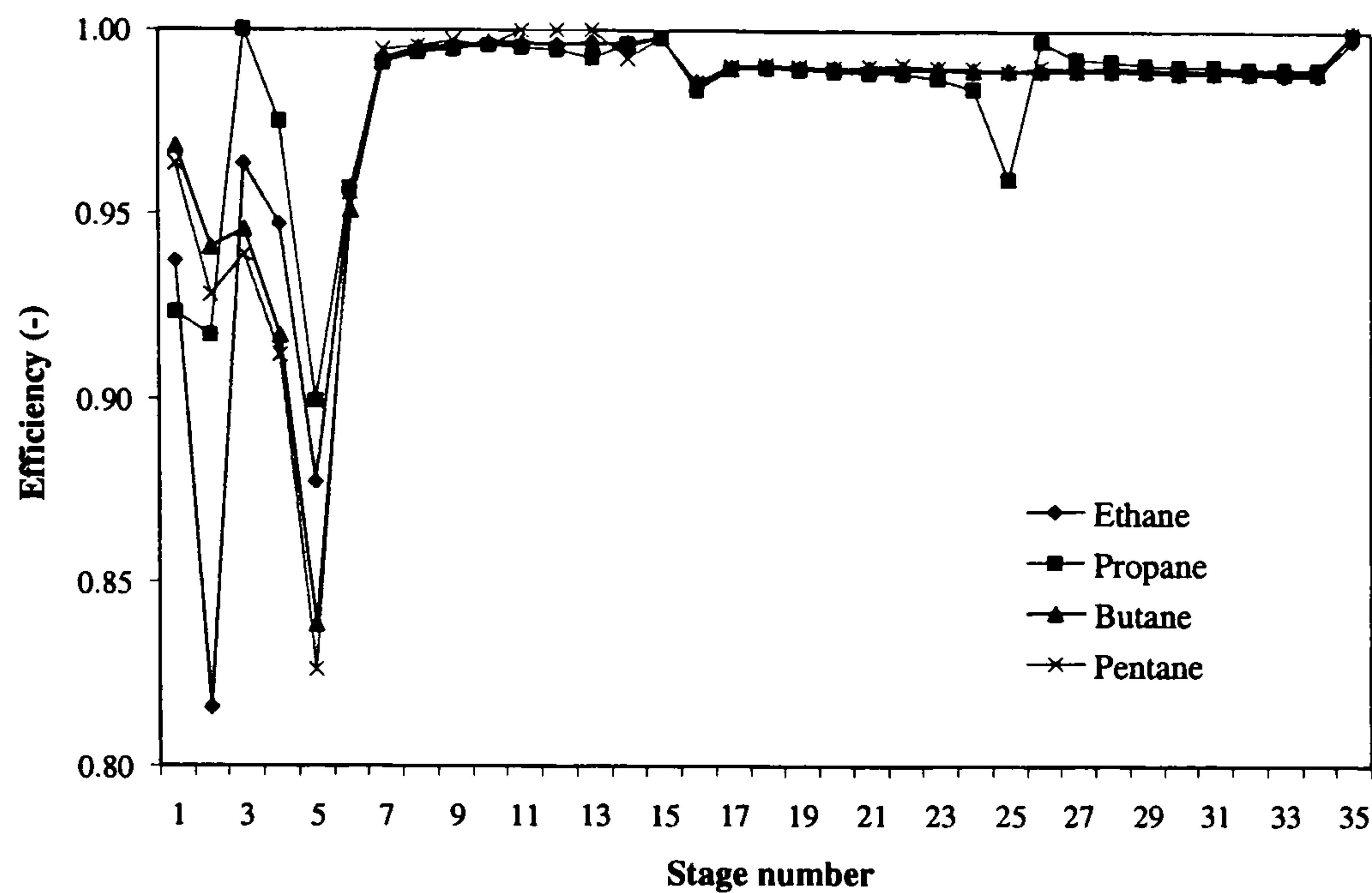


Figure 5.5: Efficiency calculated for the depropanizer column

5.5 where the calculated component efficiency-like parameters are shown. An important point to note here is that all the component efficiency-like parameters again lie between 0 and 1, varying between 0.8 and 1, with the largest deviations from unity observed at the top of the column. The simulations with the non-equilibrium model for this system again showed the same phenomena as for the esterification case. The calculated vapour compositions used in the calculations of the efficiency-like parameters are shown in Fig. 5.6. This result is not surprising since perfect mixing in the bulk phases have been assumed. If measured composition values are used, perfect mixing probably will not be valid, resulting in erratic efficiency values. This condition can be simulated by adding noise (for example, randomly change the simulated compositions by a factor of $(1e - 03)$ to the simulated steady state compositions (the efficiencies vary between $-\infty$ and ∞)). Figure 5.7 shows the calculated erratic component efficiencies with 'noise' added to the calculated compositions for the non-equilibrium model.

If we compare our results with those of Taylor and Krishna (1993) we can observe a large disagreement. From practical experience of this column it

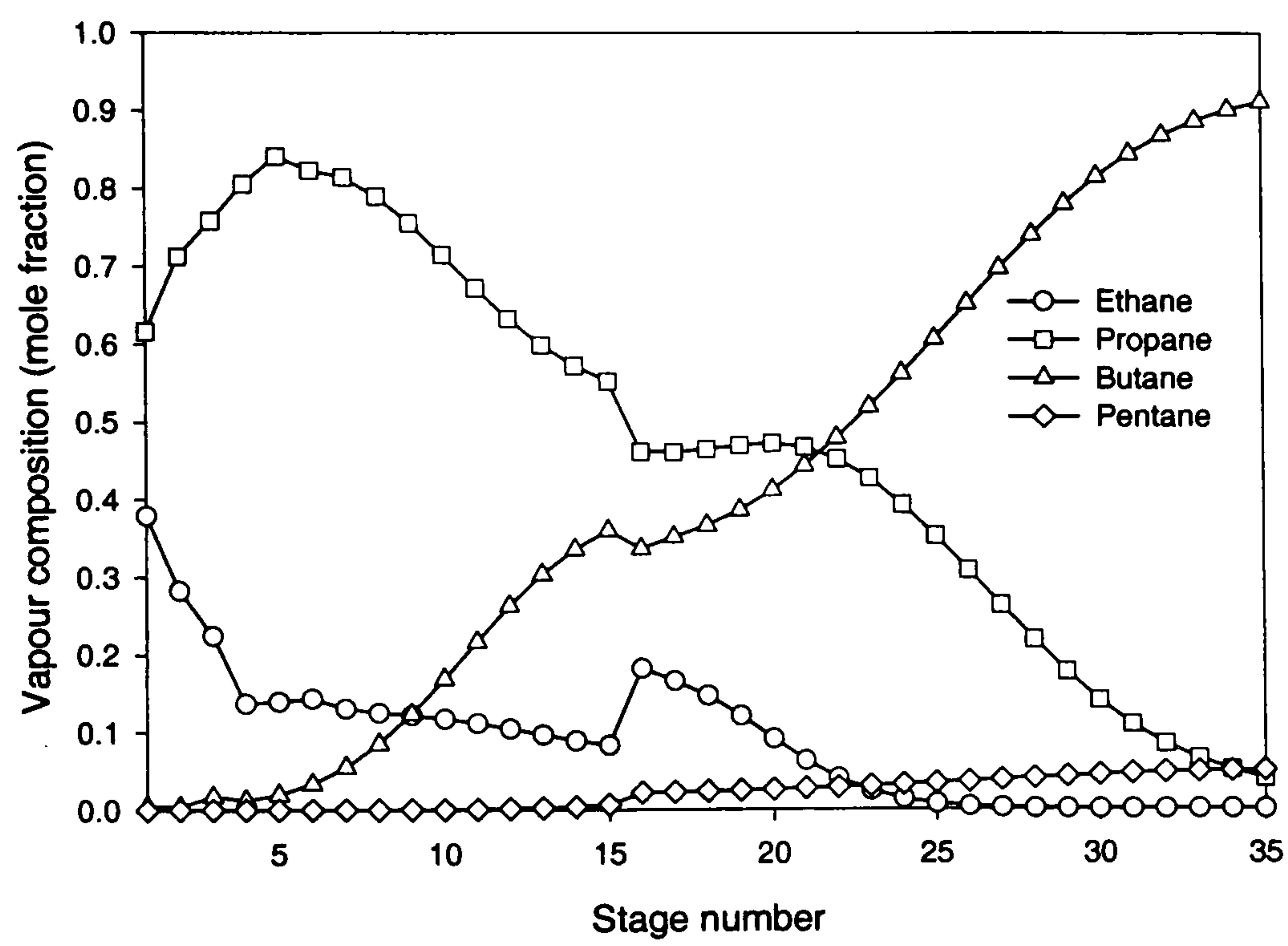


Figure 5.6: Vapour composition for the depropanizer column

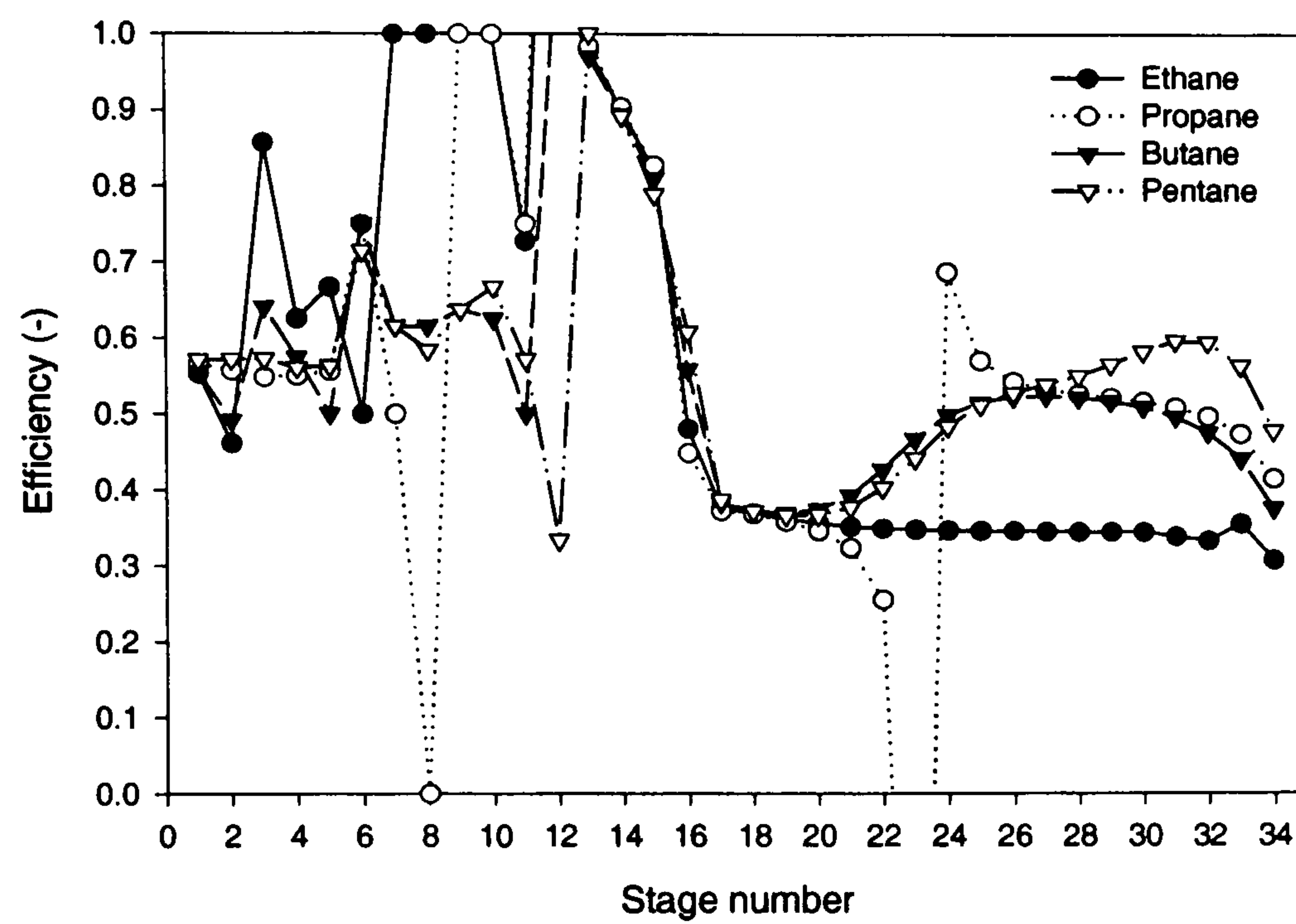


Figure 5.7: Efficiency calculated for the depropanizer column far from steady-state

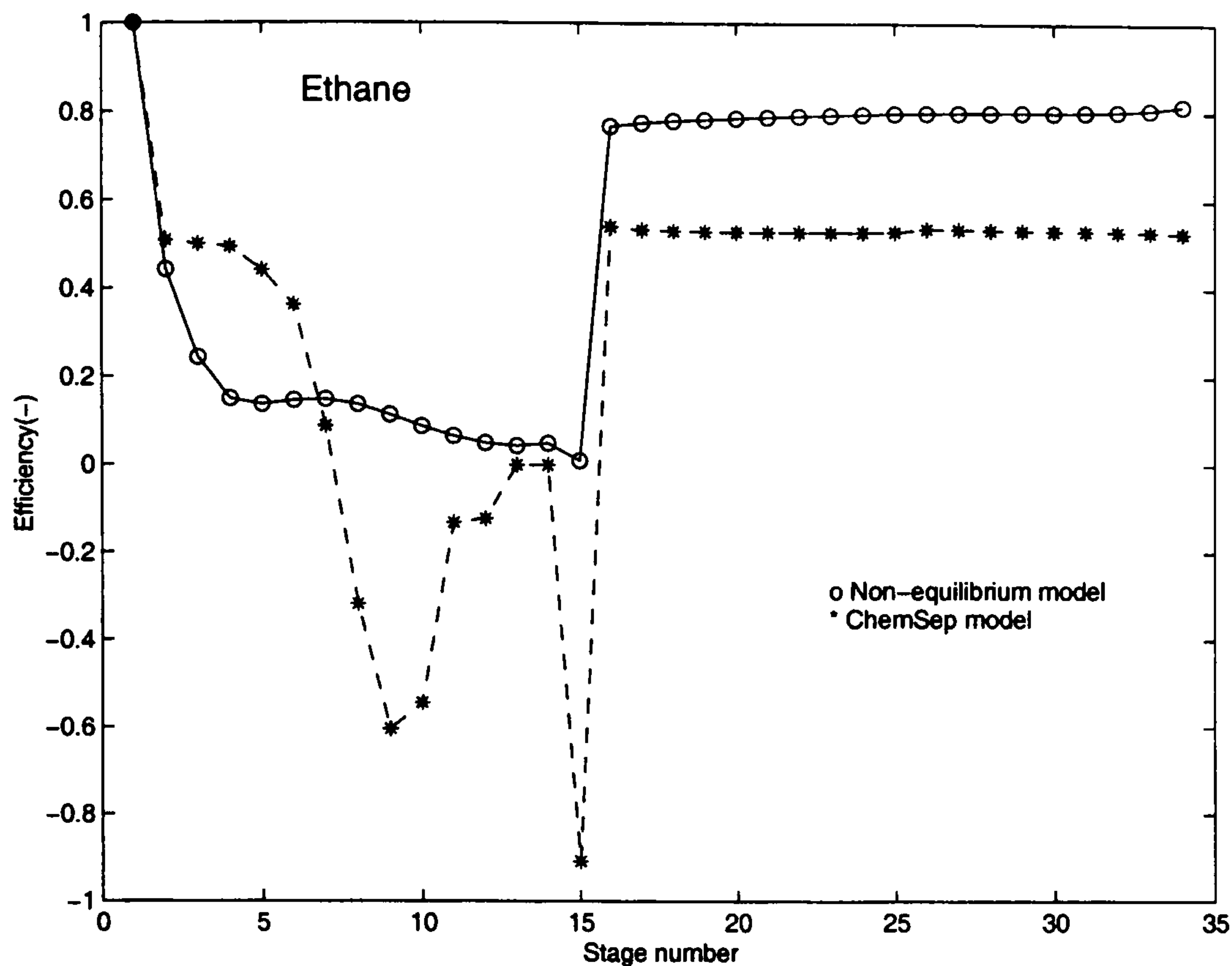


Figure 5.8: Efficiency calculated for the depropanizer, compared with those of ChemSep: Ethane

is known that the global efficiency of this column is around 0.7, which are actually less than those predicted by the non-equilibrium model in this work.

Looking back at the assumptions made when formulating the problem, we decide to include resistance in the liquid phase, which has been considered negligible. Re-running the simulations, now considering both resistances, we obtain a global efficiency of around 0.7. Results are close to Taylor and Krishna (1993) but still we get the efficiencies in the bandwidth 0-1. This can be seen from Figs. 5.8 and 5.9 where the efficiency for ethane and propane are calculated with the non-equilibrium model and plotted against the efficiency calculated using the ChemSep program (Kooimann and Taylor, 1996).

The main point of the difference, is the way y_i^* is calculated. In this work, y_i^* is calculated using the composition at the interface, ie. $y_i^* = x_i^I K(i)$, while Taylor and Krishna, for example, utilise the composition in the bulk of the liquid, ie. $y_i^* = x_i K(i)$. This will not lead to the same value if mass transfer resistance has been considered in the liquid film or the bulk liquid is not perfectly mixed. The fact that real tray efficiencies should remain in the

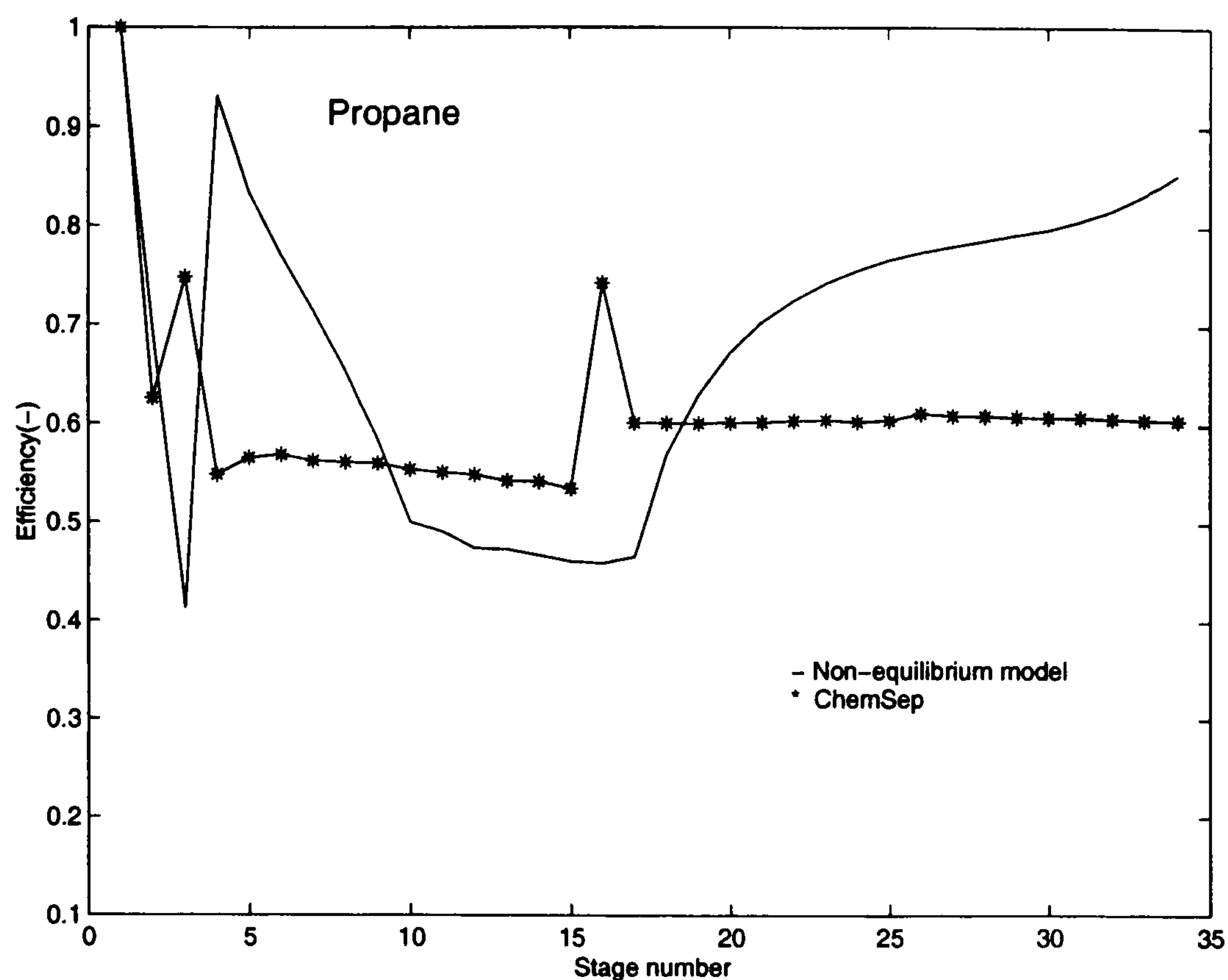


Figure 5.9: Efficiency calculated for the depropanizer, compared with those of ChemSep: Propane

limit 0-1 is not claimed here. However, efficiencies are very much composition dependent, so that, depending which compositions have been considered, different results are going to be obtained. With the definition presented in this work, the efficiency-like parameters will stay within the 0-1 limit. Considering other definitions of efficiency, it is clear that they can go beyond the 0-1 limit, however it is still uncertain if the definition is consistent as well as if the use of bulk composition for calculating the equilibrium composition is correct.

Taylor and Krishna (1993) in the concluding remarks of Chapter 13 (Multi-component Distillation: Efficiency Models) also pointed out that the component efficiencies are very sensitive to the computed equilibrium composition, y^* . They also claim that it is possible to obtain completely different efficiencies by using a different thermodynamic model for computing y^* , which is not surprising. However, it could even be possible to get different efficiencies utilising the same thermodynamic model but only changing the interaction parameters, and surprisingly here both models or parameter sets give a good representation of the vapour-liquid equilibrium data.

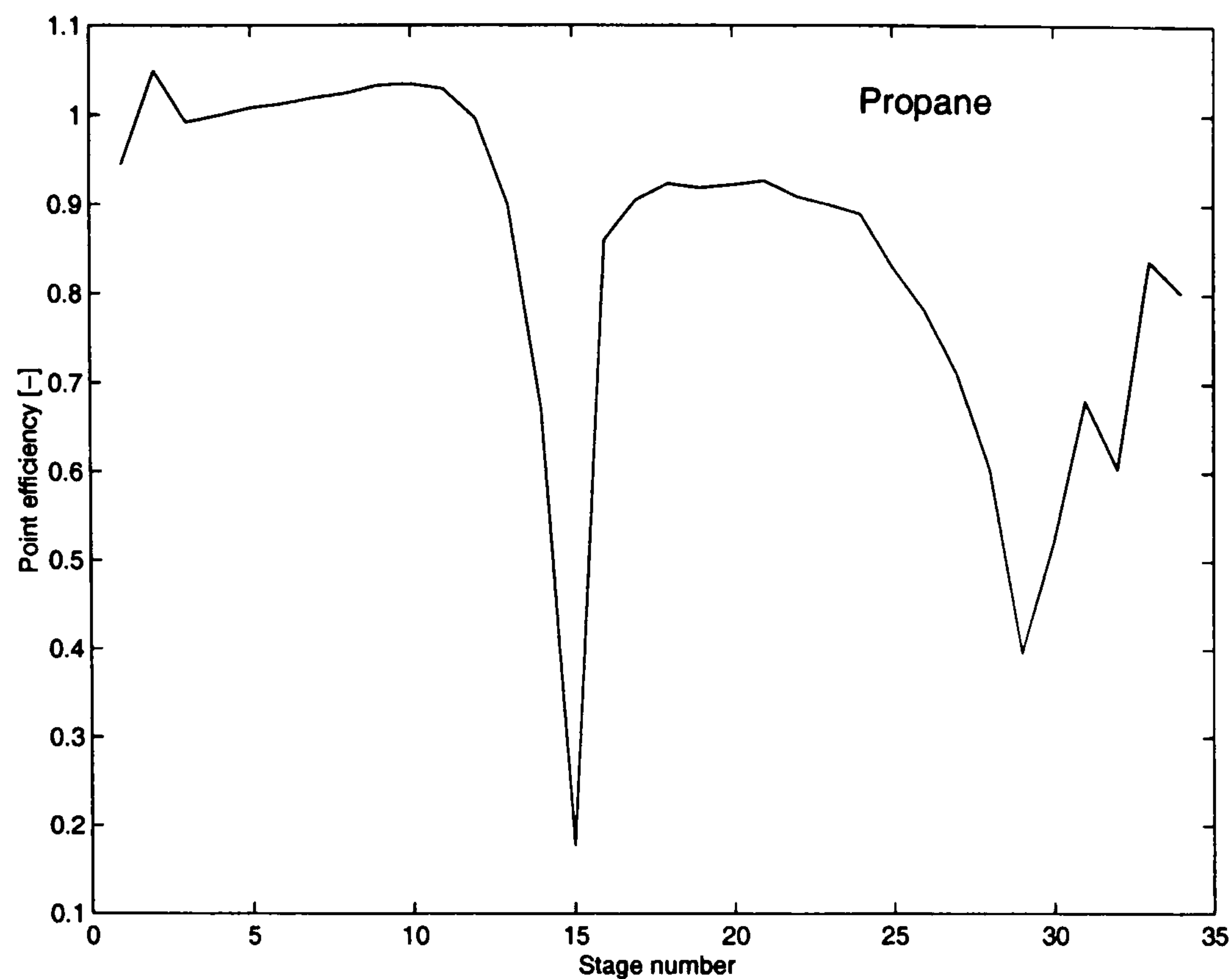


Figure 5.10: Point Efficiency for the depropanizer column: Propane

This is exactly what it is possible to observe in this work. Even when vapour and liquid composition are quite well matched, efficiencies are not.

In order to compare the well-known Murphree efficiency and efficiencies calculated through knowledge of the mass transfer, point efficiencies have also been calculated for the depropanizer column. Figure 5.10 shows the results. Completely different values are obtained. More experience with this kind of efficiency could help in understanding which one is the 'right' one.

Efficiency remarks

In general, there are a few points that should be marked in our definition of efficiency as well as model assumptions. The following conditions, which follow from the assumption of perfect mixing in the bulk phase, must apply:

- a). if $y_{i,p} > y_{i,p+1}$, then $y_{i,p}^* > y_{i,p+1}$, therefore $0 < E_M < 1$.
- b). if $y_{i,p} < y_{i,p+1}$, then $y_{i,p}^* < y_{i,p+1}$, therefore $0 < E_M < 1$.

The conditions, a.) and b.), are fixed by the thermodynamics of the mixture. The equilibrium composition for a light component is always higher than its corresponding non-equilibrium value. Similarly, the equilibrium composition of a heavy component is less than the corresponding non-equilibrium value.

These conditions are always satisfied in the simulation results when the convergence is tight enough. When composition changes between plates are small, quite accurate simulation results are needed because several places after the decimal point are significant. With all this we can conclude that while the non-equilibrium models give more accurate composition and temperature profiles than the equilibrium models, and provide more useful information, they are not able to match experimental tray efficiency values because compositions satisfy conditions a.) or b.) This does not mean that experimental values of efficiencies are wrong, it just means that the non-equilibrium models developed, including the one presented in this work, still are theoretically limited by the assumption of perfect mixing of the bulk phase, given by conditions a.) and b.).

5.3 Illustration of Hybrid Modelling Approach

With the results obtained in the previous Sections, the solution of hybrid models can now be highlighted. The depropanizer column and the esterification column are used as examples of the hybrid modelling approach. The results from the combined model for the esterification, which reproduces the experimental data quite accurately using approximately 20% less in computational time, are shown.

Using the tray efficiency parameters from the non-equilibrium model in the equilibrium model, simulations have been performed for the depropanizer column. A specified efficiency for the equilibrium model of 0.85 is used. A hybrid model switching between non-equilibrium and equilibrium model has also been performed. The top section has been simulated with the non-equilibrium model and the bottom section with the equilibrium model, as suggested by the efficiency analysis.

The results in Figs. 5.11 and 5.12 show the simulated liquid and vapour composition profiles for the case of equilibrium model with fixed efficiency. *HM* in these Figures refers to simulations with fixed column efficiency, while the

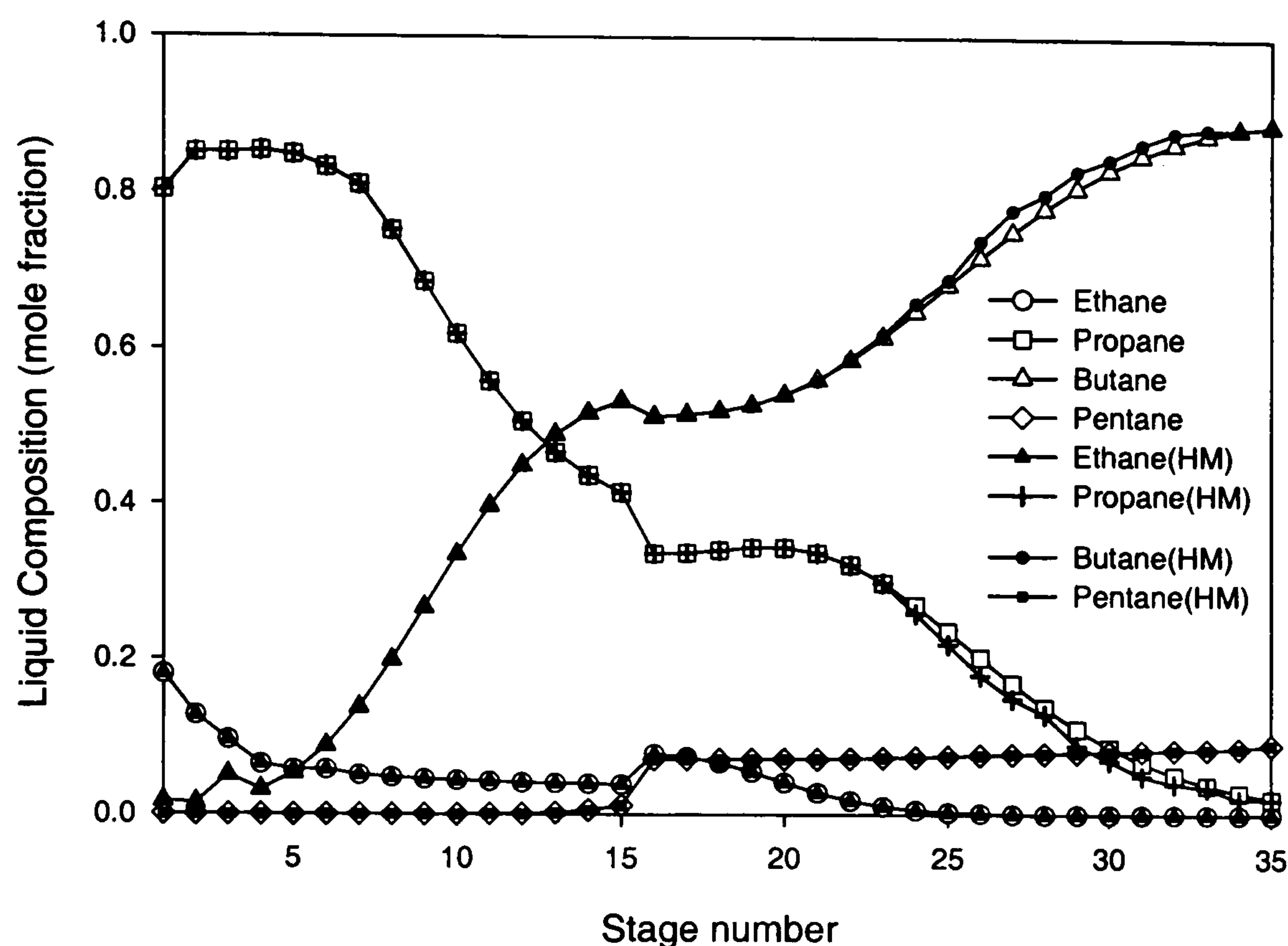


Figure 5.11: Liquid composition profile with equilibrium model with fixed efficiency and non-equilibrium model

other results are the ones obtained from the non-equilibrium model. A simple switch from the non-equilibrium model to the equilibrium model at the converged steady state with the non-equilibrium model performs this simulation (time used to converge the non-equilibrium model: 2.53 min., time for the hybrid model: 1.25 min. in a SUN-Ultra 1 Workstation).

With a fixed column efficiency value (for equilibrium model), small deviations can be noted. However, for the hybrid model, not surprisingly, hardly any variation can be noted.

The same procedure has been repeated for the esterification case. In this

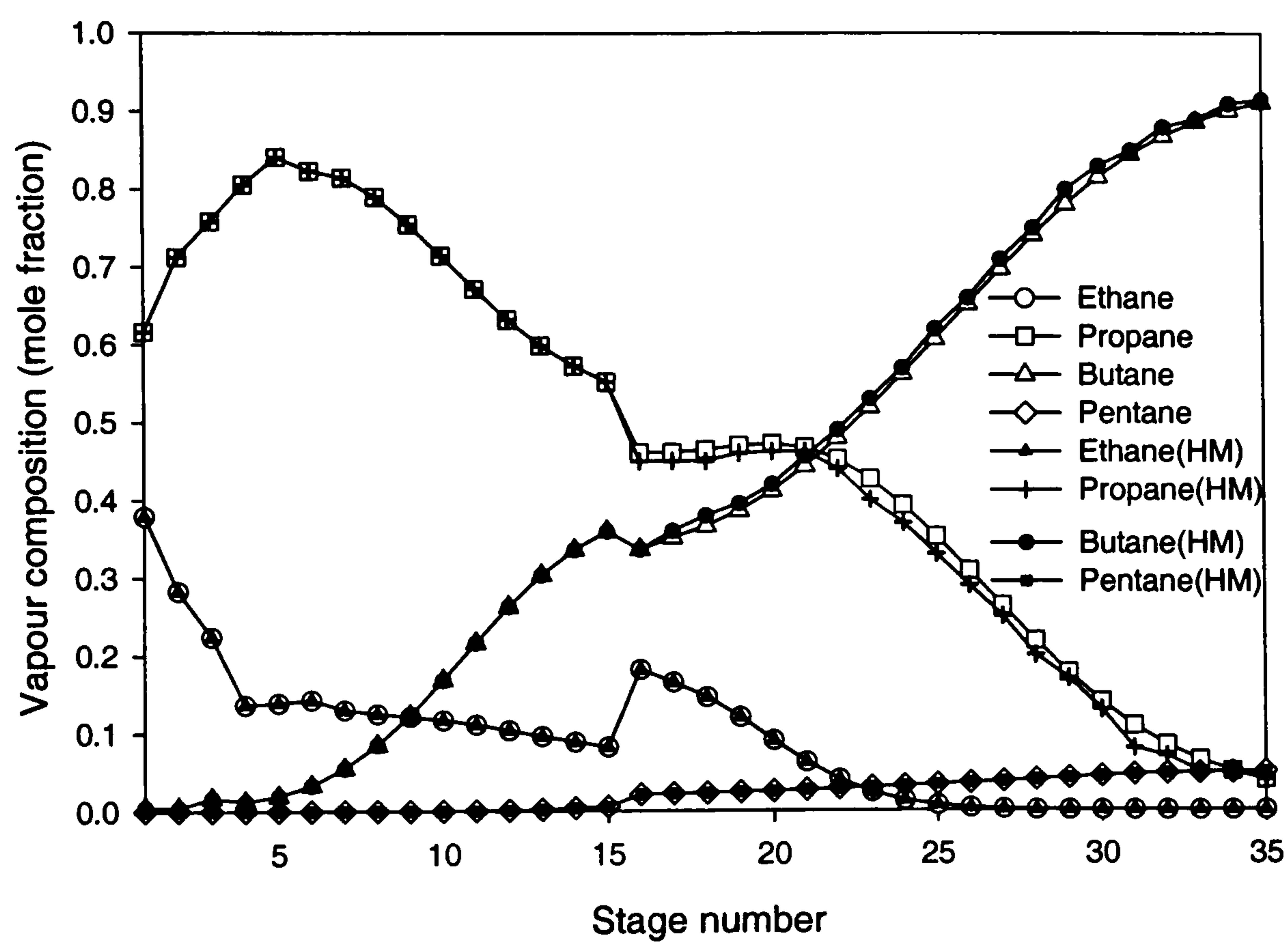


Figure 5.12: Vapour composition profile with equilibrium model with fixed efficiency and non-equilibrium model

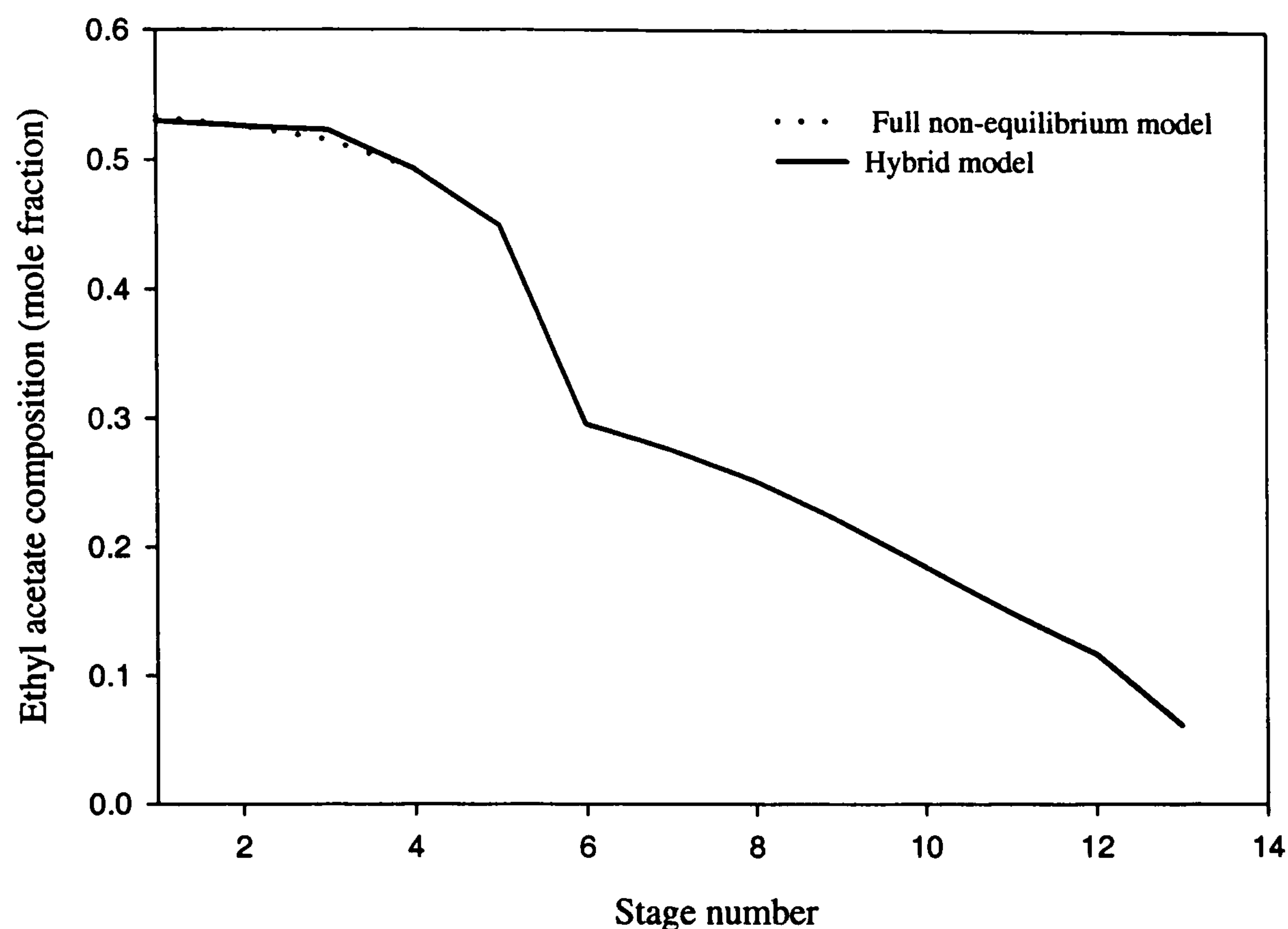


Figure 5.13: Hybrid model applied to the esterification column

case, according to the efficiency and the excess Gibbs free energy analysis, a specified efficiency for the equilibrium model of 0.6 has been used. The hybrid model, comprising stages 1 to 3 simulated with equilibrium model and stages 4-13 simulated with non-equilibrium model, has also been performed.

The results obtained from the hybrid model are presented in Fig. 5.13. Small deviations in the composition values (bottom of the column) in the hybrid model of combined non-equilibrium and equilibrium models, compared with the full non-equilibrium model (time used to converge the non-equilibrium model: 2.13 min., time for the hybrid model: 1.46 min. in a SUN-Ultra 1 Workstation).

5.4 Conclusions

The general(hybrid) model contributes to the development of a computer aided environment which facilitates the understanding of the reactive distillation operation and the solution of different simulation problems. The new model features have been validated through reactive and non-reactive systems. The hybrid modelling approach not only allows different model types in the modelling of a single distillation column, but also the use of different simulation modes during the solution of a specific simulation problem.

The hybrid modelling approach provides a powerful analysis tool through which the importance of terms in the different models can be established. In principle, the non-equilibrium model should provide a more correct and consistent prediction of the behaviour of the reactive distillation system. The non-equilibrium model, however, is more time consuming and requires information on a greater number of model parameters. Use of a suitable hybrid model, whenever applicable, makes the solution more efficient without appreciable loss of model accuracy.

In addition to the analysis presented in this Chapter, the hybrid models, ICAS or *gPROMS* can also be used for other types of analysis, such as bifurcation (which has already been shown in Chapter 4), controllability and dynamic optimization.

Analysis with the hybrid model in terms of controllability and dynamic optimization is presented in the following Chapter.

Chapter 6

Controllability Issues and Dynamic Optimization

Reactive distillation systems require tight process control to ensure that deviations from the ‘optimum’ can be handled adequately. The development of a good process control scheme requires the identification of the process objectives, translation of these objectives to possible or achievable control objectives and the integration with the control strategy.

Reactive distillation differs from conventional distillation due to the presence of reactions. It has been proven that this phenomena has a significant influence on the performance of the control system (Sneesby *et al.*, 1997).

Obviously, the main objective of any process is to maximise profitability. The objective for the reaction part of the column should be to maximise the reactant conversion, while the objective for the separation part should be to maximise the purity of the products. Hence, the full column should fulfil the overall objective (maximise profitability) by achieving in each process (reaction and separation) the particular objective.

Other process objectives such as contamination problems when working with dangerous products or to maximise the catalyst life can also be included.

Before starting to implement any controller design some ideas about how easy is to control a reactive distillation unit are needed. What to measure? What to manipulate? What are the best pairings?

Newells and Lee *et al.*(1987) presented some qualitative rules answering these questions:

- control outputs that are not self-regulating
- control outputs that have favourable dynamics characteristics
- select inputs that have large effects on the outputs
- select inputs that rapidly affect the controlled variables

These questions are characteristic of the control of the process itself: *controllability*. Thus, *controllability* is independent of the controllers and can only be changed when the design of the unit is changed (Skogestad *et al.*, 1990). This is then the main reason for controllability analysis made at the design stage.

For control system design, many mathematical methods are used, but for controllability the results only provide a broad indication. A number of ‘tedious’ simulations normally replaces this analysis.

Important features on controllability of reactive distillation are described in this Chapter. A linear model is shown. Configuration is defined as well as measurements, manipulated variables and disturbances.

In the second section of this Chapter dynamic optimization is addressed. The optimal control results show that integrated design-control techniques should be applied to reactive distillation columns.

6.1 Controllability Issues

There has been very little research in the area of controllability of reactive columns. However some research has been presented for reactive batch distillation (Sørensen, 1994).

In engineering practice a plant is called ‘controllable’ if the plant is able to achieve the specified control objectives (Rosenbrock,1970).

All controllability assessments studies have been proposed with the main idea of perfect control. This idea is limited by time delays, right-half plane zeroes, model uncertainty and manipulated variables constraints. Controllability analysis is an extensive area of research but only some characteristics are presented here.

Most of the controllability analysis found in the literature is presented in terms of linear measures. Although it may seem restrictive usually it is not, since the most important non-linearity, given by the constraints in the inputs, can be handled with linear analysis (Skogestad *et al.*, 1990). However, non-linear simulations are always required to confirm the results obtained from the linear analysis.

The procedure for controllability analysis in this work is described by the following main steps (Wolff *et al.*, 1992) starting with the linearised model,

- scale the plant;
- compute controllability measures; and,
- analyse controllability.

To analyse the controllability of reactive columns a control configuration must be assumed. There is probably no single configuration that can be the best for all the columns (Skogestad *et al.*, 1990). Because of the large number of possible control configurations there is a clear need for tools that can assist in the selection of the best possible configuration.

In the following Sections a linear model, some issues about scaling, controllability tools and possible control configurations are presented.

6.1.1 Linear Model

Applying linear control theory to nonlinear systems is an approach adopted by several authors who have demonstrated its success on a number of realistic examples. The works reported by Morari *et al.*(1985), Barton and Perkins (1986), Perkins and Wong (1985) among others, confirmed that the closed loop performance of the control system was consistent with the predictions of the theory.

Almost all the tools developed for controllability analysis are in terms of linear models: RGA, poles, zeroes, condition number, etc.). So that, in order to analyse the controllability of reactive columns a linear model is needed. Based on the non-linear model of Chapter 3, a linear model has been developed by linearising the equations at an operating point. This operating point is the steady-state condition and since the linearisation is done around this point, the linearised model will only be valid for small deviations from the steady-state and the validity of the model should be probed.

A linear model of any process can be described by the following equations,

$$\dot{x} = Ax + Bu + Ed \quad (6.1)$$

$$y = Cx + Du + Fd \quad (6.2)$$

where,

$$x = [all\ states]^T \quad (6.3)$$

$$y = [measurements\ variables]^T \quad (6.4)$$

$$u = [control\ variables]^T \quad (6.5)$$

$$d = [disturbance\ variables]^T \quad (6.6)$$

Applying Laplace transformation to the linear model, we get,

$$y(s) = G(s)u(s) + G_d(s)d(s) \quad (6.7)$$

where $G(s)$ and $G_d(s)$ are transfer functions models which describes the effect on the output of the input and disturbances.

The objective is to keep the outputs close to their set-points (r), i.e, $e = y - r$, and to reject disturbances. The ideal control will accomplish this by inverting the process such that the manipulated inputs become,

$$u = G^{-1}r - G_d^{-1}d \quad (6.8)$$

When deriving the linear model, measurements, manipulated (control) variables and disturbances have been defined as,

- The measured variables are temperatures and/or, composition of the products (it is assumed that these variables can be practically measured!). Interest in controlling these variables comes from previous results in controlling distillation columns as well as reactive batch distillation (Skogestad *et al.*, 1990; Sørensen, 1994).
- The manipulated variables are the distillate flow and the vapour boil-up and/or the heat of the reboiler.
- Disturbances are in feed flow-rate and in feed composition. The selection of disturbances in the feed composition will offer also an indirect way of looking at disturbances on the reaction parameters. Disturbances in the feed composition affects the reaction stoichiometry.

The linear and non-linear models are compared by looking at Fig. 6.1. A 10% step in distillate flow rate are introduced to both models. The linear model (shown in the top graph) describes the responses in the same way as the non-linear model (bottom graph) (the axes for the top graph are the same as for the bottom graph: Ethyl acetate composition at the top of the column vs. time). The linear model can be then used for controllability and control studies not too far from the linearised point, i.e. only for small disturbances (Skogestad *et al.*, 1990).

6.1.2 Scaling

Why is it important to scale the plant?

Most of the controllability measures are scale dependent. It is crucial that variables are scaled properly. One way of scaling is described in the following (Skogestad and Postlethwaite, 1996),

- Inputs (u): normalise u_j with respect to its allowed range.
- Outputs (y): normalise e_i with respect to its allowed range.
- Disturbances (d): normalise d_k with respect to its allowed range.

Another way, which also achieves the same objectives, is to scale the transfer matrices G and G_d , assuming that the allowed magnitude of the signals d , u , e and r do not vary with the frequency (Havre and Skogestad, 1992). The later is the scaling adopted in this work.

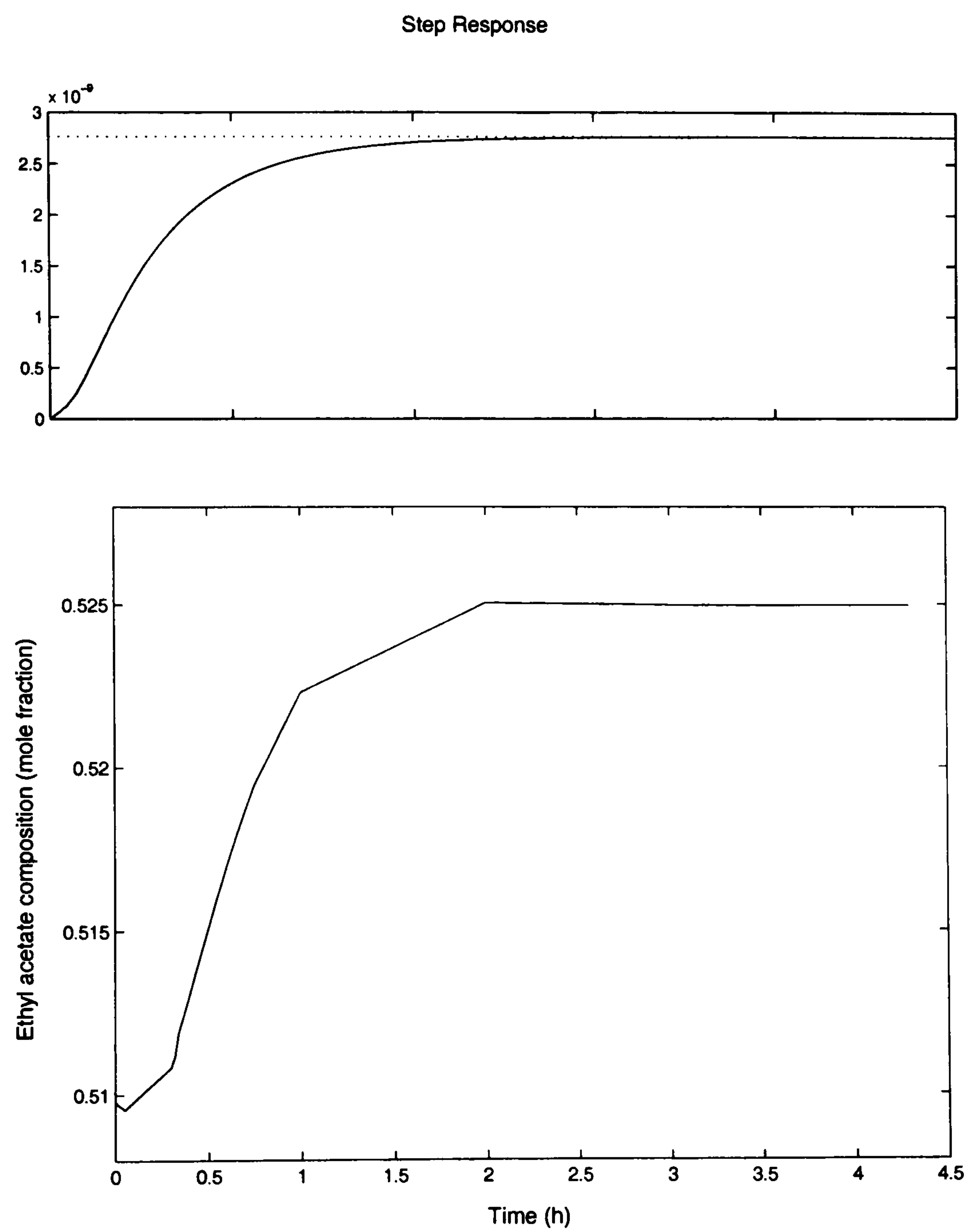


Figure 6.1: Response obtained from the linear and non-linear model (10% step change).

6.1.3 Controllability Tools

Which tools for controllability analysis are available?

- Functional controllability

The first thing that should be checked is that the plant is functionally controllable (Skogestad and Postlethwaite, 1996).

Essentially, a plant is not functionally controllable if the rank of $G(s)$ is for all s less than the number of outputs that we want to control. This is extended for square plants to the requirement that $\det(G(s))$ should be different from 0. For unstable plants it should be checked that the unstable states are state controllable and state observable. Nevertheless, this is not important because the states we really care about are in the output vector y .

- Right half plane zeroes and time delays

Right-half plane zeroes (RHP-zero): a zero is defined as the value for s for which $G(s)$ loses rank (for square matrices this may be computed as the solution of $\det(G(s))$). A RHP-zero of $G(s)$ limits the achievable bandwidth of the plant and this holds regardless of the type of controller used (Holt and Morari, 1985). RHP-poles also put limitations on the control system through stability considerations. If there are RHP-zeros and poles in the same direction, it is important that the RHP-pole at p is located at a higher frequency than the RHP-zero at z , i.e., $p > z$.

Time delays have essentially the same effect as RHP-zeros.

- Singular value decomposition

Singular value decomposition (SVD) of any matrix G is:

$$G = U \Sigma U^H. \quad (6.9)$$

There will be $\text{rank}(G)$ singular values. The SVD is useful to examine which manipulated input combinations have the largest effect and which disturbances give the largest output variations.

- Condition number

The ratio between the maximum singular value and the minimum singular value is the condition number. Plants with large condition numbers are ‘ill-conditioned’, and require widely different input magnitudes depending on the direction of the desired output (Skogestad and Postlethwaite, 1996). The process is sensitive to plant/model mismatch when the condition number is high.

- Relative gain array

The relative gain array (RGA) defined by Bristol (1966) for a square plant is defined as the ratio of the ‘open-loop’ and ‘closed-loop’ gains between input j and output i . Plants with large RGA are ‘ill-conditioned’. The RGA is scaling independent and ideally should be a diagonally dominant matrix. In this case the control loops are largely decoupled. The general rule about pairing is to pair the controlled outputs y_i with the manipulated variables u_j in such way that the RGA values are positive and as close as possible to unity. RGA can also be calculated as a function of frequency. If the large values of RGA are at high frequencies plants are difficult to control. One should ‘never’ use a controller with large RGA values (Skogestad, 1992). One big disadvantage of RGA is that it contains no information about disturbances and dynamic behaviour of the plant.

6.1.4 Control Configurations

The control configurations of a distillation column can be divided into two categories:

- Basic Configurations
- Ratio Control Schemes

Table 6.1 summarises the basic configurations:

Both LD and VB configurations are feasible but lead to bad level control which affects composition control (via the overall mass balance) and reduces control response.

Configuration	Primary Manipulated Variable	Secondary Manipulated Variable
LV	reflux rate or reboiler duty	reboiler duty or reflux rate
LB	bottoms rate	reflux rate
LD	distillate rate	reflux rate
DV	distillate rate	reboiler duty
DB	distillate rate	bottoms rate
VB	bottoms rate	reboiler duty

Table 6.1: Basic control configurations

The LV configuration is the most common used in the industry. The main advantage of this configuration is that the manipulated variables affect directly to compositions.

The LV configuration is sensitive to disturbances when no control is used but rather insensitive with one-point control. In this configuration, the RGA is expected to be large for high purity columns with large reflux.

The DB configuration it is believed violates the mass balance and is normally not considered although its effectiveness has been demonstrated experimentally (Skogestad *et al.*, 1990). This configuration was considered as a non viable alternative on a long term basis, however on a short term basis it does not behave unreasonably. If D and B are adjusted for a long time then the column will end by being filled up or emptied. This configuration then is actually rather good when using composition feed-back control.

For the DV configuration the RGA elements are always small contrary to the DB configuration where the RGA elements are infinite at steady state (thus, the RGA is not a reliable measure for this configuration).

For the ratio control scheme many combinations are possible, but the more common are presented in Table 6.2. (L/D)(V/B) has been recommended by Skogestad and Morari, 1987. Its known as 'the double ratio' scheme. The ratio control scheme is advantageous for double composition control but not for single composition control. This scheme creates implicit decoupling (as well as all the ratio schemes).

Configuration	Primary Manipulated Variable	Secondary Manipulated Variable
(L/D)V	reboiler duty	reflux ratio
(L/D)(V/B)	reflux ratio or boil-up ratio	boil-up ratio or reflux ratio
(V/B)L	reflux ratio	boil-up ratio

Table 6.2: Ratio control configurations

Important differences between configurations are related to interaction when using single-loop controllers (Shinskey, 1984) and sensitive to input gain uncertainty when using decoupler for two-point control. In both cases a large value of RGA at the frequency range of the closed-loop results in control problems.

Recent work has been presented in the literature for an ETBE (ethyl-tert-butyl-ether) production (Sneesby *et al.*, 1997). They recommended two configurations: LV and LB, both for a single composition control. They found that the location of the temperature control is critical and can dramatically affect the stability of the control scheme. This is due to the interactions between the chemical and phase equilibria. Dynamic simulation for studying the responses of the system was recommended.

A model for reactive distillation columns including control system and the possibility of coupling additional columns was derived by Bock *et al.*(1997b). They analysed sensitivities to manipulated variables and disturbances in a reactive distillation column and a coupled recovery column for the esterification of myristic acid. Based on this the SISO (to make it simple) control structure was carried out.

Bock *et al.*(1997b) also found that the influence of the reaction temperature profile within the reactive column has to be known, when the temperature is used as a reference variable for the purity. They controlled the system using two SISO-control loops, as only one was not sufficient to ensure conversion. They kept the temperature at the top of the column constant by manipulating the heat supply at the top of the column, which leads to a very fast control loop due to its proximity; and the temperature in the middle of the column is kept constant by manipulating the heat of the reboiler. In most of the cases the disturbances were eliminated quite well. A long time was required to achieve the set-point when the influence of the reaction could not

be compensated by a manipulated variable.

For this work the DV configuration has been chosen.

6.1.5 Examples of Application

It is known that the interactions between the top and bottom of distillation columns are very large. Changing conditions at the top will lead to changes in the bottom, and *vice versa*. Because of this distillation columns are known as very difficult or impossible to control.

Using two single control loops it may be possible to control both the top and the bottom of the column.

In the case of reactive distillation it is desirable to control not only the composition of the product, but also the loss of reactants that may be at the other end of the column so that only one point control will not be able to achieve this.

The temperature of the reactive section may be another variable desirable to control, however, in this work it is not considered. For the examples studied it seems to be sufficient to control compositions or top and bottom temperatures. Controlling these variables the temperature in the reactive section (or in the column itself, in the case of full reactive column) suffices to achieve desirable temperature profiles.

The DV-configuration was adopted for this controllability analysis:

DV-configuration: controlling the distillate flow and the reboiler heat duty (or vapour boil-up) to control the distillate composition (or temperature) and the bottom composition (or temperature):

<i>Manipulated variable</i>	<i>Controlled variable:</i>
D	X_D or X_B (or, T_B or T_D)
V	X_D or X_B (or, T_B or T_D)

Procedure

Assuming that we have made a decision on the plants inputs and outputs, we want to analyse the model G to investigate what control performance can be expected. The procedure is described from Skogestad and Postlethwaite (1996) and is only an extension from the procedure presented above. The controllability indices are described below.

- Linearise the model.
- Scale all the variables (inputs, outputs, disturbances, references) to obtain a scaled model.
- Check functional controllability.
- Compute the poles.
- Compute the zeroes.
- Obtain the frequency response $G(j\omega)$ and compute the RGA matrix.
- Compute the singular values of $G(j\omega)$ and plot them as function of frequency.
- Compute condition number: the ratio between the minimum and maximum singular value.
- Analyse.

For the results shown in this thesis, the hybrid model included into the ICAS simulator has been linearised, however, *gPROMS* also allows the linearisation of models. All the controllability indices have been obtained using *MATLAB*.

MTBE Production

The MTBE production column has been first analysed by a series of simulations. The steady state for which multiple solutions exist was taken for study. Methanol is fed in tray 10 while the butenes remain fed at stage 11. Simulations have been performed with the non-equilibrium model and it was assumed to have 1 hour disturbance for changes in feed flows and composition, reboiler heat duty and distillate flow-rate. Full results can be found in

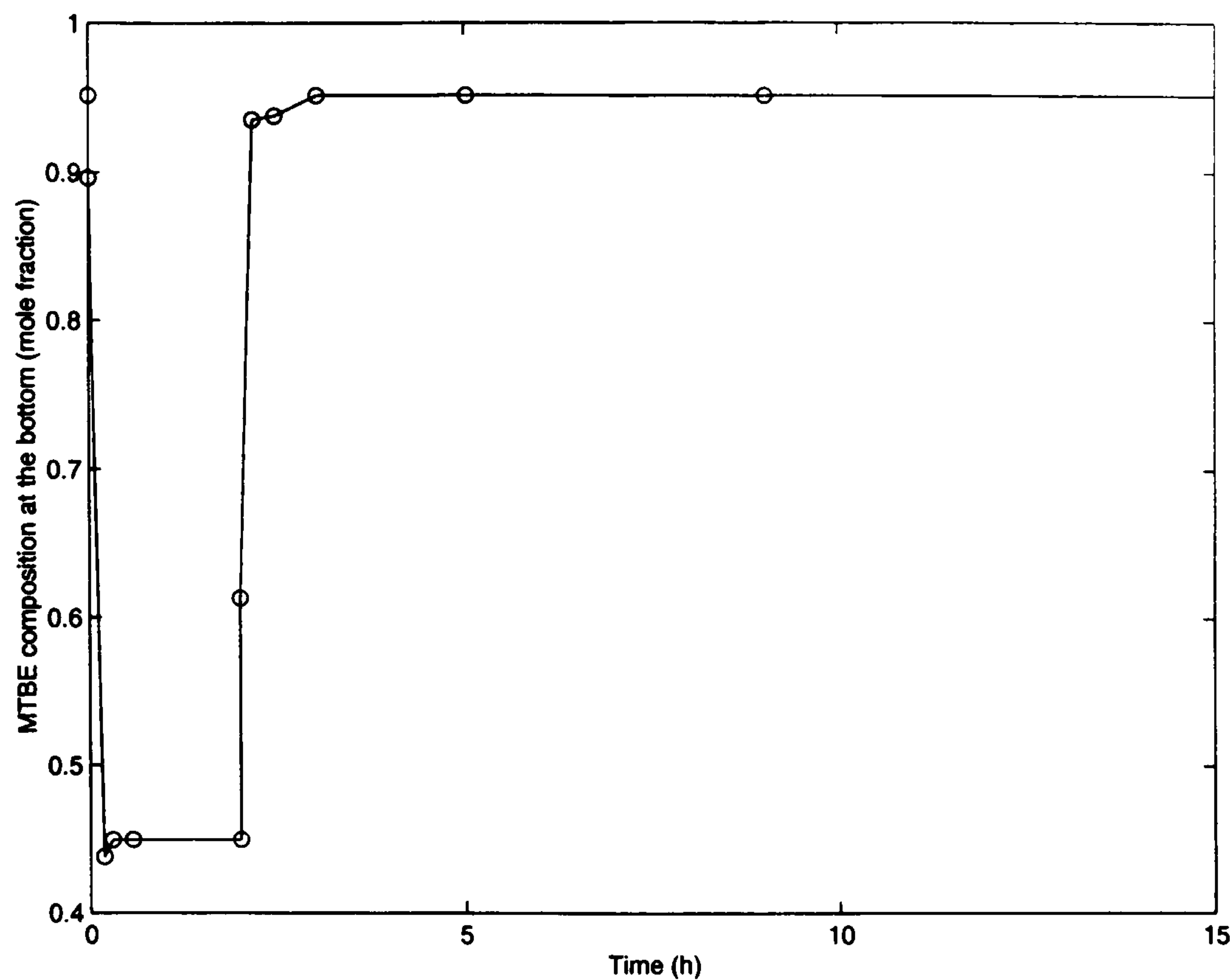


Figure 6.2: High conversion of MTBE as result of 10% increase in reboiler heat duty.

Appendix B. The reboiler heat duty was found to be a very sensitive variable. There is a range of values giving the high conversion solution. Below or above that range the system drastically changes to the low conversion solution (see Figs. 6.2, 6.3). This confirms the results obtained by the continuation method (bifurcation analysis in Chapter 5).

Through simulation it has been shown that adding or reducing the number of stages does not improve the column performance. However in many cases it may worsen performance, as can be seen from Fig 6.4 where 5 reactive stages have been added to the system. The purity of MTBE at the bottom of the column is reduced to almost half of the purity achieved by the nominal design.

If any changes in the number of stages is desirable then the ratio between the size of the stripping section and the reactive section, as well as between the rectification section and the reactive column should be changed. (see Appendix B for more detail explanations).

Secondly the controllability analysis following the procedure described above

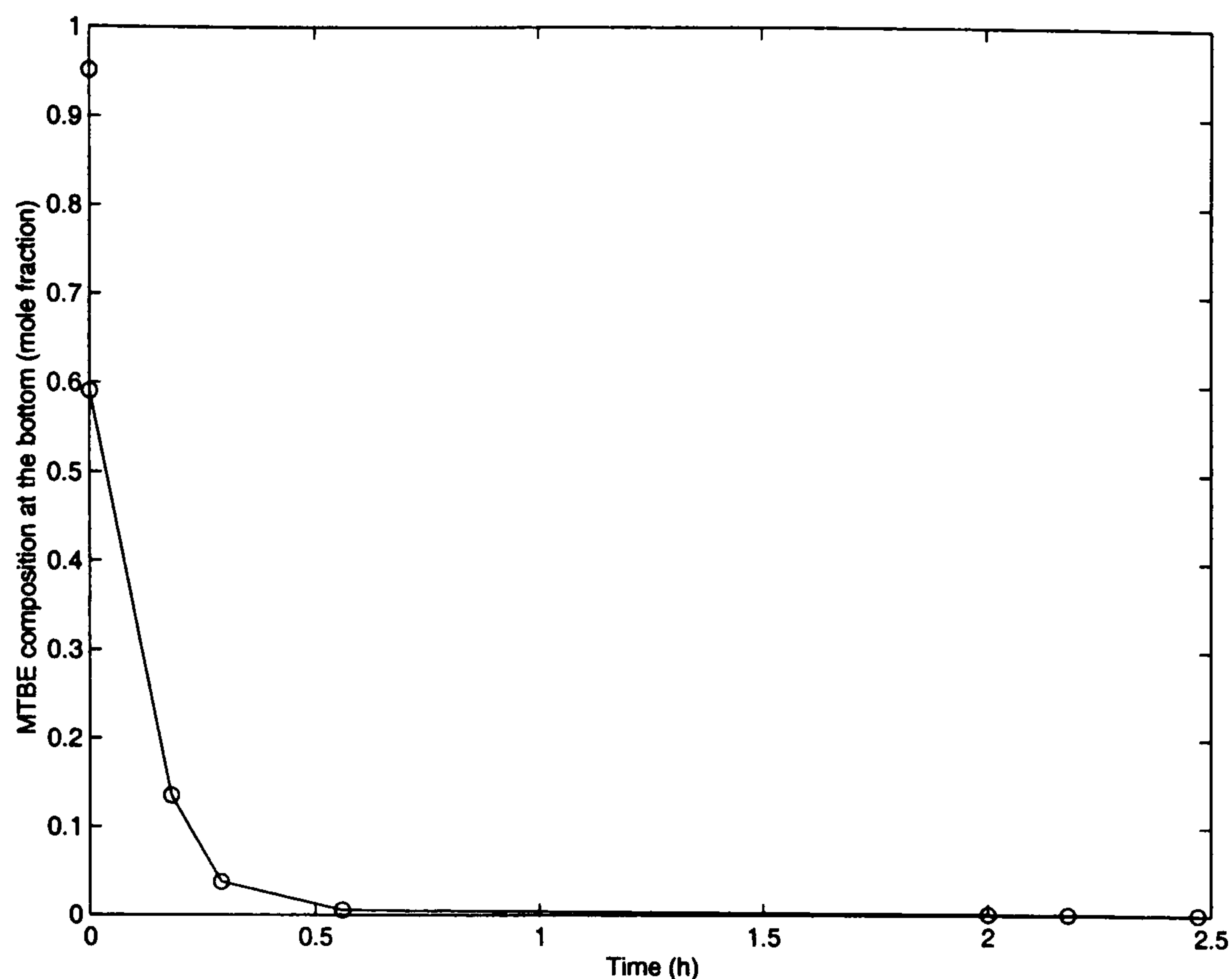


Figure 6.3: Low conversion of MTBE as a result of 15% decrease in reboiler heat duty.

was studied. Once again in this analysis, the steady state with multiple solutions is analysed (methanol is fed in tray 10 while the butenes remain fed at stage 11). Three cases were analysed for the DV-configuration as can be seen from Table 6.3. Some controllability indices obtained are summarised in Table 6.4. Accounting for the process dynamics some controllability indices, such as RGA and singular values were calculated over a range of frequencies. The results from the frequency-dependent analysis are the same as obtained for the steady-state analysis. Detailed calculations are in Appendix B.

From the analysis of all the indicators (steady-state and frequency dependent) it can be seen that:

- all the poles of the systems have negative real parts, indicating stability of the open-loop system,
- all the cases studied present RHP-zeroes, limiting the achievable control performance,
- the processes are very sensitive to plant/model mismatch, according to the high condition number,

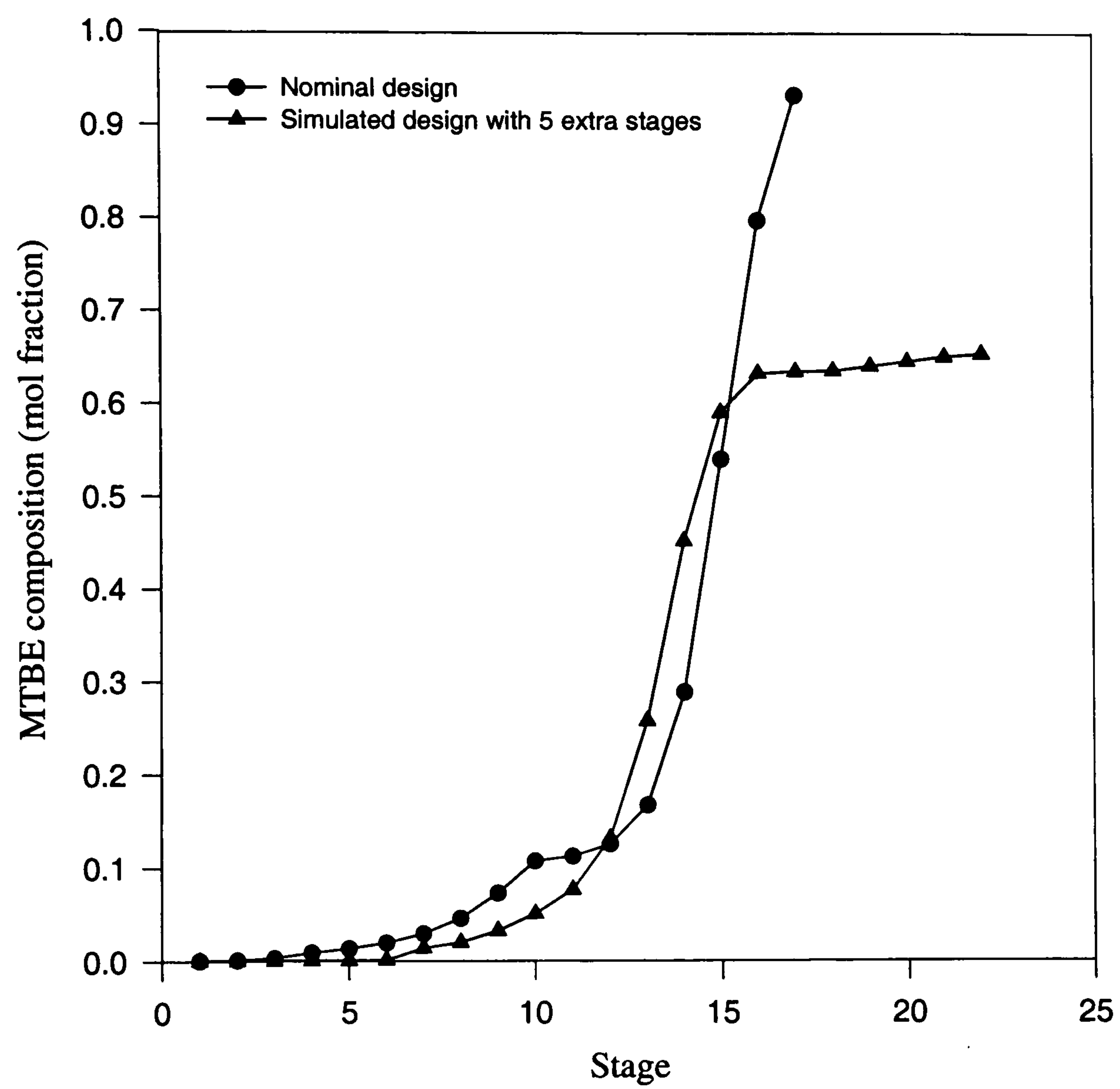


Figure 6.4: Lower purity of MTBE as a result of adding extra reactive stages

Cases	Measured Variables	Disturbances
Case 1	$x_{MTBE,D}$ $x_{MTBE,B}$	$x_{isobutene,F}$ T_F
Case 2	$x_{MTBE,D}$ T_B	$x_{isobutene,F}$ T_F
Case 3	T_D T_B	$x_{isobutene,F}$ T_F

Table 6.3: Measured variables for the controllability study on MTBE production

Case	RGA	Singular values	Condition Number	RHP-zeroes
1	1.063 -0.06 -0.06 1.063	$min = 0.0223$ $max = 2.8356$	127.16	yes
2	1.047 -0.047 -0.047 1.047	$min = 0.00387$ $max = 0.12200$	31.52	yes
3	0.71 0.29 0.29 0.71	$min = 0.000316$ $max = 0.320000$	1012.7	yes

Table 6.4: Controllability indices for the MTBE production

- from the RGA values for the three cases, the following control pairings can be suggested,

Manipulated variable: Controlled variable:

$$\begin{array}{cc} D & x_{MTBE,D} \\ V & T_B \text{ or } x_{MTBE,B} \end{array}$$

Temperatures are easy to measure in a distillation column, and they have a linear dependence with the control measure. The pairing of the vapour-boil-up should be done with the temperature in the bottom of the column probably in spite of the very small minimum singular value (compared with that of Case 1).

- the minimum singular value is very small in all the cases, suggesting that large magnitude inputs may be needed to obtain the desired outputs.

Ethyl Acetate Production

The controllability analysis following the procedure described above was also studied for the esterification column. The column studied in Chapter 4 using

the equilibrium model with tray efficiency is taken for the linearisation and controllability analysis. Three cases were analysed for the DV-configuration as presented in Table 6.5. Some results showing the controllability indices are given in Table 6.6 (full results are shown in Appendix B).

Cases	Measured Variables	Disturbances
Case 1	T_D T_B	$x_{ethanol,F}$ T_F
Case 2	$x_{EtAc,D}$ $x_{EtAc,B}$	$x_{ethanol,F}$ T_F
Case 3	$x_{EtAc,D}$ $x_{EtAc,B}$	$x_{isobutene,F}$ F_F

Table 6.5: Measured variables for the controllability study on ethyl acetate production

Case	RGA	Singular values	Condition Number	RHP-zeroes
1	1.17 - 0.17 0.17 1.17	$min = 0.00106$ $max = 8.08000$	7622.64	yes
2	1.05 - 0.05 -0.05 1.05	$min = 0.00018$ $max = 0.24400$	1355.56	yes
3	1.02 - 0.02 -0.02 1.02	$min = 0.0008$ $max = 0.1317$	164.62	no

Table 6.6: Controllability indices for the ethyl acetate production

From the analysis of all the indicators (steady-state and frequency dependent) it can be seen that:

- all the poles of the systems have negative real parts, indicating stability of the open-loop system,
- almost all the cases studied but one present RHP-zeroes, limiting the achievable control performance, there is not RHP-zeroes for Case 3, it may be noted that the temperature measurements or disturbances are generating the RHP-zeroes in the system,
- the processes are very sensitive to plant/model mismatch, according to the condition number (very high),

- from the RGA values for the three cases, the following control pairings can be suggested,

Manipulated variable: *Controlled variable:*

D	$x_{EtAc,D}$
V	$x_{EtAc,B}$

- the minimum singular value is very small in all the cases, suggesting that large magnitude inputs may be needed to obtain the desired outputs.

6.2 Dynamic Optimization

If we wish to determine, for example, the optimal diameter of the reactive column in addition to the optimal way of operating the column over the time then we need to use *dynamic optimization*.

Since operation and design problems are of transient nature then both are applications of dynamic optimization, which is also known as *optimal control*.

The dynamic optimization in this work is carried out by using *gPROMS* and *gOPT* (PSE Ltd., 1997). In general, *gPROMS* is able to solve problems described by the following items,

Mathematical Problem

We consider a process described by:

$$g(x(t), \dot{x}(t), y(t), u(t), v) = 0 \quad (6.10)$$

where, $x(t)$ and $y(t)$ are the differential and algebraic variables, $\dot{x}(t)$ are the time derivatives, $u(t)$ the control variables and v the time invariant parameters to be determined by the optimization.

Initialisation

gPROMS assumes that the initial condition of the system is described by:

$$g(x(0), \dot{x}(0), y(0), u(0), v) = 0 \quad (6.11)$$

By performing dynamic simulation we will completely determine the transient response of the system, once the time variation of the control is fixed.

Objective Function

gPROMS/gOPT seeks to determine:

- t_f , the time horizon,
- v , the value of the time invariant parameters,
- the time variation of the control variables over the entire time horizon

as well as to minimise or maximise the final value of a single variable, z ,

$$\min_{t_f, u(t), v, t \in [t, t_f]} z(t_f) \quad (6.12)$$

z is either the differential variables x or the algebraic variables y :

$$z(t_f) = \int_0^{t_f} \Phi(x(t), \dot{x}(t), y(t), u(t), v) dt \quad (6.13)$$

Bounds of the optimal decision variables

$$t_f^{\min} \leq t_f \leq t_f^{\max} \quad (6.14)$$

$$u^{\min} \leq u(t) \leq u^{\max} \quad (6.15)$$

$$v^{\min} \leq v \leq v^{\max} \quad (6.16)$$

$$\forall t \in [0, t_f]$$

End point constraints

These are conditions that must be satisfied at the end of the operation.

$$equality \implies w(t_f) = W^* \quad (6.17)$$

$$inequality \implies w^{\min} \leq w(t_f) \leq w^{\max} \quad (6.18)$$

Path constraints

These are conditions that must be satisfied at all the time during the operation.

$$w^{min} \leq w(t_f) \leq w^{max} \quad \forall t \in [0, t_f] \quad (6.19)$$

Classes of control variable profile

gPROMS offers several possibilities, but this is the one utilised within this work,

- Piecewise constant control: the controls remain constant at a certain value over a certain part of the time horizon before jumping discretely to a different value over the next time interval.

Solution

The solution comprises the following:

- the value of the time horizon, t_f ,
- the values of the time invariant parameters,
- the variation of the control variables over the time horizon.

The dynamic optimization problem is solved as:

- parametrisation of the control variables
- fix the parameters values
- use DA-SOLV to integrate the system and get the sensitivity information
- use SRQPD to solve NLP to get the new set of values.

The control vector parametrisation approach (Vassiliades *et al.*, 1994a,b) is implemented within the *gPROMS* process modelling (PSE Ltd.,1997). The approach converts the problem of solving a dynamic optimization problem (DAE, initial estimates, junction conditions and point equality and inequality constraints) to a finite dimensional nonlinear programming (NLP). The solution of the NLP are calculated via the solution of a multistage DAE system

in the variable sensitivities. The control parametrisation approach requires that the DAE system of the problem being solved must have a solution for any set of values of the decision variables may take.

Other method of solving dynamic optimization has been developed by Biegler and co-workers (Cuthrell and Biegler, 1988). In their approach the differential equations are discretised by using Lagrange form polynomials and orthogonal collocation. The resulting algebraic approximations are then written as constraints in an NLP. The solution of large NLP's is still under study, for that, the method works quite well for small systems but starts to fail when large number of equations are needed to represent the physical problem, since all the equations are discretised.

6.2.1 Optimization problem

This study addresses some aspects of optimal control of a reactive distillation column. The esterification column was used as an example since this is the system that, using equilibrium models with tray efficiency, can accurately represent experimental data.

Problem statement:

The system under consideration is shown in Fig. 6.5. Table 6.7 gives the structure of the optimization problem.

The overall objective is to design the column (diameter, areas of reboiler and condenser) to give feasible operation over a finite time horizon of interest (10 hours) while maximising profitability, *i.e.* minimising the total annualised cost.

$$\text{minimise Cost} = \text{minimise } (C_{shell} + C_{tray} + C_{hx} + C_{op}) \quad (6.20)$$

where C_{shell} is the cost of the column shell, C_{tray} is the cost of the tray, C_{hx} is the heat exchangers cost (for the reboiler and condenser), and C_{op} is the operating cost.

There are constraints on the maximum loss of product in the bottom as well

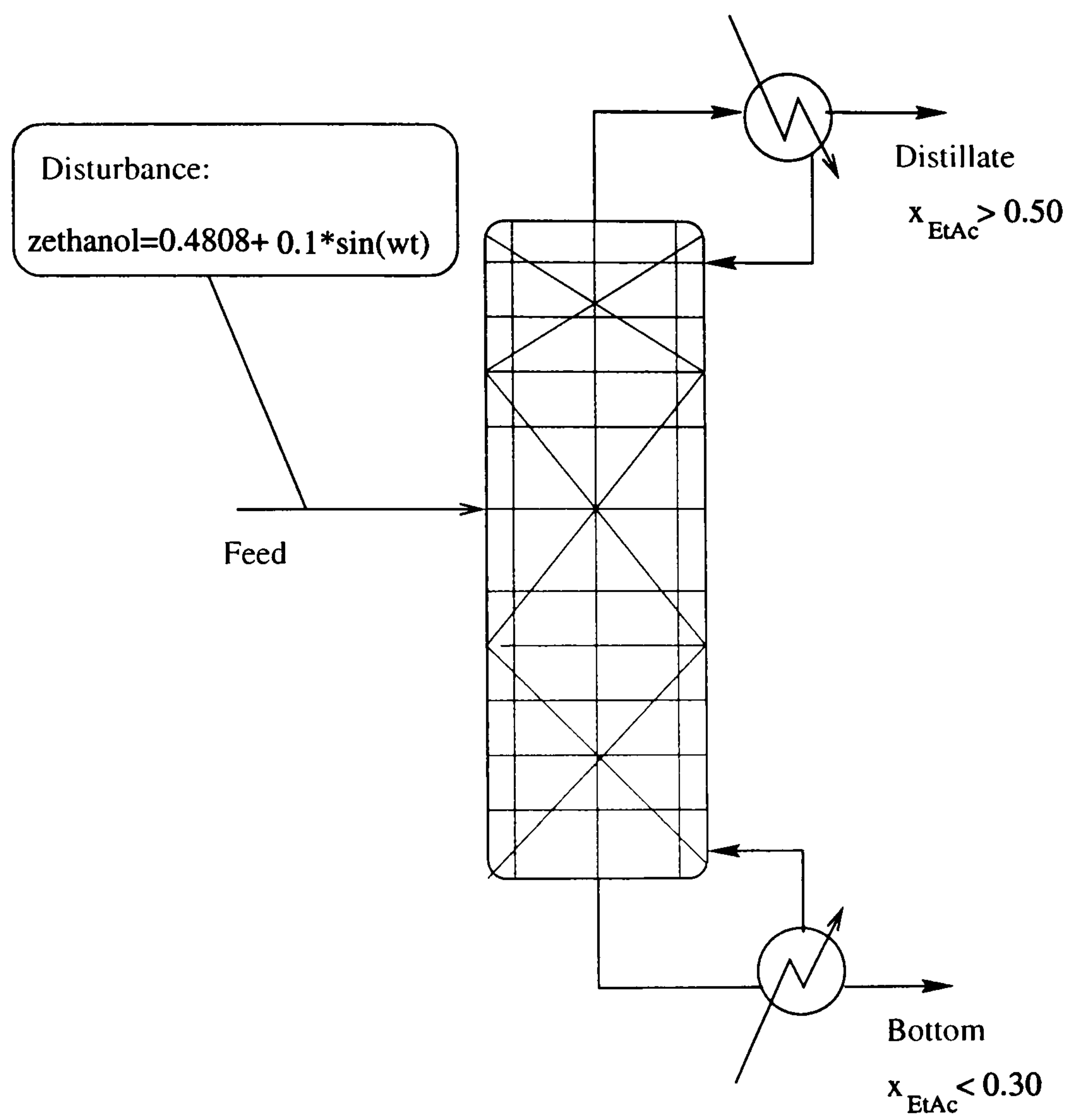


Figure 6.5: Reactive distillation column for the design study

Objective function:	total annualised cost
Fixed:	number of trays (13) feed location (tray 6)
Optimized-variables	diameter of the column ($3m \leq D_1 \leq 6m$) ($4m \leq D_2 \leq 8m$) areas of condenser and reboiler
Specifications:	ethyl acetate top composition ($x_{top} \geq 0.525$) ethyl acetate bottom composition ($x_{bot} \leq 0.3$)
Disturbance:	feed composition (sinusoidal, 1h period)
Control variables:	distillate flow-rate ($1000 \leq Dist \leq 3800(mol/h)$) reboiler heat duty ($0.25 \times 10^7 \leq Q \leq 0.9 \times 10^6(MJ/h)$)

Table 6.7: Optimization details

as on the minimum purity of product in the distillate. The system is subject to a sinusoidal disturbance in the feed composition. Manipulated variables for control are the heat of the reboiler and the distillate flow-rate according to the suggestions from the previous controllability studies.

The problem comprises 2609 variables. The objective function together with disturbances and constraints are given in Appendix C.

Results

The nominal design for the reactive column was tested (through simulation) in the presence of a disturbance. The disturbance was a sinusoidal feed composition. As expected there were a large number of constraint violations. The most important was the violation of the top composition, as can be seen from Fig. 6.6, where the composition of ethyl acetate goes beyond the limits (minimum purity at the top should be 0.525). This highlights the need for controlling the system.

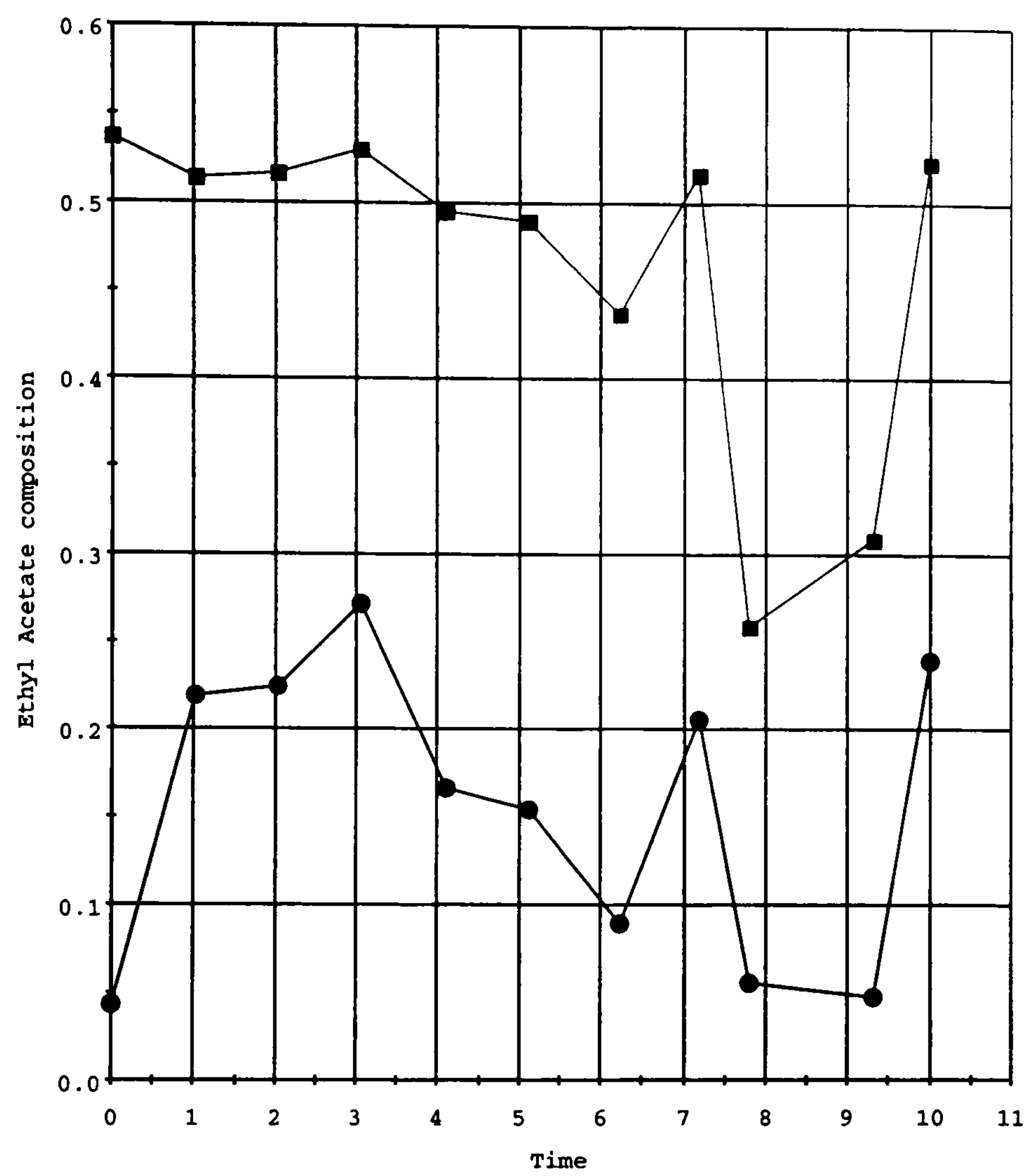


Figure 6.6: Top and bottom compositions of ethyl acetate. Results from the simulated nominal case with disturbance.

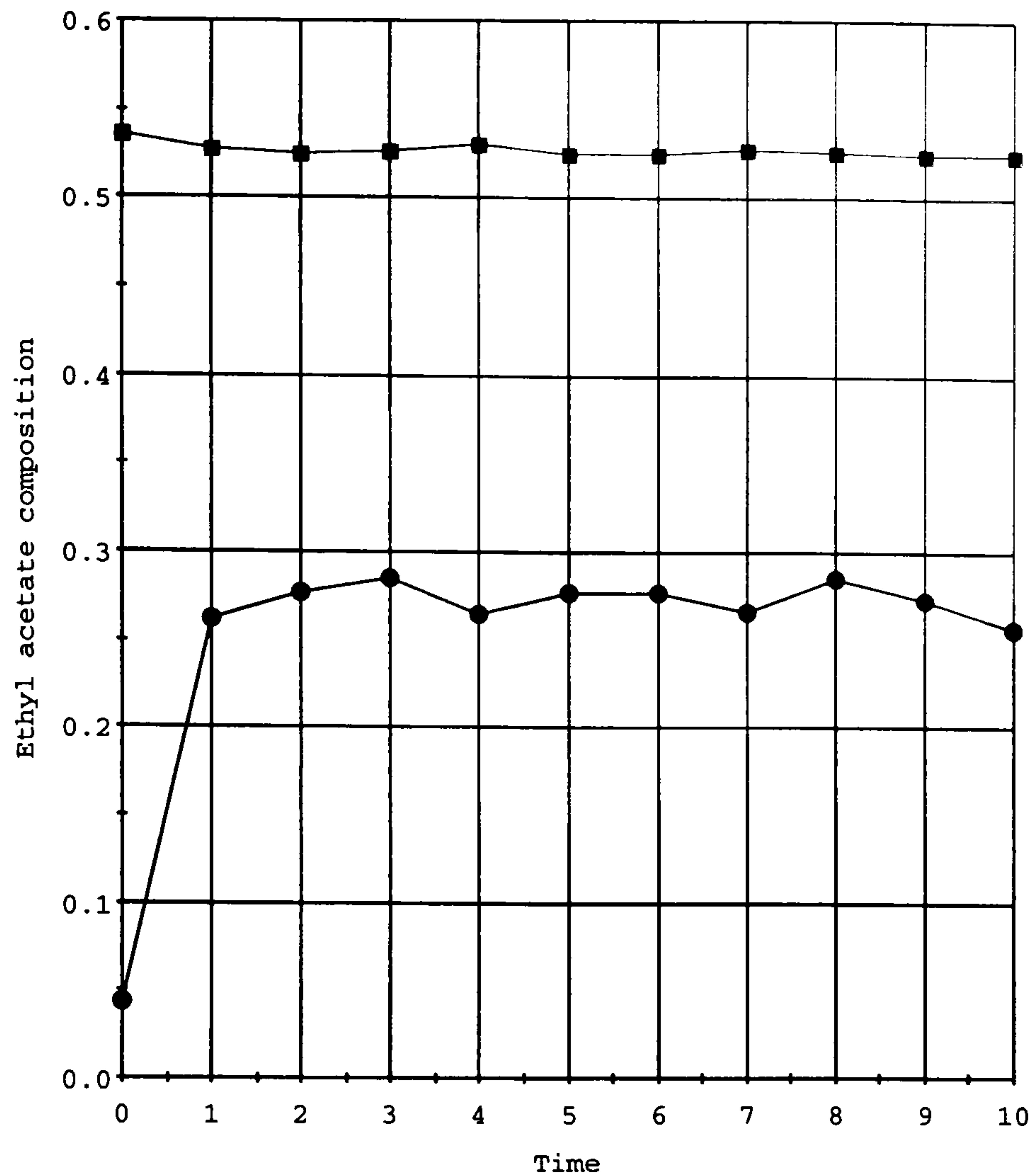


Figure 6.7: Ethyl acetate composition. Results from the dynamic optimization.

Dynamic optimization was carried out, controlling the reboiler heat duty and the distillate flow-rate. The results are shown in Fig. 6.7. Table 6.8 compares the nominal and the optimal values obtained. For the optimal solution there are no constraints violations. The system is rejecting the disturbance while the top product specification is maintained, by increasing the heat of the reboiler, this implies that the reaction rate is increased (explaining why the bottom purity increases although remaining below the upper bound). It can be noted as well, that while the operating cost is increased because of the reboiler heat duty increase, a notable reduction in the capital cost is made by a reduction in the column diameter.

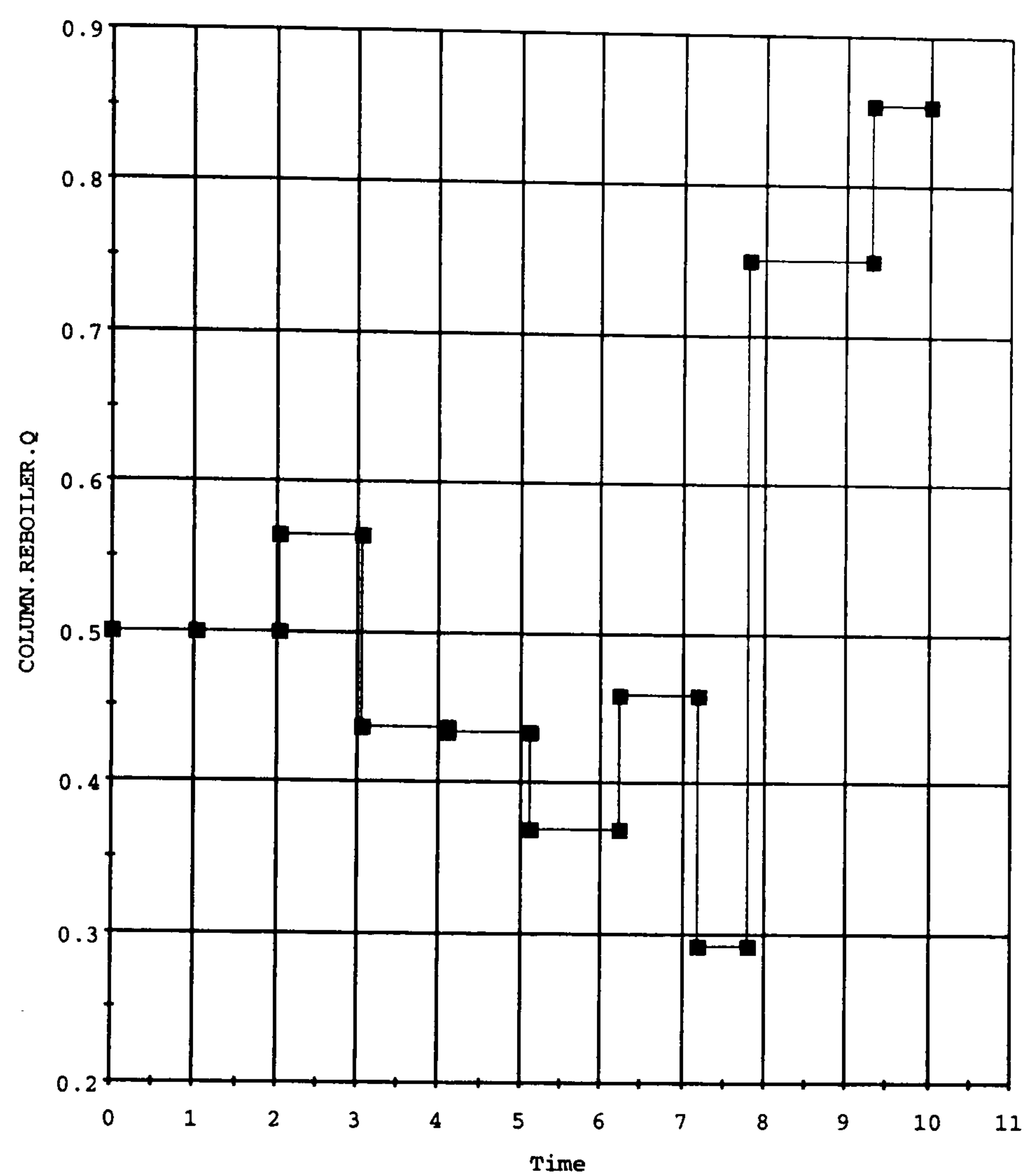


Figure 6.8: Controlled variable: Reboiler Heat Duty($\times 10^6(MJ/h)$). Results from the dynamic optimization.

Variable	Nominal	Optimal
Diameter	5.6/6.25m	4.5/5m
Reboiler heat duty	$0.58 \times 10^6 MJ/h$	$0.85 \times 10^6 MJ/h$
Distillate flow-rate	1150 <i>Kmol/h</i>	737.87 <i>Kmol/h</i>

Table 6.8: Optimization results: nominal and optimal values

6.3 Conclusions

Controllability studies have been performed for two reactive systems. The results from this analysis have been applied for the solution of the optimal control problem.

Following the controllability studies an optimal control problem has been solved. From these results the optimal design of reactive distillation columns has been determined.

The optimal solution found is limited to the objective function, proposed disturbance, and to the model as defined. Certainly, other types of disturbances and uncertainties should be included in the optimization problem, however experimental (or plant) data to corroborate the results are not available. The approach can be used for this analysis and is generally applicable for other similar systems.

The results presented open up a broad area for research. Nowadays, large optimization problems can be solved without much trouble, and simultaneous design of reactive distillation columns and their associated control structure, subject to disturbances as well as uncertainties can be solved for the optimal solution.

Chapter 7

General Conclusions and Future Work

The main contributions of this thesis have been:

- A hybrid model for continuous staged reactive and non-reactive distillation columns.

The hybrid modelling approach allows different model types in the modelling of a single distillation column. It also allows the use of different simulation modes during the solution of a specific simulation problem. The framework developed helps to avoid problems of mismatch between model and simulation results as well as between the two forms of models.

- New tools for the analysis of distillation columns.

The importance of terms in the different models can be established. The analysis of the Gibbs free energy as a function of time has been used as a measure of distance from the equilibrium. Bifurcation analysis for reactive columns gives the existence or not of multiple solutions.

- Controllability analysis.

For the first time controllability analysis has been addressed for reactive distillation columns. The controllability indices have helped to determine the best control structure for the problem studied.

- Dynamic optimization

As well as controllability issues, for the first time, to the best of our knowledge, dynamic optimization has been performed for continuous reactive distillation systems. The work presented here, although limited

in scope, opens a new area of study for the interaction between design and control of reactive distillation columns.

The simulation and design of hybrid (reactive and non-reactive) distillation columns with different types of models and combination of them is made possible through the framework developed in this thesis. Different analysis tools, such as tray efficiency values, monitoring of the Gibbs free energy, bifurcation analysis, are available within the framework. Moreover, controllability indices can be determined as a first step towards developing the control structure and finally the optimal design of reactive distillation columns can be found through dynamic optimization.

The motivation for this study has been the interactions between reaction and separation that a reactive column offers. Increased interest in the units for applications in fine chemicals and pharmaceuticals manufacturing, as well as in the commodity industry chemical industry, has also been an incentive of this work.

The work has been mainly focused in developing models (dynamic and steady state) which are sufficiently rigorous to illustrate the complex behaviour of continuous staged reactive distillation columns. The thesis addresses different aspects of operation, simulation and design of reactive distillation columns.

A novel integrated model has been presented, given the hybrid modelling approach. The integration of different types of models as well as modes of simulation gives a new tool for the design of reactive columns.

Controllability issues have also been addressed for reactive distillation columns. However, this analysis has only been investigated for specific cases and it should be studied in greater depth. Assessment of controllability in process design should include many other aspects such as the ability of the system to handle process uncertainties.

Optimal control or dynamic optimization has been addressed in this work. This constitutes a major area of work that would benefit for future work leading from the results obtained in this work.

The following future work is suggested:

- First of all the need for experimental data must be highlighted, since real data is seriously lacking in the open literature.
- The non-equilibrium model should be more thoroughly tested when both mass transfer resistances in the liquid and vapour film are included. Models that consider reaction in the liquid film may be needed in cases of fast reactions, and should be included in the general framework (although at the present such models have not given much advantage over the models which does not consider reaction in the liquid film).
- The effect of changing correlations in the models should be investigated.
- Controllability may be carried out in terms of non-linear models.
- Dynamic optimization should be carried out in order to determine the optimal control structure and parameters together with the design of the reactive column at minimum annualised cost. It has been shown that the simultaneous design of the process and the control structure offers great advantages over sequential design (Mohideen *et al.*, 1996; Bansal *et al.*, 1999). Important savings can be made by utilising the simultaneous approach as well as the possibility of detecting control problems that might not be detected when the design is already made.

Nomenclature

a	Activity coefficient [-]
a	Interfacial area [m^2/m^3]
a'	Interfacial area per unit volume of froth [m^2/m^3]
A	Area [m^2]
A_b	Bubbling area [m^2]
A_p	Specific surface area of the packing [m^2/m^3]
A, B, C, \dots	Coefficients in correlations
C	Concentration [$kmol/h$]
Ca^l	Liquid capillary number [-]
df	Driving force
D_f	Fick's coefficient [m^2/s]
D_{ij}	Maxwell-Stefan diffusivity (Inverse friction coefficient) [m^2/s]
D_{ij}^0	Diffusion coefficient of species i in infinite low concentration in species j [cm^2/s]
D_p	Packing size [m]
DS_p	Heat of reaction [$J/Kmol$]
eq	Amount of acid groups on the resin per unit mass [eq]
E_a	Activation energy [$J/Kmol$]
E^M	Efficiency parameter [-]
E_p^M	Murphree tray efficiency [-]
EL	Liquid entrainment [$Kmol/h$]
EV	Vapour entrainment [$Kmol/h$]
f_{ij}	Friction factor [-]
F	Feed flow [$Kmol/h$]
F_s	Superficial factor [-]
G^E	Excess Gibbs free energy [$J/Kmol$]
h_f	Froth height [m]
h_w	Exit weir height [m]
H	Height of the packing section [m]
H	Enthalpy [$J/Kmol$]
H^E	Enthalpic hold up [$J/Kmol$]

Hl	Liquid enthalpy [$J/Kmol$]
Hlf	Enthalpy of a liquid feed [$J/Kmol$]
Hvf	Enthalpy of a vapour feed [$J/Kmol$]
Hv	Vapour enthalpy [$J/Kmol$]
J	Molar diffusion flux [$mol/m^2 s$]
K	Matrix of volumetric mass transfer coefficients [s^{-1}]
K	Equilibrium constant [-]
K_{eq}	Chemical equilibrium constant [-]
L	Liquid flow rate [$Kmol/h$]
m	Hold-up [$Kmol/h$]
\overline{M}, M	Molecular weight [$Kg/Kmol$]
n_i	Mass transfer rate [$Kmol/h$]
N	Number of transfer unit
$N_{i,p}$	Molar flux of species i at a particular point in the two phase dispersion [$mol/m^2 s$]
NC	Number of components
Np	Products
Nr	Reactants
NR	Number of reactions
P	Pressure [atm]
P^{sat}	Vapour pressure [atm]
PL	Liquid extracted from (or added to) any stage [$Kmol/h$]
PV	Vapour extracted from (or added to) any stage [$Kmol/h$]
Q	Volumetric flow rate [m^3/s]
R	Gas constant [$J/Kmol K$]
Re	Reynolds number [-]
$S_{i,p}$	Reaction rate in the liquid bulk [$Kmol/h$]
Sc, S_c	Schmidt number [-]
Sh	Sherwood number [-]
t	Time [h]
t_g	Gas contact time [h]
t_l	Liquid-phase residence time [h]
T	Temperature [K]
u_s	Superficial vapour velocity [m^2/s]
v	Velocity [m^2/s]
V	Molecular diffusion volumes [-]
V	Molar volume at the normal boiling point of the solute [cm^3/mol]
V	Vapour flow rate [$Kmol/h$]
x	Liquid composition [-]
$x_i x_j$	Factor of concentration weight
y	Vapour composition [-]

Z Liquid flow path length [m]

Greek letters:

α	Heat transfer coefficient [W/m^2K]
Δy	Point efficiency [-]
Γ	Factor accounting for thermodynamic non idealities [-]
γ	Activity coefficient [-]
ΔH^{vap}	Enthalpy of vaporisation [$J/Kmol$]
ψ	Energy flux [W/m^2]
ϕ	Fugacity coefficient [-]
ϕ_p	Heat transfer rate [W]
$\bar{\rho}$	Density of mixture [$Kmol/m^3$]
ρ	Density of pure components [$Kmol/m^3$]
λ	Thermal conductivity [$W/(mK)$]
Λ	Thermodynamic factor []
μ	Viscosity [cP]
μ_i	Chemical potential [$J/Kmol$]
ν	Stoichiometric coefficient []
σ	Surface tension [N/m]

Superscript

L	Liquid
V	Vapour

Subscript

cp	Heat capacity
i, j	Components
p	Tray
r	Reduced
ΔH	Enthalpy

Mathematical Symbols:

∇	Gradient
$[]$	Matrix
${}^{-1}$	Inverse of a matrix

Abbreviations:

AA	Acetic acid
AE	Algebraic equation
BDF	Backwards differentiation formulae
DAE	Differential algebraic equation

<i>EOS</i>	Equation of state
<i>Et</i>	Ethyl
<i>EtAC</i>	Ethyl acetate
<i>MTBE</i>	Methyl-tert-butyl ether
<i>ODE</i>	Ordinary differential equation
<i>RHS</i>	Right hand side
<i>SRK</i>	Soave-Redlich-Kwong
<i>W</i>	Water

References

AIChE, 1958, Bubble Tray Design Manual, *AIChE*, New York.

Agarwal, S., and Taylor, R., 1994, Distillation Column Design Calculations Using a Non-equilibrium Model, *Ind. Eng. Chem. Res.*, 33, 2631.

Al-Jarallah, A.M., Siddiqui, M.A.B., and Lee, A.K.K., 1988, Kinetics of Methyl Tertiary Butyl Ether Synthesis Catalized by Sulfuric Acid, *Chem. Eng. J.*, 39, 169.

Ancillotti, F., Massi Mauri, M., Pescarollo, E., and Romagnoni, L., 1978, Mechanisms in the Reaction between Olefins and Alcohols Catalysed by Ion Exchange Resin, *J. Molec. Catal.*, 46, 49.

ASPEN PLUS User Guide, 1997, *Aspen Technology*.

Backhaus, A.A., 1921, U.S. Patent 1400849.

Bansal, V., Ross, R., Perkins, J.D., and Pistikopoulos, E.N., 1999, The Interactions of Design and Control: Double Effect Distillation, *J. Proc. Control*, accepted.

Barbosa, D., and Doherty, M.F., 1987, Theory of Phase Diagrams and Azeotropic Conditions for Two-Phase Reactive Systems, *Proc. R. Soc. London*, A14, 443.

Barbosa, D., and Doherty, M.F., 1988a, The Influence of Equilibrium Chemical Reactions on Vapor Liquid Phase Diagrams, *Chem. Eng. Sci.*, 43, 529.

Barbosa, D., and Doherty, M.F., 1988b, The Simple Distillation of Homogeneous Reactive Mixtures, *Chem. Eng. Sci.*, 43, 541.

Barton, G.W., and Perkins, J.D., 1986, A Case Study of Dynamic Simulation in Control System Design, presented at Technology & Industry, Sydney.

Bird, R.B., Stewart, W.E., and Lightfoot, E.N., 1960, Transport Phenomena, *John Wiley & Sons Ltd.*, New York.

Bock, H., Jimoh, M., and Wozni, G., 1997a, Analysis of Reaction Distillation Using the Esterification of Acetic Acid as an Example, *Chem. Eng. Technol.*, 20, 182.

Bock, H., Wozni, G., and Gutsche, B., 1997b, Design and Control of a Reaction Distillation Column Including the Recovery System, *Chem. Eng. Proc.*, 36, 101.

Bondy, R.W., 1991, Physical Continuation Approaches to Solving Reactive Distillation Problems, *AIChE Meeting*, Los Angeles.

Bøssen, B.S., Jørgensen, S.T., and Gani, R., 1993, Simulation, Design and Analysis of Azeotropic Distillation Operations, *Ind. Eng. Chem. Res.*, 32, 620.

Bravo, J.L., and Fair, J.R., 1982, Generalised Correlation for Mass Transfer in Packed Distillation Columns, *Ind. Eng. Chem. Proc. Des. Dev.*, 21, 170.

Bristol, E.H., 1966, On a New measure of Interactions for Multivariable Process Control, *IEEE Trans. Automatic Control*, AC-11, 133.

Cameron, I.T., Ruiz, C.A., and Gani, R., 1986, A Generalized Model for Distillation Columns-II, Numerical and Computational Aspects, *Comp. Chem. Eng.*, 10, 199.

Ciric, A.R., and Gu, D., 1994, Synthesis of Nonequilibrium Reactive Distil-

lation Processes by MINLP Optimization, *AIChE J.*, 40, 1479.

Colombo, F., Cori, L., Dalloro, L., Delogu, P., 1983, Equilibrium Constant for the Methyl Tertiary Butyl Ether Liquid Phase Synthesis by Using UNIFAC, *Ind. Eng. Chem. Fundam.*, 22, 219.

Chang, Y.A. and Seader, J.D., 1988, Simulation of Continuous Reactive Distillation by a Homotopy-Continuation Method, *Comp. Chem. Eng.*, 12, 1243.

Chen, G.X., and Chuang, K.T., 1995, Liquid-Phase Resistance to Mass Transfer on Distillation Trays, *Ind. Eng. Chem. Res.*, 34, 3078.

Cuthrell, J.E., and Biegler, L.T., 1988, On the Optimization of Differential-Algebraic Process Systems, *AIChE J.*, 33, 1257.

Daubert, T.E., and Danner, R.P., 1986, DIPPR Data Compilation, *AIChE*: New York.

Dribika, M.M., and Sandall, O.C., 1979, Simultaneous Heat and Mass Transfer for Multicomponent Distillation in a Wetted-wall Column, *Chem. Eng. Sci.* 34, 733.

Fuller, E.N., Ensley, K., and Giddings, J.C., 1969, Diffusion of Halogenated Hydrocarbons in Helium. The Effect of Structure on Collision Cross Section, *J. Phys. Chem.*, 73, 3679.

Fuller, E.N., Schettler, P.D., and Giddings, J.C., 1966, A New Method for Prediction of Binary Gas-Phase Diffusion Coefficients, *Ind. Eng. Chem.*, 58, 19.

Fredenslund, Aa., Gmehling, J., and Rasmussen, P., 1977, Vapour-Liquid Equilibria Using UNIFAC, Elsevier.

Gani, R. and Cameron, I.T., 1989, Extension of Dynamic Models of Distillation Columns to Steady State Simulation, *Comp. Chem. Eng.*, 13, 271.

Gani, R., Hytoff, G., Jacksland, C., and Jensen, A.K., 1997, An Integrated Computer Aided System for Integrated Design of Chemical Processes, *Comp. Chem. Eng.*, 21, 1135.

Gani, R., Ruiz, C.A., and Cameron, I.T., 1986, A Generalized Model for Distillation Columns-I, *Comp. Chem. Eng.*, 10, 181.

Gicquel, A., and Tork, B., 1983, Synthesis of Methyl Tertiary Butyl Ether Catalized by Ion-Exchange Resin- Influence of Methanol Concentration and Temperature, *J. of Catalysis*, 83, 9.

Glansdorf, P., and Prigogine, I, 1971, Thermodynamic Theory of Structure, Stability and Fluctuations, *John Wiley & Sons Ltd.*, NewYork.

Gokhale, V., Hurowitz, S., and Riggs, J.B., 1995, A Comparison of Advanced Distillation Control Techniques for a Propylene/Propane Splitter, *Ind. Eng. Chem. Res.*, 34, 4413.

Górak, A., 1987, Simulation Methods for Steady State Multicomponent Distillation in Packed Columns, *ICHEME Symposium Series*, A413.

gPROMS User Guide, 1997, Process Systems Enterprise Ltd., London, U.K.

Jacobs, R., and Krishna, R., 1993, Multiple Solutions in Reactive Distillation for methyl Tertiary-Butyl Ether Synthesis, *Ind. Eng. Chem. Res.*, 32, 1706.

Jelinek, J. and Hlavacek, V., 1976, Steady State Countercurrent equilibrium Stage Separation with Chemical Reaction by Relaxation Method, *Chem. Eng. Commun.*, 2,79.

Hauan, S., Hertzberg, T., and Lien, K.M., 1995, Why Tertiary Butyl Ether Production by Reactive Distillation May Yield Multiple Solutions, *Ind. Eng. Chem. Res.*, 34, 987.

Havre, K., and Skogestad, S., 1996, Input/Output Selection and Partial Control, *IFAC World Congress, San Francisco, USA*, Vol.M, 181.

Hayden, J.C., and O'Connell, J.P., 1975, A Generalised Method for Predicting Second Virial Coefficients, *Ind. Engng. Chem. Proc. Des. Dev.*, 14, 209.

Higler, A., Taylor, R. and Krishna, R., 1997, Modeling of a Reactive Separation Process Using a Non-Equilibrium Stage Model, *AIChE Annual Meeting*.

Higler, A., Taylor, R. and Krishna, R., 1998, Modeling of a Reactive Separation Process Using a Non-Equilibrium Stage Model, *Comp. Chem. Eng.*, 22, S111.

Higler, A., Taylor, R. and Krishna, R., 1999a, Nonequilibrium Modelling of Reactive Distillation: Multiple Steady States in MTBE Synthesis, *Chem. Eng. Sci.*, 54, 1389.

Higler, A., Taylor, R. and Krishna, R., 1999b, The Influence of Mass Transfer and Mixing on the Performance of a Tray Column for Reactive Distillation, *Chem. Eng. Sci.*, 54, 2873.

Hilborn, R.C., 1994, Chaos and Nonlinear Dynamics (An Introduction to Scientists and Engineers), *Oxford University Press Inc., USA*.

Holland, C.D., 1981, Fundamentals Multicomponent Distillation, Mc Graw Hill, New York.

Holt, B.R. and Morari M., 1985, Design of Resilient Processing Plants. 4.The Effects of Right Half-Plane Zeroes on Dynamic Resilience, and 5.The Effect of Dead time on Dynamic Resilience., *Chem. Eng. Sci.* 40, 59 and 1229.

Ismail Rahim, S., 1998, A Generalised Modular Framework for the Synthesis of Nonideal Separation and Reactive Separation Processes, Thesis, University of London, 1998.

Kang, Y.W., Lee, Y.Y., and Lee, W.K., 1992, Vapour-Liquid Equilibria with Chemical Reaction. Equilibrium-Systems Containing Acetic-Acid, Ethyl-alcohol, Water and Ethyl-acetate, *J. Chem. Eng. Japan*, 25, 649.

Kayhand, F., Sandall, O.C., and Mellichamp, D.A., 1977, Simultaneous Heat

and Mass Transfer in Binary Distillation-II Experimental, *Chem. Eng. Sci.* 32, 747.

Kenig, E., and Górak, A., 1995, A Film Model-Based Approach for Simulation of Multicomponent Reactive Separation, *Chem. Eng. Prog.*, 34, 97.

Kenig, E., Schneider, R., and Górak, A., 1999, Rigorous dynamic modelling of complex reactive absorption processes, *Chem. Eng. Sci.*, 54, 1347.

King, J.C., 1980, Separation Processes, *McGraw-Hill*, New York.

Kister, H.Z., 1992, Distillation Design, *McGraw-Hill*, New York.

Kister, H.Z., 1990, Distillation Operations, *McGraw-Hill*, New York.

Kooijman, H.A., and Taylor, R., 1995, Nonequilibrium Model for Dynamic Simulation of Tray Distillation Columns, *AIChE J.*, 41, 1852.

Kooijman, H.A., and Taylor, R., 1996, ChemSep Technical Manual, v3.01.

Komatsu, H., 1977, Application of the Relaxation Method for Solving Reactive Distillation Problems, *J. Chem. Eng. Japan*, 10, 200.

Komatsu, H., and Holland, C.D., 1977, A New Method of Convergence for Solving Reacting Distillation Problems, *J. Chem. Eng. Japan*, 10, 292.

Kreul, L.U., Górak, A., Dittrich, C., and Barton, P.I., 1998, Dynamic Catalytic Distillation: Advanced Simulation and Experimental Validation, *Comp. Chem. Eng.*, 22, S371.

Kreul, L.U., Górak, A., and Barton, P.I., 1999, Modeling of Homogeneous Reactive Separation Processes in Packed Columns, *Chem. Eng. Sci.*, 54, 19.

Krishna, R., and Standart, G.L., 1976, A Multicomponent Film Model Incorporating a General Matrix Method of Solution to the Maxwell-Stefan Equations, *AIChE J.*, 22, 383.

Krishnamurthy, R., and Taylor, R., 1982, Calculation of Multicomponent Mass Transfer at High Transfer Rates, *Chem. Eng. J.*, 25, 47.

Krishnamurthy, R., and Taylor, R., 1985, A Non-Equilibrium Stage Model of Multicomponent Separation Processes, Part I and II, *AIChE J.*, 31(3), 449.

Kubíček, M., 1976, Algorithm 502. Dependence of Solutions of Non-linear Systems on Parameter, *ACM Trans. Math. Software*, 2, 98.

Kubíček, M., and Marek, M., 1983, Computational Methods in Bifurcation Theory and Dissipative Structures, *Springer-Verlag*, New York.

Luyben, W.L., 1974, Process Modelling, Simulation, and Control for Chemical Engineers, *McGraw-Hill*, New York.

Mess, A.I., 1981, Dynamics of Feedback Systems, *Wiley*, New York

Michelsen, M.L., 1995, Basic Concepts in the Calculation of Chemical Equilibrium, presented at *Nordic Conference on Reactive Separation Systems*, Technical University of Denmark, Denmark.

Mohideen, M.J., Perkins, J.D., and Pistikopoulos, E.N., 1996, Optimal Design of Dynamics Systems under Uncertainty, *AIChE J.*, 42, 2251.

Morari, M., 1985, Robust Stability of Systems with Integral Control, *IEEE Transactions on Automatic Control*, 30, 574.

Nelson, P.A., 1971, Countercurrent Equilibrium Stage Separation with Reaction, *AIChE J.*, 17, 1043.

Onda, K., Takeuchi, H., and Okomoto, Y., 1968, Mass Transfer Coefficients Between Gas and Liquid Phases in Packed Columns, *J. Chem. Eng. Japan*, 1,56.

Papaeconomou, I., 1999, CAPEC Internal Report, *DTU, Denmark*.

Pelkonen, S., Górak A., Kooijman, H., and Taylor, R., 1997, Operation of a Packed Distillation Column: Modelling and Experiments, *ICHEME. Distillation and Absorption* 97, 269.

Perkins, J.D., and Wong, M.P.F., 1985, Assessing Controllability of Chemical-Plants, *Chem. Eng. Res. Des.*, 63, 358.

Pérez-Cisneros, E.S., Schenk, M., and Gani, R., 1997a, A New Approach to Reactive Distillation Modelling and Design, *ICHEME Symposium Series*, 142, 715.

Pérez-Cisneros, E.S., Gani, R., and Michelsen, M.L., 1997b, Reactive Separation Systems. Part I: Computation of Physical and Chemical Equilibrium, *Chem. Eng. Sci.*, 52, 527.

Pérez-Cisneros, E.S., Schenk, M., Gani, R., and Pilavachi, P.A., 1996, Aspects of Simulation, Design and Analysis of Reactive Distillation Operations, *Comp. Chem. Eng.*, 20, S267.

Petersen, C.K., 1989, *PATH User's Guide*. Department of Applied Mathematical Studies and Centre for Nonlinear Studies, University of Leeds, U.K.

Pilavachi, P.A., Schenk, M., and Gani, R., 1999, Aspects of Chemical and Physical Equilibrium and Energy Requirements in Distillation, *ICHEME*, submitted.

Pilavachi, P.A., Schenk, M., Pérez-Cisneros, E.S., and Gani, R., 1997, Modelling and Simulation of Reactive Distillation Operations, *I&CE Research*, 36, 3188.

Powers, M.F., Vickery, D.J., Arehole, A., and Taylor, R., 1988, A Nonequilibrium Stage Model of Multicomponent Separation Processes-V. Computational Methods for Solving the Model Equations, *Comp. Chem. Eng.*, 12, 1229.

Reid, R.C., Prausnitz, J.M., and Poling, B., 1987, *The Properties of Gases*

and Liquids, *McGraw-Hill*, New York-London.

Rehfinger, A., and Hoffmann, U., 1990, Kinetics of Methyl Tertiary Butyl Ether Liquid Phase Synthesis Catalyzed by Ion Exchange Resin-I. Intrinsic Rate Expression in Liquid Phase Activities, *Chem. Eng. Sci.*, 45, 1605.

Rosenbrock, H.H., 1970, State-space and Multivariable Theory, Nelson, London.

Rovaglio, M., and Doherty, M.F., 1990, Dynamics of Heterogeneous Azeotropic Distillation Columns, *AIChE J.*, 36, 39.

Ruiz, C.A., Basualdo, M.S., and Scenna, N.J., Reactive Distillation Dynamic Simulator, *Trans IChemE*, 70, 363.

Ruiz, C.A., Cameron, I.T., and Gani, R., 1988, A Generalized Dynamic Model for Distillation Columns-III. Study of Startup Operations, *Comp. Chem. Eng.*, 12, 1.

Saito, S., Michishita, T., and Maeda, S., 1971, Separation of Meta- and Para- Xylene Mixture by Distillation Accompanied by Chemical Reactions, *J. Chem. Eng. Japan*, 4, 37.

Sawistowski, H., and Pilavakis, P.A., 1979, Distillation with Chemical Reaction in a Packed Column, *IChemE Symposium Series*, 56.

Sawistowski, H., and Pilavakis, P.A., 1982, Vapor-Liquid-Equilibrium with Association in Both Phases - Multicomponent Systems Containing Acetic Acid, *J. Chem. Eng. Data*, 27, 64.

Scenna, N.J., Ruiz, C.A., and Benz, S., 1998, Dynamic simulation of start-up procedures of reactive distillation columns, *Comp. Chem. Eng.*, 22, S719.

Schrans, S., de Wolf, S., and Baur, R., 1996, Dynamic Simulation of Reactive Distillation: An MTBE Case Study, *Com. Chem. Eng.*, 20, S1619.

Scheiber, I., and Marek, M., 1995, Chaotic Behaviour of Deterministic Dissipative Systems, *Cambridge University Press*, Cambridge.

Seader, J.D., 1989, The Rate-Based Approach for Modelling Staged Separations, *Chem. Eng. Prog.*, 85, 41.

Sennewald, K., Gehrmann, K., and Schafer, S., 1971, Column for Carrying Out Organic Chemical Reactions in Contact with Fine Particulate Catalysts, US Patent 3,579,309.

Sivasubramanian, M.S., and Boston, J.F., 1990, The Heat and Mass Transfer Rate-Based Approach for Modelling Multicomponent Separation Processes, *Com. Appl. Chem. Eng.*, 331.

Skogestad, S., 1997, Dynamics and Control of Distillation Columns- A Critical Survey, *Modelling, Identification and Control*, 18, 177.

Skogestad, S., Lundstrom, P., and Jacobsen, E.W., 1990, Selecting the Best Distillation Control Configuration, *AIChE J.*, 36, 753.

Skogestad, S., and Morari, M., 1987, Control Configuration Selection for Distillation-Columns, *AIChE J.*, 10, 1620.

Skogestad, S., and Postlethwaite, I., 1996, Multivariable Feed-Back Control, *John Wiley & Sons Ltd.*, England.

Sneesby, M.G., Tade, M.O., Datta, R., and Smith, T.N., 1997, ETBE Synthesis via Reactive Distillation. 2. Dynamic Simulation and Control Aspects, *Ind. Eng. Chem. Res.*, 36, 1870.

Solari, H.G., Natiello, M.A., and Mundlin, G.B., 1996, Nonlinear Dynamics: a Two-Way Trip from Physics to Math,

Sørensen, E., 1994, Studies on Optimal Operation and Control of Batch Distillation Columns, PhD. Thesis, University of Thronheim, Norway.

Sundmacher, K., 1995, Reaktivdestillation mit katalytischen Fuellkoerperkack-

ungen ein neuer Process zur Herstellung der Kraftstoffkomponente MTBE, PhD Thesis, CUTECH Institute, Clausthal-Zellerfeld, Germany.

Sundmacher, K., and Hoffmann, U., 1996, Development of a New Catalytic Distillation Process for Fuel Ethers via a Detailed Nonequilibrium Model, *Chem. Eng. Sci.*, 51, 2359.

Suzuki, I., Komatsu, H., and Hirata, M., 1970, Formulation and Prediction of Quaternary Vapor-Liquid Equilibria Accompanied by a Chemical Reaction, *J. Chem. Eng. Japan*, 3, 152.

Suzuki, I., Yagi, H., Komatsu, H., and Hirata, M., 1971, Calculation of Multicomponent Distillation Accompanied by a Chemical Reaction, *J. Chem. Eng. Japan*, 4, 26.

Stewart, W.E., and Prober, R., 1964, Matrix Calculation of Multicomponent Mass Transfer in Isothermal Systems, *Ind. Eng. Chem. Fundam.*, 3, 224.

Taylor, R., Kooijman, H.A., and Hung, J.S., 1994, A Second Generation Nonequilibrium Model for Computer-Simulation of Multicomponent Separation Processes, *Comp. Chem. Eng.*, 18, 205.

Taylor, R., Kooijman, H.A., and Woodman, M.R., 1992, Industrial Applications of a Nonequilibrium Model of Distillation and Absorption Operations, *ICHEME Symposium Series*, A415.

Taylor, R., and Krishna, R., 1993, Multicomponent Mass Transfer, Wiley, New York.

Taylor, R., and Lucia, A., 1995, Modelling and Analysis of Multicomponent Separation Processes, *AIChE Symposium Series*, 91, 19.

Thompson, J.M.T., and Stewart, H.B., 1986, Nonlinear Dynamics and Chaos: Geometrical Methods for Engineers and Scientists, *Wiley, New York*.

Toor, H.L., 1964, Solution of the Linearized Equations of Multicomponent Mass Transfer, *AIChE J.*, 10, 448.

Ung, S., and Doherty, M.F., 1995a, Vapour-Liquid Phase Equilibrium in Systems with Multiple Chemical Reactions, *Chem. Eng. Sci.*, 50, 23.

Ung, S., and Doherty, M.F., 1995b, Vapour-Liquid Phase Equilibrium in Systems with Multiple Chemical Reactions, *Ind. Eng. Chem. Res.*, 34, 2555.

Ung, S., and Doherty, M.F., 1995c, Necessary and Sufficient Conditions for Reactive Azeotropes in Multi-Reactions Systems, *AIChE J.*, 41, 2383.

Venkataraman, S., Chan, W.K., and Boston, J.F., 1990, Reactive Distillation Using ASPEN PLUS, *Chem. Eng. Prog.*, 86(8), 45.

Vogelphol, A., 1979, Murphree Efficiencies in Multicomponent Systems, *ICHEME Symposium Series* 2(56), 25.

Wesseling, J.A., 1997, Non-equilibrium Modelling of Distillation, *Chem. Eng. Res. Des.*, 75, 519.

Wesseling, J.A., and Krishna, R., 1990, Mass Transfer, *Ellis Horwood, Chichester, England*.

Whitman, W.G., 1923, A Preliminary Experimental Confirmation of the Two-Film Theory of Gas Absorption, *Chem. Metall. Eng.*, 29, 146.

Wilke, C.R., and Chang, P., 1955, Correlation of Diffusion Coefficients in Dilute Solutions, *AIChE J.*, 1 264.

Wolff, E.A., Skogestad, S., Hovd, M., and Mathisen, K.W., 1992, A Procedure for Controllability Analysis, *IFAC Workshop, London, UK*.

Zheng, Y., and Xu, X., 1992, Study on Catalytic Distillation Processes. 2. Simulation of Catalytic Distillation Processes - Quasi-Homogeneous and Rate-based Model, *Trans. IChem. E* 70, Part A, 465.

Appendix A

Properties

A.1 Enthalpy

The component liquid enthalpy is calculated from a polynomial expression for the heat capacity taken from the DIPPR data bank (Daubert and Danner, 1986).

$$h_i^L = \int_{T_o}^T (A_{cp} + B_{cp}T + C_{cp}T^2 + D_{cp}T^3 + E_{cp}T^4)dT \quad (\text{A.1})$$

Mixture liquid enthalpy is calculated by means of the following equation,

$$H^L = \sum_{i=1}^{NC} x_i(h_i^L - h_r^L) \quad (\text{A.2})$$

where h_r^L is a reference enthalpy.

The vapour enthalpy is calculated through the liquid enthalpy and the heat of vaporisation. For the heat of vaporisation the DIPPR data bank (Daubert and Danner, 1986) is again used. The expression is as follows,

$$H_i^{vap} = A_{\Delta H}(1 - T_r)^{(B_{\Delta H} + C_{\Delta H}T_r + D_{\Delta H}T_r^2 + E_{\Delta H}T_r^3)} \quad (\text{A.3})$$

$$T_r = \frac{T}{T_C} \quad (\text{A.4})$$

$$\Delta H^{vap} = \sum_{i=1}^{NC} x_i H_i^{vap} \quad (\text{A.5})$$

Mixture vapour enthalpy is calculated by,

$$H^V = \sum_{i=1}^{NC} y_i (h_i^L - \Delta H^{vap}) \quad (\text{A.6})$$

A.2 Density

Component density of the liquid phase is calculated with the DIPPR data bank (Daubert and Danner, 1986).

$$\rho_{Li} = \frac{A_\rho}{B_\rho^{(1+(1-\frac{T}{C_\rho})^{D_\rho})}} \quad (\text{A.7})$$

Mixture density is calculated through,

$$\frac{1}{\bar{\rho}_{Lp}} = \frac{1}{\sum_{i=1}^{NC} \rho_{Li,p} x_{i,p}} \quad (\text{A.8})$$

Density of the vapour phase is calculated from the equation of state (or ideal gas law).

A.3 Viscosity

Viscosity for liquid and vapour phase are calculated through a suitable correlation given by Daubert and Danner (1986),

$$\mu_i^v = \frac{A_{\mu v} T^{B_{\mu v}}}{(1 + C_{\mu v}/T + D_{\mu v}/T^2)} \quad (\text{A.9})$$

$$\mu_i^l = \exp(A_{\mu l} + B_{\mu l}/T + C_{\mu l} \ln(T) + D_{\mu l} T^{E_{\mu l}}) \quad (\text{A.10})$$

Mixture viscosity is calculated through,

$$\mu_L = \exp\left[\sum_{i=1}^{NC} \ln \mu_i^l x_{i,p} + 1/2 \sum_{i \neq j} x_i x_j G_{ij}\right] \quad (\text{A.11})$$

$$\mu_V = \sum_{i=1}^{NC} \frac{\mu_i^l y_{i,p}}{\sum_{j=1}^{NC} y_j \phi_{ij}} \quad (\text{A.12})$$

where

$$\phi_{ij} = \frac{[1 + (\mu_i/\mu_j)^{1/2}(M_j/M_i)^{1/4}]^2}{[8(1 + M_i/M_j)]^{1/2}} \quad (\text{A.13})$$

A.4 Surface Tension

Surface tension for pure components is calculated with DIPPR data bank (Daubert and Danner, 1986):

$$\sigma_i = A_\sigma * (1 - T_r)^{B_\sigma} + C_\sigma T_r \quad (\text{A.14})$$

For mixtures an approximate estimate is used:

$$\bar{\sigma}^{1/4} = \sum_{i=1}^{NC} x_i \sigma_i^r \quad (\text{A.15})$$

with $r = -3$ to $r = 1$ is usually used.

A.5 Thermal Conductivity

Thermal conductivity for pure components is calculated with DIPPR data bank (Daubert and Danner, 1986):

$$\lambda_i = \frac{A_\lambda T^{B_\lambda}}{1 + C_\lambda/T + D_\lambda/T^2} \quad (\text{A.16})$$

Mixture thermal conductivity is calculated through the following expression,

$$\bar{\lambda}_L = \sum_{i=1}^{NC} \sum_{j=1}^{NC} \rho_i \rho_j \lambda_{ij} \quad (\text{A.17})$$

$$\lambda_{ij} = 2(\lambda_i^{-1} + \lambda_j^{-1})^{-1} \quad (\text{A.18})$$

$$\rho_i = \frac{x_i V_i}{\sum_{j=1}^{NC} V_j} \quad (\text{A.19})$$

$$\bar{\lambda}_V = \frac{\sum_{i=1}^{NC} y_i \lambda_i^v}{\sum_{j=1}^{NC} y_j \phi_{ij}} \quad (\text{A.20})$$

where ϕ_{ij} is the interaction parameter for gas mixture viscosity.

A.6 Binary Diffusion Coefficients

The relationship between the Fick's diffusion coefficient and the Maxwell-Stefan diffusion coefficients is given by:

$$D_f = D\Gamma$$

where D_f is the Fick's coefficient, D is the Maxwell-Stefan coefficient and Γ is a factor accounting for thermodynamic non-idealities. For ideal systems both coefficients are identical ($\Gamma = 1$).

Fick's diffusion coefficient incorporates two aspects: *a*) significance of inverse drag and *b*) the thermodynamic non-idealities.

Fick's coefficients are less easy to interpretate physically than the Maxwell-Stefan coefficients. (Taylor and Krishna, 1993).

- Vapour phase

Reid *et al.* (1987) and Daubert and Danner (1986) recommend the use of a correlation due to Fuller *et al.* (1966,1969) to calculate the diffusion coefficients and this is the one used in this work.

$$D_f = CT^{1.75} \frac{\sqrt{[(M_1 + M_2)/M_1 M_2]}}{P(\sqrt[3]{V_1} + \sqrt[3]{V_2})^2} \quad (\text{A.21})$$

with T in kelvin(K), P in Pa , M_1 and M_2 in g/mol and $C = 1.013e-02$, D will be in (m^2/s) . The terms V_1 and V_2 are the molecular diffusion volumes and are calculated by summing atomic contribution in the components.

- Liquid phase

For the liquid phase, Wesselingh and Krishna (1990) suggested the following model for the limiting diffusivities:

$$D_{ij} = (D_{ij}^o D_{ji}^o)^{1/2} \quad (\text{A.22})$$

where the D° coefficients are calculated with the method due to Wilke and Chang (1955):

$$D_{12}^\circ = 7.4e - 08 \frac{(\phi_2 M_2)^{1/2} T}{\mu_2 V_1^{0.6}} \quad (\text{A.23})$$

where D° is the diffusion coefficient of species 1 (the solute) present in infinitely low concentration in species 2 (the solvent), cm^2/s ; M_2 is the molar mass of the solvent, g/mol ; T is the temperature, K ; μ_2 is the viscosity of the solvent, cP ; and V_1 is the molar volume at the normal boiling point of the solute, cm^3/mol .

Appendix B

Results

B.1 Simulation Results for MTBE

- Changes in Feed Rate

The transient response to a 10% decrease in methanol feed flow rate with vapour boil-up and distillate held constant is shown in Fig. B.1.

Without a decrease in the vapour boil-up input, there was a decrease in the bottom flow rate which means low MTBE production.

The composition of the bottom shifted to higher MTBE concentration (actually the global isobutene conversion did not considerably changed). The temperature in the column increased accordingly as the reboiler remained in phase equilibrium. After the disturbance the column recovers its original steady state.

Increasing the methanol feed flow rate in 10% makes the system unstable, going to a low conversion solution without recovering from that. The transient is shown in Fig. B.2.

The control of the stoichiometric ratio is rather complicated, specially because the feed composition will not be accurately (it will probably depends on a process upstream). The unreacted methanol is recovered with the MTBE in the bottoms of the column, and the amount of methanol in the reactive zone increases the isobutene conversion.

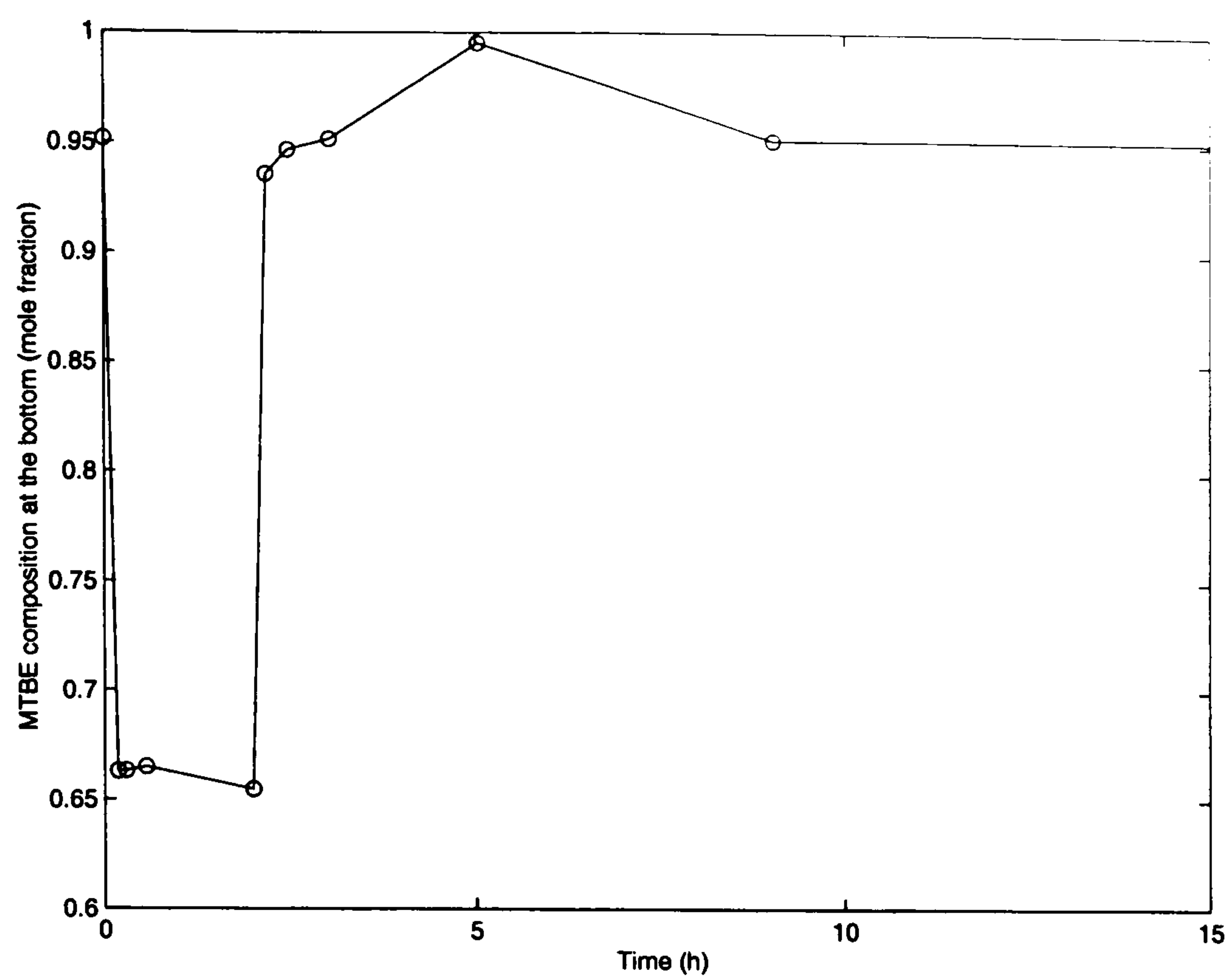


Figure B.1: Decreasing 10% methanol feed flow-rate.

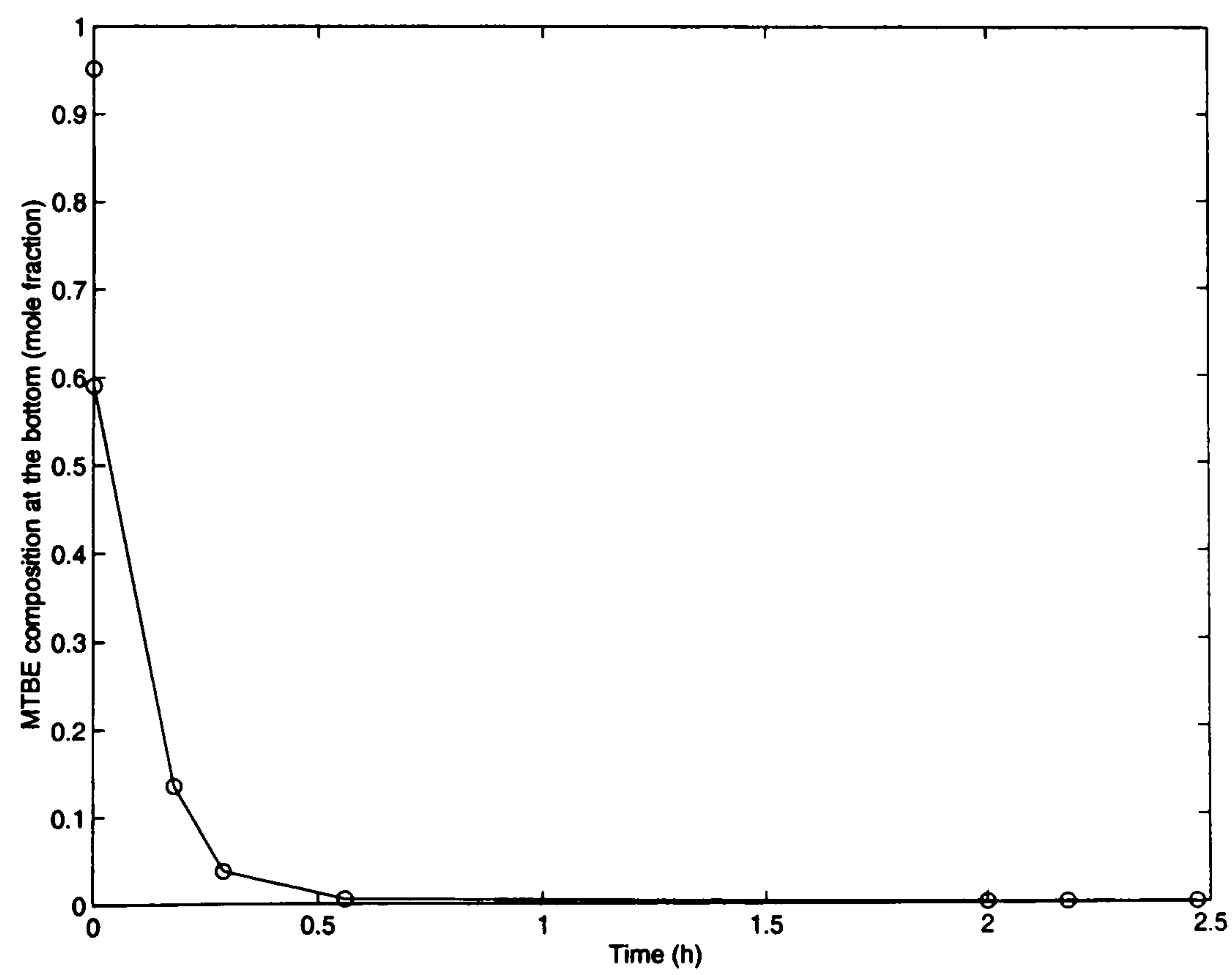


Figure B.2: Increasing 10% methanol feed flow-rate.

A compromise must be determined between isobutene conversion (increases as methanol increases) and ether purity (which falls as methanol increases). High MTBE purity can be produced with a lower methanol excess, but some excess should be used to suppress side reactions.

- Changes in Feed Composition

The isobutenes feed composition is fixed by upstream plant operations and usually varies between 15 and 55% of isobutene, depending in the process upstream (which units and catalyst are employed). Increasing the concentration of isobutene could have some effects on the reactive distillation columns operations, such as:

- reactant concentration in the reaction zone increase, with a ‘favourable’ effect in the reaction equilibrium,
- reactive section temperature and reactive section gradient of temperature increase with effect on the reaction equilibrium, and
- the specific reboiler duty must be decreased to maintain product specifications or conditions.

Fig. B.3 shows the transient response to a 10% of isobutene feed composition increased. The global isobutene conversion increased by the additional driving force for the reaction as well as MTBE purity in the bottoms. The bottom temperature follows the composition changes.

When the isobutene composition decreases is interesting to notice that the system is going to low conversion solution. A step change (15% decreasing isobutene feed composition) makes the system go to very low MTBE production and it will not go back to the high conversion solution again, when the composition is back to the normal amount. This effect is shown in Fig. B.4.

If the step change is only 10% then a small change is produced and the reactive column will recover after some time (Fig. B.5).

The temperature in the reactive section increased and exceeded the limit for the catalyst temperature degradation.

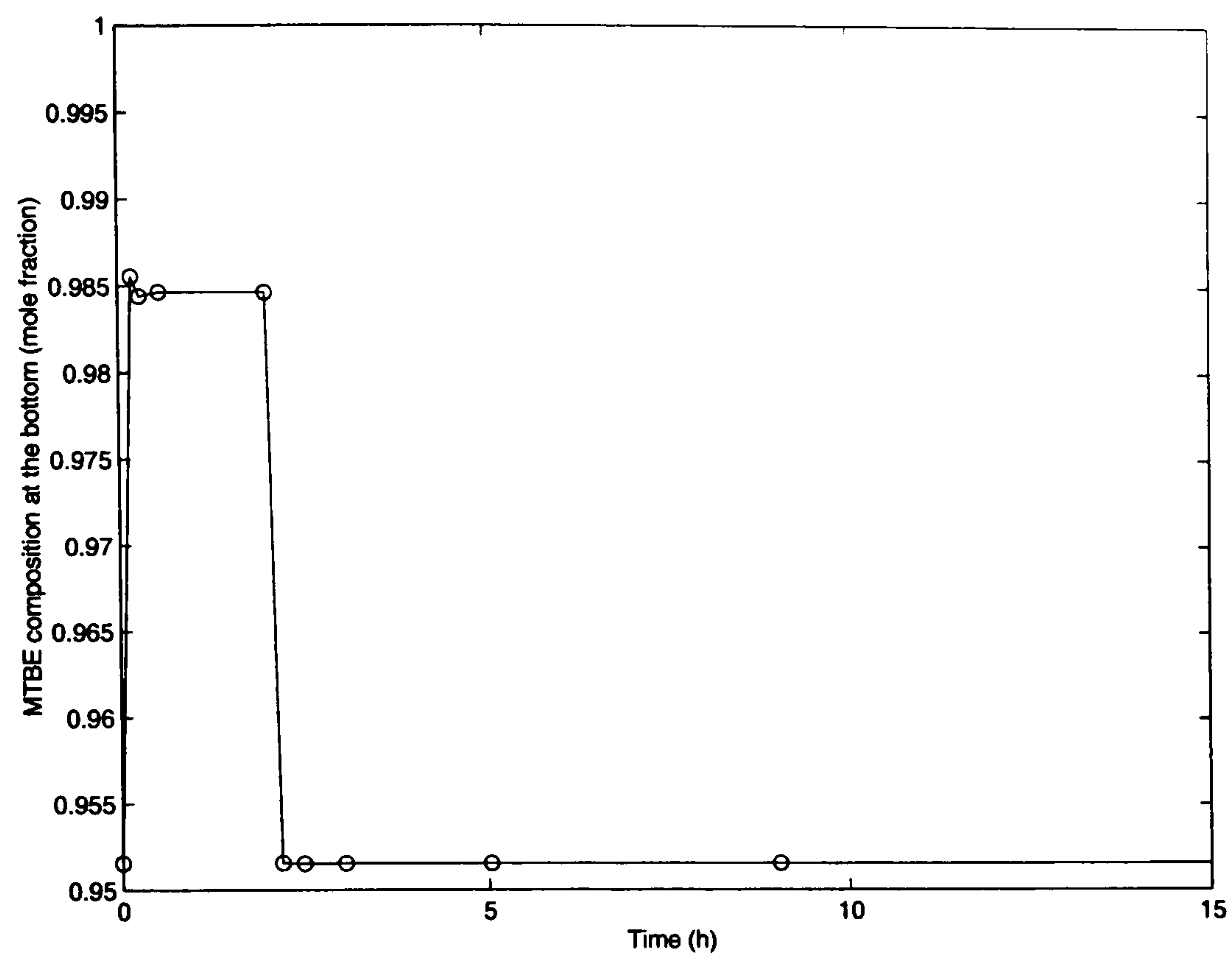


Figure B.3: Increasing 10% isobutene feed composition.

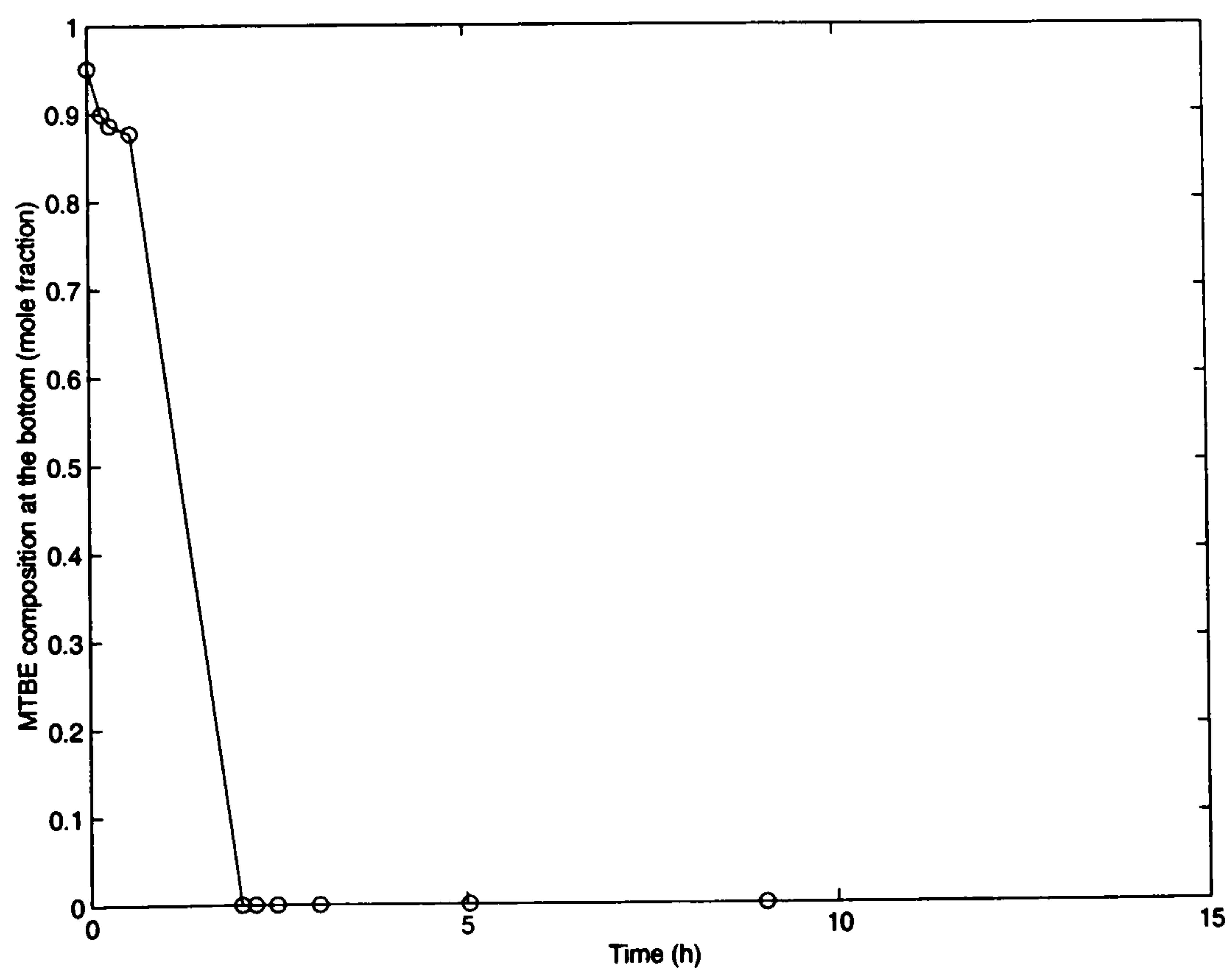


Figure B.4: Decreasing 15% isobutene feed composition.

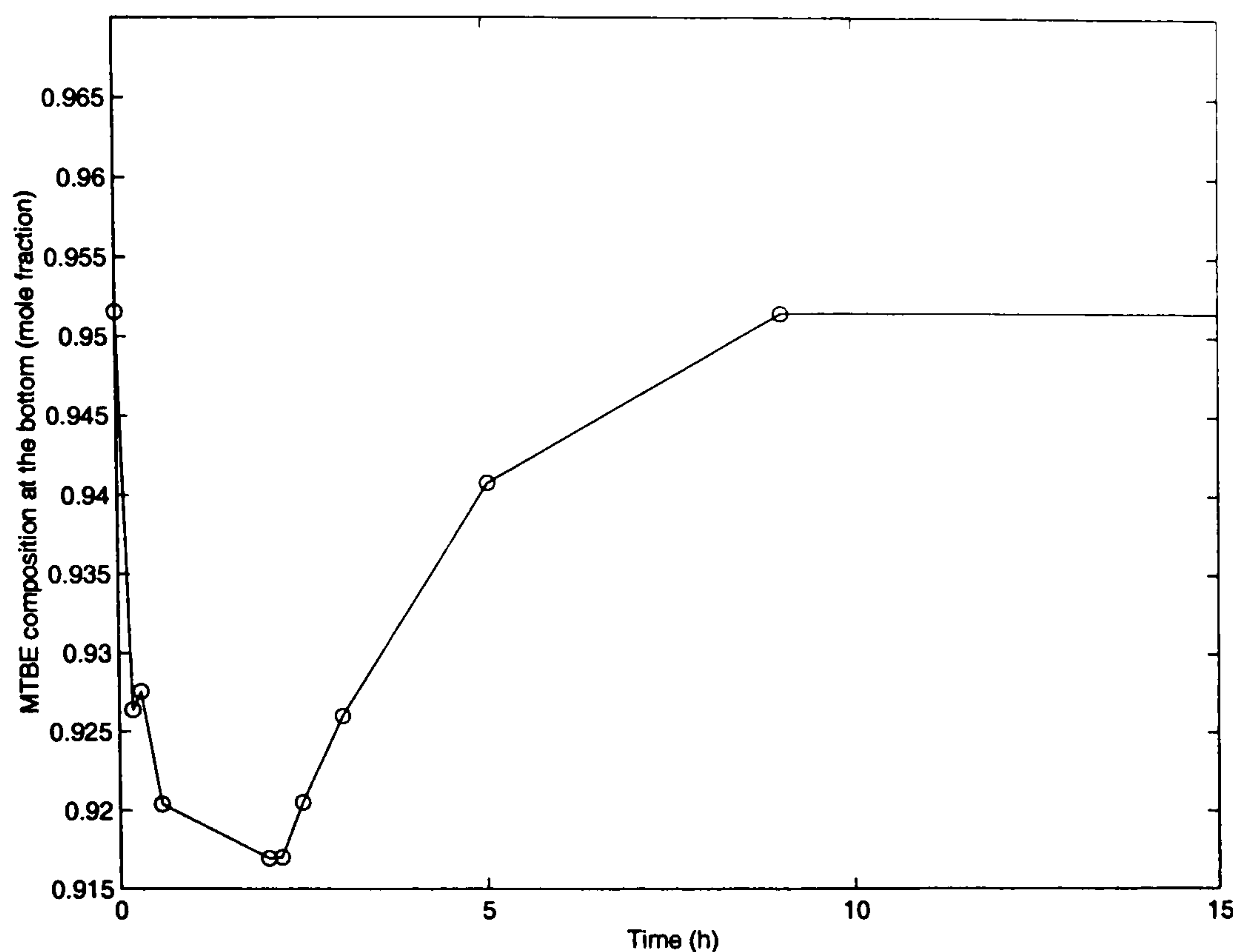


Figure B.5: Decreasing 10% isobutene feed composition.

Decreasing the methanol feed flow rate will help to maintain the desired conditions.

- Effects of Reactive and Non-Reactive Stages

Increasing or decreasing the number of reactive stages from the 'optimum' produced a bad interaction between the phase equilibrium and the chemical reaction which leads to high decomposition of product on the lower reactive stages.

The rectification zone of a reactive distillation column should remove the inert (light component, n-butene, in this case) from the reactive section and recycle unreacted reactant (isobutene) to the reactive section.

The stripping section should remove the the MTBE from the reactive section to maintain good reaction conditions and purify the product as well as prevent the loss of reactants with the product.

Even though the separation objectives are clear, increasing in rectification or stripping stages is not necessarily good for the reaction section conditions.

If the rectification zone is increased too much will result in loss of isobutene in the distillate, and if the stripping zone is increased too much methanol will be moved away from the reaction section.

B.1.1 Controllability Analysis for the MTBE production

Three cases are presented:

Case1

The input variables (u) are given by,

$$u = \begin{bmatrix} D \\ V \end{bmatrix} \quad (\text{B.1})$$

The disturbances (d) are considered as follows,

$$d = \begin{bmatrix} x_{isobutene,F} \\ T_F \end{bmatrix} \quad (\text{B.2})$$

while the measurements variables (y) are,

$$y = \begin{bmatrix} x_{MTBE,D} \\ x_{MTBE,B} \end{bmatrix} \quad (\text{B.3})$$

The transfer function G (after scaling) is given by,

$$G = \begin{bmatrix} 2.8325 & 0.1254 \\ 0.0388 & 0.0288 \end{bmatrix} \quad (\text{B.4})$$

The reactive column is functional controllable. The $\det G(s)$ is different from zero.

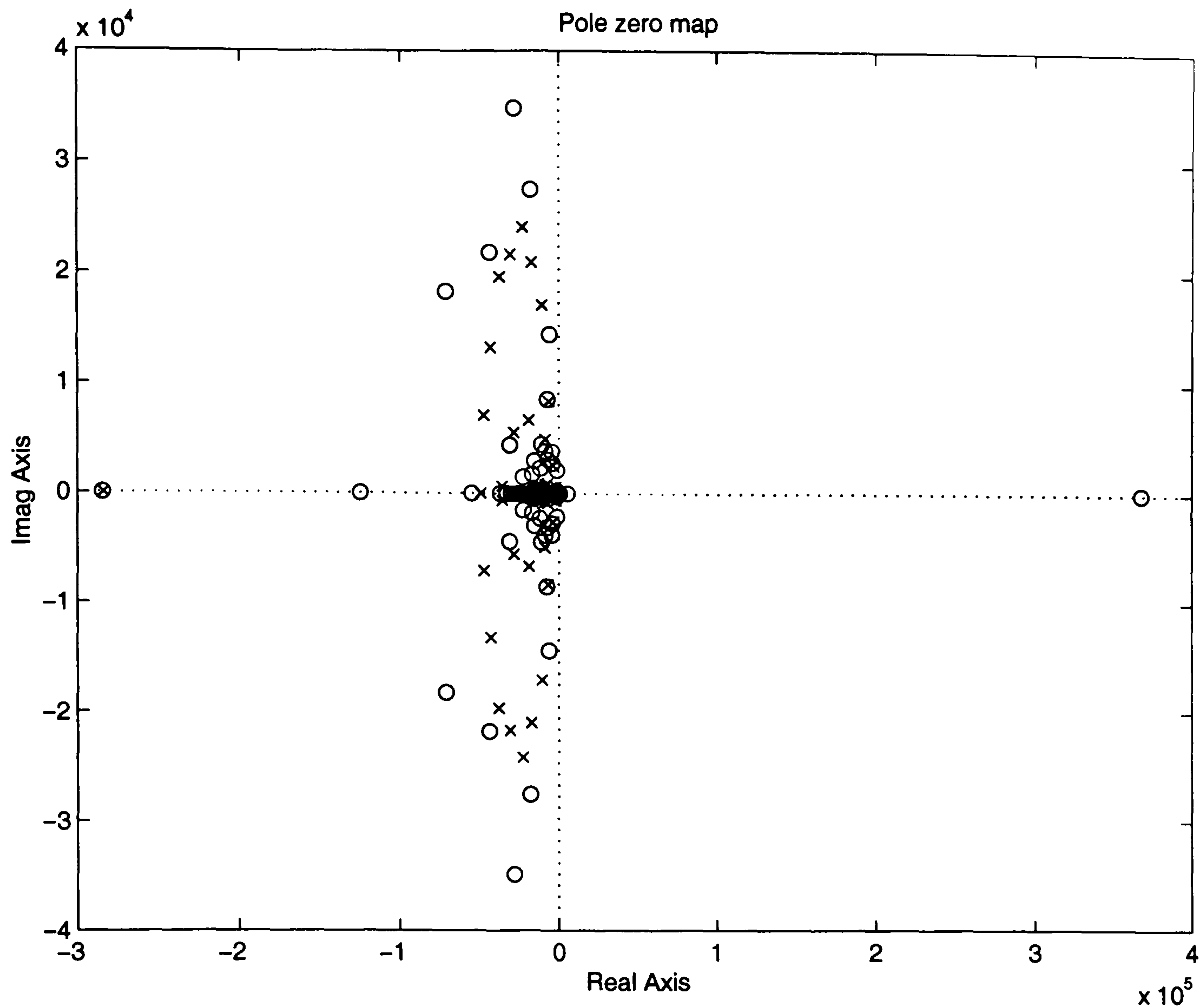


Figure B.6: Poles and Zeroes for Case 1 (MTBE)

- Computation of poles and zeroes

All poles are in the left half plane (system stable). Existence of RHP-zeroes. As can be seen from Fig.B.6.

- RGA

The steady-state RGA matrix is given by,

$$RGA = \begin{bmatrix} 1.06340 & -0.0634 \\ -0.0634 & 1.06340 \end{bmatrix} \quad (B.5)$$

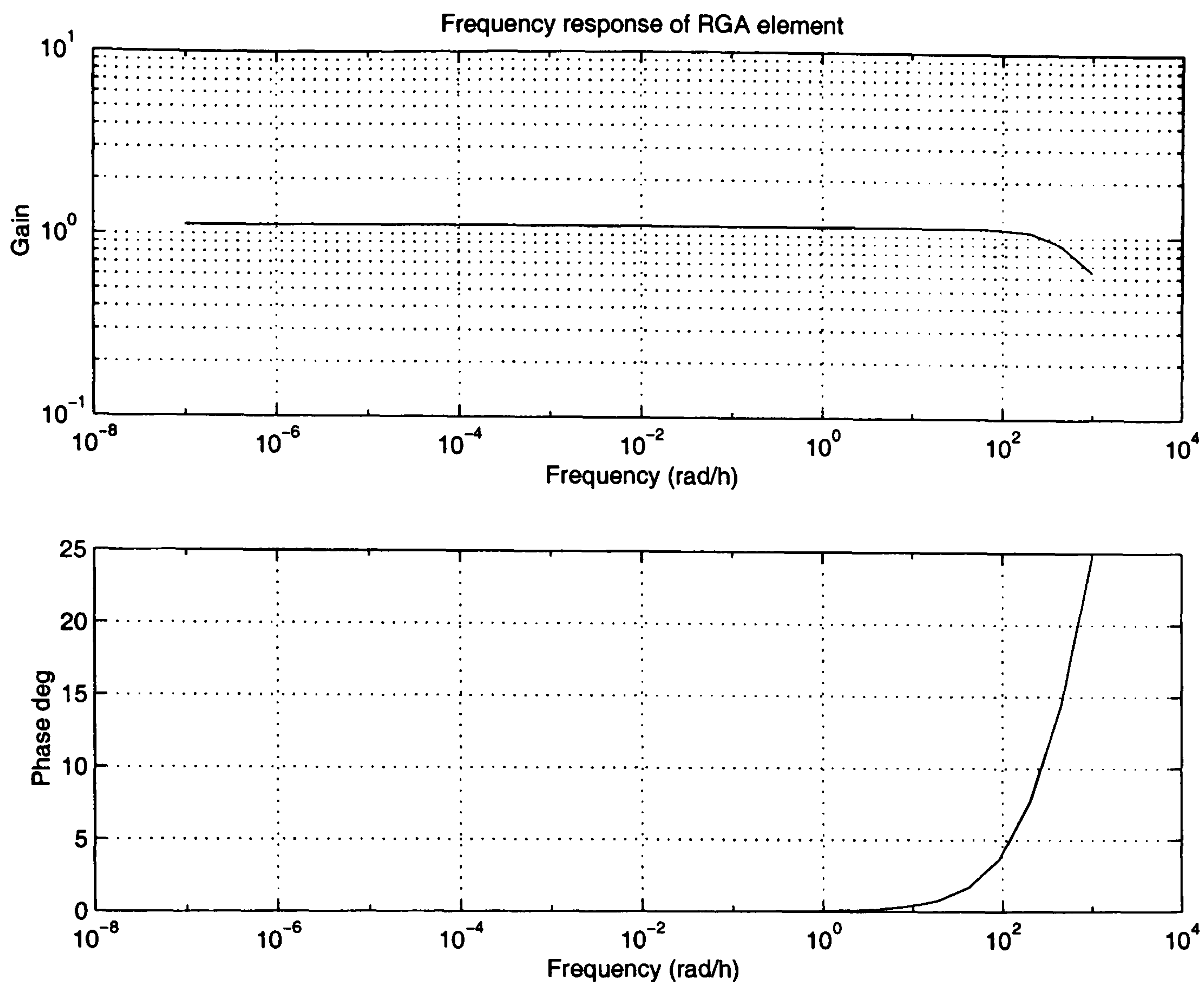


Figure B.7: RGA element (1,1) as a function of the frequency for Case 1 (MTBE)

The 1,1 element of the matrix can be plotted as a function of the frequency, as can be seen in Fig. B.7. The values of RGA are close to 1 at any frequency, only at high very high frequencies takes some smaller values. The pairing of distillate and composition is a good choice.

- Singular value

The singular values are :

$$\underline{\sigma} = 0.0223 \quad (\text{B.6})$$

$$\overline{\sigma} = 2.8356 \quad (\text{B.7})$$

The singular values at every frequency are given in Fig. B.8

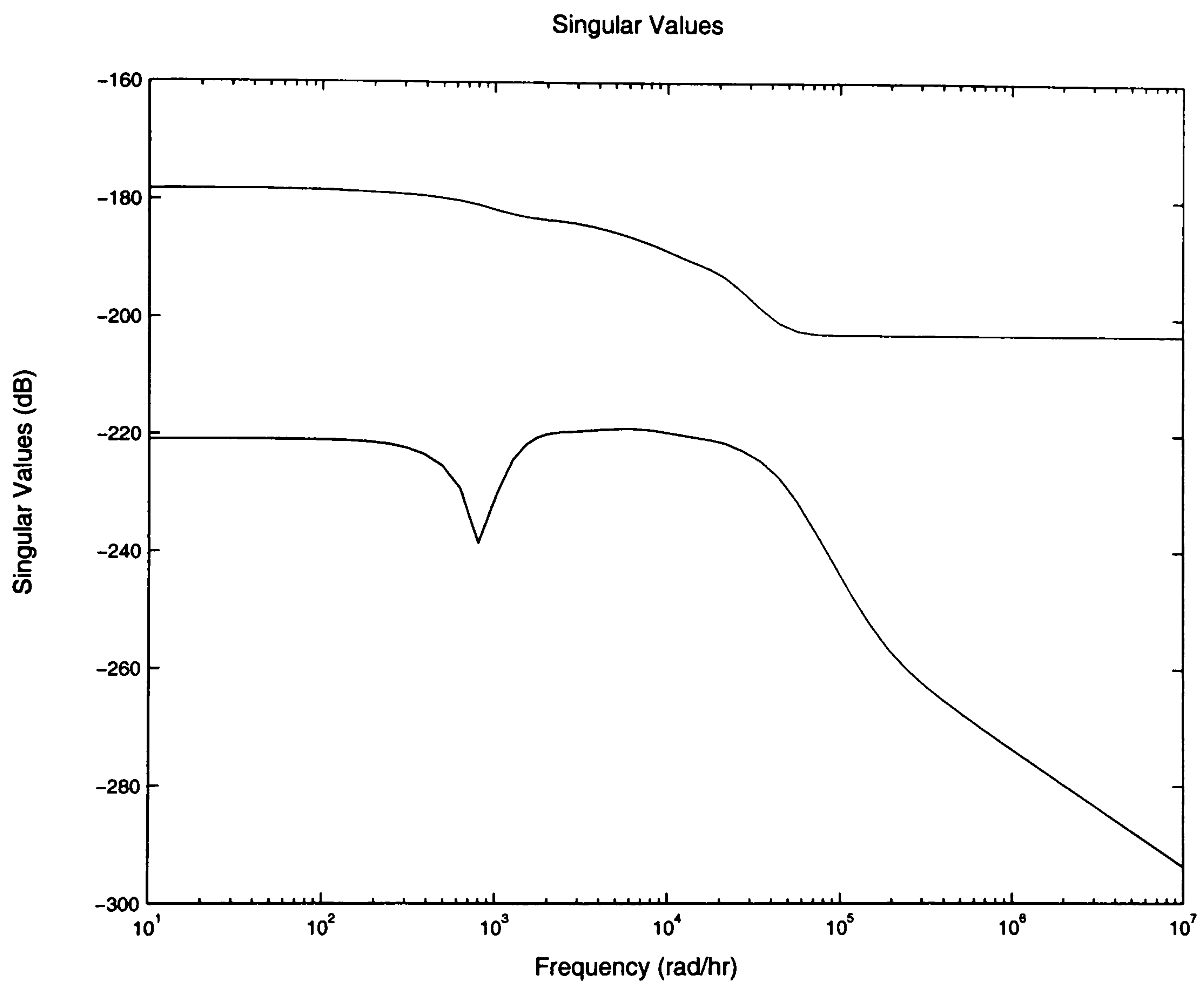


Figure B.8: Singular values for Case 1(MTBE)

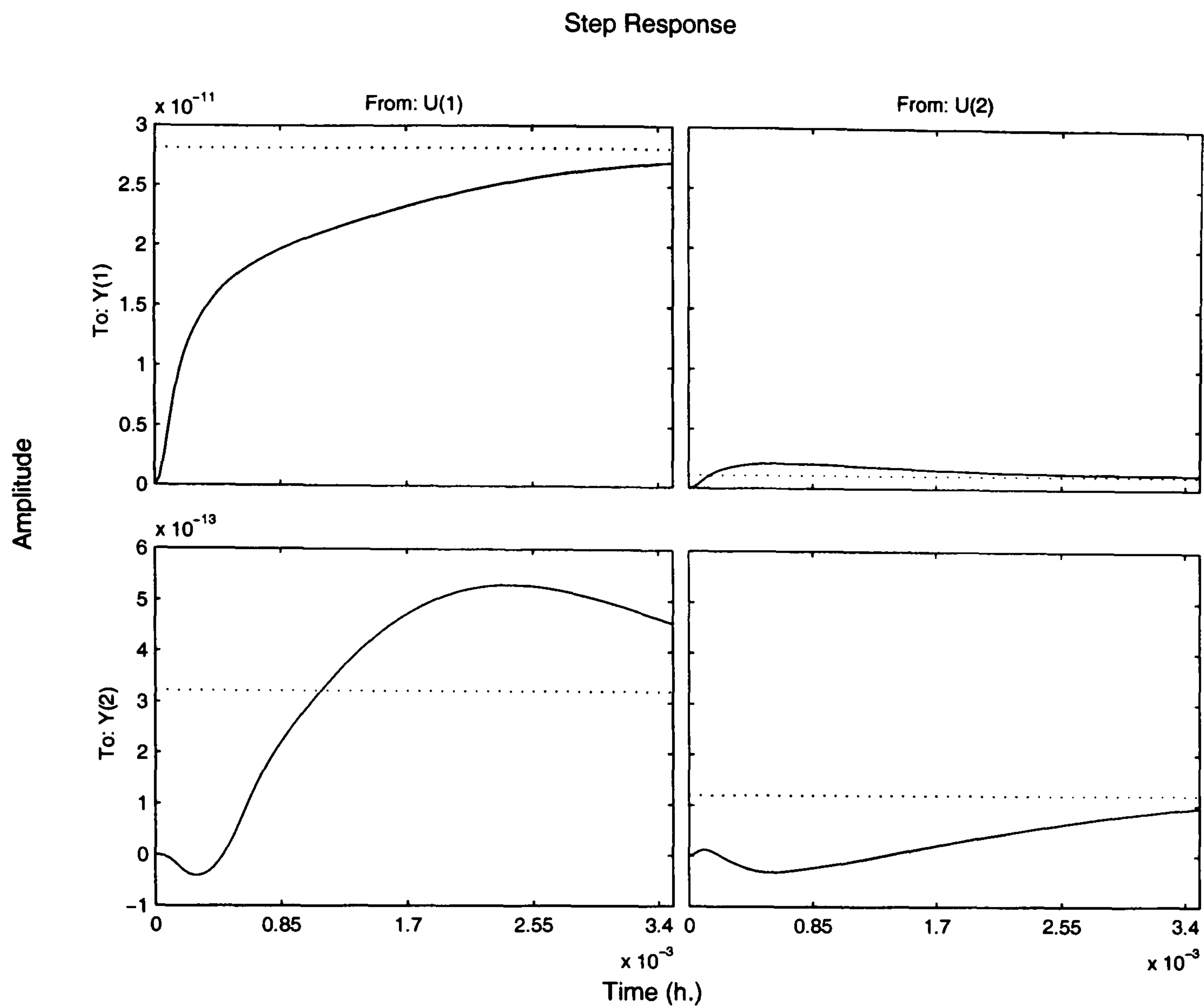


Figure B.9: Step response for Case 1 (MTBE). (10% step size)

Analysis

The condition number is large (≈ 127) but not too large. The RGA values are small, and since the condition number is not really high it should not be a problem to control this column. The pairing of distillate with the product composition and the bottom with the composition at the bottom of the column is the best, which is physically logical. The only negative effect are the RHP-zeros which implies inverse response, as can be seen from Fig. B.9.

Case2

The input variables (u) are given by,

$$u = \begin{bmatrix} D \\ V \end{bmatrix} \quad (\text{B.8})$$

The disturbances (d) are considered as follows,

$$d = \begin{bmatrix} x_{isobutene,F} \\ T_F \end{bmatrix} \quad (\text{B.9})$$

while the measurements variables (y) are,

$$y = \begin{bmatrix} x_{MTBE,D} \\ T_B \end{bmatrix} \quad (\text{B.10})$$

The transfer function G is given by,

$$G = \begin{bmatrix} 0.1223 & 0.00410 \\ 3.88e-05 & 2.88e-05 \end{bmatrix} \quad (\text{B.11})$$

The reactive column is functional controllable. The $\det G(s)$ is different from zero.

- Computation of poles and zeroes

All poles are in the left half plane (system stable). Existence of RHP-zeroes. As can be seen from Fig.B.10.

- RGA

The steady-state RGA matrix is given by,

$$RGA = \begin{bmatrix} 1.0475 & -0.0475 \\ -0.0475 & 1.0475 \end{bmatrix} \quad (\text{B.12})$$

The 1,1 element of the matrix can be plotted as a function of the frequency, as can be seen in Fig. B.11. The values of RGA tends to 1 at high frequencies, which confirms that the pairing u1-y1 is a good choice.

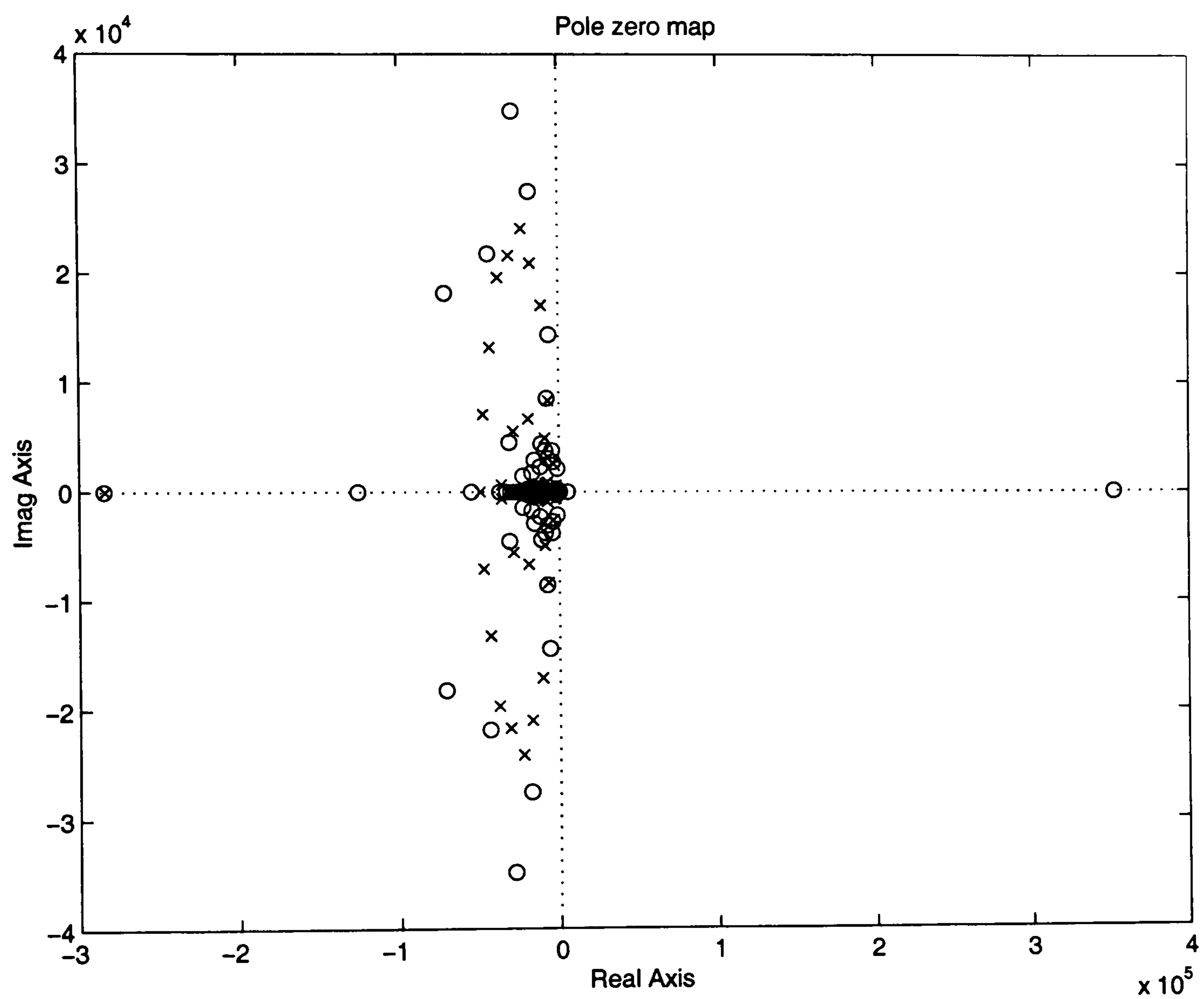


Figure B.10: Poles and Zeroes for Case 2 (MTBE)

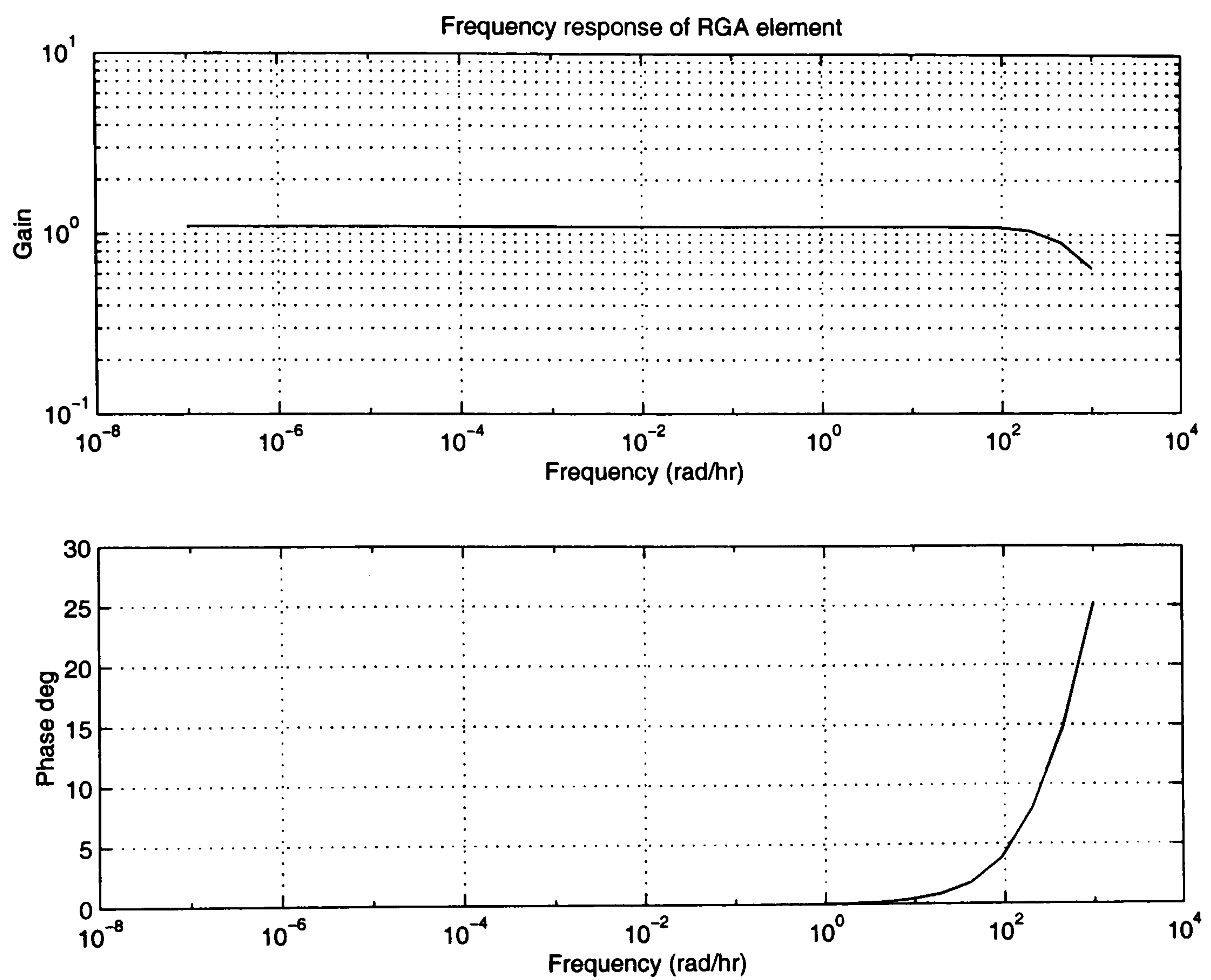


Figure B.11: RGA element (1,1) as a function of the frequency for Case 2 of MTBE

- Singular value

The singular values are :

$$\underline{\sigma} = 0.00387 \quad (B.13)$$

$$\overline{\sigma} = 0.122 \quad (B.14)$$

Analysis

The condition number is large (≈ 31.5), but not too large. The RGA values are small, indicating that the interactions are not strong. A negative effect are the RHP-zeroes. The inverse response can be seen from Fig. B.12. It should not be a problem in controlling this column.

Case3

The input variables (u) are given by,

$$u = \begin{bmatrix} D \\ V \end{bmatrix} \quad (B.15)$$

The disturbances (d) are considered as follows,

$$d = \begin{bmatrix} x_{isobuten,F} \\ T_F \end{bmatrix} \quad (B.16)$$

while the measurements variables (y) are,

$$y = \begin{bmatrix} T_D \\ T_B \end{bmatrix} \quad (B.17)$$

The transfer function G is given by,

$$G = \begin{bmatrix} 0.12230 & 0.00410 \\ -0.0077 & 0.00060 \end{bmatrix} \quad (B.18)$$

The reactive column is functional controllable. The $\det G(s)$ is different from zero.

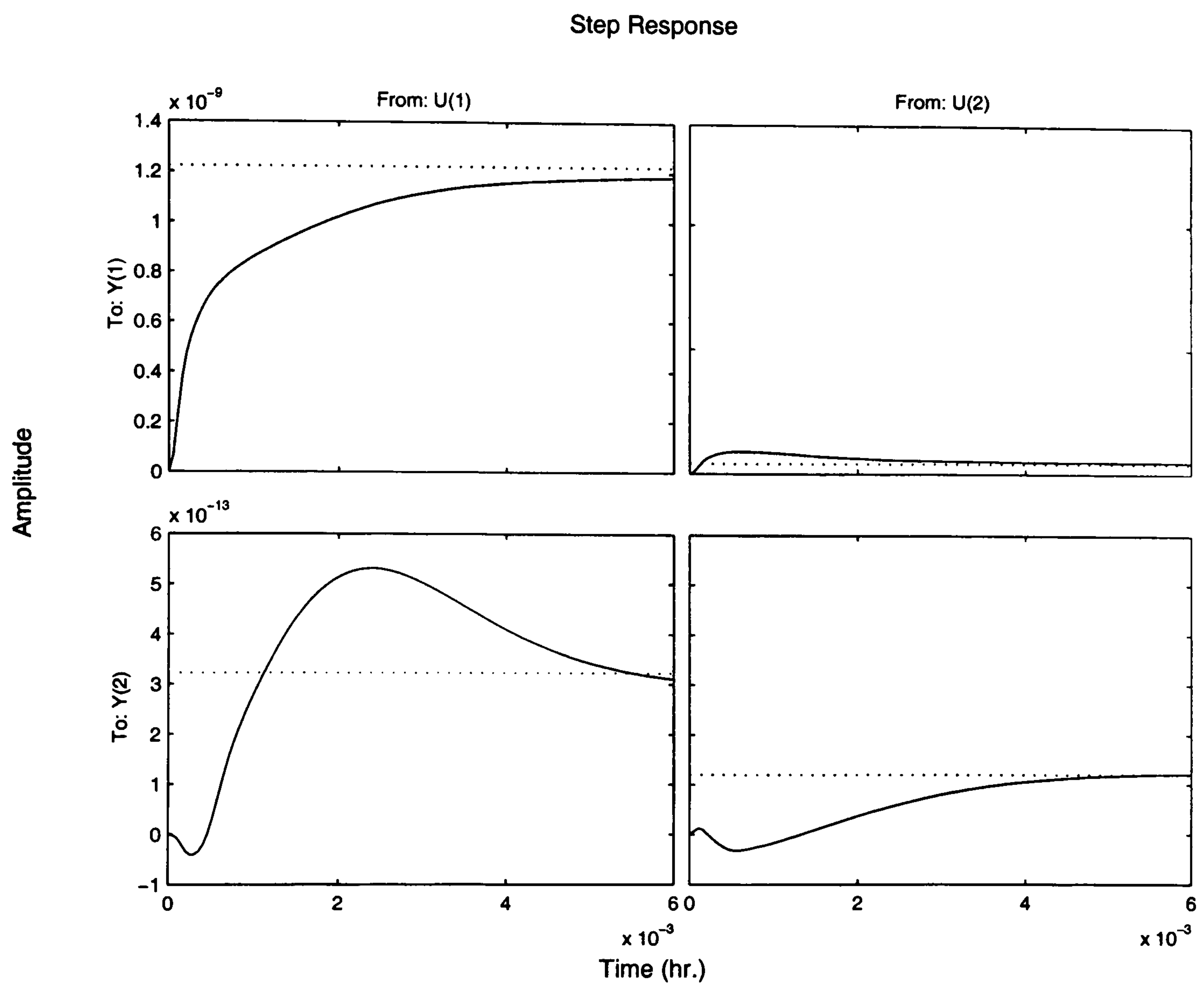


Figure B.12: Step response for Case 2 (MTBE). (10% step size)

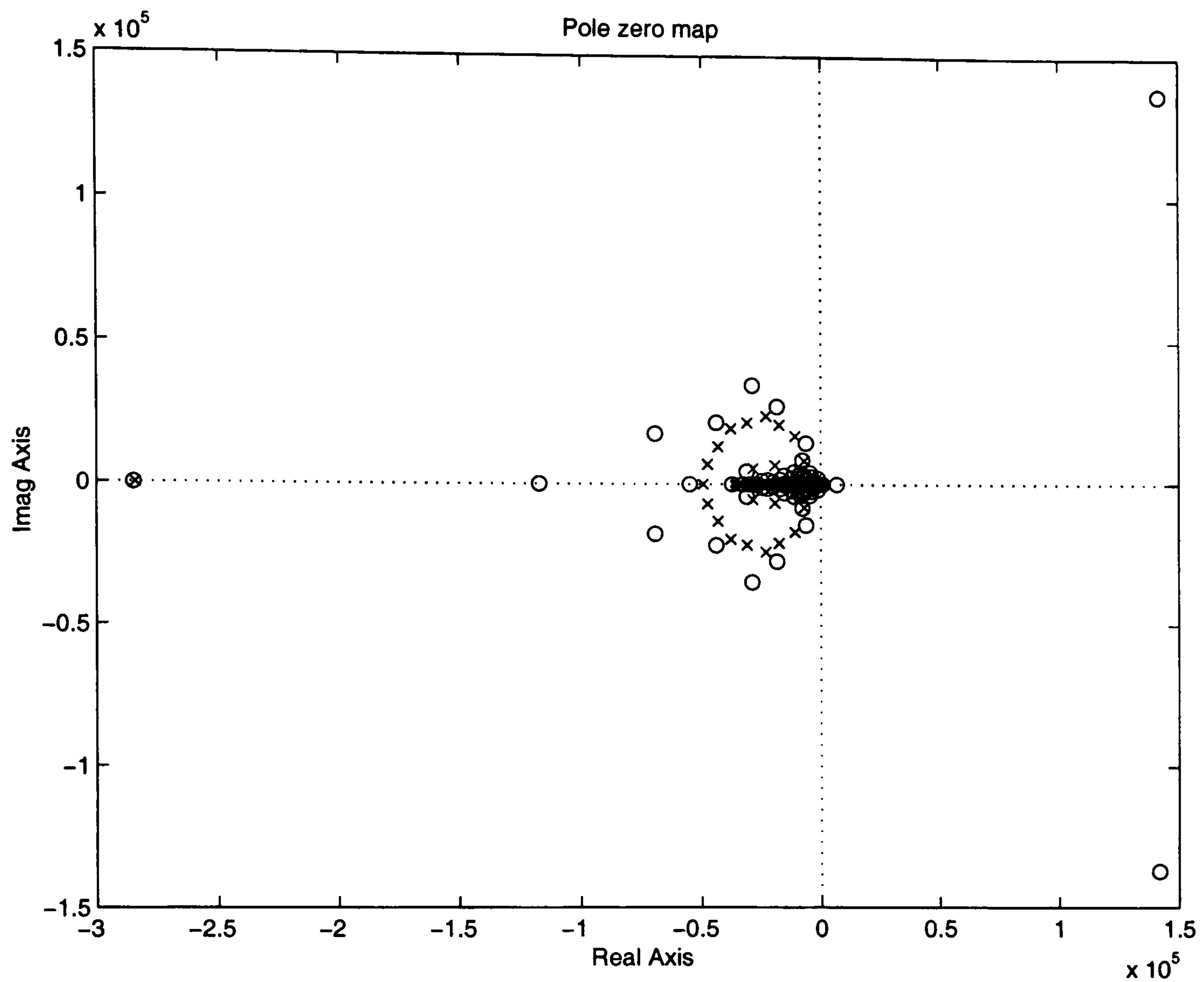


Figure B.13: Poles and Zeroes for Case 3 (MTBE)

- Computation of poles and zeroes

All poles are in the left half plane (system stable). Existence of RHP-zeroes. As can be seen from Fig.B.13.

- RGA

The steady-state RGA matrix is given by,

$$RGA = \begin{bmatrix} 0.71 & 0.29 \\ 0.29 & 0.71 \end{bmatrix} \quad (B.19)$$

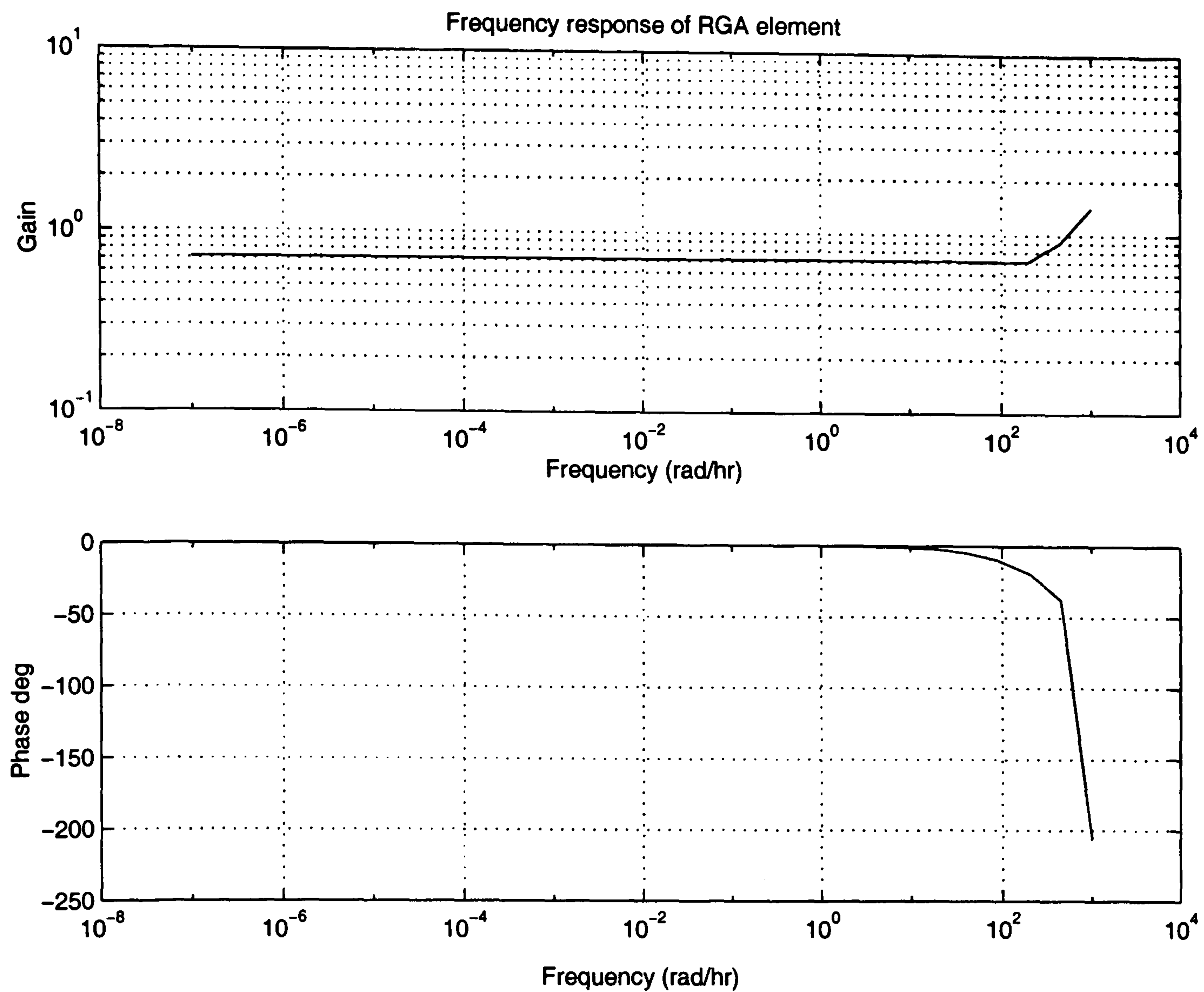


Figure B.14: RGA element (1,1) as a function of the frequency for Case 3 (MTBE)

The 1,1 element of the matrix can be plotted as a function of the frequency, as can be seen in Fig. B.14. The values of RGA tends to 1 at high frequencies, which confirms that the pairing u_1 - y_1 is a good choice.

- Singular value

The singular values are :

$$\underline{\sigma} = 0.000316 \quad (B.20)$$

$$\overline{\sigma} = 0.32 \quad (B.21)$$

Singular values for every frequency are given in Fig. B.15.

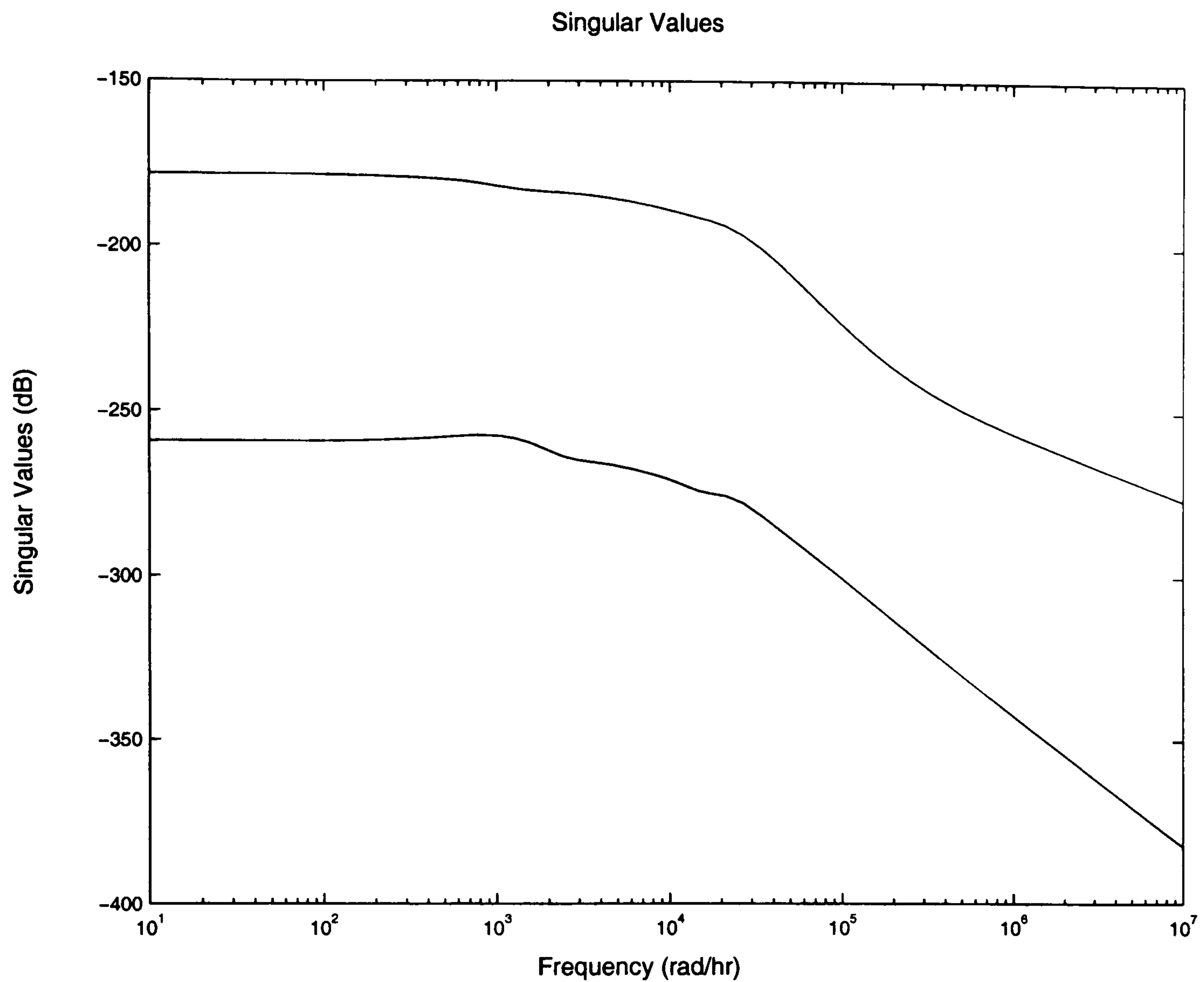


Figure B.15: Singular values for Case 3 (MTBE)

Analysis

The condition number is large (≈ 1012.93). The RGA values are different from unity, indicating that the interactions are strong. Another negative effect are the RHP-zeroes. The inverse response can be seen from Fig. B.16.

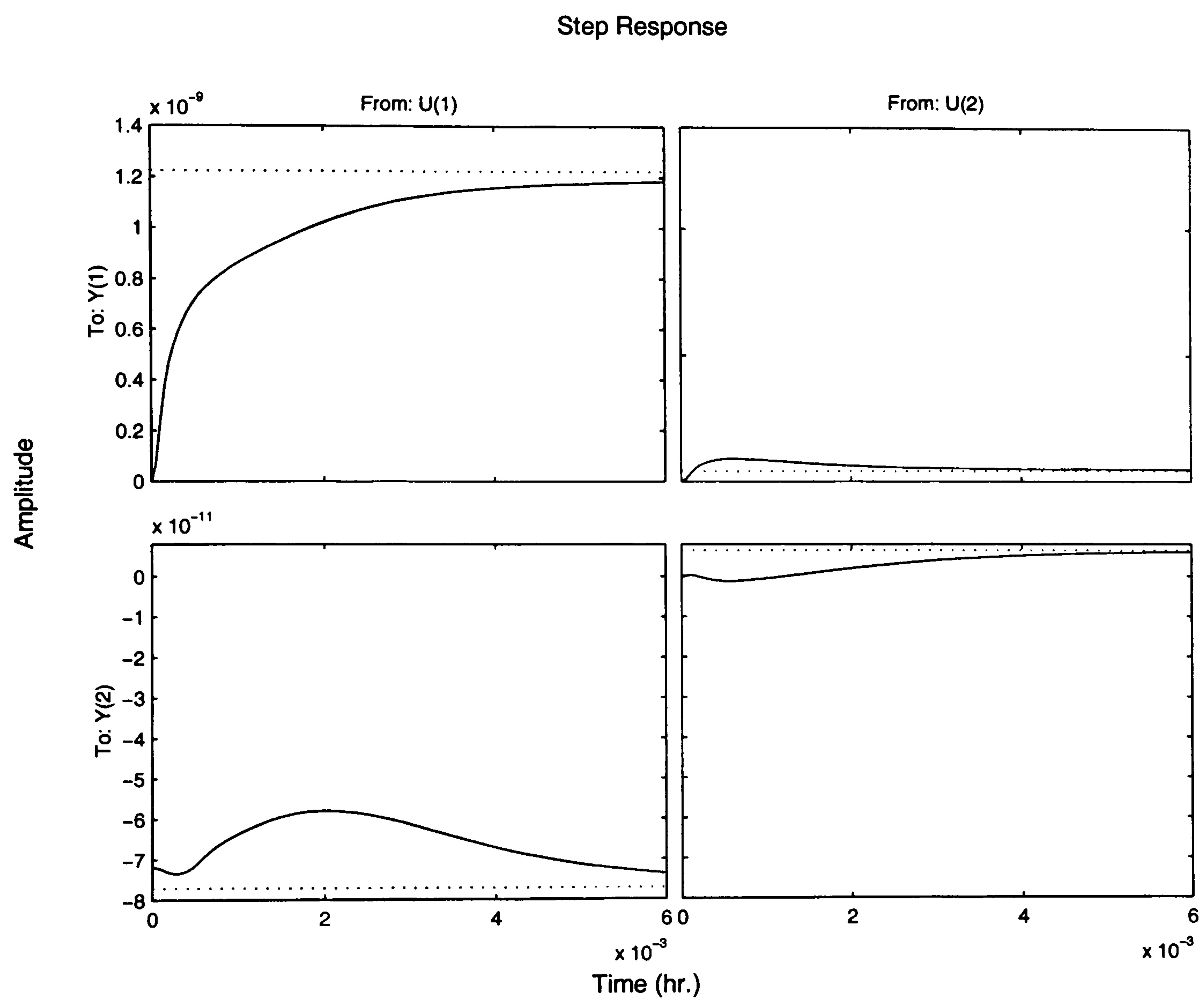


Figure B.16: Step response for Case 3 (MTBE). (10% step size)

B.2 Esterification of Acetic Acid with Ethanol

For the case of the esterification we have assumed the 0.00387D-V configuration.

Case1

The input variables (u) are given by,

$$u = \begin{bmatrix} D \\ V \end{bmatrix} \quad (\text{B.22})$$

The disturbances (d) are considered as follows,

$$d = \begin{bmatrix} x_{ethanol,F} \\ T_F \end{bmatrix} \quad (\text{B.23})$$

while the measurements variables (y) are,

$$y = \begin{bmatrix} T_D \\ T_B \end{bmatrix} \quad (\text{B.24})$$

The transfer function G is given by,

$$G = \begin{bmatrix} 3.282 & -0.0015 \\ -7.387 & 4.53e - 04 \end{bmatrix} \quad (\text{B.25})$$

The reactive column is functional controllable. The $\det G(s)$ is different from zero.

- Computation of poles and zeroes

All poles are in the left half plane (system stable). Existence of RHP-zeroes. As can be seen from Fig.B.17.

- RGA

The steady-state RGA matrix is given by,

$$RGA = \begin{bmatrix} 1.1726 & -0.1726 \\ -0.1726 & 1.1726 \end{bmatrix} \quad (\text{B.26})$$

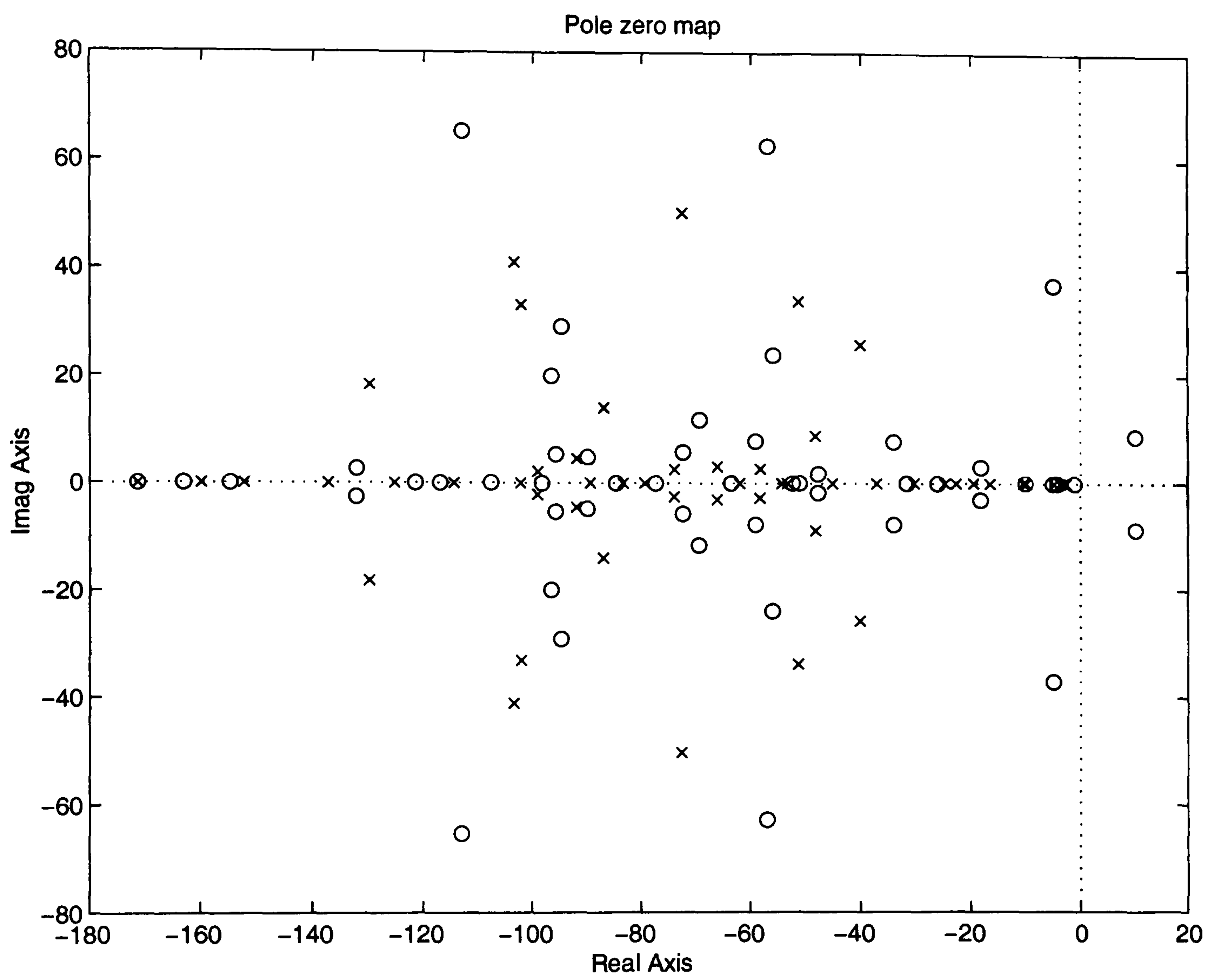


Figure B.17: Poles and Zeroes for Case 1 (Esterification)

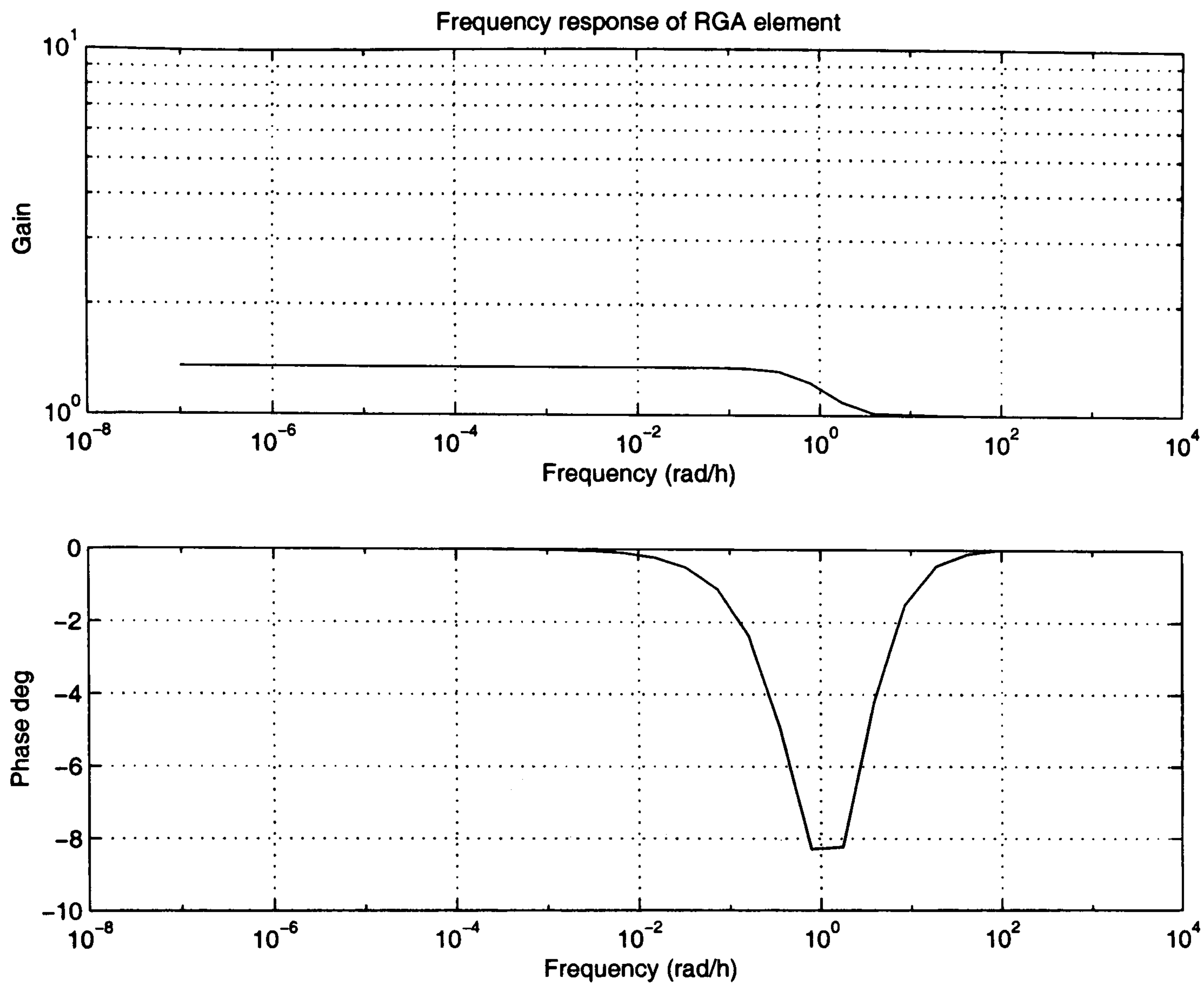


Figure B.18: RGA element (1,1) as a function of the frequency for Case 1 (Esterification)

The 1,1 element of the matrix can be plotted as a function of the frequency, as can be seen in Fig. B.18. The values of RGA tends to 1 at high frequencies, which confirms that the pairing u_1 - y_1 is a good choice.

- Singular value decomposition

The matrix G is decomposed into its singular value giving,

$$G = U \Sigma V^H \quad (\text{B.27})$$

for our case,

$$U = \begin{bmatrix} 0.4064 & 0.9137 \\ -0.9137 & 0.4064 \end{bmatrix} \quad (\text{B.28})$$

$$\Sigma = \begin{bmatrix} 8.08 & 0 \\ 0 & 1.06e-03 \end{bmatrix} \quad (\text{B.29})$$

$$V^H = \begin{bmatrix} 0.9900 & -0.417e-05 \\ -0.417e-05 & -0.9900 \end{bmatrix} \quad (\text{B.30})$$

Where the matrix Σ gives the singular values in the main diagonal.

Analysis

Since there are elements in $G(s)$ smaller than 1 in magnitude this suggests that may be control problems with input constraints.

The 1,1 element of the gain matrix G is 3.282. Thus, an increase in u_1 (distillate) yields a large steady-state change in y_1 (temperature of distillate), that is the outputs are very sensitive to changes in u_1 . In contrary an increase in u_2 (vapour boil-up) gives $y_2 = -0.0015$, a small change and in the opposite direction of that for the increase in u_1 (the opposite analysis to this is for u_2).

If both u_1 and u_2 (distillate and vapour-boil-up) are increased simultaneously, the overall steady-state change in y_1 is $(3.282 - 0.0015) = 3.2805$, which indicates that the temperature is strongly dependent on internal changes of flows. This can also be seen from the smallest singular value: 0.00106.

From the input singular vector,

$$u = \begin{bmatrix} 0.9137 \\ 0.4064 \end{bmatrix} \quad (\text{B.31})$$

we see that the effect is to move the outputs in the same direction, which will lead to a relative short control action to keep both temperature at the desired values simultaneously.

The condition number is rather large (≈ 7620), due to the very small minimum singular value. Although the RGA values are relatively small, the high value of the condition number implies control problems as well as the RHP-zero, which is also very close to the origin (RHP-zeros close to the origin are the most difficult to overcome). The RHP-zero also implies inverse response, as can be seen from Fig. B.19.

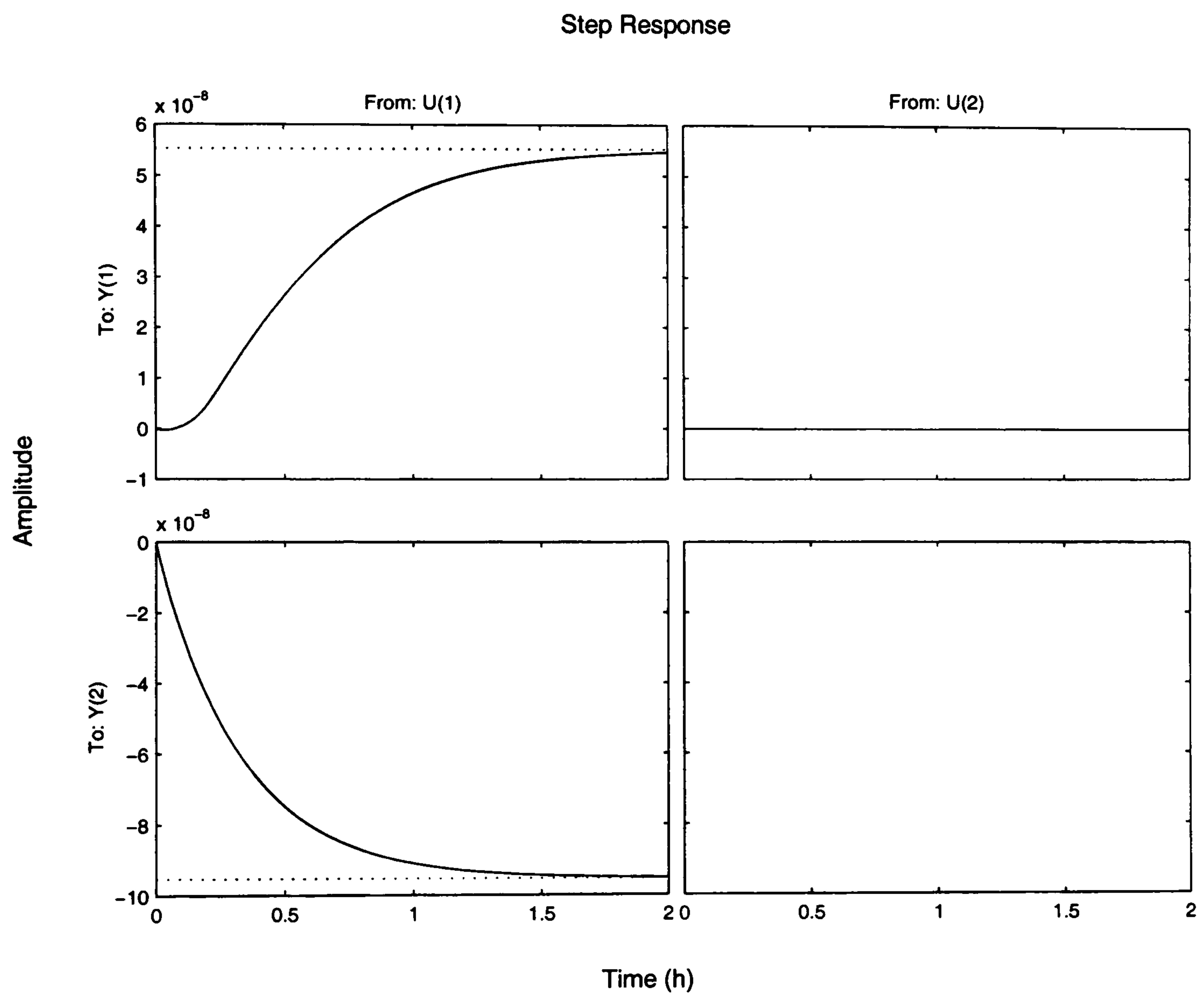


Figure B.19: Step response for Case 1 (Esterification). (10% step size)

Case2

The input variables (u) are given by,

$$u = \begin{bmatrix} D \\ V \end{bmatrix} \quad (\text{B.32})$$

The disturbances (d) are considered as follows,

$$d = x_{\begin{smallmatrix} ethanol, F \\ T_F \end{smallmatrix}} \quad (\text{B.33})$$

while the measurements variables (y) are,

$$y = \begin{bmatrix} x_{4D} \\ x_{1B} \end{bmatrix} \quad (\text{B.34})$$

For this case the transfer function G is given by,

$$G = \begin{bmatrix} 0.2440 & -1.152e - 03 \\ -0.042 & 1.033e - 05 \end{bmatrix} \quad (\text{B.35})$$

- Computation of poles and zeros

All poles are in the left half plane (system stable). Existence of RHP-zeros. Poles and zeroes map is shown in Fig. B.20

- RGA

The RGA matrix is given by,

$$RGA = \begin{bmatrix} 1.055 & -0.055 \\ -0.055 & 1.055 \end{bmatrix} \quad (\text{B.36})$$

The 1,1 element of the matrix can be plotted as a function of the frequency, as can be seen in Fig. B.18. The values of RGA tends to 1 at high frequencies, which confirms that the pairing u1-y1 is a good choice.

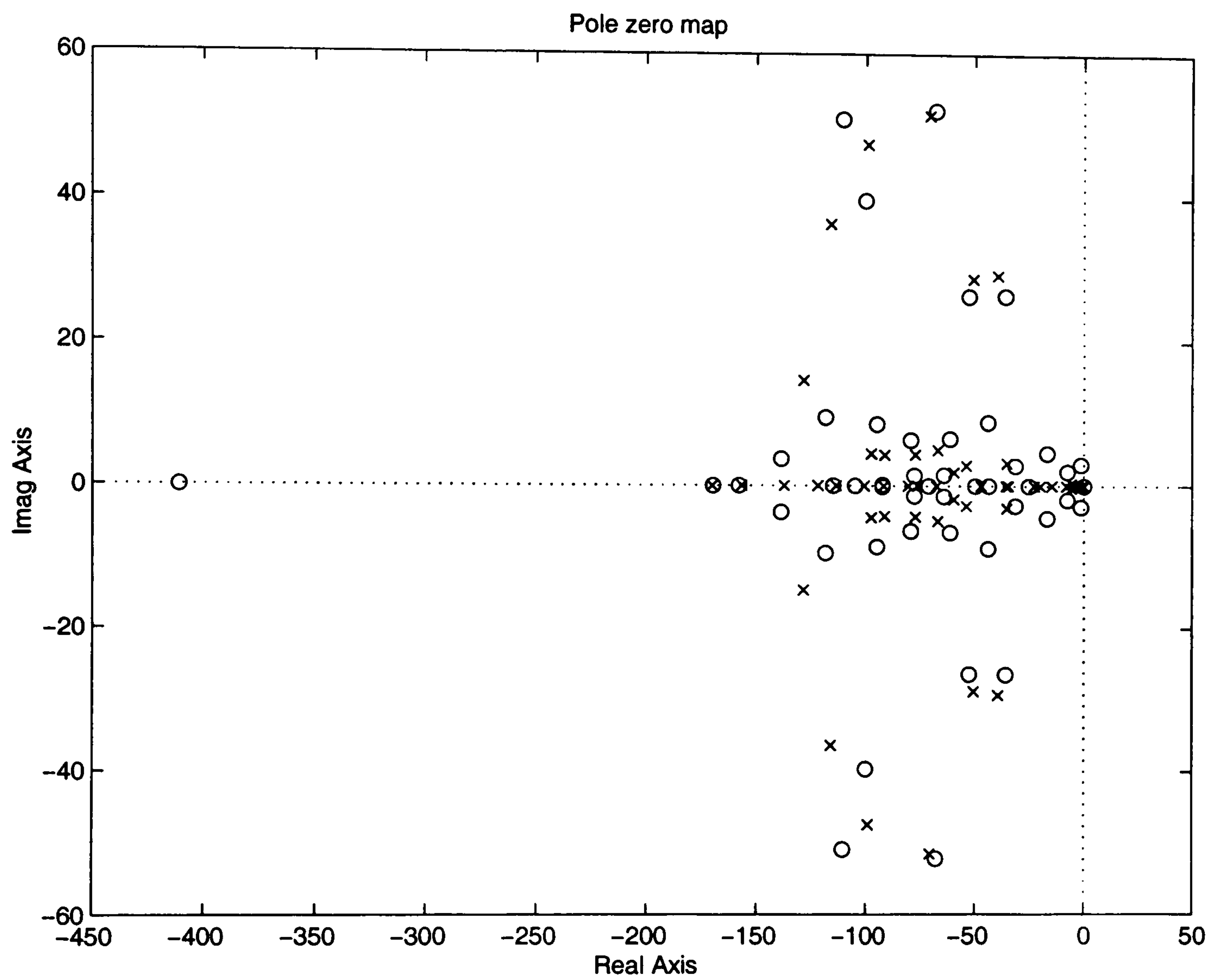


Figure B.20: Poles and zeroes for Case 2 (Esterification)

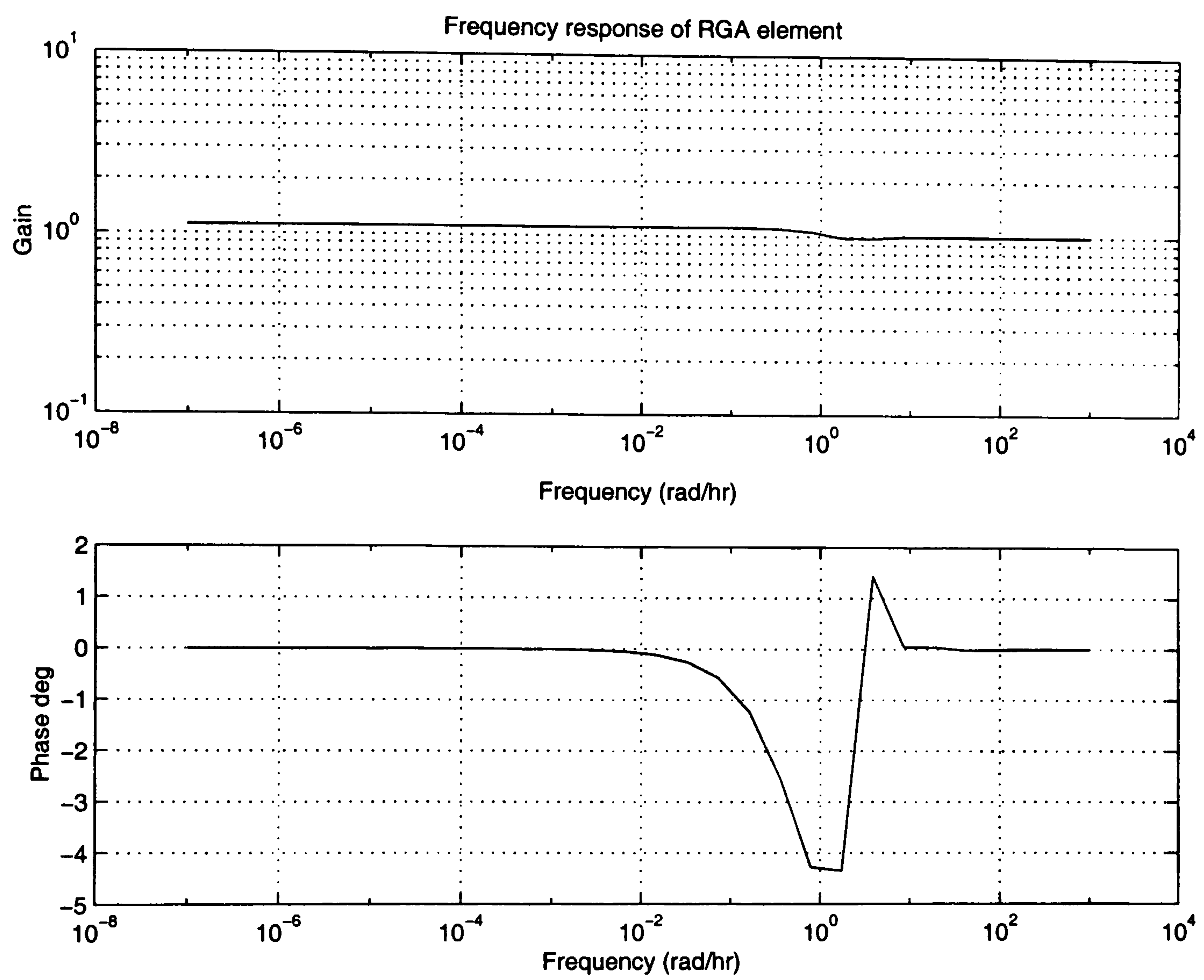


Figure B.21: RGA element (1,1) as a function of the frequency for Case 2 (Esterification)

- Singular value decomposition

The matrix G is decomposed into its singular value giving,

$$G = U \Sigma V^H \quad (\text{B.37})$$

for our case,

$$U = \begin{bmatrix} 0.9855 & -0.1693 \\ -0.1693 & -0.9855 \end{bmatrix} \quad (\text{B.38})$$

$$\Sigma = \begin{bmatrix} 0.244 & 0 \\ 0 & 1.875e-04 \end{bmatrix} \quad (\text{B.39})$$

$$V^H = \begin{bmatrix} -0.999 & 0.471e-03 \\ -0.471e-03 & 0.9900 \end{bmatrix} \quad (\text{B.40})$$

Where the matrix Σ gives the singular values in the main diagonal. Singular values as a function of the frequency are given in Fig. B.22.

Analysis

Since there are elements in $G(s)$ smaller than 1 in magnitude this suggests that there may be control problems with input constraints.

The 1,1 element of the gain matrix G is 0.2440. Thus, an increase in u_1 (distillate) yields a small steady-state change in y_1 (composition of distillate), that is the outputs are not sensitive to changes in u_1 . Similarly an increase in u_2 (vapour boil-up) gives $y_2 = -0.0012$, a small change and in the opposite direction of that for the increase in u_1 (the same analysis to this keeps for u_2).

If both u_1 and u_2 (distillate and vapour-boil-up) are increased simultaneously, the overall steady-state change in y_1 is $(0.244 - 0.0012) = 0.2428$, which indicates that compositions are weakly dependent on internal changes of flows. From the input singular vector,

$$u = \begin{bmatrix} 0.9855 \\ -0.1693 \end{bmatrix} \quad (\text{B.41})$$

we see that the effect is to move the outputs in the opposite direction. This will lead to a large control action to keep both composition at the desired

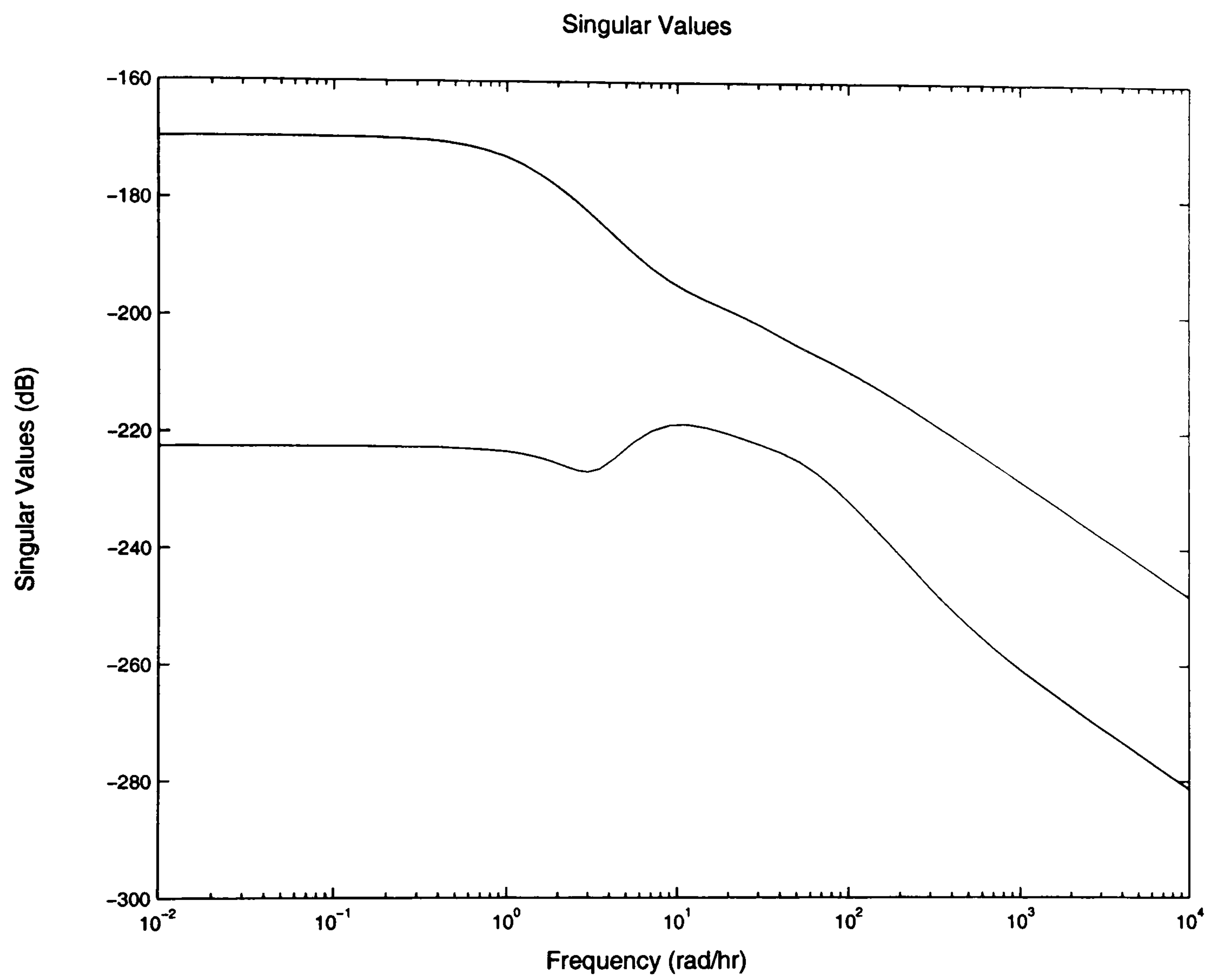


Figure B.22: Singular values for Case 2 (Esterification)

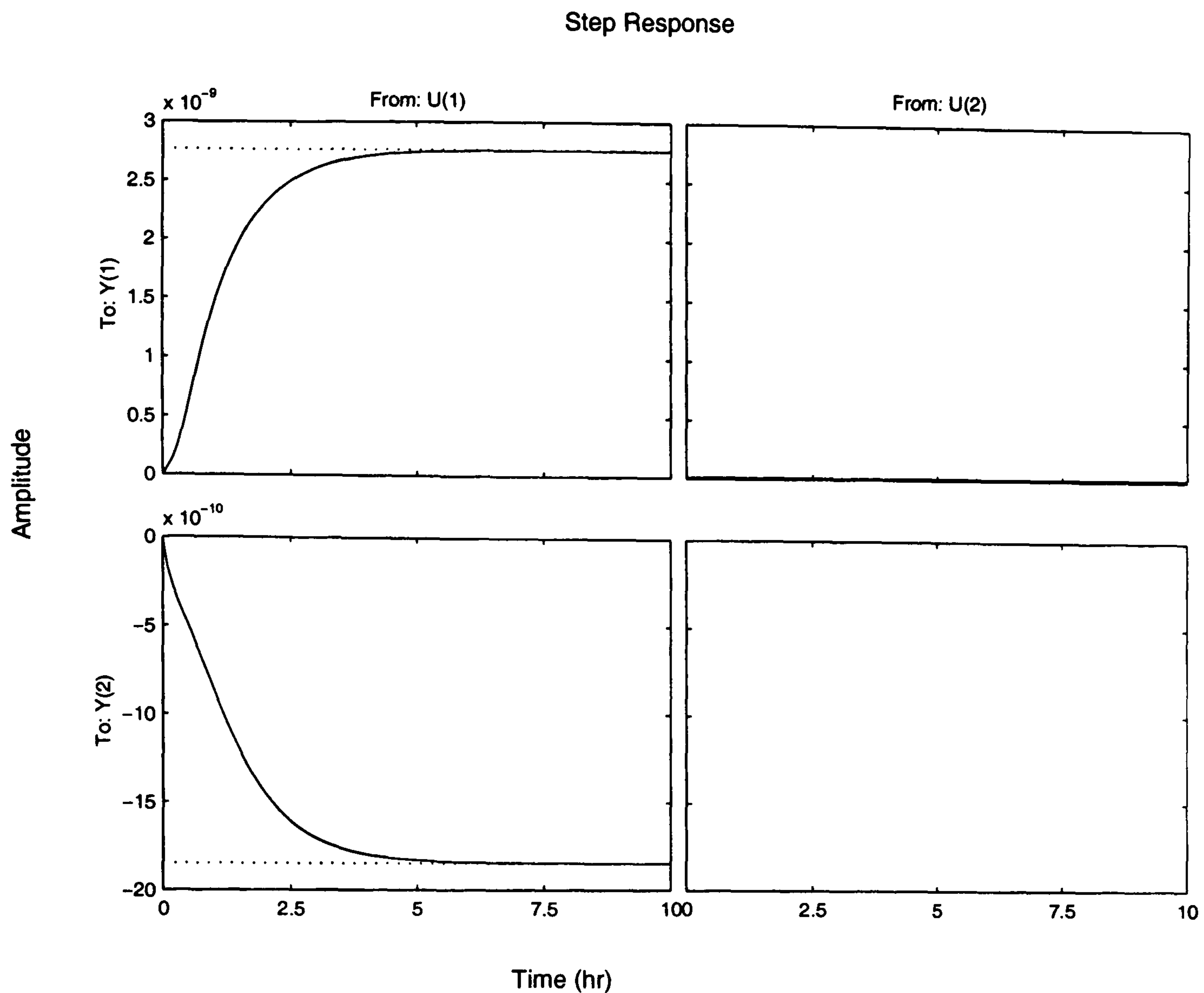


Figure B.23: Step responses for Case 2 (Esterification). (10% step size)

values simultaneously.

The condition number is rather large (≈ 1300), due to the very small minimum singular value. Although the RGA values are relatively small, the high value of the condition number implies control problems as well as the RHP-zero, which is also very close to the origin. The inverse response can be seen from Fig. B.23.

Case3

The input variables (u) are given by,

$$u = \begin{bmatrix} D \\ V \end{bmatrix} \quad (\text{B.42})$$

The disturbances (d) are considered as follows,

$$d = \begin{bmatrix} x_{1F} \\ x_{4F} \end{bmatrix} \quad (\text{B.43})$$

while the measurements variables (y) are,

$$y = \begin{bmatrix} x_{4D} \\ x_{1B} \end{bmatrix} \quad (\text{B.44})$$

For this case the transfer function G is given by,

$$G = \begin{bmatrix} 0.1091 & 1.4e - 02 \\ -0.0738 & -2.58e - 05 \end{bmatrix} \quad (\text{B.45})$$

- Computation of poles and zeros

All poles and zeros are in the left half plane (system stable). Fig. B.24.

- RGA

The RGA matrix is given by,

$$RGA = \begin{bmatrix} 1.0274 & -0.0274 \\ -0.0274 & 1.0274 \end{bmatrix} \quad (\text{B.46})$$

RGa as a function of the frequency is given in fig. B.25.

- Singular value

The singular values as a function of the frequency are given in Fig. B.26.

Analysis

The condition number is not too large (≈ 165), and the RGA values are very close to unity in the main diagonal. The RHP-zero disappears if the disturbance on the feed temperature is not present. Step changes are shown in Fig. B.27.

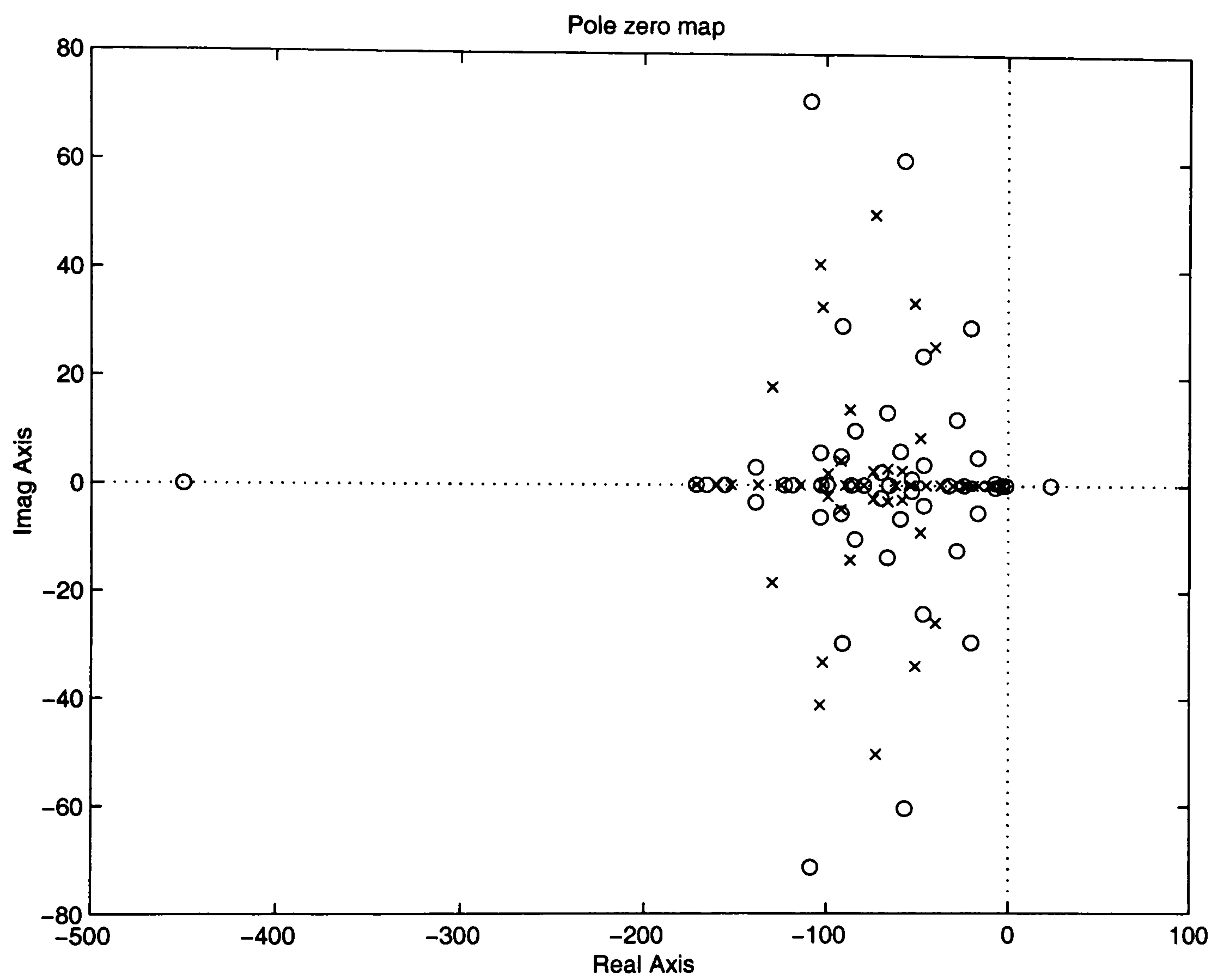


Figure B.24: Poles and zeros for Case 3 (Esterification)

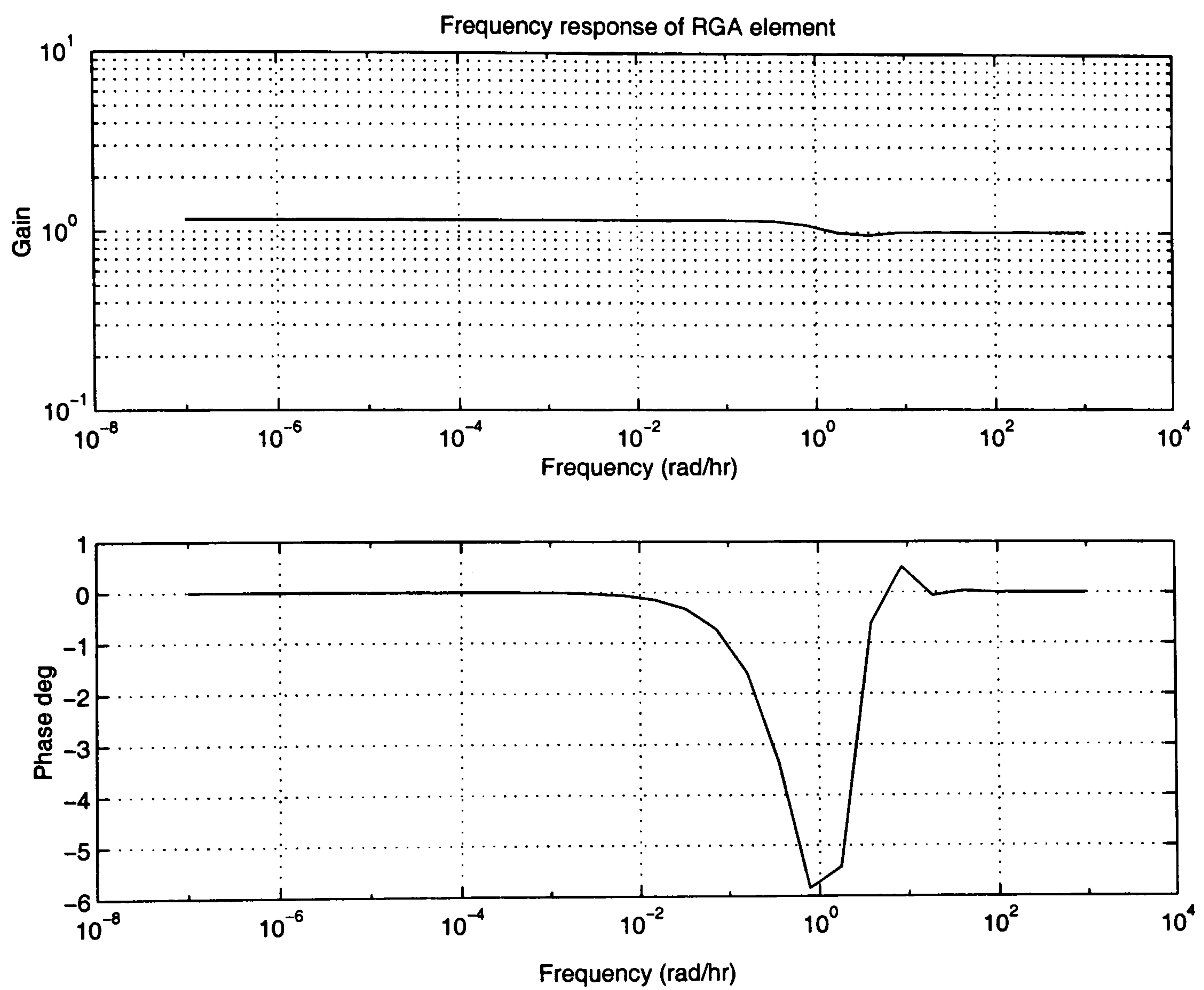


Figure B.25: RGA element (1,1) as a function of the frequency for Case 3 (Esterification)

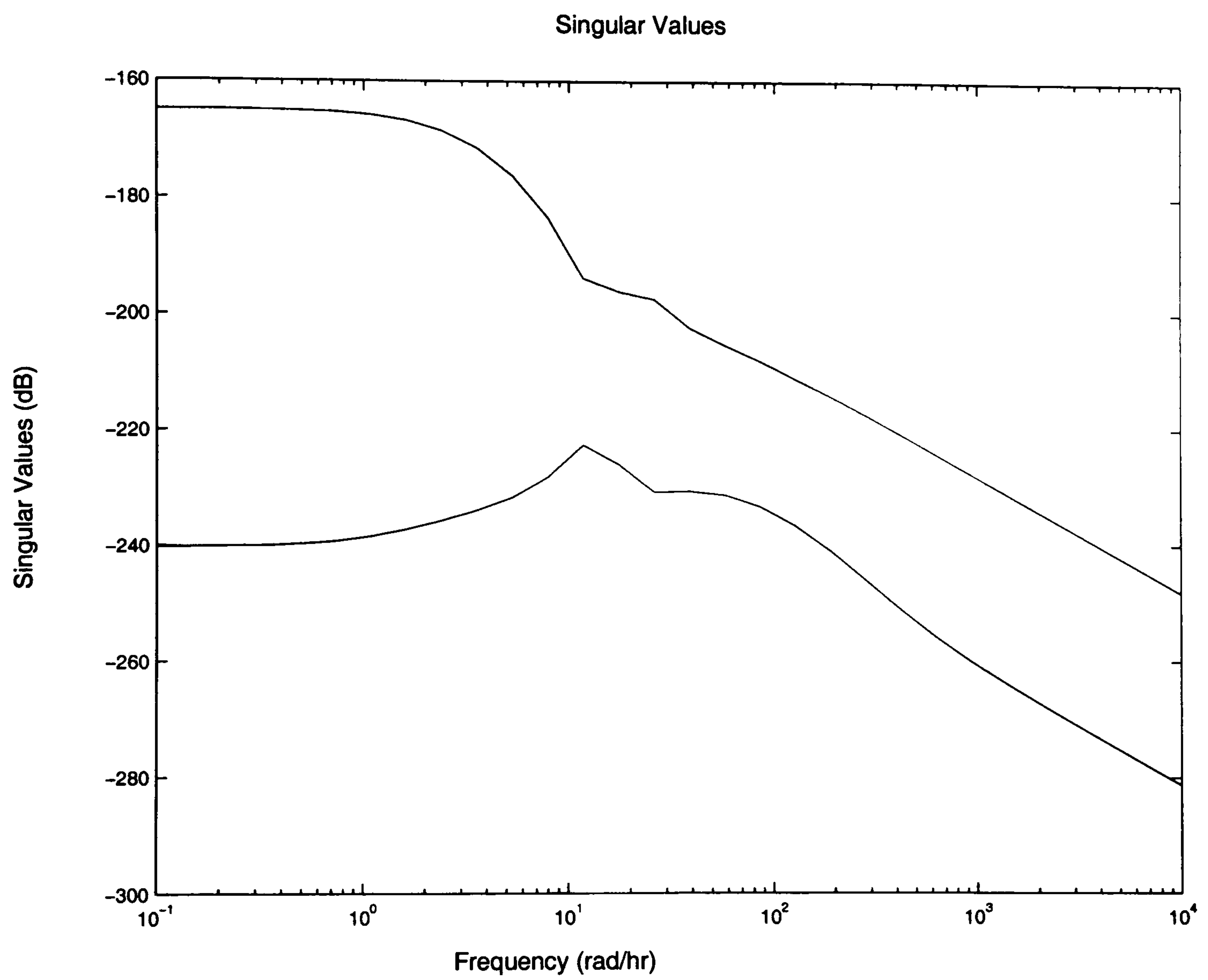


Figure B.26: Singular values for Case 3 (Esterification)

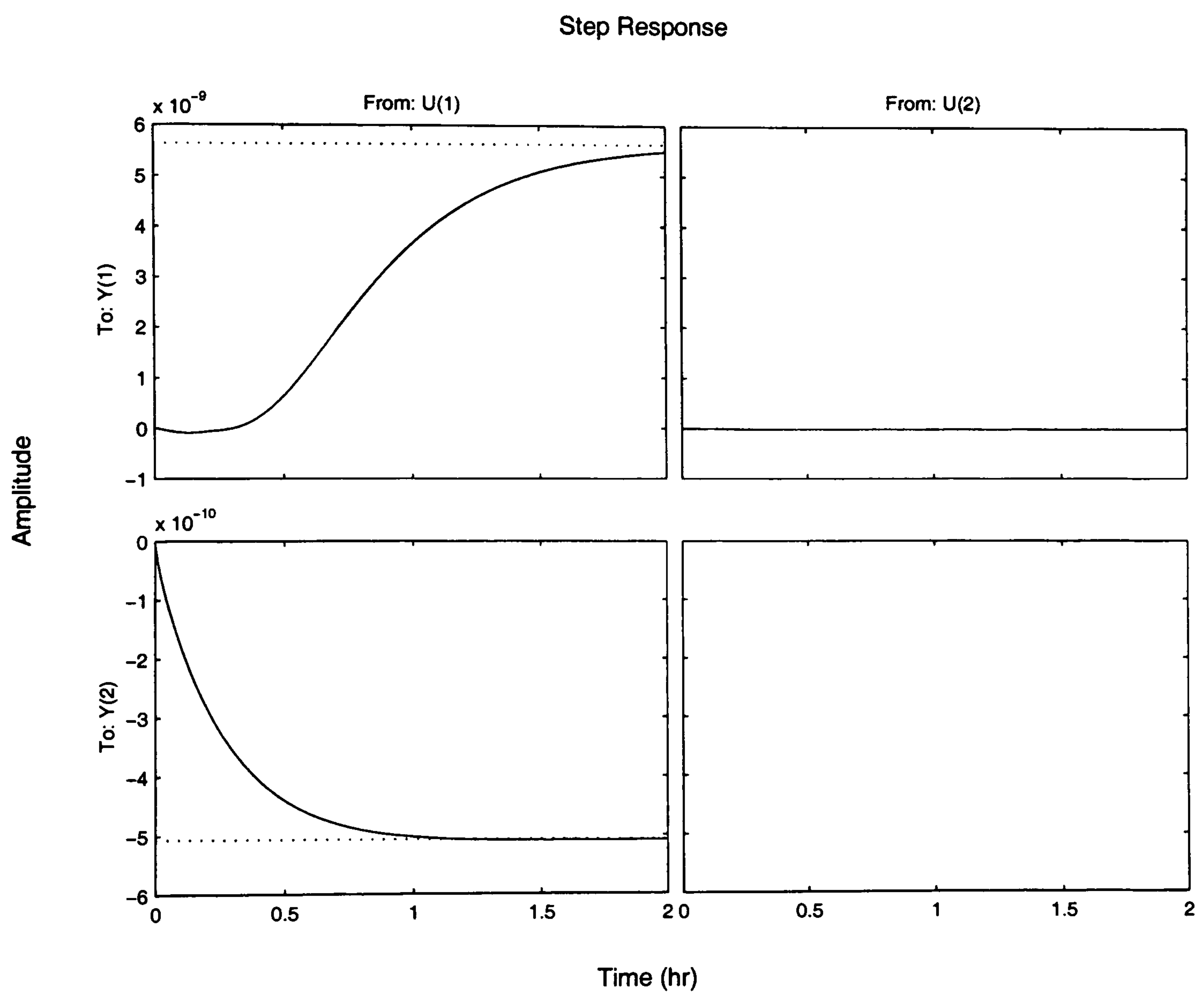


Figure B.27: Step responses for Case 3 (Esterification). (10% step size)

Appendix C

Optimization

C.1 Objective Function and Disturbances

Objective Function

The objective function is composed by capital and operating costs. The annualised investment cost is determined by the cost of the column, its internal, and reboiler and condenser.

$$\text{minimise Cost} = \text{minimise}(C_{shell} + C_{tray} + C_{hx} + C_{op}) \quad (C.1)$$

where C_{shell} , C_{tray} , C_{hx} and C_{op} are given by,

$$C_{shell} = \frac{1}{3} \left(\frac{M\&S}{280} \right) (101.9D_t)(2.18 + F_c) \sum_p (H_o + \sum_{p' < p} 2A_{p'})^{0.802} (Z_p - Z_{p+1}) \quad (C.2)$$

where,

A is a constant equal to 101.9;

$M\&S$ is the Marshall and Swift index equal to 800;

B is a constant equal to 2.18;

H_o is the sum of the spacing at the top and bottom of the column equal to 1m.;

F_c is the material of construction factor equal to 1.05;
 D_t is the column diameter (variable); and,
 A_p' is a dummy variable which is a function of tray spacing and is set to 1 for a tray spacing of 2 feet.

$$C_{tray} = \left(\frac{M\&S}{280} \right)^{4.7} D_t^{1.55} F_c \sum_p 2Z_p \quad (C.3)$$

where,

$M\&S$ is the Marshall and Swift index equal to 800;
 F_c is the material of construction factor equal to 1.

The column diameter, D_t , its easily calculated from the internal vapour flow-rate, and the materials of construction factors will be constant for a given system.

$$C_{hx} = \frac{1}{3} \left[\frac{M\&S}{280} \right] 101.3(2.29 + F_{cc})(A_c^{0.65} + A_r^{0.65}) \quad (C.4)$$

where,

$M\&S$ is the Marshall and Swift index equal to 800;
 F_{cc} is the material of construction factor for heat-exchanger equal to 1.30;
 A_c and A_r are the condenser and reboiler areas (variables), respectively.

$$C_{op} = Q_c C_{water} + Q_r C_{steam} \quad (C.5)$$

The cost of steam and cooling water is computed directly, hence, C_{water} is the cost of cooling water (2.8573E-4 dollars per kgmol); and C_{steam} is the cost of steam (3.63763E-3 dollars per kg).

Disturbances

Sinusoidal in feed composition:

$$z_{AA} = z_{AA} + 0.15 \sin(wt) \quad (C.6)$$

$$z_{Et} = z_{Et} + 0.15 \sin(wt) \quad (C.7)$$